AD_____

Award Number: W81XWH-12-2-0138

TITLE: Investigating Metabolic Control of Persister Formation in Biofilms

PRINCIPAL INVESTIGATOR: Mark P. Brynildsen, Ph.D.

CONTRACTING ORGANIZATION: TRUSTEES OF PRINCETON UNIVERSITY, THE
1 NASSAU HALL
PRINCETON NJ 08544-2001

REPORT DATE: October 2013

TYPE OF REPORT: Annual

PREPARED FOR: U.S. Army Medical Research and Materiel Command
Fort Detrick, Maryland 21702-5012

REPORT DOCUMENTATION PAGE

Form Approved
OMB No. 0704-0188

1. REPORT DATE	2. REPORT TYPE	3. DATES COVERED
october 2013	Annual	30September2012-29Septmeber2013

4. TITLE AND SUBTITLE
Investigating Metabolic Control of Persister Formation in Biofilms

5a. CONTRACT NUMBER
W81XWH-12-2-0138

5b. GRANT NUMBER
W81XWH-12-2-0138

5c. PROGRAM ELEMENT NUMBER

6. AUTHOR(S)
Mark P. Brynildsen, Stephanie M. Amato, Christopher H. Fazen, Theresa Henry
Mehmet A. Orman, Elizabeth L. Sandvik, Katherine Volzing

E-Mail: mbrynild@princeton.edu

5d. PROJECT NUMBER

5e. TASK NUMBER

5f. WORK UNIT NUMBER

7. PERFORMING ORGANIZATION NAME(S) AND ADDRESS(ES)
TRUSTEES OF PRINCETON UNIVERSITY, THE
1 NASSAU HALL
PRINCETON NJ 08544-2001

8. PERFORMING ORGANIZATION REPORT NUMBER

9. SPONSORING / MONITORING AGENCY NAME(S) AND ADDRESS(ES)
U.S. Army Medical Research and Materiel Command
Fort Detrick, Maryland 21702-5012

10. SPONSOR/MONITOR'S ACRONYM(S)

11. SPONSOR/MONITOR'S REPORT NUMBER(S)

12. DISTRIBUTION / AVAILABILITY STATEMENT
Approved for Public Release; Distribution Unlimited

13. SUPPLEMENTARY NOTES

14. ABSTRACT

Bacterial persistence is a phenomenon in which a small fraction of a bacterial population enters dormancy in otherwise growth-promoting conditions to survive future stress. These survivors are responsible for the relapse of biofilm infections, and thus a greater understanding of their formation will lead to more effective therapies against biofilm-utilizing pathogens, such as Pseudomonas aeruginosa, *Escherichia coli*, *Acinetobacter baumannii*, and *Staphylococcus aureus*. We have discovered that diauxic carbon shifts stimulate the generation of persisters in planktonic cultures, and hypothesized that metabolic transitions generate persisters in biofilms. In this project, we are identifying metabolic transitions in biofilm communities of *E. coli*, *P. aeruginosa*, and *S. aureus* that generate persisters, and using genetic and biochemical techniques to reconstruct the underlying signaling pathways. During this reporting period we discovered that specific carbon source transitions in *E. coli* biofilms stimulate persister formation through a ppGpp and nucleoid-associated protein dependent pathway. In addition, preliminary data suggests that nitrogen source transitions in *P. aeruginosa* biofilms and carbon source transitions in *S. aureus* biofilms stimulate persister formation. Further, we have developed a rapid method to assay persister metabolic activity. Support from this grant has led to three publications and one submitted manuscript thus far.

15. SUBJECT TERMS
Antibiotic tolerance, bacterial persistence, nutrient transitions, biofilms

16. SECURITY CLASSIFICATION OF:			17. LIMITATION OF ABSTRACT	18. NUMBER OF PAGES	19a. NAME OF RESPONSIBLE PERSON
a. REPORT	b. ABSTRACT	c. THIS PAGE			USAMRMC
U	U	U	UU	191	19b. TELEPHONE NUMBER *(include area code)*

Table of Contents

ANNUAL REPORT

Introduction

Bacterial persistence is a phenomenon in which a small fraction of a bacterial population enters dormancy in otherwise growth-promoting conditions to survive future stress (*e.g.*, antibiotic treatment)[1]. These survivors are responsible for the relapse of biofilm infections, and thus a greater understanding of their formation will lead to more effective therapies against biofilm-utilizing pathogens, such as *Pseudomonas aeruginosa*, *Escherichia coli*, *Acinetobacter baumannii*, and *Staphylococcus aureus*. We have discovered that diauxic carbon shifts stimulate the generation of persisters in planktonic cultures, and believe this to be a general phenomenon in response to metabolite fluctuations. Biofilms are highly heterogeneous communities in which the microenvironment of encased bacteria changes considerably as the film matures[2-4]. We hypothesized that metabolic transitions generate persisters in biofilms, and that a mechanistic understanding of such phenomena will lead to novel treatment strategies. In this project, we are identifying metabolic transitions in biofilm communities of *E. coli*, *P. aeruginosa*, and *S. aureus* that generate persisters, and using genetic and biochemical techniques to reconstruct the underlying signaling pathways. This effort will elucidate how metabolism controls persister formation in biofilms, and identify targets of therapeutic interest for the reduction of relapse infections from biofilms in combat-wounded personnel.

Body

This section has been segregated into research accomplishments and future work.

Research Accomplishments

Statement of Work Task 1: Determine carbon source shifts that stimulate persister formation in biofilms.

The purpose of this task was to perform a phenotypic screen in order to identify carbon source transitions that stimulate persister formation in biofilms of *E. coli*, *P. aeruginosa*, and *S. aureus*.

As detailed in our first quarterly report, we found the MBEC biofilm culturing method, which was originally proposed, to be problematic, since it was difficult to unambiguously claim that cells collected after sonication were solely those from the biofilm (Figure 1). This prompted us to switch to the colony biofilm culturing method, where only biofilm cells are present, and thus persisters can be unequivocally attributed to the biofilm state (Figure 2). Though the method unambiguously measures persisters from biofilm populations, it is not nearly as high-throughput as the MBEC method (6-well plates compared to 96-well plates, variable solid media compared to liquid media), and thus experiments are more cumbersome and time consuming.

E. coli carbon source transitions

Previously, we had discovered that diauxic carbon source transitions generated persisters in planktonic *E. coli* cultures. A publication describing this phenomenon and its underlying mechanism has been published in *Molecular Cell*[5] (Appendices), and this award was acknowledged for its support of the development and testing of cAMP-CRP and ppGpp transcriptional reporters used in that study (Figure 3 and Figure 4). These reporters were used in the corresponding biofilm study described below, which is currently under review at *PLoS One* (Appendices).

Since the clinical relevance of bacterial persistence is largely associated with the biofilm state, we sought to determine whether carbon source transitions could be a source of persisters in *E. coli* biofilms. To accomplish this, we identified experimental conditions where nutrient availability to biofilm cells could be controlled exogenously (Figure 5). In brief, young biofilms

were used to avoid the inherent nutrient heterogeneity of mature biofilms[6,7], and the colony biofilm culturing method was used to eliminate any contribution from planktonic cells (Figure 5A). Colony biofilm culturing was found to exhibit uniform diauxic growth in biofilm cells (Figure 5BCD), and to demonstrate that young biofilms were present on the time-scale of our experiments, biofilms were imaged with confocal microscopy and compared to samples where an equal number of planktonic cells were seeded onto the membrane just prior to imaging (Figure 6). The presence of cell clusters in the biofilm sample demonstrates that these young films are immobilized cells growing in surface-attached communities. We note that the strain constructed to perform these imaging experiments was used in a study of persister metabolism we published in *Antimicrobial Agents and Chemotherapy*[8] (Appendices), and this award was acknowledged for its support.

To enumerate persisters in biofilms, we needed to identify an ofloxacin (OFL) concentration and treatment time that yielded a biphasic kill curve and persister level that was invariant with respect to higher antibiotic concentrations. First we tested numerous OFL concentrations at 6 hours of treatment, since this time far exceeded that which we have identified to be necessary in stationary phase cultures[8,9]. These experiments indicated that delivery of 200μL of 10μg/mL OFL to colony biofilms was sufficient to eliminate persister dependency on the OFL concentration (Figure 2D left), and subsequent time course experiments indicated that 5 hours of treatment was sufficient to enumerate persisters (Figure 7). When a panel of diauxic and non-diauxic media compositions were tested for persister formation, we found significant increases for diauxic transitions when compared to the glucose-only control, whereas transitions to the non-diauxic substrates fructose and gluconate failed to increase persisters beyond the glucose-only control (Figure 7). Using glucose-fumarate as a model diauxic transition, we tested a fumarate-only control to determine whether the increase in persisters was due to growth on the less favorable substrate or the transition from glucose to fumarate. Figure 7C demonstrates that persister formation was a result of the carbon source transition, and not growth on fumarate. From here we went on to identify the underlying formation pathway, which is further detailed in Task 4 and Task 5.

P. aeruginosa carbon source transitions

Following the approach laid by our *E. coli* work, we first needed to identify an OFL concentration and treatment time that yielded a biphasic kill curve and persister level that was invariant with respect to higher antibiotic concentrations. First we tested numerous OFL concentrations at 6 hours of treatment, and found that 200μL of 150μg/mL OFL was sufficient to eliminate persister dependency on the OFL concentration (Figure 2D right). Further, subsequent time course experiments indicated that 5 hours of treatment was sufficient to enumerate persisters (Figure 8). When a panel of diauxic and non-diauxic media compositions were tested, we observed persister formation for specific diauxic transitions (glycerol, fructose) when compared to the fumarate-only control, whereas transitions to the non-diauxic substrate succinate failed to increase persisters beyond the fumarate-only control (Figure 9). To determine whether growth on the less favorable substrates or the carbon source transition was responsible for persister formation, we measured persisters from glycerol-, fructose-, glucose-, and succinate-only controls. Interestingly, these controls suggested that growth on the less favorable substrate was the cause of persister formation (Figure 10), which differed from the phenomenon observed in *E. coli*. Since we observed extremely poor growth in our sole glycerol and fructose controls, suggesting that growth rate effects may dominate persistence measurements in those samples, we rationalized that replacing the LB overnights with minimal media overnights would allow better growth and an opportunity to detect transition-dependent persister formation. However, experiments performed with minimal media overnights produced qualitatively similar results to those obtained with LB overnights (Figure 11). To determine if this phenomenon was specific to the biofilm state, we performed analogous experiments with

planktonic cultures of *P. aeruginosa*. Unfortunately, OFL persisters are rare in planktonic *P. aeruginosa* cultures, and in our experiments we often found them to be under our limit of detection, so we were unable to conclusively demonstrate whether this phenomenon translated to planktonic conditions.

The biofilm data we obtained suggests that OFL persistence in *P. aeruginosa* is largely dependent on the carbon source, which conceivably occurs through growth-rate effects. However, if persistence were exclusively growth-rate dependent, a non-growing *P. aeruginosa* population should not exhibit biphasic killing, and a single, constant killing rate should be observed. Interestingly, Figure 12 shows that this simply is not true, and two distinct killing regimes are observed even for a non-growing population. Our plan to investigate the link between metabolism of less favorable growth substrates, growth-rate, and OFL persistence is discussed in the Future Work section.

S. aureus carbon source transitions

S. aureus is an auxotroph for numerous amino acids[10], and therefore cannot grow on minimal media containing just carbon source and salts as *E. coli* and *P. aeruginosa* can. The chemically-defined media we initially planned to use for *S. aureus* was described by Miller and Fung[11]. Two alternative media, with fewer amino acids, have been described by Rudin and colleagues (AAM+)[12] and Lee and colleagues (AAM-)[10], and we tested whether these media could support glucose-dependent biofilm growth of *S. aureus*. Figure 13 demonstrates that AAM+ supports *S. aureus* growth that is glucose-dependent, whereas AAM- does not support biofilm growth in the presence or absence of glucose. Therefore, AAM+ was chosen for all *S. aureus* experiments. To determine the carbon source utilization pattern of *S. aureus*, we performed planktonic growth experiments where AAM+ media with 0.1 g/L glucose was supplemented with 166.5mM carbon of secondary carbon source. Planktonic conditions were chosen for these assays because we have observed with *E. coli* and *P. aeruginosa* that carbon source utilization in the biofilm state closely resembles that of the planktonic state, and planktonic assays allow for a higher degree of parallelization. These experiments demonstrated three utilization patterns, non-diauxic (gluconate, glycerol, fructose, ribose), diauxic (pyruvate, oxaloacetic acid, lactose), and absence of growth on secondary carbon sources (α-ketoglutarate, succinate, fumarate, acetate, arabinose) (Figure 14). Since *S. aureus* growth on defined media is slow and experiments last longer than 24 hours, we judiciously chose to investigate persister formation for nutrients that exhibited diauxic growth with glucose (lactose and pyruvate).

To determine the antibiotic concentration to use for persister enumeration from *S. aureus* biofilms grown on AAM+, we treated 6-hr grown films with different concentrations of ciprofloxacin (CIP) and monitored CFUs after 5, 8, 16, 24, and 48 hours. Ciprofloxacin was chosen since it is has been the more prevalent fluoroquinolone used to investigate *S. aureus* persistence[13,14]. These experiments indicated that delivery of 200μL of 400μg/mL CIP to colony biofilms was sufficient to eliminate persister dependency on the CIP concentration (Figure 15A), and subsequent time course experiments indicated that 24 hours of treatment was sufficient to enumerate persisters (Figure 15B).

When diauxic nutrient transitions were investigated for their ability to form persisters in *S. aureus* biofilms, we found that glucose-lactose colony biofilms exhibited increased persister formation compared to glucose-only and glucose-pyruvate biofilms (Figure 16). To determine

whether the observed persister formation is substrate- or transition-dependent we will measure persisters from lactose-only controls.

Statement of Work Task 2: Determine nitrogen source shifts that stimulate persister formation in biofilms.

The purpose of this task was to perform a phenotypic screen in order to identify nitrogen source transitions that stimulate persister formation in biofilms of *E. coli*, *P. aeruginosa*, and *S. aureus*.

E. coli nitrogen source transitions

E. coli uses NH_4^+ as its preferred nitrogen source, and we began by identifying an NH_4^+ concentration that would support colony biofilm growth for approximately 3-4 doublings (Figure 17). From this data, we determined that inoculation of each membrane with cells suspended in 0.25mM NH_4^+ media was sufficient for our purposes. To determine if nitrogen source transitions stimulate persister formation in *E. coli* biofilms, arginine and glutamine were provided at 20mM nitrogen as the sole nitrogen source in the agar, and as controls, 20mM NH_4^+ and nitrogen source-free agar were used. As depicted in Figure 17B, all samples grew comparably during the first 4 hours (common period of NH_4^+ consumption) and divergence became apparent by the 5 hour time point. The nitrogen-source free control demonstrates that secondary nitrogen sources were consumed by the colony biofilms. When persister levels in the biofilms were enumerated, we observed persister formation in biofilms supplied with arginine in the agar, whereas biofilms supplied with NH_4^+ and glutamine in the agar failed to form persisters (Figure 17C). In fact, the persister level for glutamine supplied biofilms was less than that for the NH_4^+ supplied biofilms. This result likely originates from the co-utilization of glutamine and faster growth that is observed in Figure 17B. To determine whether persister formation was from the nitrogen source transition or from growth on the less favorable substrate, we measured persister levels in colony biofilms with arginine as the sole nitrogen source. Our preliminary data suggests that persister formation in NH_4^+-arginine biofilms was a result of growth on arginine and not from the nutrient transition (Figure 18). To determine if this phenomenon was specific to the biofilm state, we performed analogous experiments with planktonic cultures, and found that persister levels for NH_4^+-arginine after the transition were indistinguishable from a sole arginine control, suggesting that persister formation was due to growth on arginine and not the metabolic transition (Figure 19). For planktonic cultures, due to the comparative ease with which experiments can be parallelized, we also measured persister formation with asparagine as the secondary nitrogen source and did not observe persister formation after the nitrogen transition when compared to the NH_4^+-only control.

P. aeruginosa nitrogen source transitions

P. aeruginosa also uses NH_4^+ as its preferred nitrogen source, and we began by identifying an NH_4^+ concentration that would support colony biofilm growth for approximately 3-4 doublings (Figure 20). From this data, we determined that inoculation of each membrane with cells suspended in 0.5mM NH_4^+ media was sufficient for our purposes. To determine if nitrogen source transitions stimulate persister formation in *P. aeruginosa* biofilms, alanine, arginine asparagine, aspartate, glycine, glutamate, glutamine, serine, and threonine were provided at 30mM nitrogen as the sole nitrogen source in the agar, and as controls, 30mM NH_4^+ and

nitrogen source-free agar were used. As depicted in Figure 21, all samples grew comparably during the first 4 hours (common period of NH_4^+ consumption) and divergence became apparent by the 5 hour time point. The nitrogen-source free control demonstrates that secondary nitrogen sources were consumed by the colony biofilms. When persister levels in the biofilms were enumerated, we observed persister formation in biofilms supplied with serine, glycine, and threonine in the agar, whereas biofilms supplied with NH_4^+, glutamine, glutamate, aspartate, asparagine, arginine, and alanine in the agar failed to form persisters (Figure 21). We note that persisters in the NH_4^+-alanine samples began relatively high compared to the NH_4^+-only control, but followed a qualitatively similar persister level trend during biofilm growth. To determine whether persister formation was from the nitrogen source transition or from growth on the less favorable substrates, we measured persister levels in colony biofilms with serine and glycine as sole nitrogen sources. We did not assay threonine, because growth and persister data suggested that *P. aeruginosa* was unable to grow on threonine as the sole nitrogen source under our experimental conditions. Interestingly, the data suggest that persister formation within NH_4^+-glycine and NH_4^+-serine colony biofilms are transition-dependent, since persister levels in the NH_4^+-glycine and NH_4^+-serine exceed those within the sole glycine and sole serine controls for time periods after the nitrogen source transition (Figure 22). However, we require additional replicates to ensure the statistical significance of these findings. This is in contrast to persister formation from carbon source transitions in *P. aeruginosa* biofilms, that we found to be largely dependent on the growth substrate. This most likely reflects the greater catabolic flexibility of *P. aeruginosa* with regard to nitrogen sources, as evidenced by its improved growth on secondary nitrogen sources compared to its poor growth on secondary carbon sources. Interestingly, *E. coli* exhibits greater catabolic flexibility with regard to carbon sources when compared to nitrogen sources, and analogously, demonstrated transition-dependent persister formation with regard to carbon source transitions and substrate-dependent persister formation with regard to nitrogen source transitions.

S. aureus nitrogen source transitions

As mentioned above, *S. aureus* is an auxotroph for numerous amino acids[10]. However, the defined media compositions also include NH_4^+ at a concentration of 60.5mM. Thus far, we have not performed experiments assaying the nitrogen source transitions with *S. aureus*. This is largely due to delay in arrival of the research team and our transition to colony biofilm culturing, and to address this issue we are now enlisting the effort of 6 researchers to accomplish our SOW tasks by the end of the award period.

Statement of Work Task 3: Determine terminal electron acceptor shifts that stimulate persister formation in biofilms.

The purpose of this task was to perform a phenotypic screen in order to determine whether transitions away from O_2 stimulate persister formation in biofilms of *E. coli*, *P. aeruginosa*, and *S. aureus*.

To perform these experiments, we purchased a Coy O_2-control glovebox outfitted with an anaerobic upgrade in May, and the delivery and installation was completed in August. We performed experiments with *E. coli* at various oxygenation levels, 0, 5, 10, and 20% O_2, and then began to see inconsistencies and defects in growth. We have conducted a series of

experiments to determine the source of the growth issues and have consulted with the manufacturer, Coy Laboratories. Thus far, we have been able to conclusively demonstrate that the glovebox, heater, catalyst (for anaerobic operation), and shaking incubator are not the sources of the growth issues. In addition, we have identified the N_2 source we were using as a problem. The N_2 was supplied by building facilities (house), and using a N_2 cylinder from Airgas we observed significantly improved growth. We are currently determining if the N_2 source was the sole issue, since growth remains moderately inhibited in the glovebox compared to ambient controls. Variables that remain are the O_2 source, piping, and gas controller. The piping and controller are directly from Coy Laboratories, whereas the O_2 is from Airgas. It is possible that the house N_2 had residual effects on the piping and controller, and if this is the case we anticipate that this growth issue will be corrected as more N_2 from Airgas is used. We believe that O_2 is unlikely to be an issue, and if the piping and controller are found to be problematic we will obtain and use alternatives. Unfortunately, these technical difficulties have stalled our efforts to determine if terminal electron acceptor transitions generate persisters.

Statement of Work Task 4: Determine the role of known mediators of metabolic shifts on metabolically-controlled persister formation in biofilms
Statement of Work Task 5: Determine the role of known mediators of persistence on metabolically-controlled persister formation in biofilms
The purpose of these tasks were to examine the role of mediators of metabolism and persistence on metabolically-controlled persister formation. We have chosen to discuss these tasks together to improve the logical flow of this report. Inherently, only a subset of organisms and conditions tested in phenotypic screens of Tasks 1, 2, and 3 would be subjected to these analyses.

E. coli persister formation

For *E. coli*, we observed persister formation resulting from carbon source transitions in colony biofilms. To begin to reconstruct the signaling pathway, we inspected whether the metabolic mediator ppGpp, which was found in our planktonic study[5] to be critical for persister formation, was involved in persister formation in the biofilm state. As depicted in Figure 23, *ΔrelA* failed to generate persisters in response to diauxie in the biofilm state, suggesting that a ppGpp-dependent pathway similar to that found in planktonic cultures was operating. To identify whether mediators of chromosomal (-) supercoiling, which were also found to be critical in our planktonic study, were similarly involved in the biofilm pathway, we measured persisters in *ΔhupA*, *ΔhupB*, *ΔihfA*, *ΔihfB*, *Δhns*, *ΔseqA*, and *Δfis* strains. Interestingly, several nucloid-associated proteins (NAP) were found to be essential for persister formation from diauxic carbon source transitions in *E. coli* biofilms (Figure 24), though the specific NAP proteins involved differed between the planktonic and biofilm states. Recently, Lon has been implicated in ppGpp-dependent persister formation in *E. coli* biofilms[15], therefore, we tested *Δlon* for its ability to eliminate persister formation from carbon source transitions. As depicted in Figure 25, persister levels in *Δlon* colony biofilms were lower than that of wild-type, but persister formation from carbon source transitions remained in the absence of Lon.

P. aeruginosa persister formation

For *P. aeruginosa*, we have recently identified nitrogen-source transitions as a potentially transition-dependent phenomenon, and thus, have not yet started to mechanistically build back

the formation pathway. However, in preparation for these steps, we experimented with protocols to perform targeted-chromosomal mutations in *P. aeruginosa*[16-18]. Using a *P. aeruginosa* version of the λ-Red recombinase technique, we successfully generated chromosomal deletions of *pilTU*, *lasI*, *fhp*, and *nirS* in *P. aeruginosa*. *fhp* and *nirS* deletions were chosen due to their importance in nitrate- and nitrite-respiration, and therefore, may prove useful for our investigations into terminal electron acceptor transitions. *lasI* was chosen due to its role in quorum sensing, and *pilTU* was selected as the first deletion to perform in order to replicate the results of a study whose authors were advising us on genetic manipulations of *P. aeruginosa*.

S. aureus persister formation

For *S. aureus*, we have identified glucose-lactose transitions to be of potential interest, but we still need to determine whether persister formation is substrate- or transition-dependent. However, we have begun to prepare for the necessary genetic manipulations we will need once an interesting transition has been identified. Specifically, genetic manipulation of *Staphylococcus aureus* Newman will be performed using the methods described by Monk and colleagues[19]. Chemically competent *E. coli* SA08B cells have been acquired from Lucigen containing a methylation pattern consistent with the *S. aureus* Newman strain allowing plasmid preparation in the cloning strain and direct transformation into *S. aureus* with high efficiency, a task previously greatly inhibited by the staphylococcal restriction modification barrier which quickly degrades DNA generated in many common *E. coli* cloning strains. The plasmid to be utilized in this strain and a detailed cloning protocol was obtained from Dr. Ian Monk. The pIMAY-Z plasmid is a newly modified form of the pIMAY plasmid, with the modified form containing a constitutively expressed lacZ to ease identification of plasmid loss. Use of this method should decrease the time needed to generate mutants as it eliminates the additional step of plasmid replication in an intermediate staphylococcal cloning strain, such as *S. aureus* RN4220, for successful transformation into target strains and has been reported to have increased transformation efficiency.

Methods to measure persister metabolic activity

In addition to using genetics to identify persister formation pathways, we hypothesized that an ability to measure persister metabolic activity would be useful for our mechanistic investigations. In preparation for this, we developed the first high-throughput method to rapidly measure persister metabolic activity. The method is based on metabolite-enabled aminoglycoside potentiation in persisters, and a manuscript (Appendices) describing the method has been published in *Antimicrobial Agents and Chemotherapy*[20]. In addition, we identified a metabolic dye, Redox Sensor Green, that can be used to study persister metabolism, and these findings were published in a separate article in *Antimicrobial Agents and Chemotherapy*[8] (Appendices).

Statement of Work Task 6: Measure gene expression from biofilms where metabolic control of persister formation occurs.

The purpose of this task was to identify leads to fill in mechanistic gaps in persister formation pathways. Inherently, only a subset of organisms and conditions tested in phenotypic screens of Tasks 1, 2, and 3 would be subjected to these analyses. In addition, if Task 4 and 5 were

sufficient to identify the persister formation pathway, as was the case with *E. coli* carbon source transitions, this Task would not be required.

Thus far, we have not needed to measure gene expression to identify missing links within persister formation pathways, because Task 4 and 5 have been sufficient.

Future Work

E. coli carbon source transitions

We have submitted a manuscript describing the identification of a persister formation pathway in *E. coli* biofilms to *PLoS One* and it is currently under review. Any future work associated with this aspect of the project will be in response to requests from peer reviewers and/or editors.

P. aeruginosa carbon source transitions

The experiments we have performed on *P. aeruginosa* carbon source transitions suggest that persister formation originates from growth on less favorable substrates (Figures 9, 10, 11), conceivably due to growth-rate effects. This seemingly strong dependence prompted us to ask whether the *P. aeruginosa* persister formation we observed was truly dependent on growth-rate. Inhibition of growth-rate occurs due to a multitude of reasons, and we hypothesize that the method of growth inhibition is critically important to persistence. For instance, for OFL (which we use in our experiments) cell death occurs when it binds to a functioning DNA gyrase. Therefore, we hypothesize that cultures whose growth has been slowed by DNA gyrase availability will have higher persister levels than cultures whose growth has slowed to comparable levels but through different means, such as metabolism. Analogously, if metabolism were to slow growth, but DNA gyrase activity was maintained, we would anticipate little increase in OFL persister levels. Therefore, to test these hypotheses and determine the root cause by which carbon source transitions form persisters in *P. aeruginosa* biofilms, we will construct one strain where growth rate can be controlled by expression of the fumarate transporter (DctA) and another that can be controlled by expression of DNA gyrase. We will then vary growth-rate with inducer (IPTG) and measure persister levels. If persister levels correlate to a greater extent with gyrase availability rather than growth-rate, we will generate a transcriptional fusion of the gyrase promoter and GFP, and use fluorescence activated cell sorting to determine whether *P. aeruginosa* persisters formed from carbon source transitions are enriched in the sub-population with reduced gyrase expression.

S. aureus carbon source transitions

Though glucose-lactose colony biofilms generate more persisters than glucose-only controls, we need to determine whether the persister formation is substrate- or transition-dependent. To do this we will use a lactose-only control, and reduce the inoculum cell density and glucose concentration. *S. aureus* glucose-only biofilms exhibit persister formation at densities not much greater than OD_{600} = 0.7, and therefore, by reducing the cell density and glucose concentration of the initial inoculums we can ensure that we have a larger window with which to study transition-dependent persister formation in *S. aureus* biofilms.

E. coli nitrogen source transitions

Preliminary data suggests that persister formation due to nitrogen transitions in *E. coli* biofilms is substrate-dependent. To confirm this data, we will perform additional biological replicates of the sole-arginine control. Depending on the results from our investigation into why carbon source transitions stimulate substrate-dependent persister formation in *P. aeruginosa*,

we may adopt a similar strategy to more thoroughly understand why nitrogen source transitions stimulate substrate-dependent persister formation in *E. coli*.

P. aeruginosa nitrogen source transitions

Our data suggest that transitions from NH_4^+ to glycine or serine generate persisters in *P. aeruginosa* biofilms. To further validate that this persister formation is transition- and not substrate- dependent, we will reduce the initial cell density and NH_4^+ concentration so that we will have a larger window with which to study the phenomenon. If formation is further validated to be transition-dependent, we will begin mechanistic investigations in order to delineate the underlying pathway.

S. aureus nitrogen source transitions

We have yet to assay *S. aureus* for its ability to generate persisters following nitrogen source transitions. With the arrival of the complete research team by the end of the previous reporting period, we are now in a position to perform these experiments.

Terminal electron acceptor transitions

The rate-limiting step to studying terminal electron acceptor transitions is identification of the cause of growth inhibition in the O_2-control glovebox. We are working rapidly to resolve this issue, and have identified one cause of growth inhibition thus far (house N_2). Once the growth issues with the O_2-control glovebox have been resolved we will resume our investigations of persister formation from terminal electron acceptor transitions in *E. coli*, *P. aeruginosa*, and *S. aureus* biofilms.

Key Research Accomplishments

1) Identification that carbon source transitions stimulate persister formation in *E. coli* through a ppGpp-and NAP-dependent pathway in both planktonic and biofilm states

2) Development of a method to rapidly measure persister metabolic activity in a high-throughput manner

3) Identification of a metabolic dye (RSG) that can be used to interrogate the metabolic status of persisters

4) Preliminary data suggests that specific nitrogen-source transitions stimulate persister formation in *P. aeruginosa* biofilms

5) Preliminary data suggests that specific carbon-source transitions stimulate persister formation in *S. aureus* biofilms

6) Preliminary data suggests that persister formation from nitrogen source transitions in *E. coli* originate from growth on less favorable substrate

7) Identification that persister formation from carbon source transitions in *P. aeruginosa* biofilms originate from growth on less favorable substrate

8) Determination that dormancy in division or metabolic activity are not necessary or sufficient for persistence

9) Determination that previous techniques for persister “isolation” provide highly impure samples

Reportable Outcomes

Publications and Manuscripts

1) Amato SM, Orman MA, Brynildsen MP. Metabolic control of persister formation in *Escherichia coli*. *Molecular Cell*, 2013 May 23;50(4):475-87.

2) Orman MA, Brynildsen MP. Dormancy is not necessary or sufficient for bacterial persistence. *Antimicrobial Agents and Chemotherapy*, 2013 Jul;57(7):3230-9.

3) Orman MA, Brynildsen MP. Establishment of a method to rapidly assay bacterial persister metabolism. *Antimicrobial Agents and Chemotherapy*, 2013 2013 Sep;57(9):4398-409.

4) Amato SM, Brynildsen MP. Nutrient transitions are a source of persisters in *Escherichia coli* biofilms. (under review at *PLoS One*).

Presentations

1) Amato SM, Brynildsen MP. “Nutrient-shift dependent formation of ampicillin persisters”, presented at the American Society of Microbiology’s Interscience Conference on Antimicrobial Agents and Chemotherapy, September 2013, Denver, CO.

Degrees supported by this award

1) Stephanie M. Amato: current Ph.D. student, graduation anticipated in 2015

2) Theresa Henry: current Ph.D. student, graduate anticipated in 2017

Funding applied for based on work supported by this award

1) MPB was selected as Princeton’s nominee for Pew Biomedical Scholars Program 2014 competition. The research proposed was a study of persister metabolism.

Conclusion

Research supported by this award has led to significant advances in our understanding of the role of metabolism in bacterial persistence, producing 3 publications and one manuscript that is under review. Specifically, we have identified a persister formation pathway in *E. coli* that is initiated by a metabolic stress and transduced through a novel metabolic toxin-antitoxin module (ppGpp biochemical network). In addition, downstream of ppGpp, we identified participants in the cellular process targeted by the antibiotic, that when deleted eliminate persister formation. This pathway, which is present in both planktonic and biofilm states, provides targets for therapeutic development, such as ppGpp synthase, that may prove useful for elimination of bacterial persisters in *E. coli* biofilms. Further, our preliminary data with *P. aeruginosa* and *S. aureus* biofilms suggest that persister formation from nutrient transitions is a common phenomenon present in diverse microbial species. As we continue to make progress on the Statement of Work Tasks, we will identify additional mediators of persister formation from nutrient transitions in biofilms that may prove useful as targets for the development of antipersister therapies to treat biofilm infections.

References

1 Lewis, K. (2008), Multidrug tolerance of biofilms and persister cells, *Curr Top Microbiol Immunol*, **322**, 107-131.
2 Ahimou, F., Semmens, M. J., Haugstad, G. *et al.* (2007), Effect of protein, polysaccharide, and oxygen concentration profiles on biofilm cohesiveness, *Appl Environ Microbiol*, **73**, 2905-2910.
3 Flemming, H. C. & Wingender, J. (2010), The biofilm matrix, *Nat Rev Microbiol*, **8**, 623-633.
4 Stewart, P. S. & Franklin, M. J. (2008), Physiological heterogeneity in biofilms, *Nat Rev Microbiol*, **6**, 199-210.
5 Amato, S. M., Orman, M. A. & Brynildsen, M. P. (2013), Metabolic Control of Persister Formation in Escherichia coli, *Mol Cell*, **50**, 475-487.
6 Williamson, K. S., Richards, L. A., Perez-Osorio, A. C. *et al.* (2012), Heterogeneity in Pseudomonas aeruginosa biofilms includes expression of ribosome hibernation factors in the antibiotic-tolerant subpopulation and hypoxia-induced stress response in the metabolically active population, *J Bacteriol*, **194**, 2062-2073.
7 Walters, M. C., 3rd, Roe, F., Bugnicourt, A. *et al.* (2003), Contributions of antibiotic penetration, oxygen limitation, and low metabolic activity to tolerance of Pseudomonas aeruginosa biofilms to ciprofloxacin and tobramycin, *Antimicrob Agents Chemother*, **47**, 317-323.
8 Orman, M. A. & Brynildsen, M. P. (2013), Dormancy is not necessary or sufficient for bacterial persistence, *Antimicrob Agents Chemother*, **57**, 3230-3239.
9 Allison, K. R., Brynildsen, M. P. & Collins, J. J. (2011), Metabolite-enabled eradication of bacterial persisters by aminoglycosides, *Nature*, **473**, 216-220.
10 Lee, D. S., Burd, H., Liu, J. *et al.* (2009), Comparative genome-scale metabolic reconstruction and flux balance analysis of multiple Staphylococcus aureus genomes identify novel antimicrobial drug targets, *J Bacteriol*, **191**, 4015-4024.
11 Miller, R. D. & Fung, D. Y. (1973), Amino acid requirements for the production of enterotoxin B by Staphylococcus aureus S-6 in a chemically defined medium, *Appl Microbiol*, **25**, 800-806.
12 Rudin, L., Sjostrom, J. E., Lindberg, M. *et al.* (1974), Factors affecting competence for transformation in Staphylococcus aureus, *J Bacteriol*, **118**, 155-164.
13 Keren, I., Kaldalu, N., Spoering, A. *et al.* (2004), Persister cells and tolerance to antimicrobials, *FEMS Microbiol Lett*, **230**, 13-18.
14 Johnson, P. J. & Levin, B. R. (2013), Pharmacodynamics, population dynamics, and the evolution of persistence in Staphylococcus aureus, *PLoS Genet*, **9**, e1003123.
15 Maisonneuve, E., Castro-Camargo, M. & Gerdes, K. (2013), (p)ppGpp Controls Bacterial Persistence by Stochastic Induction of Toxin-Antitoxin Activity, *Cell*, **154**, 1140-1150.
16 Choi, K. H., Kumar, A. & Schweizer, H. P. (2006), A 10-min method for preparation of highly electrocompetent Pseudomonas aeruginosa cells: application for DNA fragment transfer between chromosomes and plasmid transformation, *J Microbiol Methods*, **64**, 391-397.
17 Lesic, B. & Rahme, L. G. (2008), Use of the lambda Red recombinase system to rapidly generate mutants in Pseudomonas aeruginosa, *BMC Mol Biol*, **9**, 20.
18 Hoang, T. T., Karkhoff-Schweizer, R. R., Kutchma, A. J. *et al.* (1998), A broad-host-range Flp-FRT recombination system for site-specific excision of chromosomally-located DNA sequences: application for isolation of unmarked Pseudomonas aeruginosa mutants, *Gene*, **212**, 77-86.

19 Monk, I. R., Shah, I. M., Xu, M. *et al.* (2012), Transforming the untransformable: application of direct transformation to manipulate genetically Staphylococcus aureus and Staphylococcus epidermidis, *MBio*, **3**.
20 Orman, M. A. & Brynildsen, M. P. (2013), Establishment of a method to rapidly assay bacterial persister metabolism, *Antimicrob Agents Chemother*, **57**, 4398-4409.

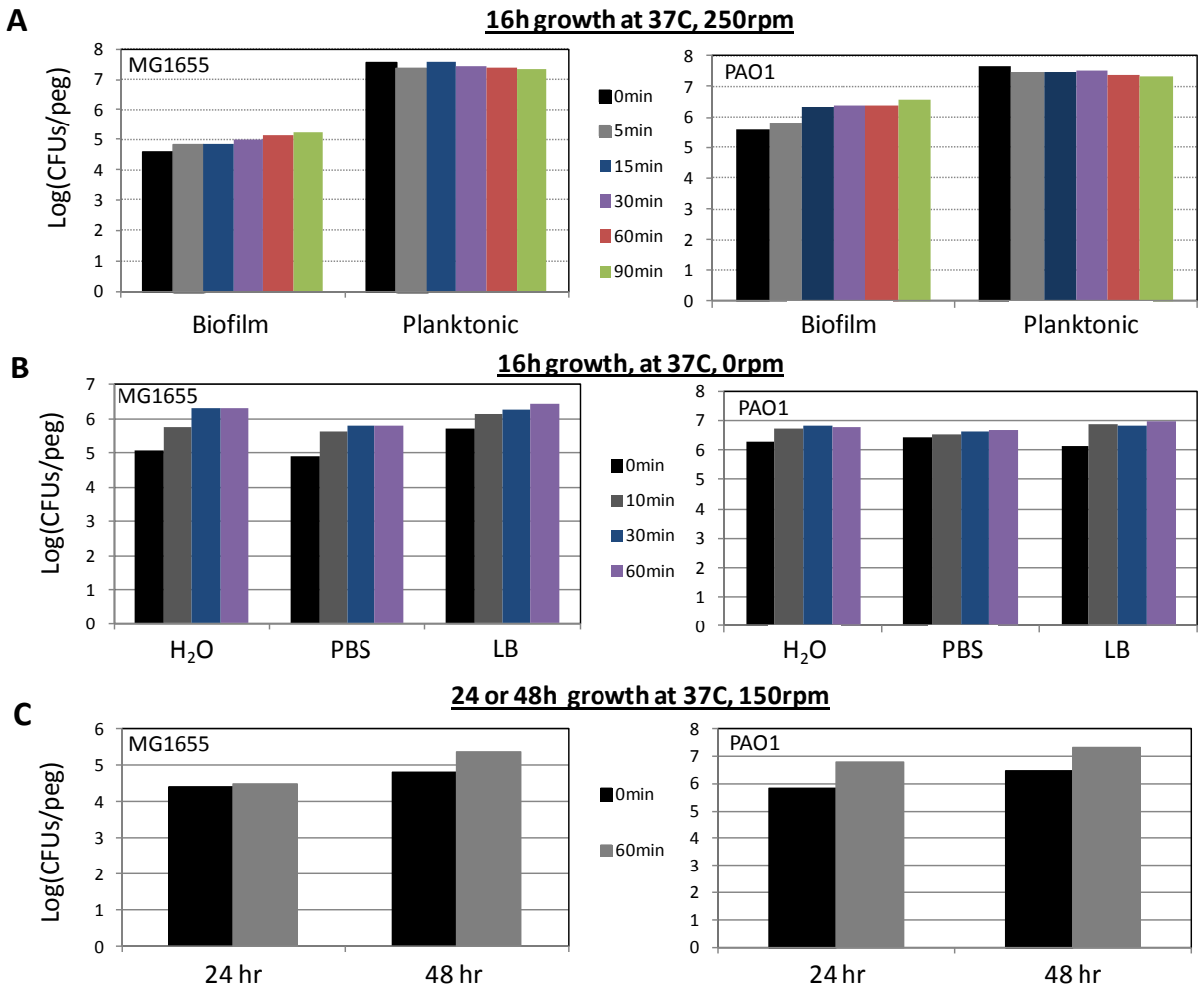

Figure 1. Effect of sonication time on biofilm and planktonic colony forming units (CFUs). **A)** *E. coli* MG1655 or *P. aeruginosa* PAO1 were incubated in 2 ml LB medium at 37°C with shaking (250 rpm) for 16 hr. The culture was diluted 100-fold in fresh LB, and 200µl of this culture was added in each well of the MBEC plate. After 16 hr of growth, shaking at 250 rpm and 37°C, the peg-lid was washed twice by immersing the pegs in PBS in a rinse plate. The pegs were then transferred to a recovery plate (having 200µl of PBS in each well) and sonicated at the times indicated. As a control, the culture was diluted 100-fold in PBS, and 200µl of this solution with planktonic cells was transferred into the wells of the recovery plate to analyze the effect of sonication time on cell viability. Sonicated samples were serially diluted and plated on LB-agar to measure CFUs/peg. **B)** Effect of rinse-medium on biofilm CFUs. **C)** Effect of culture-time on biofilm CFUs.

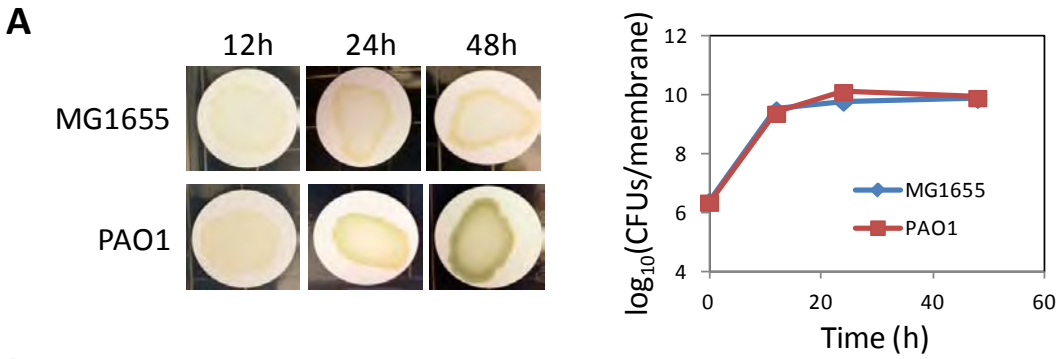
A
12h
24h
48h
MG1655
PAO1
log10(CFUs/membrane)
Time (h)
MG1655
PAO1

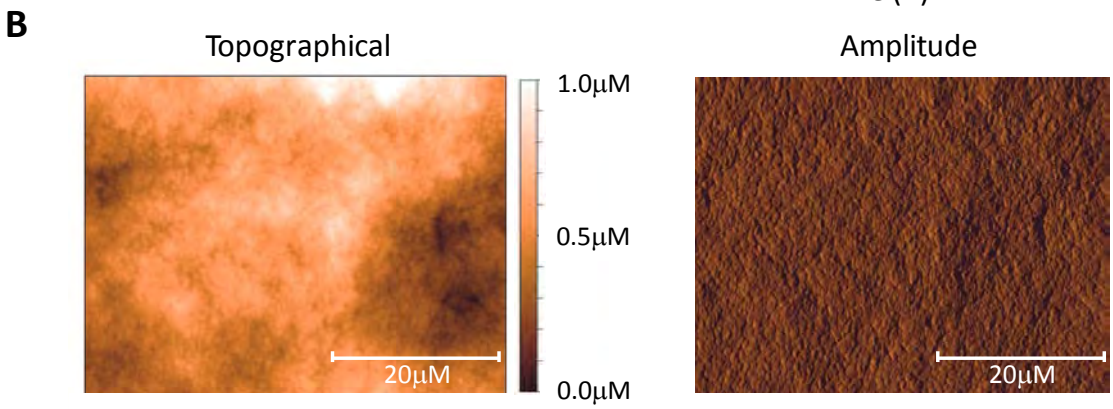
B
Topographical
Amplitude
1.0μM
0.5μM
0.0μM
20μM
20μM

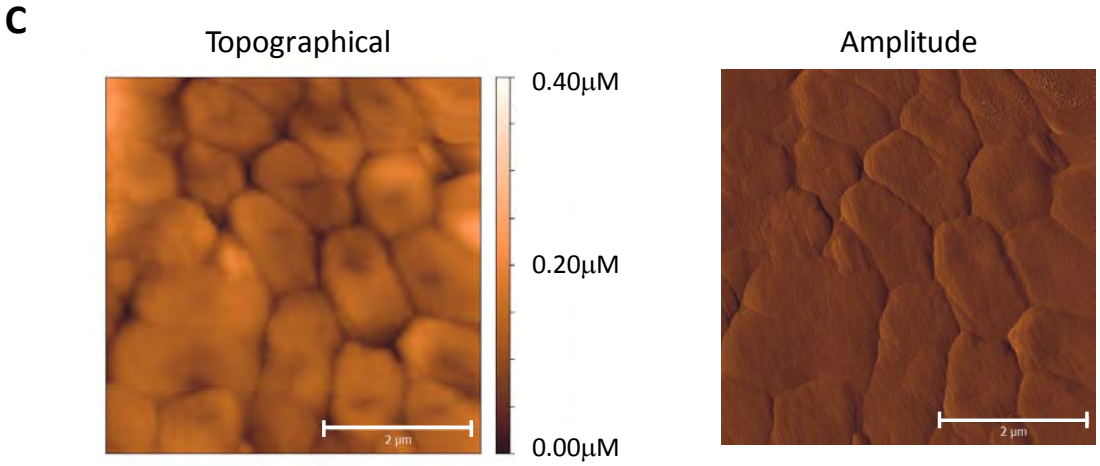
C
Topographical
Amplitude
0.40μM
0.20μM
0.00μM
2 μm
2 μm

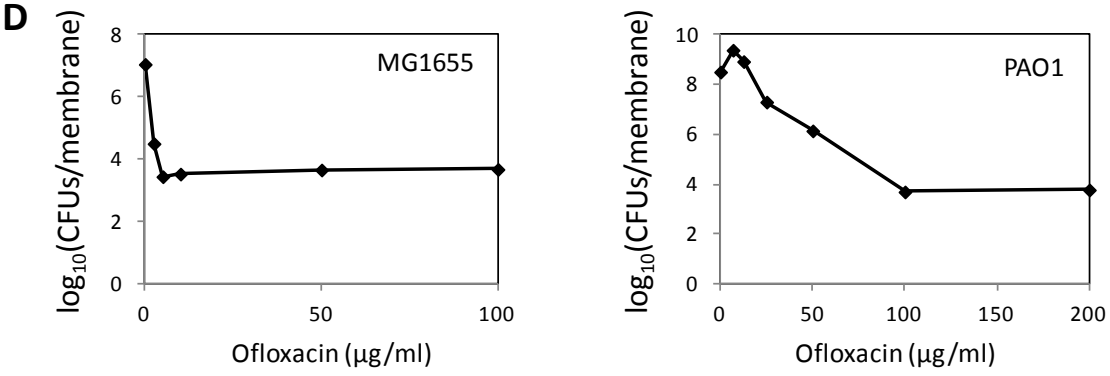
D
log10(CFUs/membrane)
MG1655
Ofloxacin (μg/ml)
log10(CFUs/membrane)
PAO1
Ofloxacin (μg/ml)

Figure 2. Culturing of colony biofilms on PES membranes. **A)** Sterile 0.2µm pore-25mm diameter PES membranes were placed aseptically onto LB-agar plates, and inoculated with 100µl of *E. coli* MG1655 or *P. aeruginosa* PAO1 overnight cultures diluted 100-fold. Samples were incubated at 37°C and transferred to 10 ml tubes pre-filled with 2 ml PBS at indicated time points. Tubes were vortexed vigorously for 1 min to separate the cells from the membrane. Cell suspensions were serially diluted and plated onto LB-agar to measure CFUs per membrane. **B)** and **C)** AFM topography and amplitude images of 24 hour *E. coli* MG1655 biofilms grown on sterile 0.2 µm pore-25mm diameter PES membranes placed aseptically on LB-agar plates. The membranes were imaged on a Veeco Dimension NanoMan AFM in tapping mode with Bruker Premium High-Resolution Tapping Mode silicon probes (RTESP). All images were obtained using a 0.5 Hz scan rate. (C) is a zoomed-in portion of (B). **D)** Persister enumeration from colony biofilms. Left: PES membranes placed on M9 minimal media plates with 10 mM glucose were inoculated with 100µl of overnight *E. coli* MG1655 culture that had been diluted to an OD_{600} = 0.1 in M9 minimal media. After 6 hours of incubation at 37°C, 200µl of ofloxacin solution at the indicated concentrations were placed on the membranes. Biofilms were treated with ofloxacin for 5 hours, separated from membranes by vortexing in PBS, washed with PBS, and plated on LB agar to measure CFUs. Right: Same as left except media was BSM with 15 mM fumarate for *P. aeruginosa* PAO1.

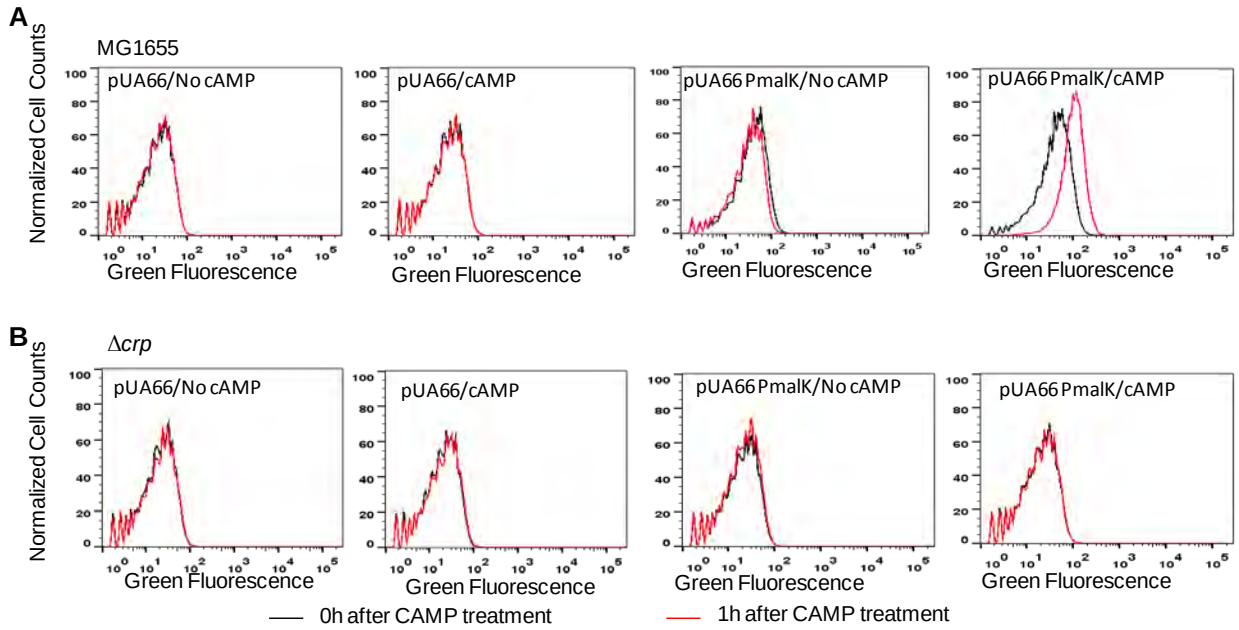

Figure 3. cAMP transcriptional reporter. **A)** Wild-type with pUA66 control or pUA66 PmalK-*gfp* were grown in 4.5mM glucose to 0.02 OD_{600} and then 8mM cAMP was added. GFP was measured prior to and 1h after cAMP addition. **B)** Same as (A) except *Δcrp* was used instead of wild-type. For flow cytometry details please see *Molecular Cell* publication within the Appendices.

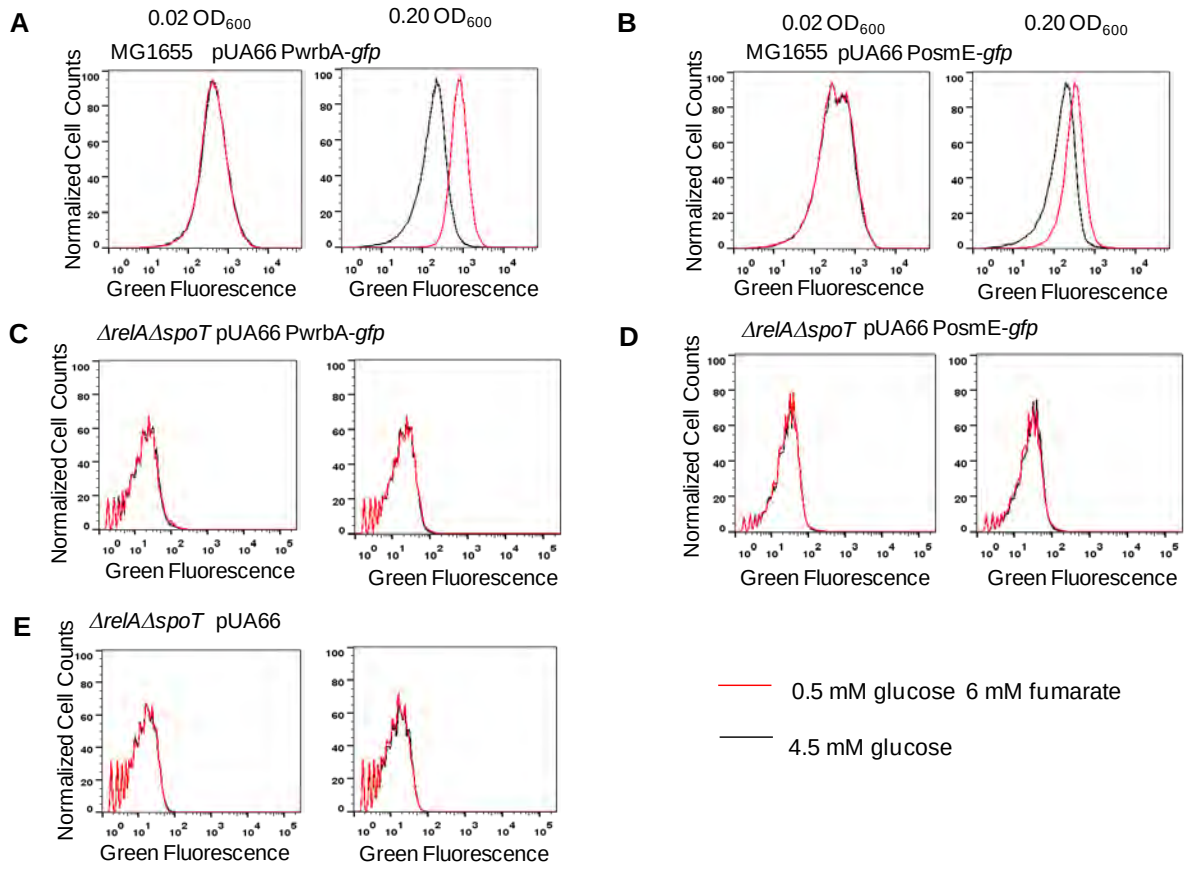

Figure 4. ppGpp transcriptional reporters. **A)** Wild-type transformed with pUA66 expressing GFP under a *wrbA* promoter, **B)** Wild-type transformed with pUA66 expressing GFP under an *osmE* promoter were grown in 4.5mM glucose or 0.5mM glucose 6mM fumarate supplemented with 400µg/mL serine and 40µg/mL aspartic acid, glutamic acid, histidine, isoleucine, leucine, phenylalanine, threonine, and valine (to allow growth of *ΔrelAΔspoT* strain). GFP fluorescence measurements were taken prior to glucose exhaustion (0.02 OD_{600}) and post glucose exhaustion (0.20 OD_{600}) using flow cytometry. **C)** *ΔrelAΔspoT* transformed with pUA66 expressing GFP under a *wrbA* promoter, and **D)** *ΔrelAΔspoT* transformed with pUA66 expressing GFP under an *osmE* promoter were grown in 4.5mM glucose or 0.5mM glucose 6mM fumarate supplemented with amino acids as described above. GFP fluorescence measurements were taken prior to glucose exhaustion (0.02 OD_{600}) and post glucose exhaustion (0.20 OD_{600}) using flow cytometry. **E)** *ΔrelAΔspoT* transformed with pUA66 vector was grown and GFP fluorescence measured under the same conditions described above as a control. For flow cytometry details please see *Molecular Cell* publication within the Appendices.

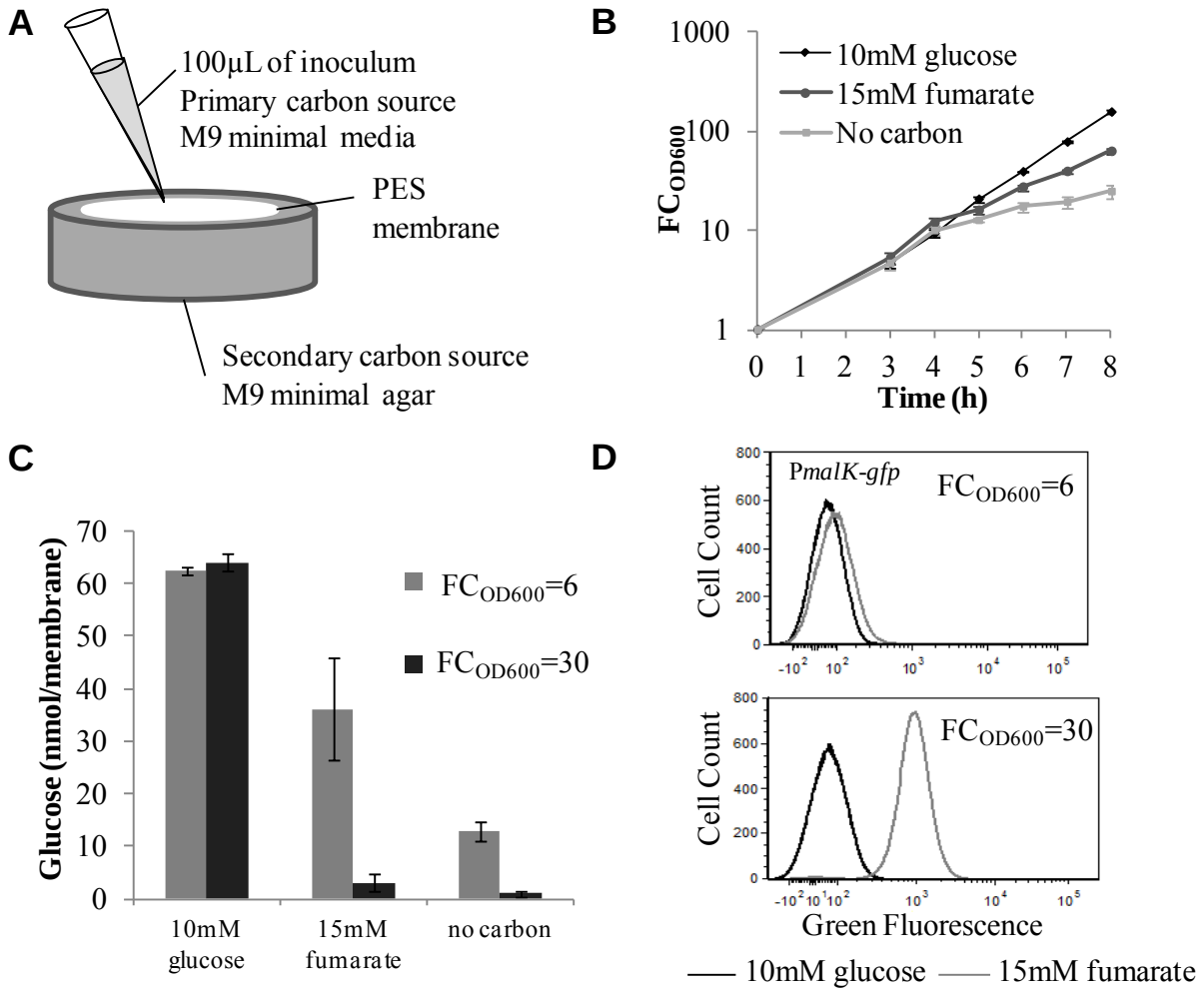

Figure 5. Method to control carbon source transitions in biofilms. **A)** Schematic of our experimental setup where cells and the primary carbon source are applied to a PES membrane set atop agar containing the secondary carbon source, glucose, or no carbon. **B)** PES membranes atop agar containing 10mM glucose, 15mM fumarate, and no carbon were inoculated with wild-type cells at 0.01 OD_{600} in 2.5mM glucose and incubated at 37°C. The OD_{600} was measured at specified time intervals and fold-change in OD_{600} (FC_{OD600}) was determined. One exponential growth phase was observed for glucose samples. Two regimes of exponential growth were observed for glucose-fumarate samples and no carbon sample exhibited limited growth after glucose exhaustion. **C)** Glucose concentration measurements were taken at each persister sampling (FC_{OD600}=6 and FC_{OD600}=30) for glucose and glucose-fumarate samples and at FC_{OD600}=6 and 2 hours post glucose exhaustion for the no carbon sample. **D)** $P_{malK\text{-}gfp}$ GFP distribution at FC_{OD600}=6 and FC_{OD600}=30 in glucose-fumarate and glucose samples. Data are averages of ≥ 3 independent experiments and error bars indicate standard deviation.

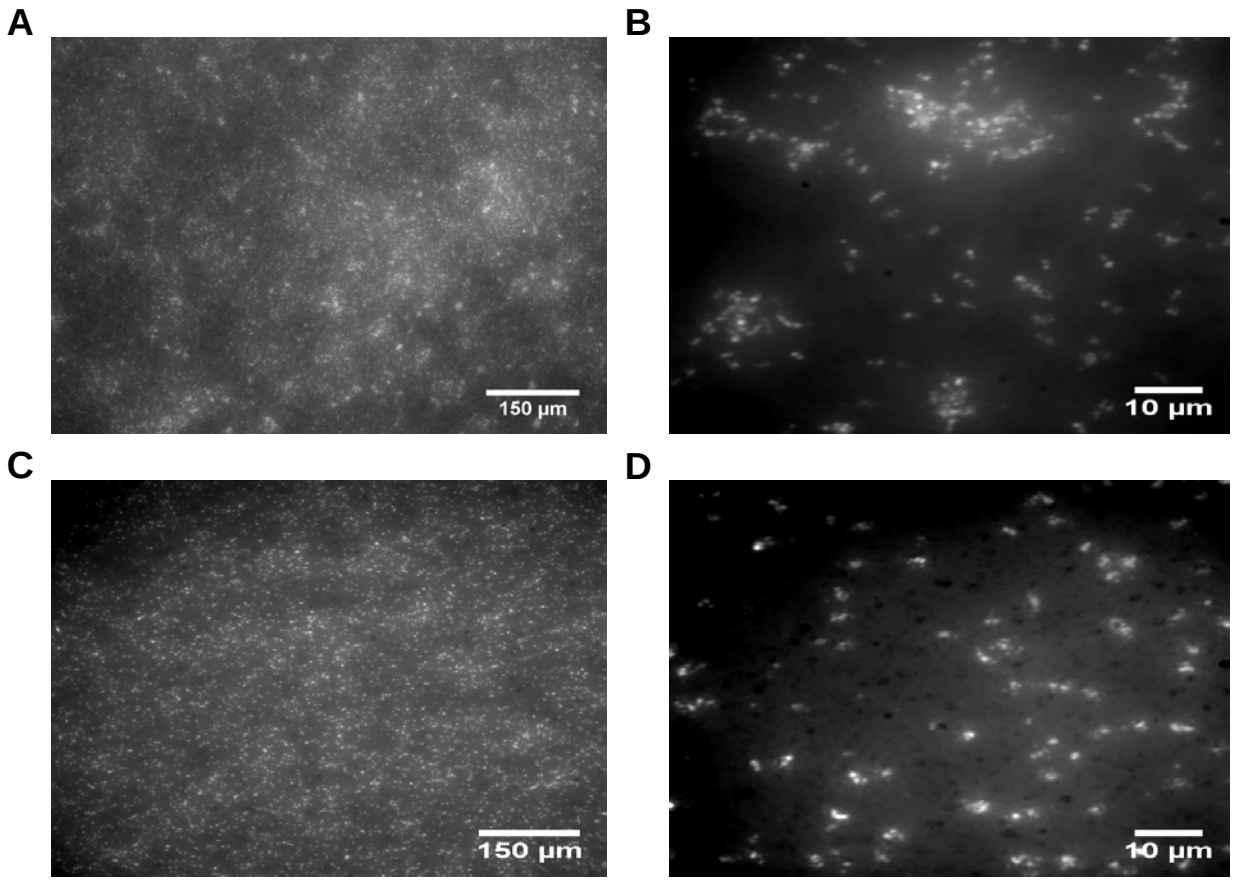

Figure 6. Imaging colony biofilms. MG1655 *lacI*^{q} P_{T5} *mCherry* cells were grown 16 h in 10mM M9 glucose with 2mM IPTG. Cells were inoculated into 2.5mM M9 glucose with 2mM IPTG at 0.01 OD_{600}. Sterilized PES membranes were aseptically placed on 10mM M9 glucose with 2mM IPTG agar. Membranes were inoculated with 100µL of cells and films were incubated at 37°C for 4hr (~3.5 doublings/ 7x10^{6} CFU/membrane). Membranes were aseptically removed from the agar and analyzed using confocal microscopy at, **A)** 10X objective and **B)** 100x objective. MG1655 *lacI*^{q} PT5 *mCherry* cells were grown 16 h in 10mM M9 glucose with 2mM IPTG. Cells were inoculated into 25mL of 10mM M9 glucose with 2mM IPTG at 0.01 OD_{600}. After ~3.5 doublings, ~7x10^{6} CFU were inoculated onto a sterilized PES membrane and analyzed using confocal microscopy at, **C)** 10x objective and **D)** 100x objective.

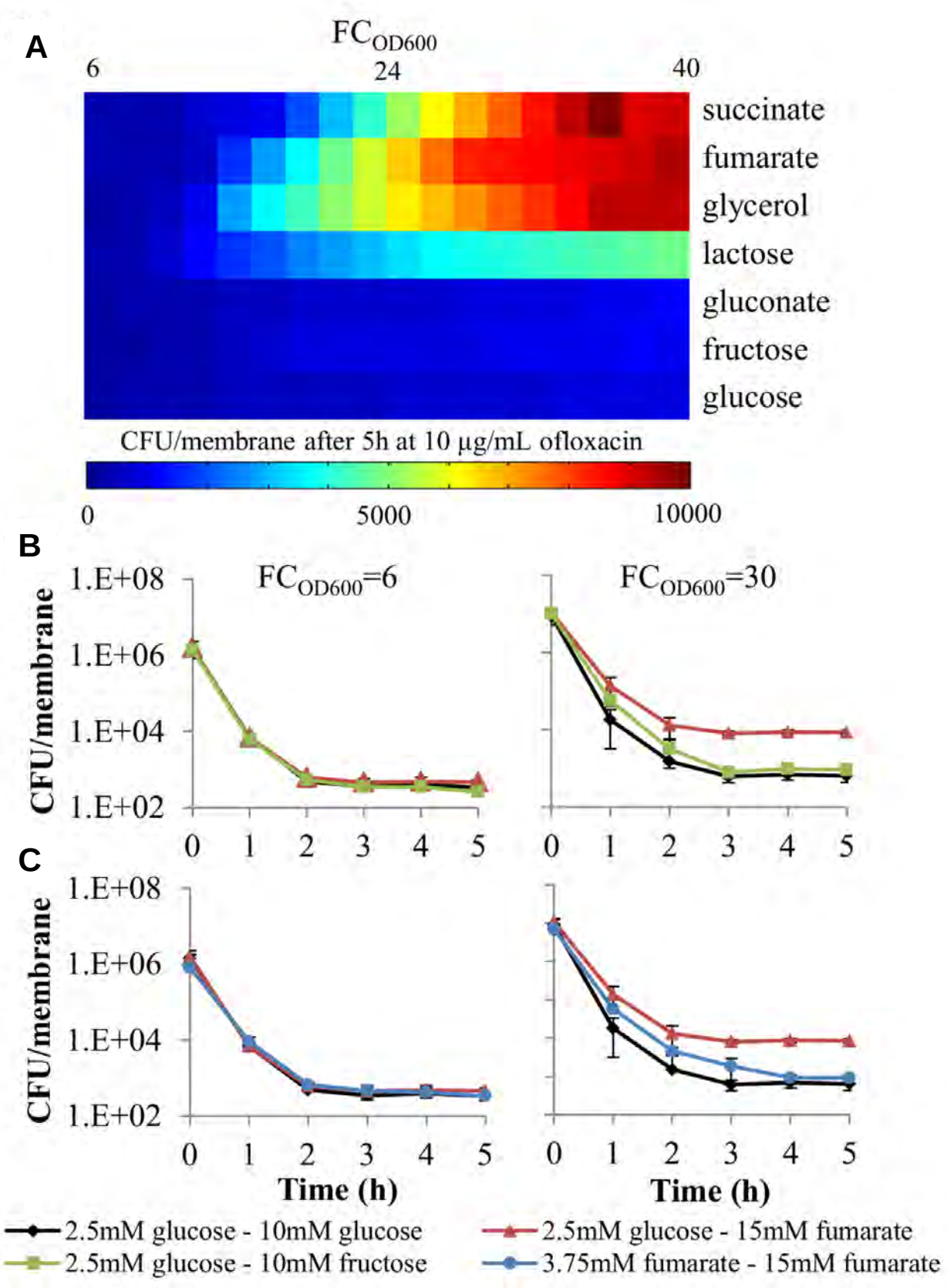
A
FC OD600
6
24
40
succinate
fumarate
glycerol
lactose
gluconate
fructose
glucose
CFU/membrane after 5h at 10 µg/mL ofloxacin
0
5000
10000
B
C
CFU/membrane
1.E+08
1.E+06
1.E+04
1.E+02
FC OD600=6
FC OD600=30
0 1 2 3 4 5
Time (h)
2.5mM glucose - 10mM glucose
2.5mM glucose - 10mM fructose
2.5mM glucose - 15mM fumarate
3.75mM fumarate - 15mM fumarate

Figure 7. Diauxic shifts stimulate persister formation in *E. coli* biofilms. **A)** *E. coli* were grown on glucose as the primary carbon source and a panel of secondary carbon sources. At hourly time points, biofilms were challenged with 200µl of 10µg/mL ofloxacin for 5 hours, aseptically removed from the agar, vortexed in 2mL PBS for 1 minute, washed, and plated to measure CFUs. To construct the color plot as a function of FC_{OD600}, as needed values plotted were interpolated from two adjacent measurements. **B)** Diauxic growth (glucose-fumarate) results in significant persister formation ($p<0.05$), whereas non-diauxic growth does not ($p>0.05$) (glucose and glucose-fructose). **C)** Growth on fumarate is not responsible for persister formation in glucose-fumarate samples, as evidenced by the sole fumarate control, which contained fumarate as the only carbon source both in the inoculum and agar. Data are averages of ≥ 3 independent experiments, error bars indicate standard deviation, and significance was assessed using the null hypothesis that the mean CFU levels in two sample sets were equal.

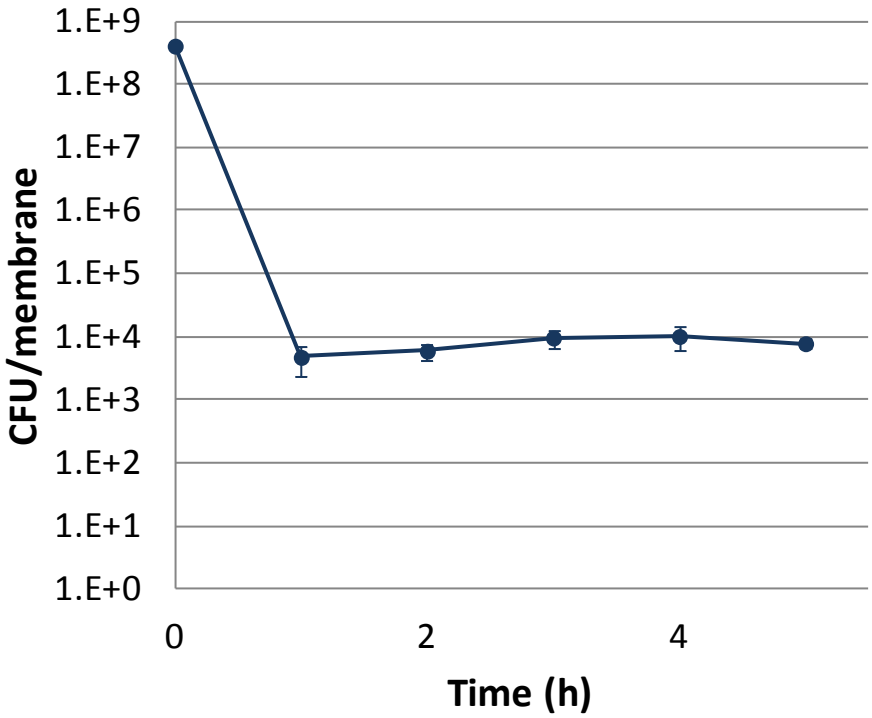

Figure 8. *P. aeruginosa* colony biofilms exhibit biphasic killing when exposed to 200μL of 150μg/mL OFL. *P. aeruginosa* PAO1 from a frozen stock were inoculated into 2 mL of LB media and grown for 16 h at 37 °C with shaking. Cells were pelleted, washed and resuspended in BSM minimal media (supplemented with 15 mM fumarate), and diluted to an OD_{600} of 0.1 in BSM minimal medium (supplemented with 15 mM fumarate). A 100 μL aliquot was transferred to sterile membranes, which had been aseptically placed on BSM minimal agar plates containing 15 mM fumarate. Samples were grown at 37 °C for 5 h. Membranes were treated with 200 μL of 150 μg/mL ofloxacin at 37 °C. Hourly, cells were removed from one of the membranes by vortexing for 1 min in 2 mL of PBS, washed twice with PBS to remove OFL, serially diluted, and plated on LB-agar to enumerate persisters. Error bars represent SEM of three replicates.

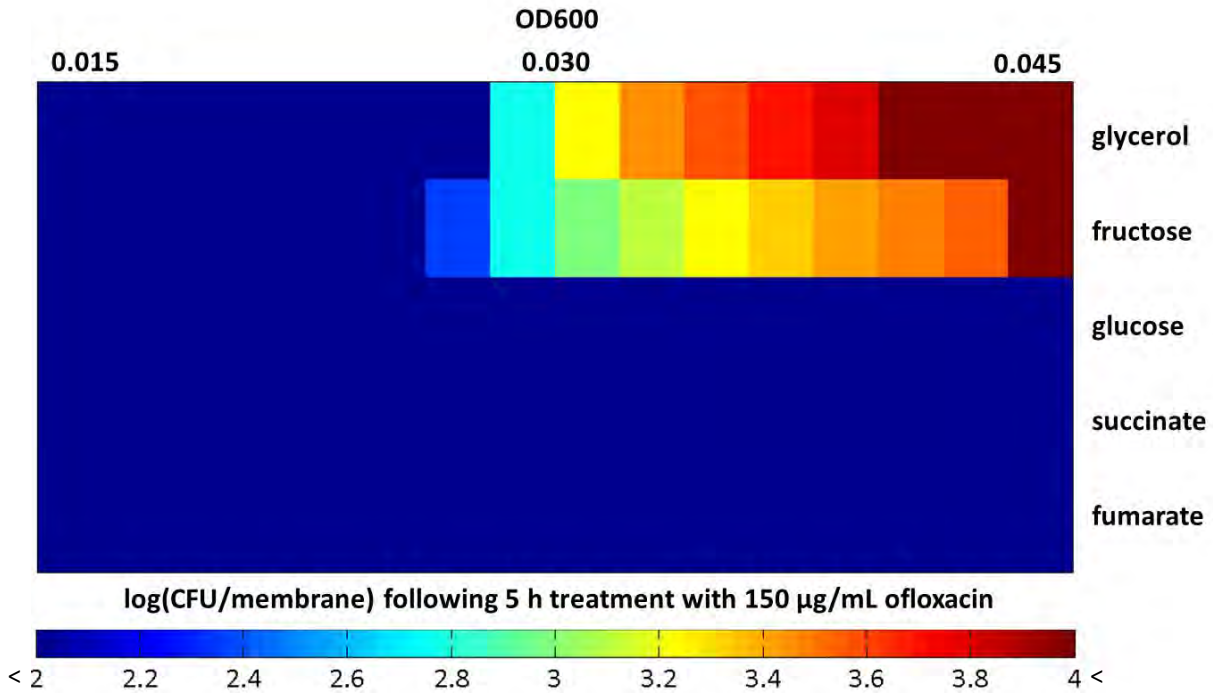

Figure 9. Carbon source transitions stimulate persister formation in *P. aeruginosa* biofilms. Overnight cultures of *P. aeruginosa* PAO1 were inoculated from frozen stock into 2 mL of LB supplemented with 15 mM fumarate and grown for 16 h at 37 °C with shaking. Overnight cultures were resuspended in BSM minimal medium with 15 mM fumarate and then diluted to an OD_{600} of 0.1 in BSM minimal medium with 15 mM fumarate. Then, 100 µL was transferred to sterile membranes, which had been aseptically placed on BSM minimal agar plates (containing 60 mM C of secondary carbon source as specified). Samples were grown at 37°C, and hourly, the untreated OD_{600} was measured, and persisters were enumerated by treating the membranes with 200 µL of 150 µg/mL ofloxacin for 5 h, after which CFUs were measured. Error bars indicated SEM of two or more replicates. CFU/membrane values for color plot were interpolated from two adjacent measurements in order to obtain values at each designated OD_{600}.

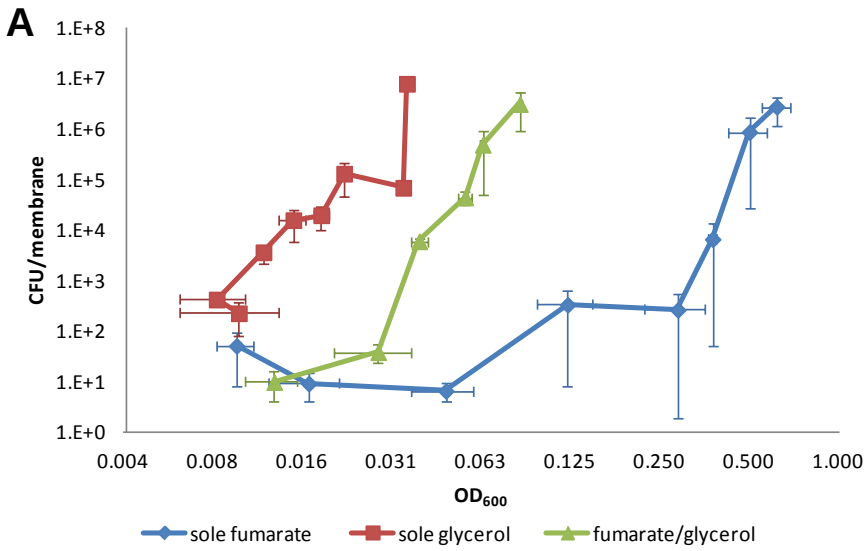
A
1.E+8
1.E+7
1.E+6
1.E+5
1.E+4
1.E+3
1.E+2
1.E+1
1.E+0
CFU/membrane
0.004
0.008
0.016
0.031
0.063
0.125
0.250
0.500
1.000
OD600
sole fumarate
sole glycerol
fumarate/glycerol

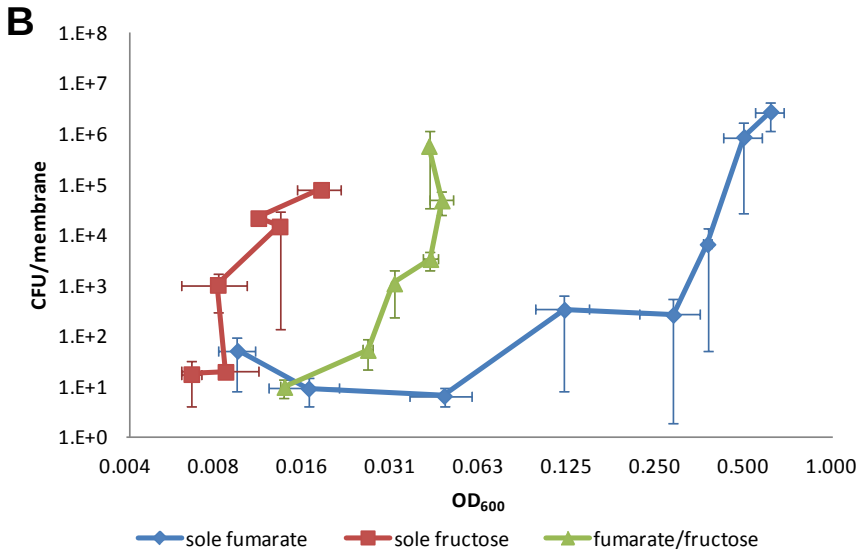
B
1.E+8
1.E+7
1.E+6
1.E+5
1.E+4
1.E+3
1.E+2
1.E+1
1.E+0
CFU/membrane
0.004
0.008
0.016
0.031
0.063
0.125
0.250
0.500
1.000
OD600
sole fumarate
sole fructose
fumarate/fructose

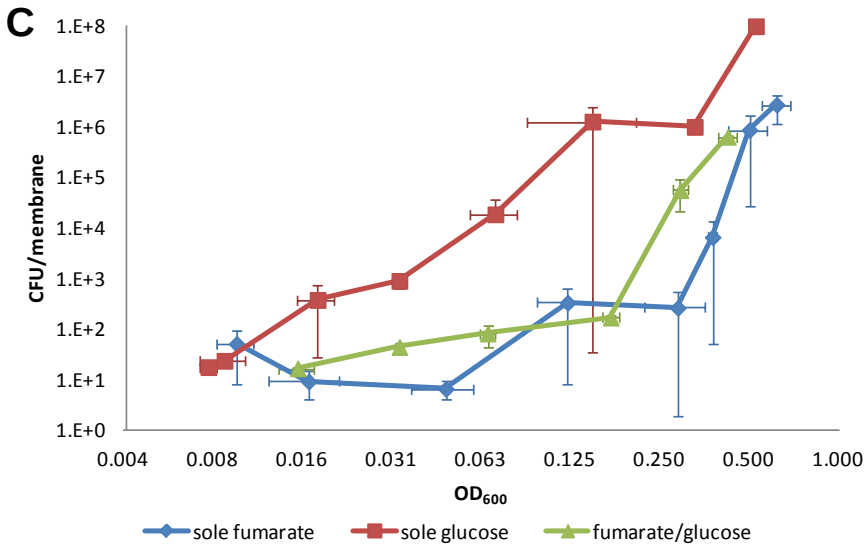
C
1.E+8
1.E+7
1.E+6
1.E+5
1.E+4
1.E+3
1.E+2
1.E+1
1.E+0
CFU/membrane
0.004
0.008
0.016
0.031
0.063
0.125
0.250
0.500
1.000
OD600
sole fumarate
sole glucose
fumarate/glucose

Figure 10. *P. aeruginosa* persister formation from carbon source transitions is substrate-dependent. *P. aeruginosa* was grown in LB with 15 mM fumarate or 60mM C of secondary carbon source for 16 h. Overnight cultures were resuspended in BSM media with 15 mM fumarate or 60mM C of secondary carbon source in sole glycerol, fructose, glucose, and succinate samples to achieve 0.1 OD_{600}. 100 µL of the cell suspensions were transferred to membranes, which had been placed on BSM minimal agar plates (containing 60 mM C of secondary carbon source). Biofilms were grown at 37 °C, and and persisters were measured hourly. Persisters were enumerated by treating membranes with 200 µL of 150 µg/mL ofloxacin for 5 h, followed by washing and plating for CFU measurements. **A)** Compares sole-glycerol, sole-fumarate, and fumarate-glycerol samples, **B)** Compares sole-fructose, sole-fumarate, and fumarate-fructose samples, **C)** Compares sole-glucose, sole-fumarate, and fumarate-glucose samples. Sole-succinate, sole-fumarate, and fumarate-succinate samples were found to be indistinguishable. Error bars indicate SEM of 2 or more replicates.

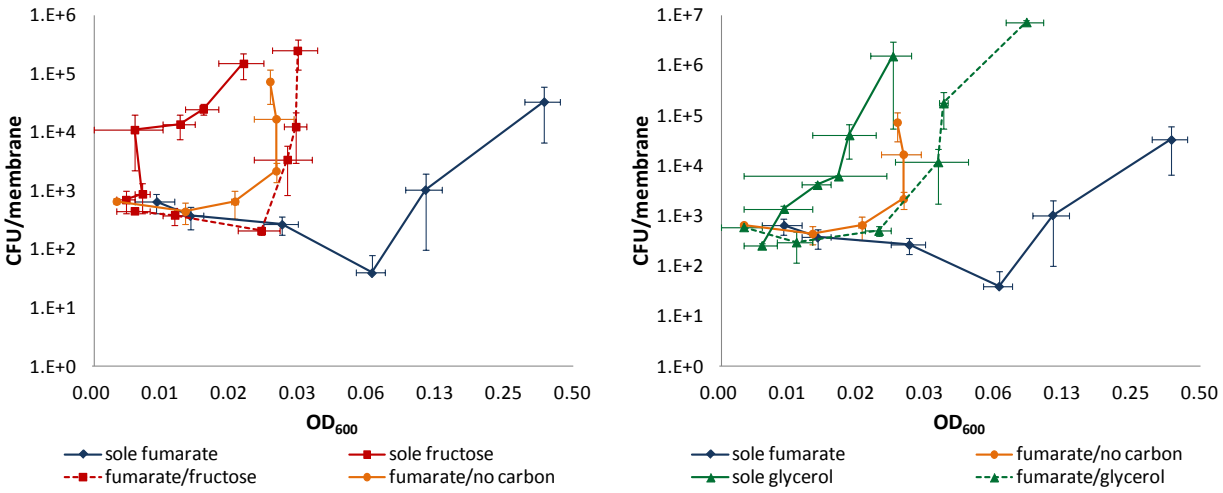

Figure 11. *P. aeruginosa* persister formation from carbon source transitions with minimal media overnights remains substrate-dependent. Frozen stock of PAO1 was used to inoculate 2 mL of LB media. Following 4 h of growth at 37°C with shaking, 2 mL of BSM minimal media supplemented with 60 mM carbon source was inoculated 1:100 and grown for 16 h at 37°C with shaking. Overnight cultures were then diluted to an OD_{600} of 0.1 in BSM minimal medium with 60 mM carbon source, and 100 µL was transferred to sterile membranes, which had been aseptically placed on BSM minimal agar plates containing 60 mM of carbon source. Samples were grown at 37°C, and at every hour, the untreated OD_{600} was measured, and persisters were enumerated by treating the membranes with 200µL of 150 µg/mL OFL for 5 h. For sole sources, only that substrate was used as the carbon source throughout all steps of the assay. For fumarate-secondary or –no carbon source, fumarate was used in the overnight and inoculum of the membrane, whereas the agar contained the secondary carbon source or was devoid of carbon source. Error bars indicate SEM of two or more replicates.

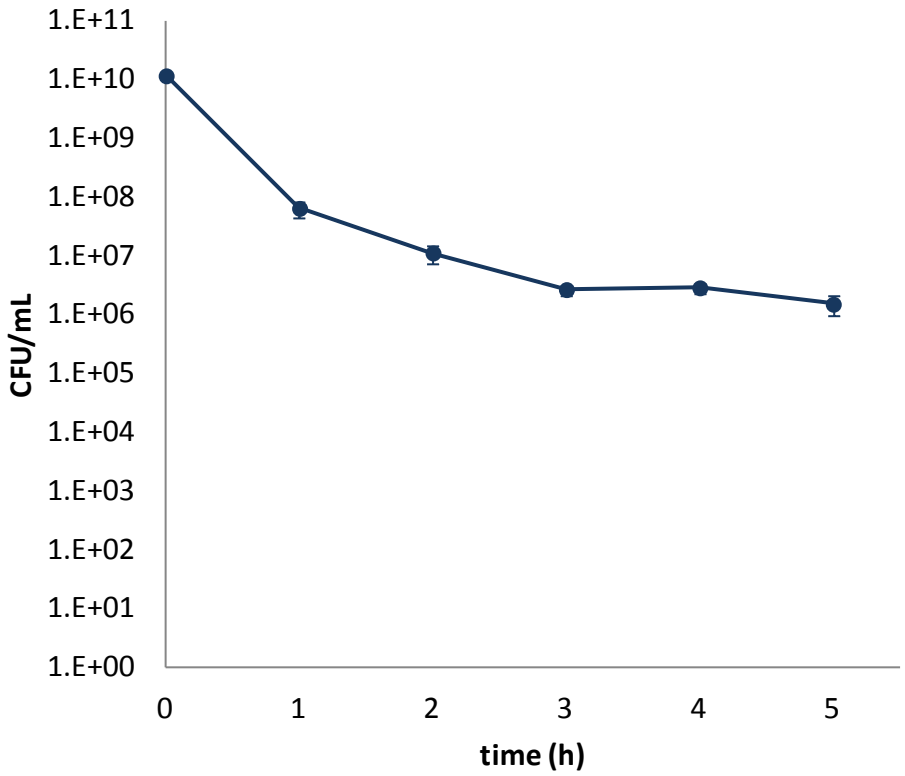

Figure 12. Non-growing *P. aeruginosa* populations exhibit biphasic kill kinetics. A 25 mL LB culture was inoculated from freezer stock and grown for 16 h in a 250 mL baffled flask at 37 °C with shaking. Five 1 mL aliquots were removed, and persisters were enumerated by treating with 50 µg/mL ofloxacin for 1–5 h at 37 °C with shaking, after which CFUs were measured by plating on LB-agar. Error bars indicated SEM of 10 replicates.

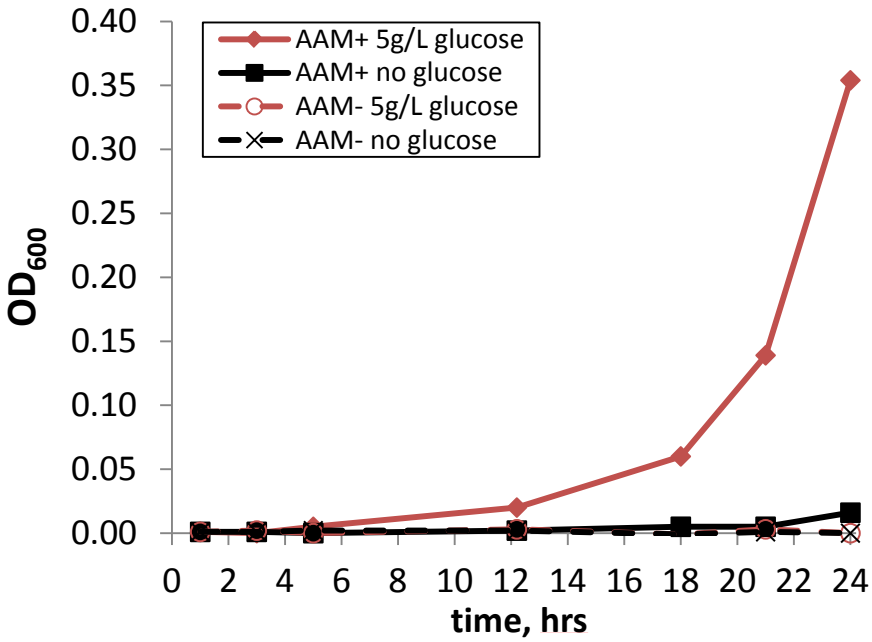

Figure 13. Defined *S. aureus* media allows glucose-dependent colony biofilm growth. *S. aureus* was grown in 2 mL of LB at 37°C for 4 h and transferred to 2 mL of AAM+ media with 5 g/L glucose for an additional 16 h. Sterile membranes were placed on agar as indicated in the legend and inoculated with 100 µL of overnight culture diluted to 0.1 OD_{600}. Biofilms were incubated at 37°C. At designated times, membranes were vortexed in PBS and OD_{600} was measured.

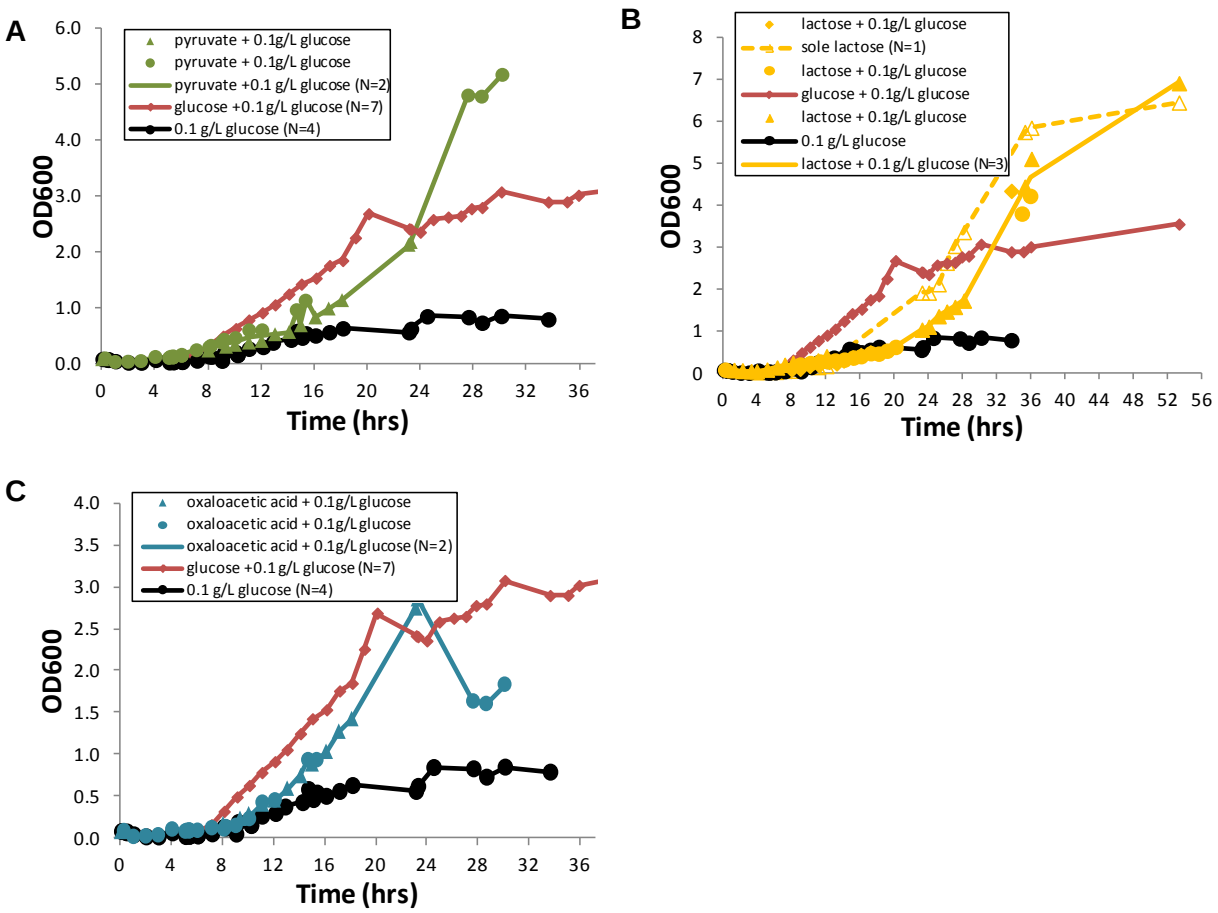

Figure 14. *S. aureus* exhibits diauxic growth with glucose and pyruvate, lactose, or oxaloacetic acid. Three mL of LB was inoculated from a frozen culture and grown for 4 hrs at 37C prior to transfer of 20 µL to 3 mL of AAM+ (5 g/L glucose) for 10 hrs additional growth at 37C. The culture was spun down and resuspended in respective AAM media substituting 5 g/L glucose (27.8 mM) with the alternate carbon source at the same molar C concentration. When indicated, flasks additionally contained 0.1 g/L glucose. The initial OD_{600} was adjusted to OD_{600}=0.1 in 25 mL in 250mL baffled flasks and grown at 37C with shaking. **A)** Growth of glucose-pyruvate compared to glucose controls, **B)** growth of glucose-lactose and lactose-only compared to glucose controls, and **C)** growth of glucose-oxaloacetic acid compared to glucose controls. Gluconate, glycerol, fructose, and ribose led to non-diauxic growth with glucose, whereas α-ketoglutarate, succinate, fumarate, acetate, arabinose grew similar to the 0.1 g/L glucose control.

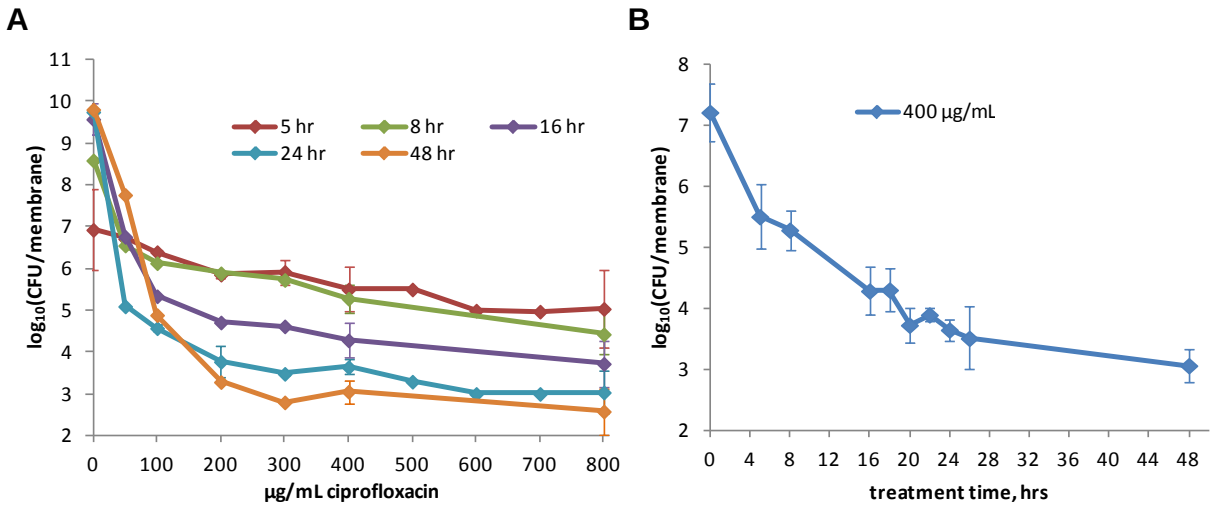

Figure 15. Determination of ciprofloxacin concentration and treatment time for *S. aureus* persister enumeration. **A)** *Staphylococcus aureus* Newman cultures were grown from frozen stock in LB for 4 hrs, and then 20 µL was transferred to 3 mL AAM (5 g/L glucose) and grown for 10 hrs at 37C. The culture was washed once and resuspended in AAM (5g/L glucose) to an OD_{600}=0.2 (inoculum). Each membrane was placed on an AAM agar plates and inoculated with 100 µL of inoculum. After 6 hrs of growth at 37C, 200 µL of 50-800 µg/mL ciprofloxacin was applied to each membrane for 5-48 hrs. At designated times, treated membranes were transferred to 15 mL tubes containing 2 mL PBS and vortexed for 1 minute. To remove antibiotic, 1mL of the suspension was centrifuged for 3 minutes at 21,000xg , 0.9 mL of the supernatant was removed and replaced with 0.9 mL PBS, and the procedure was repeated. Samples were serially diluted and plated on LB agar for CFU enumeration following overnight incubation at 37C. **B)** Biphasic killing of *S. aureus* colony biofilms after treatment with 400µg/mL CIP solution. Mean cell density +/- SD for untreated, 6hr biofilms was 7.21 +/- 0.48 $\log_{10}$(CFU/membrane) over N=4 experiments. Error bars indicate standard deviation.

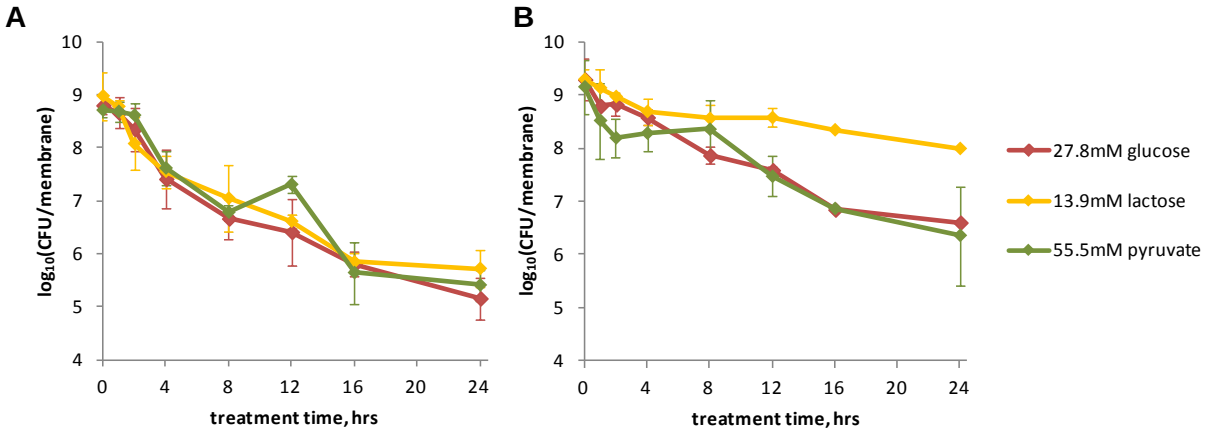

Figure 16. Glucose-lactose transitions stimulate persister formation in *S. aureus* biofilms. *S. aureus* Newman were grown from frozen stock in LB for 4 hrs then 20 µL transferred to 3 mL AAM (5 g/L glucose) and grown for 10 hrs at 37C. The culture was washed once and resuspended in AAM (5g/L glucose) to an OD_{600}=0.2 for use as inoculum. Each membrane was placed on an AAM agar plates and inoculated with 100 µL of inoculum for growth as biofilm at 37C. All biofilms were provided 5 g/L glucose (27.8 mM) in the inoculum with a secondary carbon source in the agar as indicated. Persisters were enumerated during, **A)** common period of glucose consumption (OD_{600}=0.2), and **B)** period of catabolism of the secondary carbon sources (OD_{600}=0.7). When cell densities were reached, 200 µL of 400 µg/mL ciprofloxacin was applied to each membrane for 1-24 hrs. At designated times,treated membranes were transferred to 15 mL tubes containing 2 mL PBS and vortexed for 1 minute, the antibiotic was removed by washing, and samples were serially diluted and plated on LB agar for enumeration following overnight incubation at 37C. Error bars indicate standard deviation.

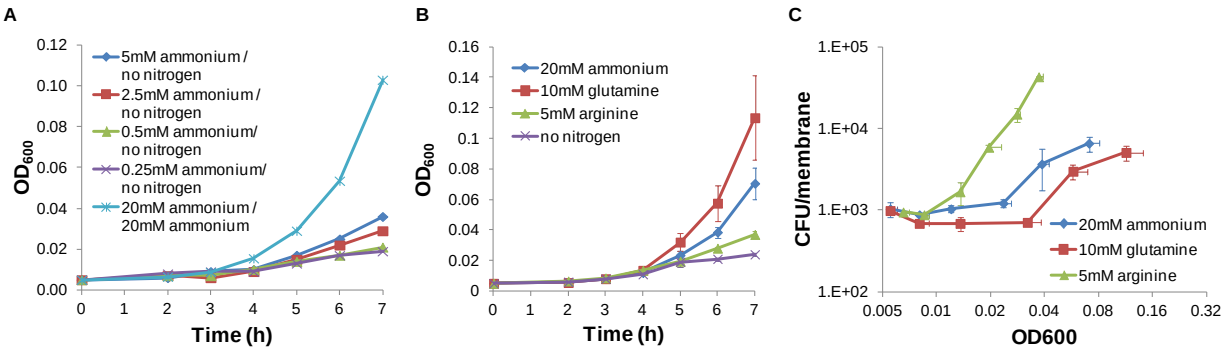

Figure 17. Nitrogen source transitions in *E. coli* biofilms. Overnight cultures in LB with 20 mM NH_4^+ were diluted to 0.1 OD_{600} in M9 minimal medium containing NH_4^+ and 100 µL was transferred to sterile PES membranes, which had been aseptically placed on M9 minimal agar plates. **A)** ON cells were diluted in 0.25, 0.5, 2.5, or 5 mM NH_4^+ and 100 µl was transferred to membranes on agar plates containing 20mM NH_4^+ or no nitrogen source. Samples were grown at 37°C and at every hour OD_{600} was measured. **B)** ON cells were diluted in 0.25mM NH_4^+ and transferred to membranes on minimal agar plates supplemented with nitrogen sources as specified. Samples were grown at 37°C and at every hour OD_{600} was measured. **C)** ON cells were diluted in 0.25mM NH_4^+ and transferred to membranes on minimal agar plates supplemented with nitrogen sources as specified. Samples were grown at 37°C and at every hour OD_{600} were measured and persisters were enumerated by treatment with 200µL of 10µg/mL ofloxacin for 5 h, after which CFUs were measured. Error bars indicate SEM of two or more replicates.

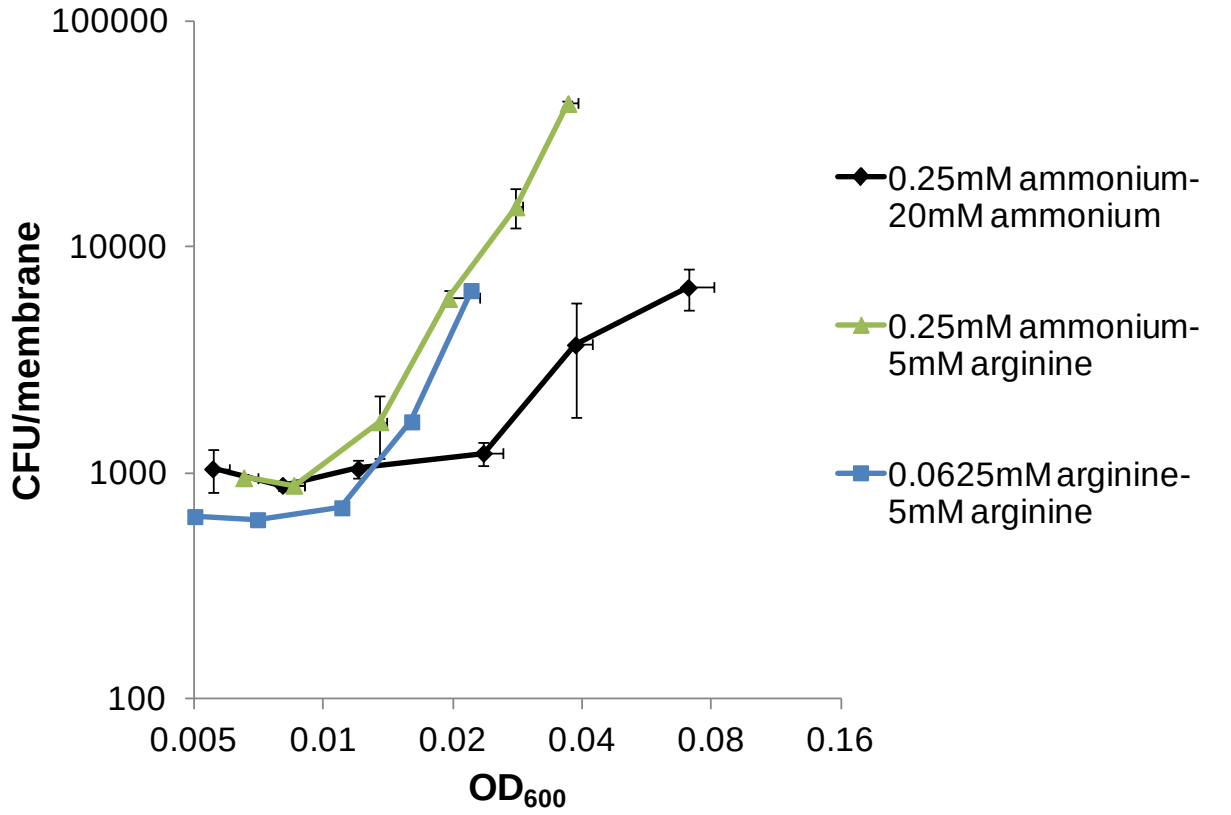

Figure 18. Preliminary data suggests that persister formation from nitrogen source transitions in *E. coli* biofilms is substrate-dependent. For sole ammonium and ammonium-arginine, ON cultures in LB with 20 mM NH_4^+ were diluted in M9 minimal medium containing NH_4^+ and 100 µL was transferred to sterile PES membranes, which had been aseptically placed on M9 minimal agar plates containing 20mM NH_4^+ or 5mM arginine. For sole arginine, ON cultures in 5mM arginine M9 minimal media were diluted in M9 minimal media containing arginine and 100 µL was transferred to sterile PES membranes aseptically placed on M9 minimal agar plates containing 5mM arginine. Samples were grown at 37°C and at every hour OD_{600} were measured and persisters were enumerated by treatment with 200µL of 10µg/mL ofloxacin for 5 h, after which CFUs were measured. Error bars indicate SEM of two or more replicates.

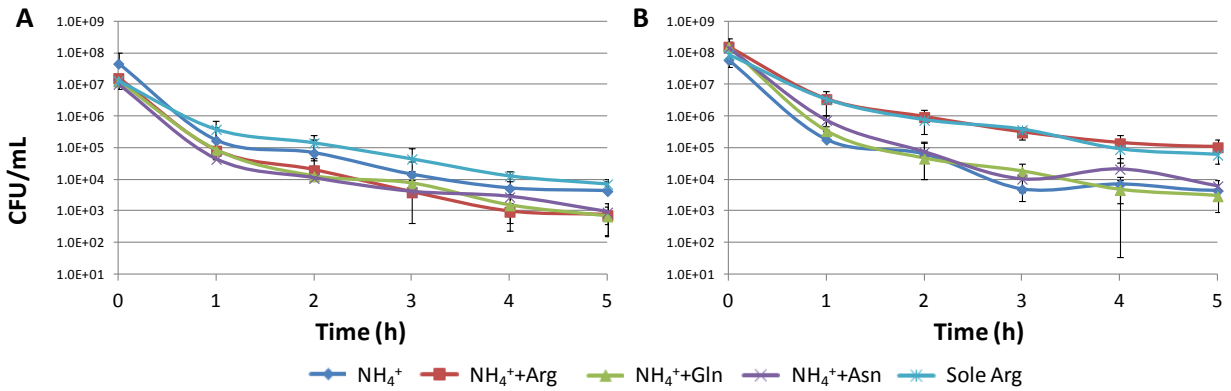

Figure 19. Nitrogen transitions in planktonic *E. coli* cultures yield persister formation that is substrate-dependent. MG1655 was grown overnight for 15h in 10mM glucose 20mM NH_4Cl and diluted into fresh media containing 0.25mM NH_4Cl and 20mM secondary nitrogen to an OD_{600} of 0.01. For the sole arginine control, MG1655 was grown overnight in 10mM glucose 5mM arginine and diluted to 0.01 OD_{600} in 5.0625mM arginine. Cells were grown and challenged with 5μg/mL OFL at, **A)** 0.02 OD_{600} representing growth on ammonium, and **B)** and 0.14 OD_{600} representing growth after ammonium exhaustion for the media that contained two nitrogen sources. Colony forming units (CFU) were quantified every hour post antibiotic treatment for 5 hours. Data are averages of 3 independent experiments and error bars indicate standard deviation.

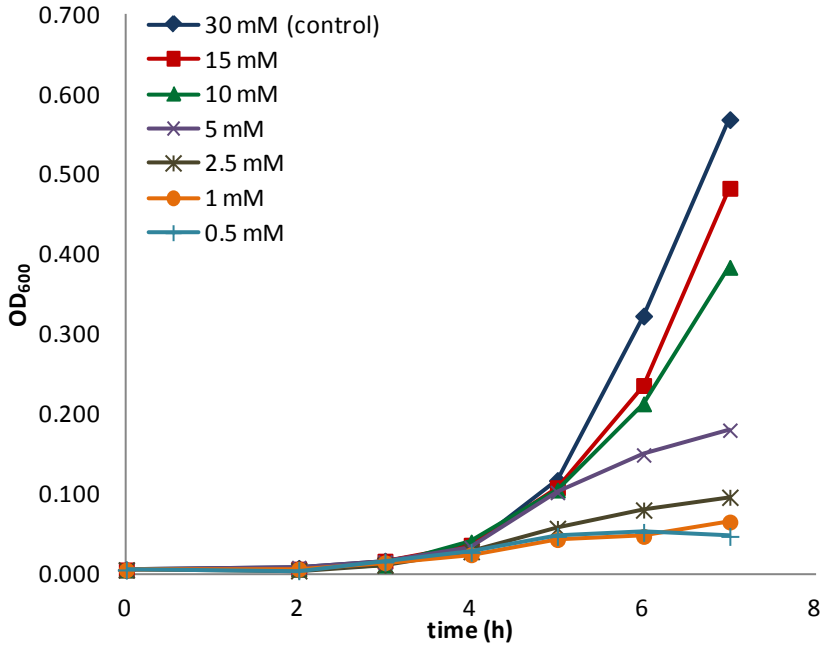

Figure 20. Identification of an NH_4^+ concentration necessary to achieve N exhaustion by ~ 3 doublings. *P. aeruginosa* PAO1 was inoculated into 2 mL of LB from frozen stock. After 4 h of growth at 37 °C with shaking, 2 mL of BSM minimal media (30 mM NH_4^+) supplemented with 40 mM fumarate was inoculated to an OD_{600} of 0.001 and grown for 16 h at 37 °C with shaking. Overnight cultures were then diluted to an OD_{600} of 0.1 in BSM (no nitrogen) minimal medium with 40 mM fumarate and varied concentrations of NH_4^+. 100 µL was transferred to sterile membranes, which had been aseptically placed on BSM minimal agar plates containing 40 mM fumarate and no nitrogen. Samples were grown at 37 °C, and the untreated OD_{600} was measured hourly.

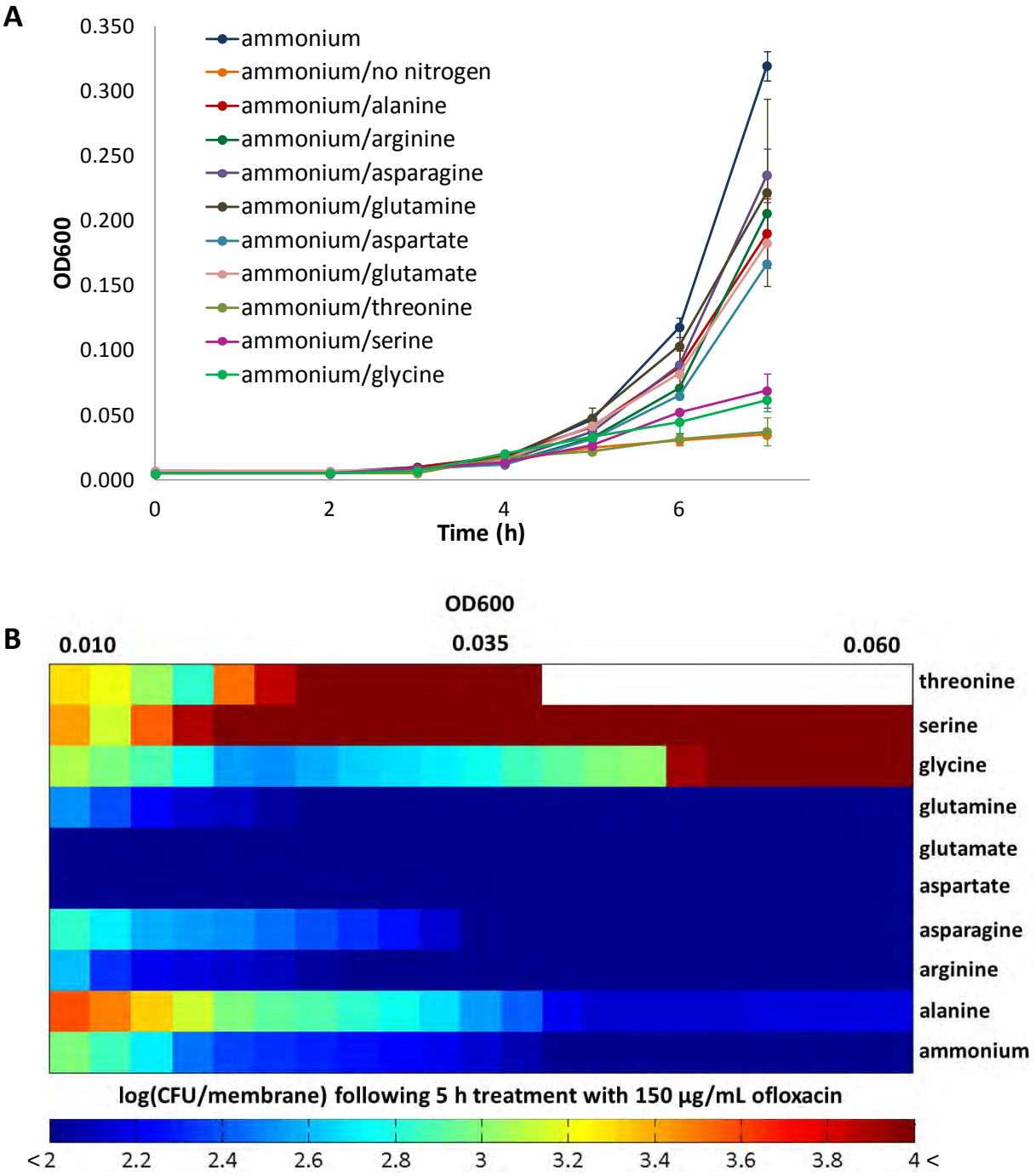

Figure 21. Nitrogen source transitions stimulate persister formation in *P. aeruginosa* biofilms. Frozen stock of PAO1 was used to inoculate 2 mL of LB media. Following 4 h of growth at 37 °C with shaking, 2 mL of BSM minimal media (30 mM NH_4^+) supplemented with 40 mM fumarate was inoculated to an OD_{600} of 0.001 and grown for 16 h at 37 °C with shaking. Overnight cultures were then diluted to an OD_{600} of 0.1 in BSM (0.5 mM NH_4^+) minimal medium with 40 mM fumarate. 100 µL was transferred to sterile membranes, which had been aseptically placed on BSM minimal agar plates containing 40 mM fumarate and 30 mM of the respective

secondary nitrogen source. Samples were grown at 37 °C, and the, **A)** untreated OD_{600}, and **B)** persisters were measured hourly. CFU/membrane values for color plot were interpolated from two adjacent measurements in order to obtain values at each designated OD_{600}. White bar for threonine indicates that the sample did not reach those cell densities during the time scale of the experiment. Error bars indicated SEM of two or more replicates.

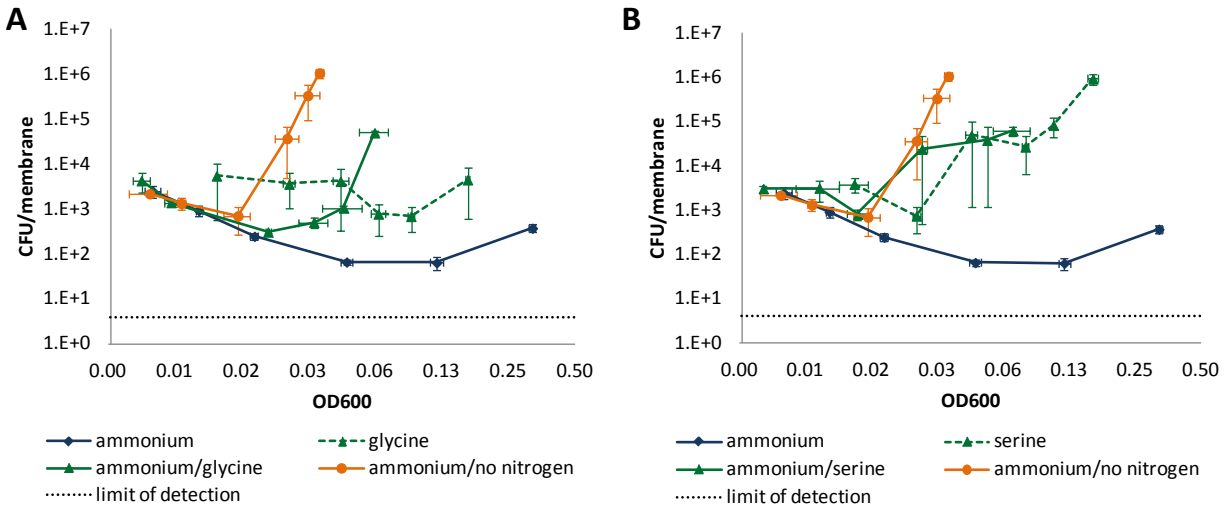

Figure 22. Preliminary data suggests that nitrogen source transitions stimulate transition-dependent persister formation in *P. aeruginosa* biofilms. Frozen stock of PAO1 was used to inoculate 2 mL of LB media. Following 4 h of growth at 37 °C with shaking, 2 mL of BSM minimal media (30 mM nitrogen source) supplemented with 40 mM fumarate was inoculated to an OD_{600} of 0.001 and grown for 16 h at 37 °C with shaking. Overnight cultures were then diluted to an OD_{600} of 0.1 in BSM (0.5 mM NH_4^+ for transitions and 0.5 mM nitrogen for sole sources) minimal medium with 40 mM fumarate. 100 µL was transferred to sterile membranes, which had been aseptically placed on BSM minimal agar plates containing 40 mM fumarate and 30 mM of the respective nitrogen source. Samples were grown at 37°C, and the untreated OD_{600} was measured hourly. Persisters were enumerated by treating with 150 µg/mL ofloxacin for 5 h, after which CFUs were measured. **A)** Persister levels for NH_4^+-only, NH_4^+-glycine, glycine-only, and NH_4^+-no nitrogen control. **B)** Persister levels for NH_4^+-only, NH_4^+-serine, serine-only, and NH_4^+-no nitrogen control. Dashed line indicates limit of detection. Error bars indicated SEM of two or more replicates.

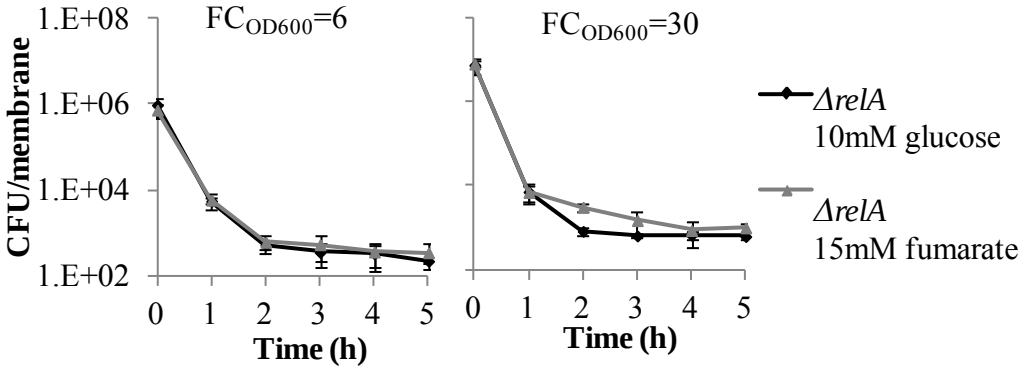

Figure 23. RelA is required for persister formation from carbon source transitions in *E. coli* biofilms. Cells were challenged with 200µL of 10µg/mL ofloxacin at FC_{OD600}=6 and FC_{OD600}=30, representing growth on glucose and growth after glucose exhaustion, respectively (except for glucose-only sample). *ΔrelA* eliminated persister formation compared to wild-type ($p<0.05$). Data are averages of 3 independent experiments, error bars indicate standard deviation, and significance was assessed using the null hypothesis that the mutant mean fold-change in persisters was equal to the wild-type fold-change in persisters.

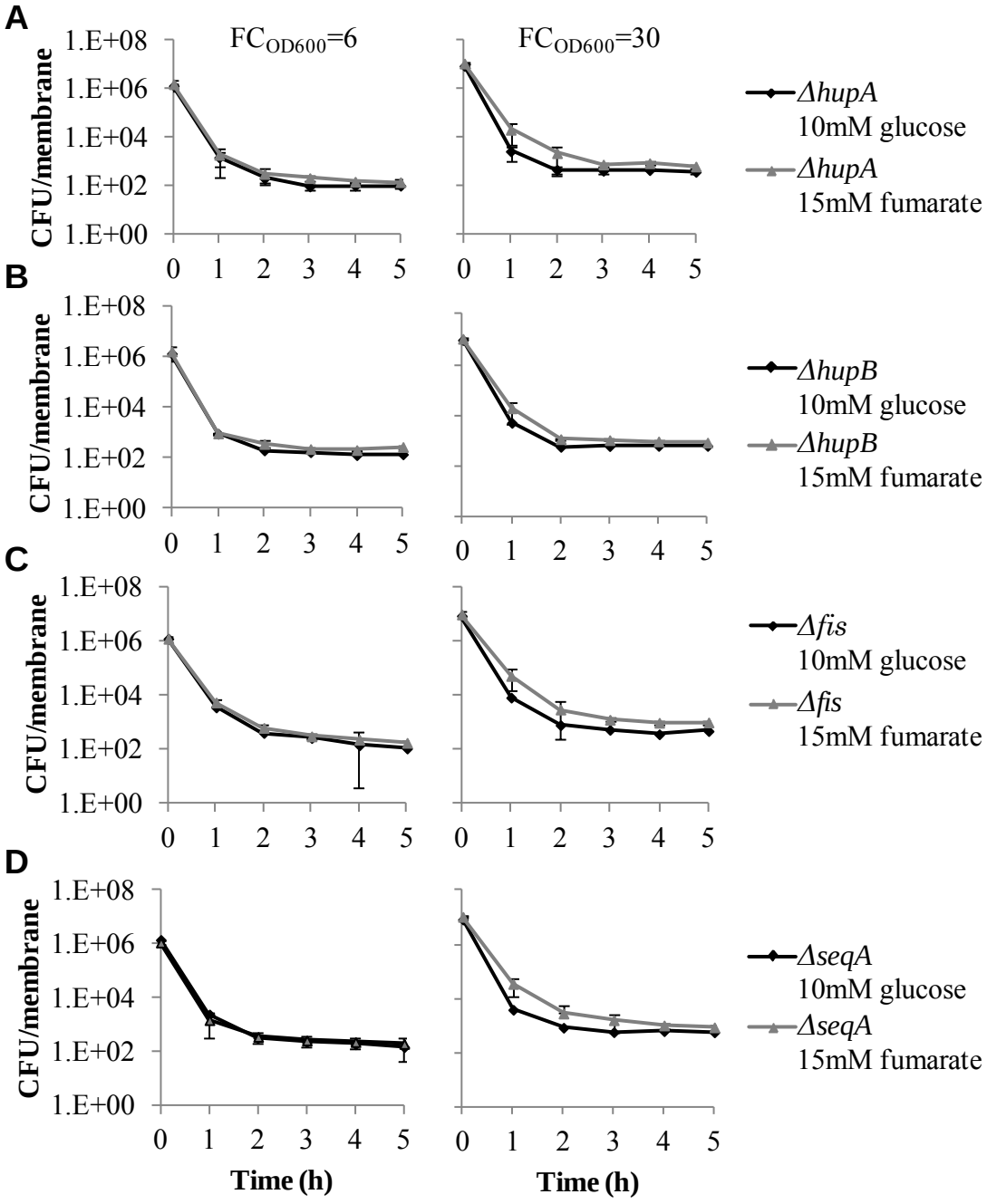

Figure 24. Nucleoid-associated proteins facilitate persister formation from carbon transitions in *E. coli* biofilms. Cells were challenged with 200µL of 10µg/mL ofloxacin at FC$_{OD600}$=6 and FC$_{OD600}$=30. Components of 3 NAPs, **A)** *Δfis,* **B)** *ΔseqA* , **C)** *ΔhupA,* and **D)** *ΔhupB* eliminated persister formation compared to wild-type ($p<0.05$). Data are averages of 3 independent experiments, error bars indicate standard deviation, and significance was assessed using the null hypothesis that the mutant mean fold-change in persisters was equal to the wild-type fold-change in persisters.

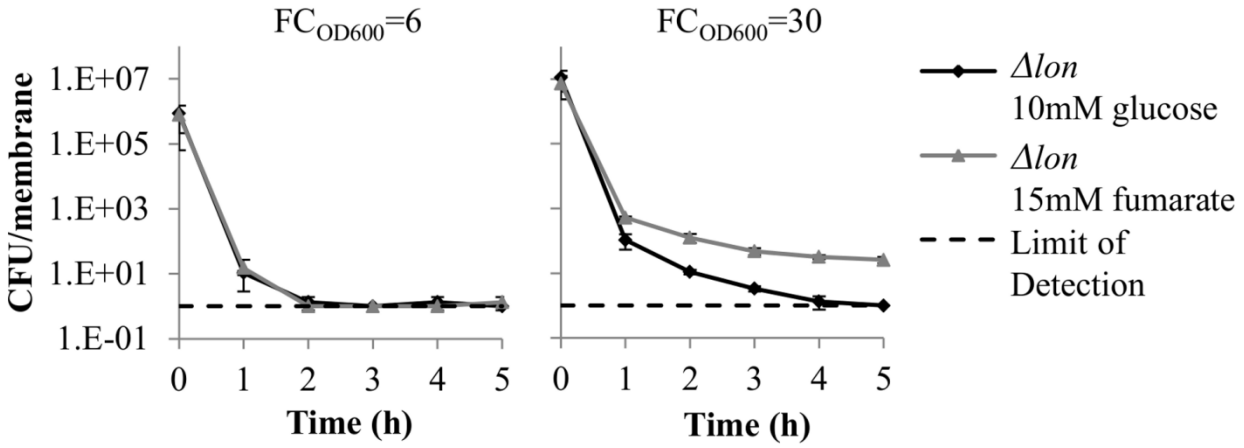

Figure 25. Involvement of Lon in persister formation from carbon source transitions in *E. coli* biofilms. Cells were challenged with 200µL of 10µg/mL ofloxacin at FC_{OD600}=6 and FC_{OD600}=30, representing growth on glucose and growth after glucose exhaustion, respectively (except for glucose-only sample). *Δlon* did not eliminate persister formation due to a carbon source transition in biofilms. The limit of detection was 1 CFU/membrane. Data are averages of 3 independent experiments and error bars indicate standard deviation.

Title

Nutrient transitions are a source of persisters in *Escherichia coli* biofilms.

Authors and Affiliations

Stephanie M. Amato[1] and Mark P. Brynildsen[1,*]

[1]Department of Chemical and Biological Engineering, Princeton University, Princeton, NJ 08544 United States of America

*Corresponding author contact information:

Phone: (609) 258-1995

Fax: (609) 258-1247

Email: mbrynild@princeton.edu

Abstract

Persisters are abundant in biofilms, though the mechanisms of their formation remain unclear. The plethora of biofilm characteristics that could give rise to persisters, including slower growth, quorum signaling, oxidative stress, and nutrient heterogeneity, have complicated efforts to delineate formation pathways that generate persisters during biofilm development. Here we sought to specifically determine whether nutrient transitions, which are a common metabolic stress encountered within surface-attached communities, stimulate persister formation in biofilms and if so, to then identify the pathway. To accomplish this, we established an experimental methodology where nutrient availability to biofilm cells could be controlled exogenously, and then used that method to discover that diauxic carbon source transitions stimulated persister formation in *Escherichia coli* biofilms. Previously, we found that carbon source transitions stimulate persister formation in planktonic *E. coli* cultures, through a pathway that involved ppGpp and nucleoid-associated proteins, and therefore, tested the functionality of that pathway in biofilms. Biofilm persister formation was also found to be dependent on ppGpp and nucleoid-associated proteins, but the importance of specific proteins and enzymes between biofilm and planktonic lifestyles was significantly different. Data presented here support the increasingly appreciated role of ppGpp as a central mediator of bacterial persistence and demonstrate that nutrient transitions can be a source of persisters in biofilms.

Introduction

Bacterial persisters are rare, phenotypic variants, whose hallmark characteristic is a transient, yet extraordinary, ability to tolerate antibiotics while their surrounding kin are killed.[1] Persisters are highly abundant in biofilms, and have been hypothesized to underlie why biofilm infections often relapse.[2,3] Persisters form during biofilm growth, and despite the identification of several important mediators, including ppGpp,[4-6] Lon,[4] RecA,[6] and YafQ,[7] the aspects of biofilm development that generate persisters, along with their respective pathways, remain ill-defined. The biofilm life-style includes numerous qualities conducive to persister formation, including slower growth,[8,9] decreased metabolism,[10] quorum signaling,[11,12] oxidative stress,[13,14] and nutrient heterogeneity.[15,16] This suggests that the composition of persister sub-populations in mature biofilms is likely heterogeneous,[10,17-19] consisting of persisters formed from different pathways in response to various signals throughout biofilm growth.

Recently, we identified a persister formation pathway in response to nutrient transitions in planktonic *E. coli* cultures.[16] Nutrient transitions are abundant in biofilms, as cells at the periphery consume favorable substrates and leave less favorable substrates and waste products available to cells deeper in the film.[5,20] Together, these phenomena suggest that nutrient transitions may be a source of persisters in biofilms. However, several studies have found that genes important to persistence in one life-style, biofilm or planktonic, are dispensable to persistence in the other.[6,7] These observations highlight the necessity to test the functionality of persister formation pathways identified under planktonic conditions in biofilm environments. To date, mechanisms of persister formation have mainly been studied in planktonic

systems,[12,14,16,21] and the extent to which these pathways operate in biofilms remains an open question.

Here we sought to determine whether carbon source transitions within biofilms generate persisters, and if so, to then identify the underlying pathway. To accomplish this, we established a biofilm culturing method where nutrient availability to cells could be controlled exogenously. Using this method, we found that diauxic transitions stimulate persister formation in *E. coli* biofilms through a pathway that involves the ppGpp synthase, RelA, and nucleoid-associated proteins (NAPs), FIS, HU, and SeqA.[22,23] This pathway is qualitatively similar to the one found in planktonic cultures, with the exceptions of only removal of one ppGpp synthase was required to eliminate persister formation and IHF was not found to participate in persister formation in biofilms. These findings provide a more thorough understanding of the importance of ppGpp to persistence in biofilms and point to nutrient transitions as an inherent characteristic of biofilm growth that has the capacity for persister generation.

Materials and Methods

Bacterial strains, plasmids, and biofilm growth conditions

E. coli MG1655 was the wild-type strain used in this study. Its genetic mutants and plasmids used here were described previously.[16] Separate colonies were used for each of three replicate experiments. Biofilm experiments were performed using colony biofilms.[20] For these experiments, cells from -80°C stock were grown for 4 h in LB, diluted 1:100 into 2mL of 10mM M9 glucose, and grown overnight for 16 h at 37°C and 250rpm. The overnight culture was diluted into fresh M9 media containing 15mM carbon to an optical density at 600nm (OD_{600}) of 0.01 and 100µL aliquots were inoculated onto sterile, polyethersulfone (PES) membranes (0.2µm pore size, 25mm diameter, Pall Corporation, Ann Arbor, MI) positioned on M9 minimal

agar plates containing either 60mM of secondary carbon, 10mM glucose, or no carbon. Plates were incubated at 37°C. To monitor growth, PES membranes were aseptically removed from the agar, vortexed in 2mL of sterile PBS for 1 minute, and the OD_{600} of the resulting cell suspensions were measured. Growth was reported as a fold change in OD_{600} (FC_{OD600}), which is the ratio of cells present on the membrane to the cells inoculated onto the membrane.

Carbon source transition assay

Colony biofilms were grown as described by diluting the overnight into fresh 15mM carbon. At desired time points, membranes containing colony biofilms were aseptically removed from the agar, vortexed in 2mL of PBS for 1 minute, and the OD_{600} was measured. OD_{600} was monitored for over 8 h of growth for specified secondary carbon sources and no carbon. Persister measurements were taken prior to glucose exhaustion (FC_{OD600}~14, Figure 1) at FC_{OD600}=6 and after glucose exhaustion at FC_{OD600}=30.

Transcriptional Reporters

MG1655 possessing pSA03, pSA04, and pSA07[16] were used as cAMP and ppGpp transcriptional reporters as indicated. Kanamycin (50µg/mL) was present during growth for plasmid retention. Cells were prepared as described above. At FC_{OD600}=6 (before glucose exhaustion) and at FC_{OD600}=30 (after glucose exhaustion), membranes were aseptically removed from the agar and vortexed in 2mL of PBS.

All strains including controls were analyzed by LSRII (BD Biosciences, San Jose, CA) flow cytometer. Microorganisms were determined using forward and side scatter parameters (FSC and SSC) and MG1655 carrying pUA66 as a control. The bacteria were assayed with a

laser emitting at 488nm for GFP, and green fluorescence was collected by 525/50 bandpass filter. Data were acquired and analyzed using FACSDiVa software (BD Biosciences, San Jose, CA).

Glucose measurements

Cells were prepared as described, and at FC_{OD600}=6 (before glucose exhaustion) and FC_{OD600}=30 (after glucose exhaustion), membranes were aseptically removed from the agar and vortexed in 1mL of PBS. For the no carbon control, samples were taken at FC_{OD600}=6 and 2 h post-glucose exhaustion. Glucose was quantified using the Amplex Red Glucose/Glucose Oxidase Kit (Invitrogen, Eugene, OR).

Persistence measurements

Persisters were enumerated by determining the number of colony forming units (CFU) after exposure to 10µg/mL ofloxacin for 5 h. At specified FC_{OD600}, colony biofilms on membranes were treated with 200µL of 10µg/mL ofloxacin applied to the top of the membrane and incubated at 37°C. At designated time points, membranes were aseptically removed from the agar, vortexed in 2mL of PBS, washed and serially diluted in PBS, and 10µL was spotted onto LB agar. Cells were stored at 4°C prior to plating as necessary, and it was confirmed that such storage did not affect CFU measurements when compared to samples plated immediately. Plates were incubated for 16 h at 37°C and CFU were measured to determine persister counts. 10-100 colonies were counted for each data point.[24]

Statistical Analysis

Statistical significance was assessed using 2-tailed t-tests with unequal variances. We previously confirmed that the data from CFU measurements can be treated as near-normally distributed with a larger sample dataset.[16] The threshold for significance was set to the p-value < 0.05.

Results and Discussion

Establishment of a method to exogenously control carbon source availability in colony biofilms

Bacteria can exhibit either diauxic or non-diauxic growth when grown in the presence of two carbon sources.[25] Diauxic growth occurs in media with multiple carbon sources when two exponential growth phases are separated by a lag period.[26] During the first growth phase, the preferential carbon source is consumed, whereas the less favorable secondary carbon source supports growth during the second growth phase. The lag period between the growth phases is associated with physiological changes required for growth on the secondary carbon source.[26] Non-diauxic growth can exhibit preferential carbon source consumption, but lacks the intermediate lag period.[27] We have previously demonstrated that diauxic carbon source transitions stimulate persister formation in planktonic *E. coli* cultures.[16] Here, we sought to investigate whether carbon source transitions stimulate persister formation during biofilm growth, and if so, identify the formation pathway responsible.

To study persister formation from carbon source transitions in biofilms, we required an experimental system where only biofilm cells were present and nutrient availability could be controlled exogenously. Biofilms are often grown in the presence of planktonic cells,[28,29] but results from these systems are complicated by biofilm dispersal, and when considering rare events such as persisters, uncertainty arises as to whether a cell originated from the biofilm or

planktonic sub-population. Given these considerations, we used the colony biofilm culturing method, where cells are grown on nutrient-permeable membranes positioned atop agar plates.[5,20,30] In this method, all bacteria are surface-attached biofilm cells and planktonic cells are absent. This culturing method also allowed exogenous control of nutrient availability to biofilm cells (Figure 1A). Glucose, the primary carbon source, was delivered with cells to the top of PES membranes and secondary carbon sources or controls (glucose and no carbon) were provided in the agar. Young biofilms were investigated to avoid the in-film nutrient gradients that are present in mature colony biofilms.[15,20] To demonstrate that the colony biofilm method produced young biofilms on the timescale of our experiments, we imaged colony biofilms 4 hours after inoculation onto the membrane using confocal microscopy and a strain producing the mCherry fluorescent protein (Figure S1). The presence of cell clusters in the biofilm sample compared to a sample where an equal number of planktonic cells were seeded onto the membrane just prior to imaging demonstrates that these young films are immobilized cells growing in surface-attached communities.

To demonstrate that exogenous control of nutrient availability was achieved with the colony biofilm method, we monitored growth, quantified the glucose concentration in membranes, and utilized a transcriptional reporter of glucose exhaustion. Using 2.5mM glucose in the inoculums, similar growth for films grown on agar containing glucose, fumarate, and no carbon was observed, indicating a common period of glucose consumption (Figure 1B). Fumarate was used here as a representative diauxic carbon source, and analogous measurements with additional secondary carbon sources are presented in the Supporting Information (Figure S2). After 4 hours (FC_{OD600}~14), growth rates of the fumarate and no carbon samples decreased, suggesting a transition away from glucose-replete conditions. Residual growth in the no carbon

sample was due to trace glucose levels, whereas growth in the fumarate sample, which far exceeded that of the no carbon sample, signified fumarate catabolism. This was confirmed by quantifying glucose in the membranes (Figure 1C). Since glucose exhaustion triggers the production of cAMP[31] resulting in cAMP-CRP transcriptional activity, we used a cAMP-CRP transcriptional reporter[16] to demonstrate that cAMP-CRP is comparable between glucose and fumarate samples during the common period of glucose consumption, and cAMP-CRP activity increased in the fumarate sample after glucose depletion (Figure 1D). These flow cytometry data, which consist of only a single, distinct peak for each sample, also suggest that the biofilm cells were exposed to similar nutrient environments. Together these data demonstrate that our experimental setup was successful in achieving well-controlled carbon source transitions in biofilms.

Carbon source transitions stimulate persister formation

After establishing a functional system for analyzing carbon source transitions in biofilms, we examined if transitions stimulate persister formation. *E. coli* persister levels were measured using ofloxacin throughout growth using glucose as the primary carbon source and a panel of secondary carbon sources that are diauxic or non-diauxic with glucose. The antibiotic treatment was delivered to the biofilms as 200µL of 10µg/mL ofloxacin evenly distributed atop the membrane to ensure full treatment of the biofilm. It was observed that diauxic media exhibited an increase in persisters to ofloxacin upon glucose exhaustion compared to the sole glucose control (Figure 2A). The non-diauxic secondary carbon sources, fructose [32] and gluconate[33] did not exhibit an increase in persisters to ofloxacin after glucose exhaustion. These results suggested that diauxic transitions stimulated formation of persisters to ofloxacin in biofilms.

To identify the underlying formation pathway, we focused on glucose-fumarate transitions, since they elicited the strongest persister formation response and were previously studied in planktonic culture.[16] For comparison, glucose-fructose transitions, which are non-diauxic, were investigated. Persister measurements were taken during growth on glucose (FC_{OD600}=6) and after glucose exhaustion (FC_{OD600}=30). During exponential growth on glucose, all persister levels were the same independent of the secondary carbon source present (Figure 2B). Persister measurements during exponential growth on the secondary carbon source exhibited a statistically significant 13-fold increase in persisters for the glucose-fumarate samples and an insignificant 1.4-fold increase for the glucose-fructose samples when compared to persister levels in the glucose-only samples at the same FC_{OD600}.

To establish that the increase in persisters was due to the transition from glucose to fumarate and not from the slower growth on fumarate, persister measurements were taken at the same film densities during growth on fumarate as the sole carbon source (fumarate provided in the inoculum and agar) (Figure 2C). The persister levels for the culture grown in the fumarate-only samples were 1.4-fold higher and not statistically different from persister levels for glucose-only samples, but were 9-fold lower and statistically different from those for the glucose-fumarate samples, which suggests that the increase in persisters was a result of the carbon source transition and not slower growth on fumarate.

Persisters form through a RelA-dependent mechanism

We next sought to determine the molecular mechanism responsible for persister formation from carbon source transitions in biofilms. Upon glucose limitation, the stringent response is activated and the metabolite ppGpp is synthesized by both RelA and SpoT.[34,35]

RelA is a ribosome-associated ppGpp synthase, whereas SpoT has both synthase and hydrolase activity.[35] We have shown previously that persister formation from carbon source transitions in planktonic cultures is dependent on the ppGpp biochemical network.[16] Therefore, we tested whether ppGpp is also essential for persister formation due to carbon source transitions in biofilms.

We measured persisters prior to and after glucose exhaustion in *ΔrelA* (Figure 3, Table S1). Deletion of the ribosome-dependent ppGpp synthase RelA resulted in an insignificant 1.6-fold increase in persisters when comparing glucose-fumarate to glucose-only samples. These data suggest that RelA is required for persister formation from carbon source transitions in biofilms. Interestingly, under planktonic conditions, *ΔrelA* was only found to reduce the quantity of persisters formed, whereas deletion of both ppGpp synthases (*ΔrelAΔspoT)* was required to eliminate persister formation.[16] This suggests that levels of ppGpp in a biofilm responding to a carbon source transition are not as significant as those in planktonic cultures. The reduced persister formation in biofilms compared to planktonic cultures (13-fold compared to ~50-fold), as well as the lack of a response from ppGpp transcriptional reporters[16] to the carbon source transition in biofilms (Figure S3) provided evidence to support this hypothesis. Despite the potentially attenuated stringent response in biofilms under our experimental conditions, ppGpp remained the driving force for persister formation from carbon source transitions.

ppGpp-dependent persister formation in biofilms requires NAPs

We next sought to determine how ppGpp in biofilms increases tolerance to ofloxacin, an antibiotic that targets DNA gyrase.[36] Previously, high levels of ppGpp have been observed to lead to relaxation of the chromosome, an indicator of reduced DNA gyrase activity.[37] Though

the mechanism underlying this phenomenon remains ill-defined, it is known that DNA gyrase, topoisomerases I, III, and IV, and NAPs work together to control the degree of (-) supercoiling of the chromosome.[37,38] Given the role of NAPs in (-) supercoiling and the discovery that several NAPs were involved in persister formation from carbon source transitions in planktonic cultures, we tested mutants of NAPs FIS, HNS, HU, IHF, and SeqA.[39-41]

We found that Δ*fis*, Δ*hupA*, Δ*hupB,* and Δ*seqA* all removed persister formation from carbon source transitions in biofilms (Figure 4), whereas Δ*ihfA,* Δ*ihfB*, and *Δhns* did not eliminate persister formation (Figure S4). Interestingly, IHF was previously found to be an important mediator of persister formation in planktonic conditions, but here was not found to be a mediator in the biofilm state. Interactions of NAPs with chromosomal DNA and one another are strongly influenced by growth rate and phase,[38,42,43] so we reason that differences in these interactions between biofilm and planktonic lifestyles underlie why IHF was only found to be important for planktonic persister formation. Together, these results demonstrate that FIS, HU, and SeqA are required for ppGpp to generate persisters in response to carbon source transitions in biofilms.

Conclusions

The clinical importance of persisters has been attributed to their presence in biofilm infections.[3,44] Though abundant in biofilms, the means by which persisters form in this bacterial life-style remain obscure. This is in part due to the environmental heterogeneity inherent to biofilm growth. Here we were able to establish an experimental protocol to study, in isolation, the effect of nutrient transitions on persistence in biofilms. Identification that diauxic carbon source transitions generate persisters to ofloxacin in biofilms led us to identify RelA and

NAPs as critical mediators of the process. ppGpp has been increasingly identified as a major mediator of persistence.[4-6,16,45] Both Nguyen and colleagues and Maisonneuve and colleagues established that ppGpp was important for persister formation in mature *E. coli* biofilms, [4,5], though the aspect of biofilm physiology that was responsible for the significance of ppGpp in persistence was undetermined. In addition, Bernier and colleagues found that ofloxacin persister formation from leucine starvation in *E. coli* biofilms was partially dependent on ppGpp.[6] Here we identified carbon source transitions as a biofilm property that generates persisters through a ppGpp-dependent mechanism. Further, we found that modulators of chromosomal (-) supercoiling were required for ppGpp to form persisters in response to carbon source transitions, providing a direct connection to the primary target of fluoroquinolones, DNA gyrase. Interestingly, Maisonneuve and colleagues found that the Lon protease was required for the ppGpp-dependent persister formation they observed.[4] We tested *Δlon* and found that removal of this protease did not eliminate persister formation in response to carbon source transitions (Figure S5). However, we note that *Δlon* did give rise to fewer persisters than wild-type, supporting its importance to persistence in *E. coli* biofilms. Increasingly, persistence has been found to depend on ppGpp, suggesting that the alarmone may be a common node for diverse formation mechanisms and thus an attractive candidate for anti-persister therapies.[46]

Acknowledgments

We thank Christina DeCoste for her technical support with flow cytometry experiments, and Professor Zemer Gitai and Albert Siryaporn for their technical support with confocal microscopy. We thank the National BioResource Project (NIG, Japan) for their support of the distribution of the Keio collection.

Funding

This work was supported by the National Science Foundation (SMA, Graduate Research Fellowship), the Department of the Army (W81XWH-12-2-0138), and with start-up funds from Princeton University.

References

1. Kint CI, Verstraeten N, Fauvart M, Michiels J (2012) New-found fundamentals of bacterial persistence. Trends Microbiol 20: 577-585.
2. Lewis K (2007) Persister cells, dormancy and infectious disease. Nat Rev Microbiol 5: 48-56.
3. Fauvart M, De Groote VN, Michiels J (2011) Role of persister cells in chronic infections: clinical relevance and perspectives on anti-persister therapies. J Med Microbiol 60: 699-709.
4. Maisonneuve E, Castro-Camargo M, Gerdes K (2013) (p)ppGpp Controls Bacterial Persistence by Stochastic Induction of Toxin-Antitoxin Activity. Cell 154: 1140-1150.
5. Nguyen D, Joshi-Datar A, Lepine F, Bauerle E, Olakanmi O, et al. (2011) Active starvation responses mediate antibiotic tolerance in biofilms and nutrient-limited bacteria. Science 334: 982-986.
6. Bernier SP, Lebeaux D, DeFrancesco AS, Valomon A, Soubigou G, et al. (2013) Starvation, together with the SOS response, mediates high biofilm-specific tolerance to the fluoroquinolone ofloxacin. PLoS Genet 9: e1003144.
7. Harrison JJ, Wade WD, Akierman S, Vacchi-Suzzi C, Stremick CA, et al. (2009) The chromosomal toxin gene yafQ is a determinant of multidrug tolerance for Escherichia coli growing in a biofilm. Antimicrob Agents Chemother 53: 2253-2258.

8. Fasani RA, Savageau MA (2013) Molecular mechanisms of multiple toxin-antitoxin systems are coordinated to govern the persister phenotype. Proc Natl Acad Sci U S A 110: E2528-2537.

9. Klumpp S, Zhang Z, Hwa T (2009) Growth rate-dependent global effects on gene expression in bacteria. Cell 139: 1366-1375.

10. Orman MA, Brynildsen MP (2013) Dormancy is not necessary or sufficient for bacterial persistence. Antimicrob Agents Chemother 57: 3230-3239.

11. Moker N, Dean CR, Tao J (2010) Pseudomonas aeruginosa increases formation of multidrug-tolerant persister cells in response to quorum-sensing signaling molecules. J Bacteriol 192: 1946-1955.

12. Vega NM, Allison KR, Khalil AS, Collins JJ (2012) Signaling-mediated bacterial persister formation. Nat Chem Biol 8: 431-433.

13. Boles BR, Singh PK (2008) Endogenous oxidative stress produces diversity and adaptability in biofilm communities. Proc Natl Acad Sci U S A 105: 12503-12508.

14. Wu Y, Vulic M, Keren I, Lewis K (2012) Role of Oxidative Stress in Persister Tolerance. Antimicrob Agents Chemother.

15. Walters MC, 3rd, Roe F, Bugnicourt A, Franklin MJ, Stewart PS (2003) Contributions of antibiotic penetration, oxygen limitation, and low metabolic activity to tolerance of Pseudomonas aeruginosa biofilms to ciprofloxacin and tobramycin. Antimicrob Agents Chemother 47: 317-323.

16. Amato Stephanie M, Orman Mehmet A, Brynildsen Mark P (2013) Metabolic Control of Persister Formation in Escherichia coli. Mol Cell 50: 475-487.

17. Allison KR, Brynildsen MP, Collins JJ (2011) Heterogeneous bacterial persisters and engineering approaches to eliminate them. Curr Opin Microbiol 14: 593-598.

18. Li Y, Zhang Y (2007) PhoU is a persistence switch involved in persister formation and tolerance to multiple antibiotics and stresses in Escherichia coli. Antimicrob Agents Chemother 51: 2092-2099.

19. Ma C, Sim S, Shi W, Du L, Xing D, et al. (2010) Energy production genes sucB and ubiF are involved in persister survival and tolerance to multiple antibiotics and stresses in Escherichia coli. FEMS Microbiol Lett 303: 33-40.

20. Williamson KS, Richards LA, Perez-Osorio AC, Pitts B, McInnerney K, et al. (2012) Heterogeneity in Pseudomonas aeruginosa biofilms includes expression of ribosome hibernation factors in the antibiotic-tolerant subpopulation and hypoxia-induced stress response in the metabolically active population. J Bacteriol 194: 2062-2073.

21. Dorr T, Vulic M, Lewis K (2010) Ciprofloxacin causes persister formation by inducing the TisB toxin in Escherichia coli. PLoS Biol 8: e1000317.

22. Dame RT, Kalmykowa OJ, Grainger DC (2011) Chromosomal macrodomains and associated proteins: implications for DNA organization and replication in gram negative bacteria. PLoS Genet 7: e1002123.

23. Dillon SC, Dorman CJ (2010) Bacterial nucleoid-associated proteins, nucleoid structure and gene expression. Nat Rev Microbiol 8: 185-195.

24. Kohanski MA, Dwyer DJ, Hayete B, Lawrence CA, Collins JJ (2007) A common mechanism of cellular death induced by bactericidal antibiotics. Cell 130: 797-810.

25. Monod J (1942) Recherches sur la croissance des cultures bacteriennes. 2nd Ed. .

26. Roseman S, Meadow ND (1990) Signal transduction by the bacterial phosphotransferase system. Diauxie and the crr gene (J. Monod revisited). J Biol Chem 265: 2993-2996.

27. Narang A, Pilyugin SS (2007) Bacterial gene regulation in diauxic and non-diauxic growth. J Theor Biol 244: 326-348.

28. Coenye T, Nelis HJ (2010) In vitro and in vivo model systems to study microbial biofilm formation. J Microbiol Methods 83: 89-105.

29. Harrison JJ, Turner RJ, Ceri H (2005) High-throughput metal susceptibility testing of microbial biofilms. BMC Microbiol 5: 53.

30. Zuroff TR, Bernstein H, Lloyd-Randolfi J, Jimenez-Taracido L, Stewart PS, et al. (2010) Robustness analysis of culturing perturbations on Escherichia coli colony biofilm beta-lactam and aminoglycoside antibiotic tolerance. BMC Microbiol 10: 185.

31. Saier MH, Ramseier, T.M., Reizer, J. (1996) Regulation of Carbon Utilization. Escherichia coli and Salmonella: cellular and molecular biology, 2nd Ed. Washington D.C.: ASM Press.

32. Clark B, Holms WH (1976) Control of the sequential utilization of glucose and fructose by Escherichia coli. J Gen Microbiol 96: 191-201.

33. Bachi B, Kornberg HL (1975) Utilization of gluconate by Escherichia coli. A role of adenosine 3':5'-cyclic monophosphate in the induction of gluconate catabolism. Biochem J 150: 123-128.

34. Traxler MF, Chang DE, Conway T (2006) Guanosine 3',5'-bispyrophosphate coordinates global gene expression during glucose-lactose diauxie in Escherichia coli. Proc Natl Acad Sci U S A 103: 2374-2379.

35. Potrykus K, Cashel M (2008) (p)ppGpp: still magical? Annu Rev Microbiol 62: 35-51.

36. Maxwell A (1997) DNA gyrase as a drug target. Trends Microbiol 5: 102-109.

37. Ferullo DJ, Lovett, S.T. (2008) The Stringent Response and Cell Cycle Arrest in Escherichia coli. PLoS Genetics: 1-15.

38. Travers A, Muskhelishvili G (2005) DNA supercoiling - a global transcriptional regulator for enterobacterial growth? Nat Rev Microbiol 3: 157-169.

39. Mott ML, Berger JM (2007) DNA replication initiation: mechanisms and regulation in bacteria. Nat Rev Microbiol 5: 343-354.

40. Ali Azam T, Iwata A, Nishimura A, Ueda S, Ishihama A (1999) Growth phase-dependent variation in protein composition of the Escherichia coli nucleoid. J Bacteriol 181: 6361-6370.

41. Kang S, Han JS, Park JH, Skarstad K, Hwang DS (2003) SeqA protein stimulates the relaxing and decatenating activities of topoisomerase IV. J Biol Chem 278: 48779-48785.

42. Dorman CJ (1991) DNA supercoiling and environmental regulation of gene expression in pathogenic bacteria. Infect Immun 59: 745-749.

43. Dorman CJ, Barr GC, Ni Bhriain N, Higgins CF (1988) DNA supercoiling and the anaerobic and growth phase regulation of tonB gene expression. J Bacteriol 170: 2816-2826.

44. Lewis K (2008) Multidrug tolerance of biofilms and persister cells. Curr Top Microbiol Immunol 322: 107-131.

45. Korch SB, Henderson TA, Hill TM (2003) Characterization of the hipA7 allele of Escherichia coli and evidence that high persistence is governed by (p)ppGpp synthesis. Mol Microbiol 50: 1199-1213.

46. Wexselblatt E, Oppenheimer-Shaanan Y, Kaspy I, London N, Schueler-Furman O, et al. (2012) Relacin, a novel antibacterial agent targeting the Stringent Response. PLoS Pathog 8: e1002925.

Figure Legends

Figure 1. Experimental approach to control carbon source transitions in biofilms. (A) A schematic of our experimental setup where cells and the primary carbon source are applied to a PES membrane set atop agar containing the secondary carbon source, glucose, or no carbon. (B) PES membranes atop agar containing 10mM glucose , 15mM fumarate, and no carbon were inoculated with wild-type cells at 0.01 OD_{600} in 2.5mM glucose and incubated at 37°C. The OD_{600} was measured at specified time intervals and FC_{OD600} was determined. One exponential growth phase was observed for glucose samples. Two regimes of exponential growth were observed for glucose-fumarate samples and no carbon sample exhibited limited growth after glucose exhaustion. (c) Glucose concentration measurements were taken at each persister sampling (FC_{OD600}=6 and FC_{OD600}=30) for glucose and glucose-fumarate samples and at FC_{OD600}=6 and 2 h post glucose exhaustion for the no carbon sample. (d) P*malK-gfp* GFP distribution at FC_{OD600}=6 and FC_{OD600}=30 in glucose-fumarate and glucose samples. Data are averages of ≥ 3 independent experiments and error bars indicate standard deviation.

Figure 2. Diauxic shifts stimulate persister formation in biofilms. (A) *E. coli* were grown on glucose as the primary carbon source and a panel of secondary carbon sources. At hourly time points, biofilms were challenged with 200µl of 10µg/mL ofloxacin for 5 h, aseptically removed from the agar, vortexed in 2mL PBS for 1 minute, washed, and plated to measure CFUs. To construct the color plot as a function of FC_{OD600}, as needed values plotted were interpolated from two adjacent measurements. (B) Diauxic growth (glucose-fumarate) results in significant persister formation ($p<0.05$), whereas non-diauxic growth does not ($p>0.05$) (glucose and glucose-fructose). (C) Growth on fumarate is not responsible for persister formation in glucose-fumarate samples, as evidence by sole fumarate control, which contained fumarate as the only

carbon source both in the inoculum and agar. Data are averages of ≥ 3 independent experiments, error bars indicate standard deviation, and significance was assessed using the null hypothesis that the mean CFU levels in two sample sets were equal.

Figure 3. RelA is required for persister formation from carbon source transitions in biofilms. Cells were challenged with 200μL of 10μg/mL ofloxacin at FC_{OD600}=6 and FC_{OD600}=30, representing growth on glucose and growth after glucose exhaustion, respectively (except for glucose-only sample). *ΔrelA* eliminated persister formation compared to wild-type ($p<0.05$). Data are averages of 3 independent experiments, error bars indicate standard deviation, and significance was assessed using the null hypothesis that the mutant mean fold-change in persisters was equal to the wild-type fold-change in persisters.

Figure 4. Nucleoid-associated proteins facilitate persister formation from carbon transitions in biofilms. Cells were challenged with 200μL of 10μg/mL ofloxacin at FC_{OD600}=6 and FC_{OD600}=30. Components of 3 NAPs (A) *Δfis,* (B) *ΔseqA* (C) *ΔhupA,* and (D) *ΔhupB* eliminated persister formation compared to wild-type ($p<0.05$). Data are averages of 3 independent experiments, error bars indicate standard deviation, and significance was assessed using the null hypothesis that the mutant mean fold-change in persisters was equal to the wild-type fold-change in persisters.

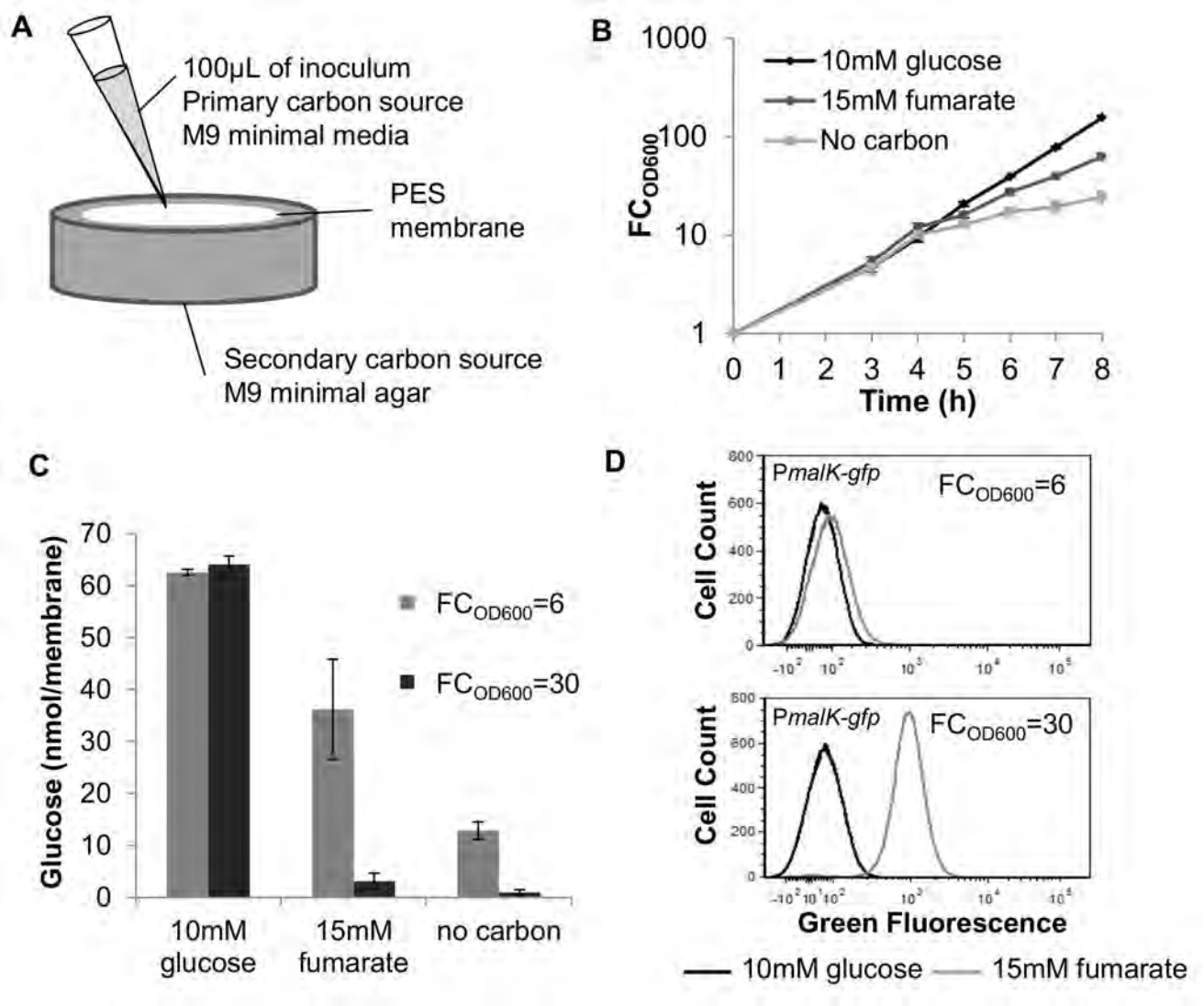
A
100µL of inoculum
Primary carbon source
M9 minimal media
PES
membrane
Secondary carbon source
M9 minimal agar
B
1000
100
10
1
FC OD600
10mM glucose
15mM fumarate
No carbon
0 1 2 3 4 5 6 7 8
Time (h)
C
Glucose (nmol/membrane)
70
60
50
40
30
20
10
0
FC OD600=6
FC OD600=30
10mM glucose
15mM fumarate
no carbon
D
PmalK-gfp
FC OD600=6
Cell Count
PmalK-gfp
FC OD600=30
Cell Count
Green Fluorescence
10mM glucose
15mM fumarate

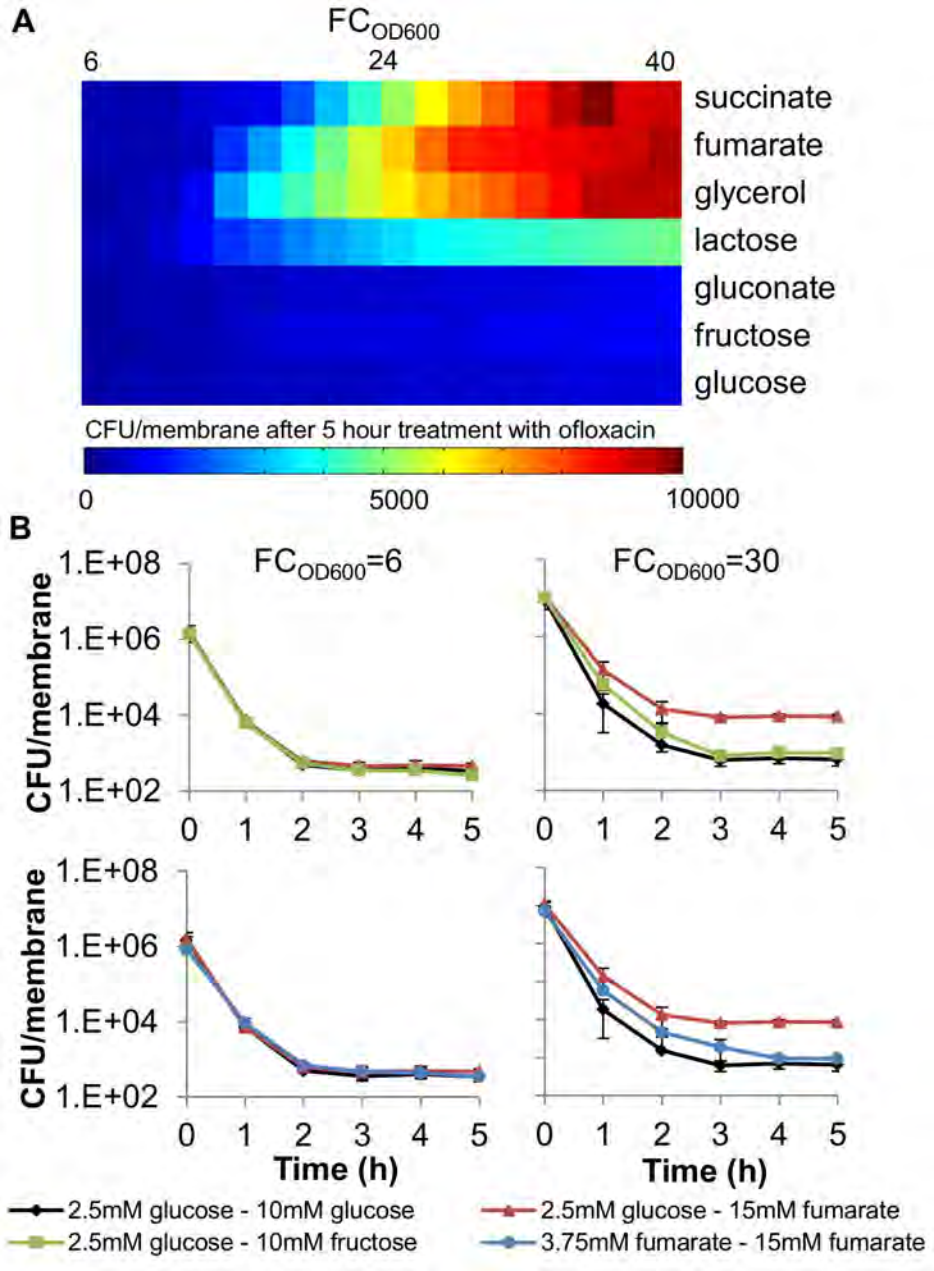
A
FC$_{OD600}$
6
24
40
succinate
fumarate
glycerol
lactose
gluconate
fructose
glucose
CFU/membrane after 5 hour treatment with ofloxacin
0
5000
10000
B
FC$_{OD600}$=6
FC$_{OD600}$=30
CFU/membrane
1.E+08
1.E+06
1.E+04
1.E+02
0 1 2 3 4 5
Time (h)
2.5mM glucose - 10mM glucose
2.5mM glucose - 10mM fructose
2.5mM glucose - 15mM fumarate
3.75mM fumarate - 15mM fumarate

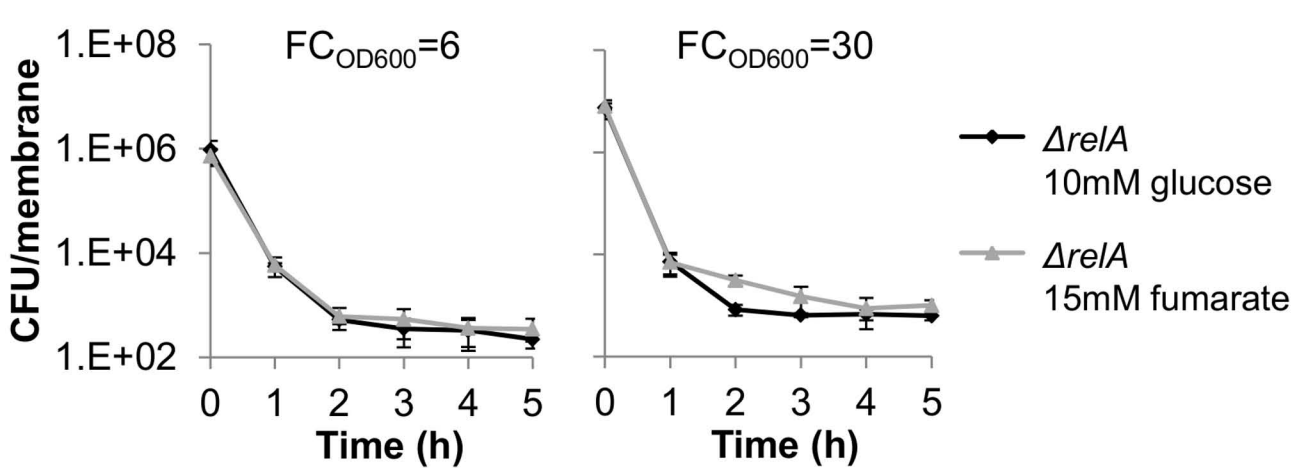
1.E+08
1.E+06
1.E+04
1.E+02
CFU/membrane
FC$_{OD600}$=6
FC$_{OD600}$=30
0 1 2 3 4 5
Time (h)
0 1 2 3 4 5
Time (h)
ΔrelA
10mM glucose
ΔrelA
15mM fumarate

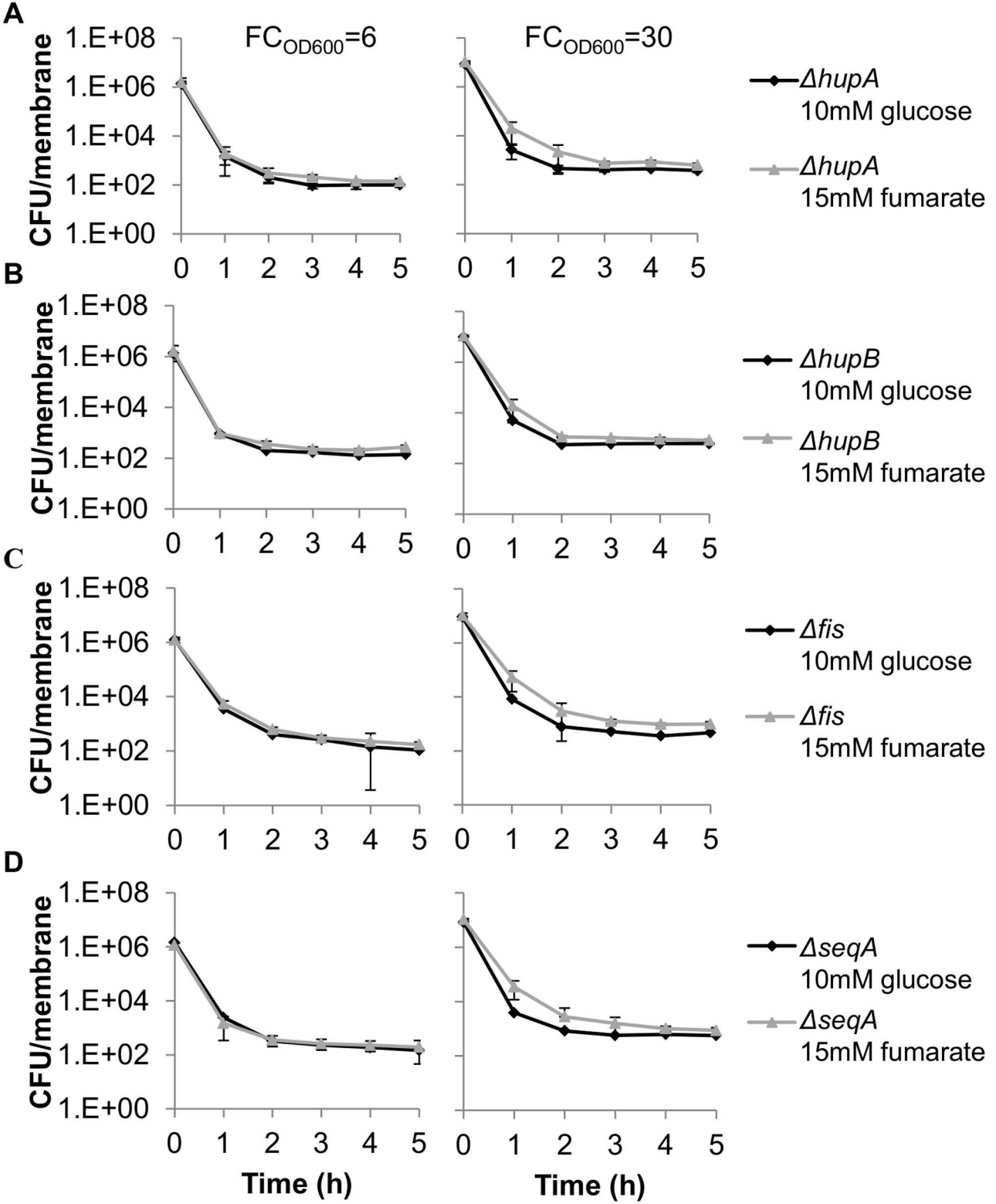
A
B
C
D
FC$_{OD600}$=6
FC$_{OD600}$=30
CFU/membrane
1.E+08
1.E+06
1.E+04
1.E+02
1.E+00
0 1 2 3 4 5
Time (h)
ΔhupA
10mM glucose
ΔhupA
15mM fumarate
ΔhupB
10mM glucose
ΔhupB
15mM fumarate
Δfis
10mM glucose
Δfis
15mM fumarate
ΔseqA
10mM glucose
ΔseqA
15mM fumarate

Supporting Information

Supporting Material and Methods

Confocal Microscopy of Colony Biofilms

E. coli MG1655 MO001, which contained a chromosomally integrated *lacI*^{q} promoter in place of the *lacI* promoter and a chromosomally integrated *T5p-mCherry* cassette in place of *lacZYA,[1]* was used to image cells grown on the PES membranes. Cells from -80°C stock were grown for 4 h in LB, diluted 1:100 into 2mL of 10mM M9 glucose with 2mM isopropyl β-D-1-thiogalactopyranoside (IPTG), and grown overnight for 16 h at 37°C and 250rpm.

For biofilm samples, the overnight culture was diluted into fresh 2.5mM M9 glucose with 2mM IPTG to an OD_{600} of 0.01 and 100µL aliquots were inoculated onto sterile, PES membranes positioned on 10mM glucose M9 minimal agar plates containing 2mM IPTG. Plates were incubated at 37°C for 4 h (~3.5 cell divisions). For planktonic samples, the overnight culture was diluted in 25mL of fresh 10mM M9 glucose with 2mM IPTG to an OD_{600} of 0.01. Cells were grown at 37°C and 250rpm until ~3.5 doublings occurred and then ~$7x10^{6}$ cells (approximately the number of cells present on the biofilm after 4 hours of growth) were applied to a sterile PES membrane.

Membranes were immobilized on a glass slide and a cover slip was placed over them prior to imaging. Imaging was performed using a Nikon Ti-E microscope (Nikon, Melville, NY), a 10X Plan Fluor Ph1 Nikon objective (0.3 NA) or 100X Plan Apo VC Nikon objective (1.4 NA), a Chroma 89014 filter set (Chroma, Bellows Falls, VT) with an ET572/35x excitation filter and ET632/60m emission filter, a Prior Lumen 200 Pro fluorescence illuminator, and an Andor iXon DU-897D camera.

Confirmation of Lon protease deletion

Genetic deletion of *lon* was transduced from the Keio collection[2] using the standard P1 phage method. The gene deletion was confirmed using PCR and two sets of primers. One set confirmed the presence of the kanamycin resistance cassette in the proper chromosomal location using a forward primer upstream of *lon*, 5'-GATTTATGGCAAGCCGGAAG-3', and a kanamycin resistance cassette reverse primer, 5'- ATGATGGATACTTTCTCGGCAGGAG-3'. The second set confirmed the absence of a duplicate gene, and contained primers within the gene of interest with an internal *lon* forward, 5'-GCGTATTTCTGCGCTCTCTG-3', and an internal *lon* reverse, 5'-TAGTGGTCGCTGAACGCTAC-3'.

Persistence measurements for Δlon

Persister enumeration for the *Δlon* strain was carried out as described in the main text with the following modification. Following antibiotic treatment at designated time points, membranes were aseptically removed from the agar, vortexed in 1mL of PBS, washed and serially diluted in PBS, and the entire sample was spotted onto LB agar to achieve a limit of detection of 1 CFU/membrane.

Supporting Figure Legends

Figure S1. Imaging colony biofilms. MG1655 *lacI*^{q} P_{T5} *mCherry* cells were grown 16 h in 10mM M9 glucose with 2mM IPTG. Cells were inoculated into 2.5mM M9 glucose with 2mM IPTG at 0.01 OD_{600}. Sterilized PES membranes were aseptically placed on 10mM M9 glucose with 2mM IPTG agar. Membranes were inoculated with 100µL of cells and films were incubated at 37°C for 4hr (~3.5 doublings/ $7x10^{6}$ CFU/membrane). Membranes were aseptically removed from the agar and analyzed using confocal microscopy at (A)10X objective and (B)100x objective. MG1655 *lacI*^{q} PT5 *mCherry* cells were grown 16 h in 10mM M9 glucose with 2mM IPTG. Cells were inoculated into 25mL of 10mM M9 glucose with 2mM IPTG at 0.01 OD_{600}. After ~3.5 doublings, ~$7x10^{6}$ CFU were inoculated onto a sterilized PES membrane and analyzed using confocal microscopy at (C) 10x objective and (D) 100x objective.

Figure S2. Growth of colony biofilms on glucose and a panel of secondary carbon sources. PES membranes atop agar containing specified secondary carbon sources were inoculated with wild-type cells at 0.01 OD_{600} in 2.5mM glucose and incubated at 37°C. The OD_{600} was measured at specified time intervals and FC_{OD600} was determined. Data are averages of ≥ 3 independent experiments and error bars indicate standard deviation.

Figure S3. ppGpp transcriptional response to carbon source transition in biofilm. MG1655 pUA66 P*osmE-gfp* and P*wrbA-gfp* cells were grown 16h in 10mM M9 glucose with 50µg/mL kanamycin and inoculated to 0.01 OD600 in 2.5mM glucose. PES membranes were placed on M9 agar with either 10mM glucose with 50µg/mL kanamycin or 15mM fumarate with 50µg/mL

kanamycin and membranes were inoculated with 100µL of cells. Films were incubated at 37°C. GFP distribution was measured at FC_{OD600}=6 and FC_{OD600}=30 for (A) P*osmE-gfp* and (B) P*wrbA-gfp* in glucose and glucose-fumarate media using flow cytometry.

Figure S4. Involvement of IHF and HNS in persister formation from carbon source transitions. Cells were challenged with 200µL of 10µg/mL ofloxacin at FC_{OD600}=6 and FC_{OD600}=30, representing growth on glucose and growth after glucose exhaustion, respectively (except for glucose-only sample). (A) *ΔihfA,* (B) *ΔihfB,* and (C) *Δhns* produced fold-change increases in persisters (glucose-fumarate persisters/glucose-only persisters) that were not significantly reduced compared to wild-type. Data are averages of 3 independent experiments, error bars indicate standard deviation, and significance was assessed using the null hypothesis that the mutant mean fold-change in persisters was equal to the wild-type fold-change in persisters.

Figure S5. Involvement of Lon in persister formation from carbon source transitions in biofilms. Cells were challenged with 200µL of 10µg/mL ofloxacin at FC_{OD600}=6 and FC_{OD600}=30, representing growth on glucose and growth after glucose exhaustion, respectively (except for glucose-only sample). *Δlon* did not eliminate persister formation due to a carbon source transition in biofilms. The limit of detection was 1 CFU/membrane. Data are averages of 3 independent experiments and error bars indicate standard deviation.

Table S1. Glucose concentrations (nmol/membrane)

	10mM glucose		15mM fumarate	
Bacterial Strain	FC_{OD600}=6	FC_{OD600}=30	FC_{OD600}=6	FC_{OD600}=30
wild-type	62.5 ± 0.61	64.1 ± 1.59	36.2 ± 9.60	3.1 ± 1.54
Δfis	50.6 ± 26.41	66.7 ± 3.30	30.2 ± 33.97	0 ± 0
Δhns	62.3 ± 2.20	61.1 ± 4.16	15.4 ± 6.72	4.5 ± 1.48
ΔhupA	65.2 ± 1.76	64.3 ± 3.56	18.2 ± 7.31	0 ± 0
ΔhupB	62.6 ± 3.85	62.2 ± 1.38	17.7 ± 1.99	0 ± 0
ΔihfA	69.6 ± 2.27	70.3 ± 2.95	17.1 ± 5.03	2.8 ± 4.32
ΔihfB	71.8 ± 2.57	73.7 ± 4.22	12.3 ± 9.25	2.3 ± 2.29
ΔrelA	61.4 ± 2.76	61.2 ± 2.42	11.1 ± 1.19	1.1 ± 0.92
ΔseqA	71.6 ± 1.98	70.0 ± 4.40	15.1 ± 3.80	0 ± 0

Table S1. Glucose concentrations (nmol/membrane). Glucose concentration measurements were taken at each FC_{OD600} = 6 and =30 for all strains in both 10mM glucose and 15mM fumarate samples. Measurements were made using an Amplex Red Glucose/Glucose Oxidase Kit (Invitrogen). Three replicates were conducted for each mutant and condition and error indicates standard deviation.

Supporting References

1. Orman MA, Brynildsen MP (2013) Dormancy is not necessary or sufficient for bacterial persistence. Antimicrob Agents Chemother 57: 3230-3239.

2. Baba T, Ara T, Hasegawa M, Takai Y, Okumura Y, et al. (2006) Construction of Escherichia coli K-12 in-frame, single-gene knockout mutants: the Keio collection. Mol Syst Biol 2: 2006 0008.

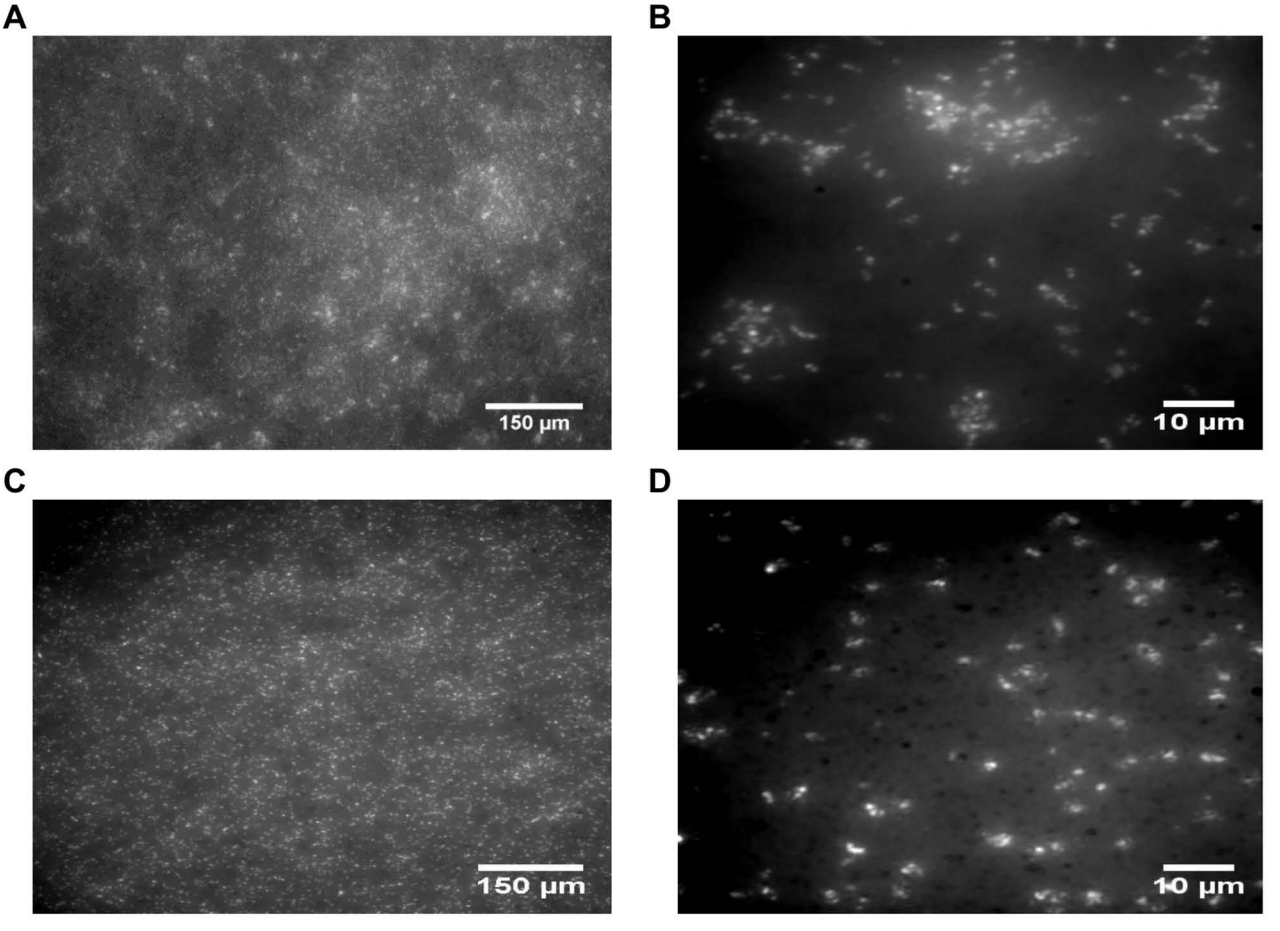
A
150 µm
B
10 µm
C
150 µm
D
10 µm

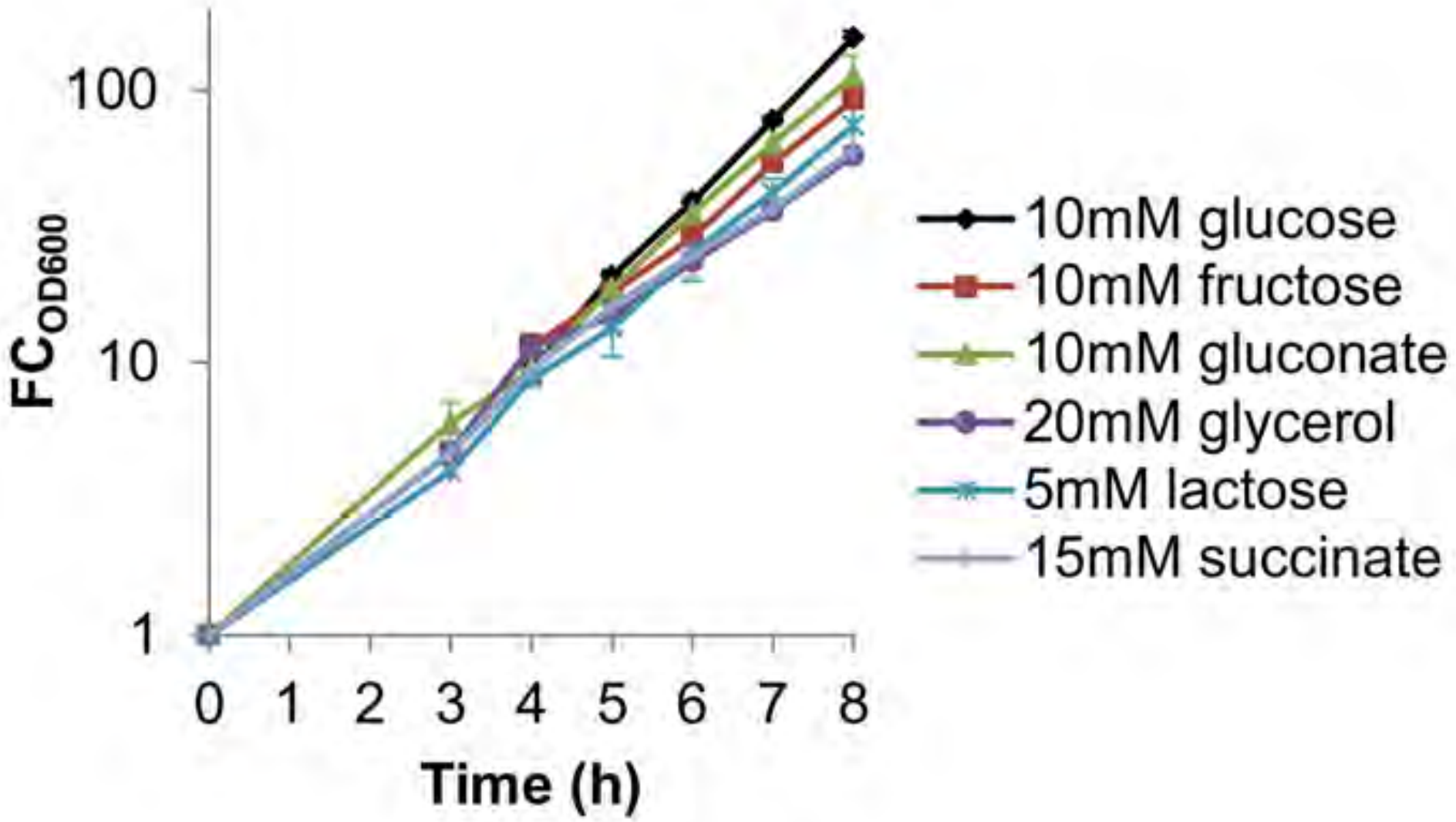
100
10
1
FC OD600
0 1 2 3 4 5 6 7 8
Time (h)
10mM glucose
10mM fructose
10mM gluconate
20mM glycerol
5mM lactose
15mM succinate

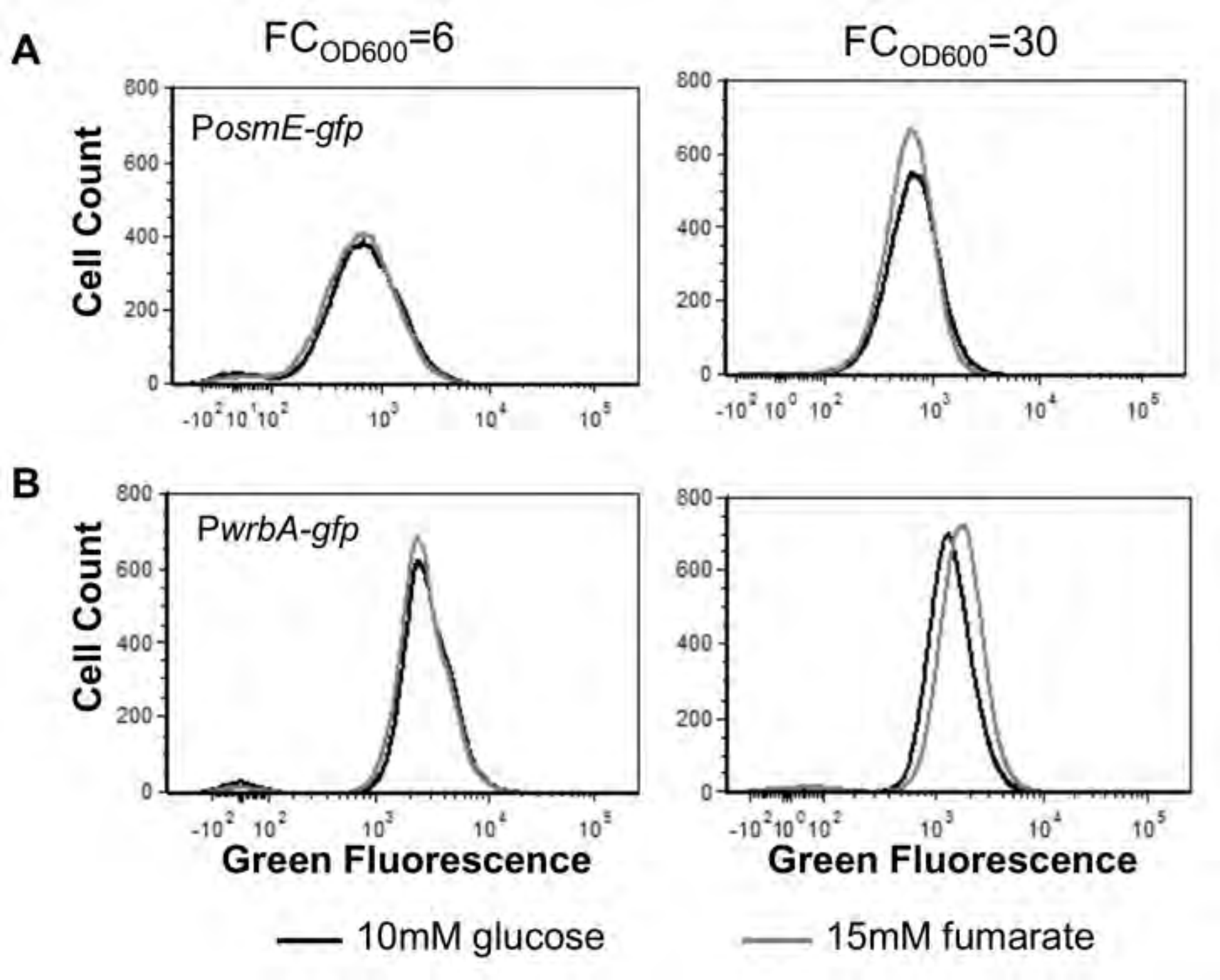
A
FC$_{OD600}$=6
FC$_{OD600}$=30
PosmE-gfp
B
PwrbA-gfp
Cell Count
Green Fluorescence
10mM glucose
15mM fumarate

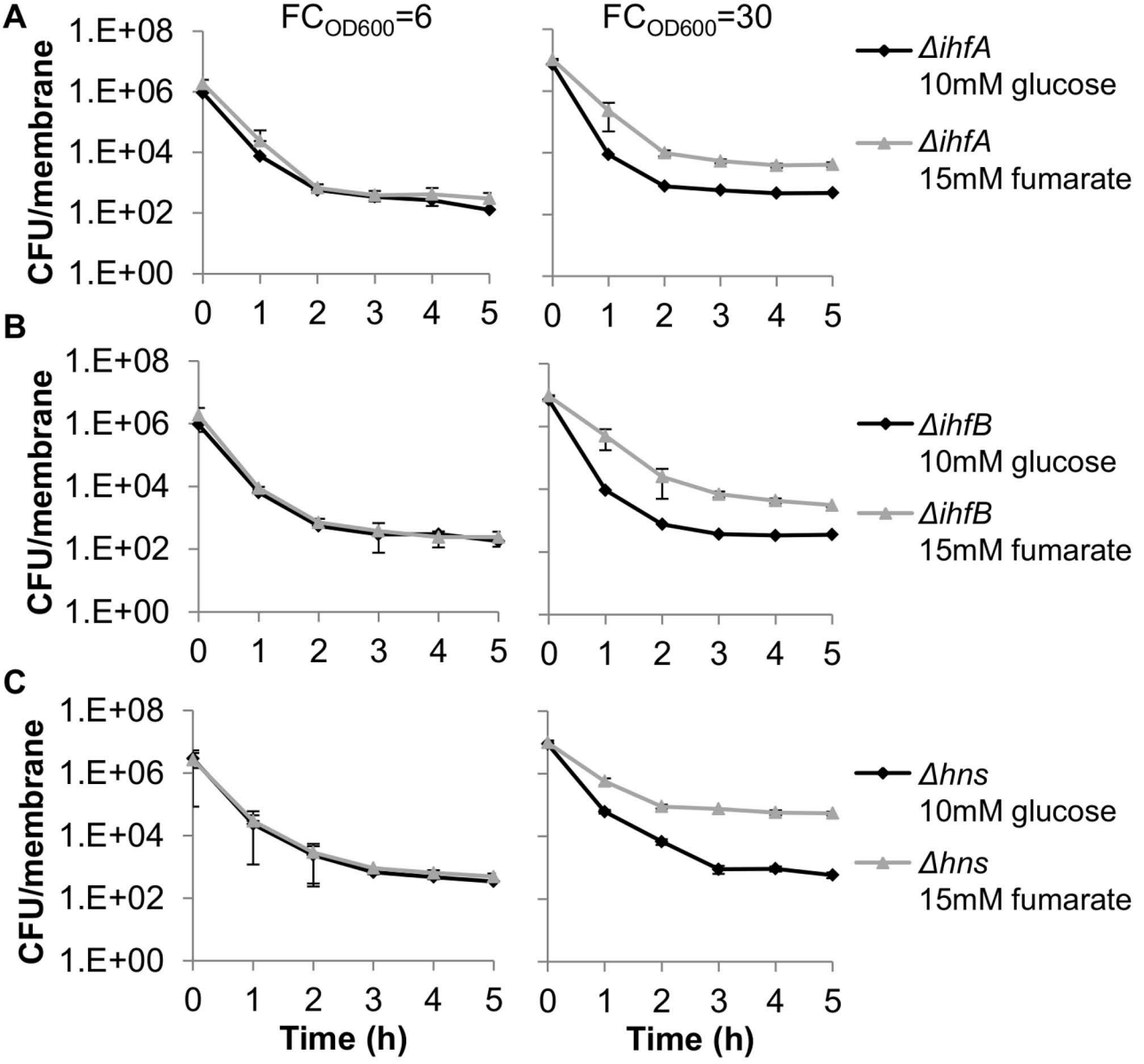
A
B
C
FC$_{OD600}$=6
FC$_{OD600}$=30
CFU/membrane
1.E+08
1.E+06
1.E+04
1.E+02
1.E+00
0 1 2 3 4 5
Time (h)
ΔihfA
10mM glucose
ΔihfA
15mM fumarate
ΔihfB
10mM glucose
ΔihfB
15mM fumarate
Δhns
10mM glucose
Δhns
15mM fumarate

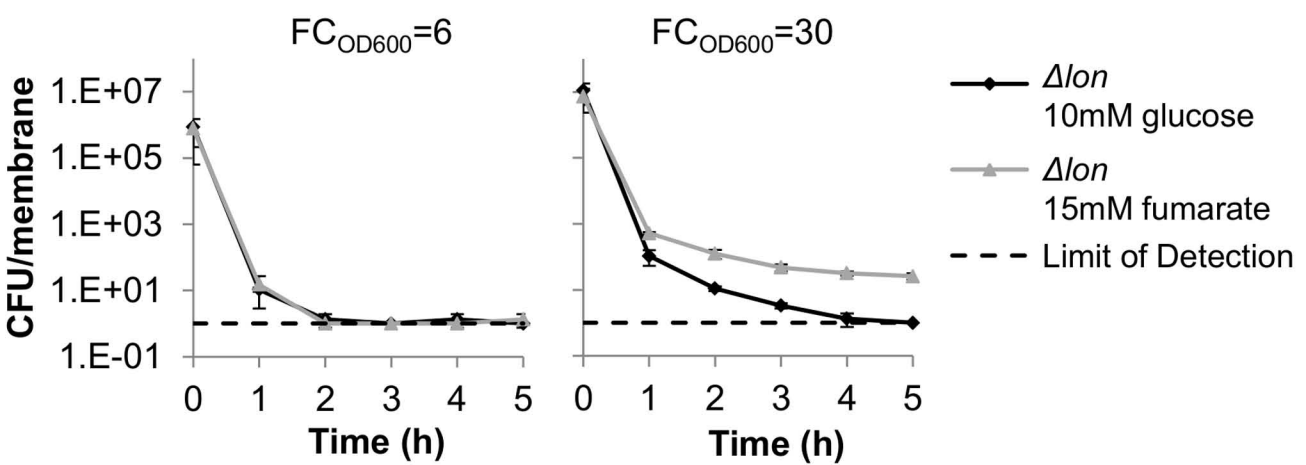
FC$_{OD600}$=6
FC$_{OD600}$=30
CFU/membrane
1.E+07
1.E+05
1.E+03
1.E+01
1.E-01
0
1
2
3
4
5
Time (h)
Time (h)
Δlon
10mM glucose
Δlon
15mM fumarate
Limit of Detection

Please cite this article in press as: Amato et al., Metabolic Control of Persister Formation in *Escherichia coli*, Molecular Cell (2013), http://dx.doi.org/10.1016/j.molcel.2013.04.002

Molecular Cell
Article

Metabolic Control of Persister Formation in *Escherichia coli*

Stephanie M. Amato,[1] Mehmet A. Orman,[1] and Mark P. Brynildsen[1,*]
[1]Department of Chemical and Biological Engineering, Princeton University, Princeton, NJ 08544, USA
*Correspondence: mbrynild@princeton.edu
http://dx.doi.org/10.1016/j.molcel.2013.04.002

SUMMARY

Bacterial persisters are phenotypic variants that form from the action of stress response pathways triggering toxin-mediated antibiotic tolerance. Although persisters form during normal growth from native stresses, the pathways responsible for this phenomenon remain elusive. Here we have discovered that carbon source transitions stimulate the formation of fluoroquinolone persisters in *Escherichia coli*. Further, through a combination of genetic, biochemical, and flow cytometric assays in conjunction with a mathematical model, we have reconstructed a molecular-level persister formation pathway from initial stress (glucose exhaustion) to the activation of a metabolic toxin-antitoxin (TA) module (the ppGpp biochemical network) resulting in inhibition of DNA gyrase activity, the primary target of fluoroquinolones. This pathway spans from initial stress to antibiotic target and demonstrates that TA behavior can be exhibited by a metabolite-enzyme interaction (ppGpp-SpoT), in contrast to classical TA systems that involve only protein and/or RNA.

INTRODUCTION

Bacterial persisters are rare, transient phenotypic variants with the ability to tolerate supralethal concentrations of antibiotics (Balaban et al., 2004; Lewis, 2010). This phenotype is characterized by a biphasic kill curve, where the first, rapid killing regime represents the death of normal cells and the second, slower killing regime indicates the presence of persisters (Keren et al., 2004; Lewis, 2010). Persisters are distinct from antibiotic-resistant cells, as their tolerances are not genetically defined. Persisters are particularly important for biofilm infections, where they are thought to underlie the propensity of such infections to relapse after the conclusion of antibiotic therapy (Lewis, 2010). The antibiotic tolerances of persisters have been attributed to transient inhibition of functions targeted by antibiotics, and although the molecular mechanisms that mediate such inhibitions remain ill defined, current research suggests that diverse stresses acting through a multitude of toxin-antitoxin (TA) modules form persisters (Dörr et al., 2010; Lewis, 2010). TA modules are attractive as terminal effectors of persistence for three reasons: (1) toxins have the ability to halt growth, thus reducing the activity of antibiotic targets (Yamaguchi and Inouye, 2011); (2) overexpression of toxins in excess of their cognate antitoxins has been shown to increase antibiotic tolerance (Dörr et al., 2010; Kim and Wood, 2010; Lewis, 2010; Vázquez-Laslop et al., 2006); and (3) TA modules exhibit bistability, the ability to produce two steady states in a clonal population (normal and persister cells) (Dubnau and Losick, 2006; Rotem et al., 2010). Each TA module is hypothesized to respond to a specific set of stresses, potentially resulting in persister heterogeneity (Allison et al., 2011; Lewis, 2010). Stresses that have been shown to form persisters can be classified into two groups, those that are from exogenous sources (e.g., antibiotic treatment), which we will call foreign stresses, and those that bacteria experience during normal growth, and thus are self-imposed (e.g., starvation), which we will call native stresses.

Dörr and colleagues have identified the most complete foreign stress persister formation pathway to date, from an initial exogenous stress (ciprofloxacin) through its signal transduction pathway (RecA, LexA) to the source of antibiotic tolerance (TisB and ATP depletion) (Dörr et al., 2010). Additional pathways originating from foreign stresses, such as acid treatment, heat shock, and oxidative stress, have been elucidated to varying degrees (Hong et al., 2012; Leung and Lévesque, 2012; Wu et al., 2012); these studies highlight the diversity of stress treatments that can form persisters.

The most complete native pathway was presented by Nguyen and colleagues, who found that the stringent response of *Pseudomonas aeruginosa* facilitated persister formation in stationary-phase and biofilm cultures by controlling reactive oxygen species metabolism (Nguyen et al., 2011). Though important mediators of this pathway were identified, a mechanistic connection from native stress to the source of bistability in antibiotic tolerance was not identified. Additional studies have found that quorum sensing, nutrient limitation, growth phase, and the biofilm lifestyle all impact persister formation (Fung et al., 2010; Grant et al., 2012; Lewis, 2010; Möker et al., 2010; Vega et al., 2012). These studies provide a wealth of knowledge on the types of native stresses that form persisters, but the mechanistic pathways that underlie the formation of persisters during normal growth remain elusive.

Inspired by previous work that found that *Escherichia coli*, *P. aeruginosa*, and *Staphylococcus aureus* persisters largely form during mid- to late-exponential phase (Keren et al., 2004), we sought to understand the molecular mechanisms by which persisters form during normal growth. During the mid- to late-exponential phase in rich media, complex nutrient transitions occur (Prüss et al., 1994; Sezonov et al., 2007), oxygen becomes

Please cite this article in press as: Amato et al., Metabolic Control of Persister Formation in *Escherichia coli*, Molecular Cell (2013), http://dx.doi.org/10.1016/j.molcel.2013.04.002

limiting and its concentration continues to decline (Tolosa et al., 2002), and higher-density phenotypes such as quorum sensing appear (Surette and Bassler, 1998). Since diverse formation mechanisms may be present, we focused on a single native stress in isolation and sought to answer the fundamental question of whether carbon source transitions stimulate persister formation, and if so, what is the underlying molecular mechanism. To accomplish this, we studied batch growth of *E. coli* in defined minimal media containing one or more carbon sources. By measuring persister levels and metabolite concentrations and using genetic perturbations, flow cytometry, and a mathematical model, we have reconstructed a mechanistic persister formation pathway from initial stress (glucose exhaustion) to a metabolic TA module, the metabolite guanosine tetraphosphate (ppGpp) and its biochemical network, and its inhibition of DNA gyrase, the primary target of fluoroquinolone antibiotics. In this pathway, ppGpp acts as the toxin, whereas SpoT, the sole ppGpp hydrolase in *E. coli*, plays the role of the antitoxin. Conventionally, TA modules are comprised of protein and/or RNA components (Wang et al., 2012; Yamaguchi and Inouye, 2011), whereas this work suggests that metabolic networks can exhibit TA-like behavior including bistability. The results described here identify a comprehensive pathway responsible for persister formation under normal growth conditions and suggest that TA-like metabolic networks may play a significant role in persister formation.

RESULTS

Diauxic Shifts Stimulate Persister Formation

When bacteria are grown in a batch culture containing two carbon sources, they exhibit a range of consumption patterns including diauxic growth and non-diauxic growth (Monod, 1942). Diauxie is characterized by exponential growth on the preferred carbon source, a growth-arrested lag phase, followed by exponential growth on the secondary carbon source (Roseman and Meadow, 1990). Non-diauxic growth can still exhibit preferential substrate consumption, while lacking the intermediate lag phase (Clark and Holms, 1976; Narang and Pilyugin, 2007), but can also result from coutilization (Bächi and Kornberg, 1975). Since persisters have been observed to form during periods of complex nutrient transitions, including shifts in carbon source (Keren et al., 2004; Prüss et al., 1994), we sought to determine if carbon source transitions stimulate persister formation.

E. coli persister levels were measured using ofloxacin (OFL) or ampicillin (AMP) throughout growth on a panel of defined minimal media containing one or two carbon sources. In *E. coli*, glucose is the preferred carbon source, preventing the consumption of most other carbon sources (Narang and Pilyugin, 2007). Therefore, glucose was used as the primary carbon source, and secondary carbon sources that are diauxic or non-diauxic with glucose were tested. Growth of all media diverged at ~0.08 optical density 600 (OD_{600}), which corresponds to the point of glucose exhaustion (Figure S1). It was observed that diauxic media exhibited an increase in persisters to OFL upon glucose exhaustion compared to the sole glucose control (Figure 1A). The non-diauxic secondary carbon source, fructose (Clark and Holms, 1976), as well as the coutilized gluconate (Bächi and Kornberg, 1975) did not exhibit an increase in persisters to OFL after glucose exhaustion. These results suggested that diauxic transitions stimulated formation of persisters to OFL. Results using AMP were similar, except that the diauxic cultures containing lactose or arabinose did not result in an increase in persisters compared to the glucose-only control (Figure S1). This suggested that separate mechanisms were likely present; therefore, we chose to focus on persisters to OFL for the remainder of this study.

To analyze this phenomenon further, we focused on diauxic growth in glucose-fumarate, since it elicited the strongest persister formation response, and growth in glucose-fructose, since it is non-diauxic and not coutilized. Persister measurements were taken during growth on glucose (0.02 OD_{600}) and after glucose exhaustion (0.12 OD_{600}). During exponential growth on glucose, all persister levels were the same, independent of the secondary carbon source present (Figure 1B). Persister measurements during exponential growth on the secondary carbon source showed a statistically significant ~50-fold increase in persisters for the glucose-fumarate culture and a statistically insignificant <2-fold increase for the glucose-fructose cultures when compared to persister levels in glucose-only culture at the same OD_{600}.

To establish that the increase in persisters was due to the transition from glucose to fumarate and not from the slower growth on fumarate, persister measurements were taken at the same cell densities during growth on fumarate as the sole carbon source (Figure 1C). The persister levels for the culture grown in fumarate-only media were 2.8-fold higher than and not statistically different from persister levels for glucose-only media, but were 15-fold lower than and statistically different from those for the glucose-fumarate media, which suggests the increase in persisters was a result of the carbon source transition rather than slower growth on fumarate.

Addition of cAMP and Bacteriostatic Agents Increase Persister Levels

We next sought to identify whether the mediators of carbon source diauxie play a role in the observed persister formation. Upon glucose limitation, two major signaling pathways are initiated, catabolite repression is released, and the stringent response is activated (Traxler et al., 2006). Adenylate cyclase (*cyaA*) is activated to synthesize cyclic AMP (cAMP), which binds to the cAMP receptor protein (CRP) to activate promoters of proteins required to metabolize carbon sources that were subject to catabolite repression (Saier et al., 1996). ppGpp synthesized by RelA and SpoT destabilizes open complex formation and represses expression of stable RNA through its interaction with RNA polymerase (RNAP) and DksA (Ferullo and Lovett, 2008; Lemke et al., 2011; Murray and Bremer, 1996). Unfortunately, Δ*cyaA* and Δ*crp* prevent resumption of growth after diauxie (Traxler et al., 2006), and *ΔrelAΔspoT* and *ΔdksA* strains are auxotrophic (Potrykus et al., 2011). Therefore, we tested whether synthetically increasing cAMP or ppGpp leads to persister formation.

Addition of cAMP to a culture growing in glucose minimal media generated a statistically significant ~20-fold increase in persisters when compared to the untreated wild-type culture, confirming that this molecule has the ability to signal persister formation (Figure 2A). This effect was absent in a *Δcrp* mutant

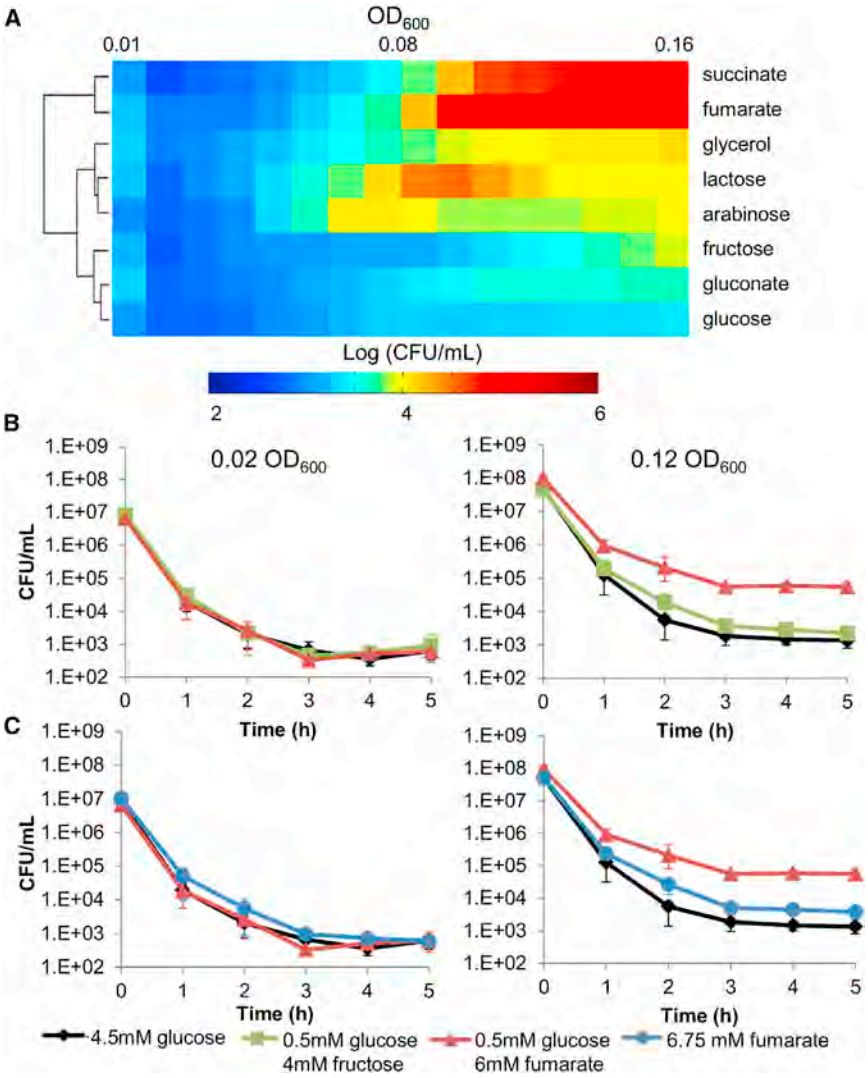

Figure 1. Diauxic Shift Stimulates Persister Formation

(A) *E. coli* were grown on glucose and a panel of secondary carbon sources. At hourly time points, aliquots of culture were removed, challenged with 5 μg/mL OFL for 4 hr, washed, and plated to measure cfu. To construct the color plot as a function of OD_{600}, cfu/mL values were interpolated from two adjacent measurements to plot persister values at the designated OD_{600}.

(B) Diauxic growth (glucose-fumarate, red) results in significant persister formation ($p < 0.05$), whereas non-diauxic growth does not ($p > 0.05$) (glucose, black; glucose-fructose, green).

(C) Growth on fumarate is not responsible for persister formation in glucose-fumarate media, as evidenced by sole fumarate control (blue). Data are averages of ≥ three independent experiments, error bars indicate data range, and significance was assessed using the null hypothesis that the mean cfu levels in two sample sets were equal. See also Figure S1.

(Figure 2B), which suggests that cAMP-CRP (cAMP receptor protein) activity was essential to persister formation. Interestingly, cAMP-CRP activates expression of RelA and DksA (Keseler et al., 2013). Therefore, we measured persister levels in response to cAMP addition in minimal glucose media supplemented with minimal concentrations of the amino acids (aa) *ΔrelAΔspoT* and *ΔdksA* require for growth (Potrykus et al., 2011). In the aa-supplemented media, wild-type cells exhibited a comparable increase in persister levels when treated with cAMP, whereas *ΔrelAΔspoT* and *ΔdksA* eliminated persister formation (Figures 2C, 2D, and S2). Removal of persister formation in these strains suggests a role for ppGpp and DksA in persister formation downstream of cAMP-CRP.

We investigated whether increased ppGpp levels, independent of cAMP, can stimulate persister formation. Serine hydroxamate (SHX), which rapidly increases intracellular ppGpp, was used to induce the stringent response (Ferullo and Lovett, 2008). However, SHX causes bacteriostasis (Tosa and Pizer, 1971), and growth inhibition alone increases antibiotic tolerance (Eng et al., 1991). As a control, we used chloramphenicol (CAM), which is also bacteriostatic but does not increase ppGpp (Rodionov and Ishiguro, 1995). A roughly 100-fold increase in persisters occurred after both SHX and CAM treatment (Figure 3A). To test if the effect of SHX was independent of ppGpp, we treated a *ΔrelAΔspoT* culture with SHX. The *ΔrelAΔspoT* strain exhibited a 15.5-fold increase in persisters after SHX treatment that was comparable to and not statistically distinguishable from the 13.2-fold increase in persisters for wild-type in analogous conditions (Figures 3B and 3C). These data suggest that multiple formation pathways may exist during diauxic transitions, since increases in cAMP and ppGpp, as well as growth inhibition, are present.

Persisters from Carbon Source Transitions Form through a ppGpp-Dependent Mechanism

We sought to separate persister formation due to growth inhibition from that of cAMP and ppGpp. To do this, we recognized that the aa supplementation required for growth of *ΔrelAΔspoT* and *ΔdksA* strains removes the lag phase associated with diauxie (Traxler et al., 2006), but glucose exhaustion and a transition to growth on fumarate still occur (Table S1 and Figure S3). In aa-supplemented media, persister measurements were taken during growth on glucose (0.02 OD_{600}) and after glucose exhaustion (0.20 OD_{600}). During exponential growth on glucose, persister levels were the same regardless of growth in either glucose or glucose-fumarate (Figure 4). After transitioning to growth on fumarate, a statistically significant increase in persister levels of ~20-fold, compared to the glucose-only control, was observed for wild-type (Figure 4A). This demonstrates

Please cite this article in press as: Amato et al., Metabolic Control of Persister Formation in *Escherichia coli*, Molecular Cell (2013), http://dx.doi.org/10.1016/j.molcel.2013.04.002

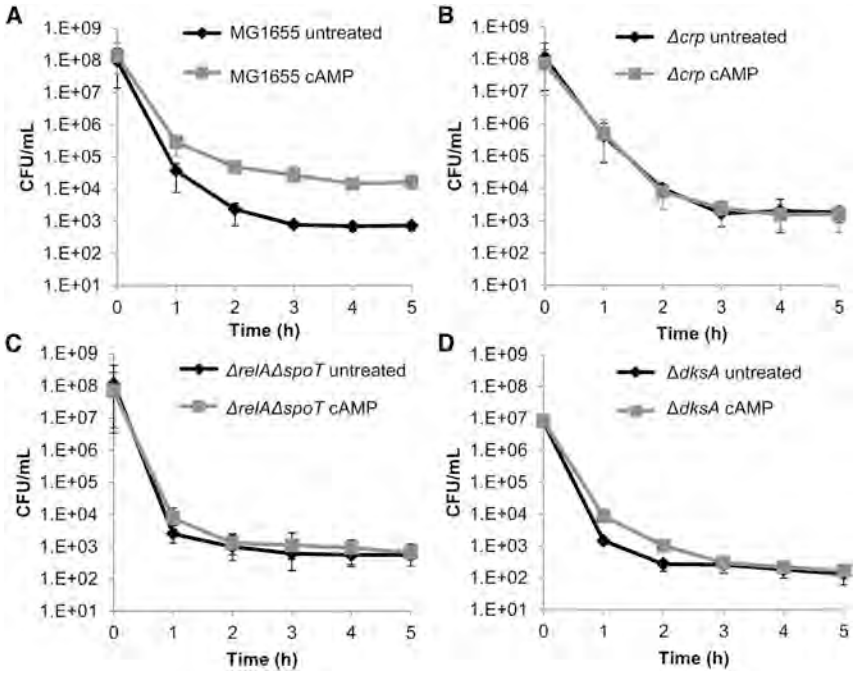

Figure 2. Role of cAMP Addition on Persistence

(A–D) At 0.02 OD_{600}, all strains were exposed to either 8 mM cAMP or no treatment. After 2 hr, survival to 5 μg/mL OFL was measured. Wild-type (A) exhibited a significant increase in persisters due to cAMP ($p < 0.05$) while *Δcrp* (B) did not. Amino acid supplementation was added to minimal media to allow growth of *ΔrelAΔspoT* (C) and *ΔdksA* (D). Wild-type measurements in the same media are provided in Figure S2. Data are averages of ≥ three independent experiments, error bars indicate data range, and significance was assessed using the null hypothesis that the mean cfu levels in two sample sets were equal.

that the carbon source transition in the absence of a diauxic lag was sufficient to stimulate persister formation. Amino acid supplementation did decrease the persister jump by ~2-fold, suggesting that growth arrest does participate in persister formation during diauxic transitions.

To explore if the cAMP-ppGpp pathway we identified plays a role in persister formation during normal growth, we measured persisters prior to and after glucose exhaustion in the aa-supplemented media for *ΔrelA*, *ΔrelAΔspoT*, and *ΔdksA*. Analogous to the diauxic media, Δ*cyaA* and Δ*crp* strains cannot resume growth on fumarate after glucose exhaustion, even in the presence of aa, so these genetic knockouts could not be tested. However, using a cAMP-CRP reporter plasmid (P*malK-gfp*), we performed fluorescence-activated cell sorting (FACS) experiments to confirm that cAMP-CRP activity increased upon glucose exhaustion in glucose-fumarate aa-supplemented media in both normal and persister cells (Figure S3 and Supplemental Experimental Procedures).

Deletions either of both ppGpp synthases or of DksA exhibited statistically significant attenuation of persister formation (Figures 4B, 4C, and 4D). Wild-type exhibited an increase of ~20-fold in persisters as a result of the carbon source transition, whereas *ΔrelA*, *ΔrelAΔspoT*, and *ΔdksA* exhibited 4-fold, 1.8-fold, and 1.5-fold increases in persisters, respectively. These results suggest that both ppGpp and DksA are essential to trigger persister formation during native carbon source transitions and that both RelA and SpoT contribute to ppGpp synthesis and persister formation under these experimental conditions.

ppGpp Biochemical Network Forms a Toxin-Antitoxin Module

With the roles of ppGpp and DksA confirmed, we sought to identify downstream components of the pathway. Unfortunately, ppGpp and DksA act as global regulators of gene expression through their interactions with RNAP (Keseler et al., 2013). Given this complexity, we focused first on identifying the terminal effector of persistence that enables bistable antibiotic tolerance under our experimental conditions. TA modules are commonly considered terminal effectors of persistence due to their bistable architecture and ability to inhibit growth. Therefore, we tested toxins that were most likely to be involved due to their relevance to persistence or association with ppGpp, cAMP, or the SOS response (Table S2). Toxins associated with the SOS response were considered due to their relevance for ciprofloxacin-induced persisters (Dörr et al., 2010), though we note that neither cAMP nor glucose exhaustion stimulated the SOS response in normal or persister cells as measured by FACS and a P*sulA-gfp* reporter plasmid (Figure S3 and Supplemental Experimental Procedures).

All toxin deletions tested exhibited an increase in persisters after carbon source transition that was quantitatively comparable and statistically indistinguishable from that of wild-type (Figure S4). These data suggest that none of the most likely TA modules are solely responsible for the ppGpp-dependent persister formation observed. We note that redundancy between TA modules has been shown to impact persistence (Maisonneuve et al., 2011) and that testing of single toxin deletions cannot rule out the possibility that multiple TA modules may be involved.

Interestingly, we observed that the biochemical reaction network of ppGpp includes a double-negative feedback loop (Figure 5A), a network architecture that can exhibit bistability (Dubnau and Losick, 2006). Furthermore, ppGpp can cause growth arrest through its interaction with RNAP (Potrykus and Cashel, 2008), and SpoT, the sole ppGpp hydrolase, cannot be knocked out in a *relA*+ background (An et al., 1979). Given that these are typical TA module characteristics (Wang and Wood, 2011; Yamaguchi and Inouye, 2011), we reasoned that the source of bistable antibiotic tolerance may lie in the ppGpp biochemical network, where ppGpp plays the role of a metabolite toxin with SpoT as its enzymatic antitoxin.

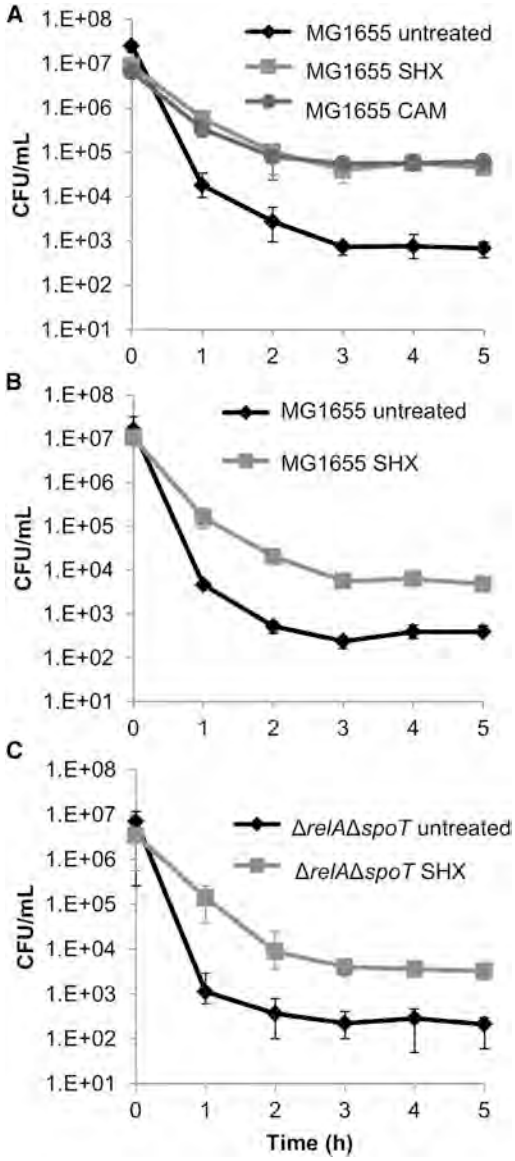

Figure 3. Role of Increased ppGpp from Serine Hydroxamate on Persistence

(A) Wild-type at 0.02 OD_{600} were exposed to either 1 mg/mL SHX, 50 μg/mL CAM, or no treatment. After 2 hr, the survival of the culture to 5 μg/mL OFL was measured.

(B and C) Cultures of wild-type (B) and Δ*relA*Δ*spoT* (C) strains were exposed to either 1mg/mL SHX or no treatment. aa-supplemented minimal media was used for both wild-type and Δ*relA*Δ*spoT*. After 2 hr, the survival of the culture to 5 μg/mL OFL was measured. Data are averages of ≥ three independent experiments, and error bars indicate data range.

To establish whether the ppGpp biochemical network can exhibit TA-like behavior, we constructed a kinetic model of the network and performed a bistability analysis (Supplemental Experimental Procedures). A typical result for bistability can be obtained, as shown in Figure 5B, with a set of physiological parameters (Tables S3 and S4). The dependence of bistability on parameter values is discussed within the Supplemental Experimental Procedures. Three steady states are present as denoted by the intersection of the nullclines. As can be seen by the projection of the phase space trajectories on the (SpoT, ppGpp) plane, two of the steady states are stable, whereas the intermediate steady state is not. One stable solution is characterized by high SpoT concentration and low ppGpp concentration, characteristic of exponentially growing *E. coli* where the ppGpp/cell can range from ~5,700–34,000 (Murray and Bremer, 1996), whereas the other stable solution is characterized by low SpoT concentration and high ppGpp concentration, corresponding to the persister state (Table S5). The ppGpp concentration is 9.9×10^5 molecules/cell in the persister state, which is beyond the population-wide average of *E. coli* upon glucose exhaustion, 2.5×10^5 molecules/cell (Murray and Bremer, 1996), but within physiological limits, since triggering the stringent response with pseudomonic acid has produced similar levels (Baracchini and Bremer, 1988). These mathematical results suggest that persisters represent an outlier population with significantly higher intracellular levels of ppGpp.

To corroborate the results of the mathematical model with experimental data, we used FACS and two stringent response reporter plasmids, P*wrbA-gfp* and P*osmE-gfp*, to measure ppGpp in the general bacterial population and persisters (Supplemental Experimental Procedures). The promoters of *wrbA* and *osmE* are known to be activated by ppGpp (Durfee et al., 2008; Traxler et al., 2011), and we demonstrated that each reported on ppGpp levels under the experimental conditions investigated by confirming that *ΔrelAΔspoT* eliminated the increased fluorescence observed from P*wrbA-gfp* and P*osmE-gfp* in response to glucose-fumarate transitions in aa-supplemented media (Figure S4). Using these ppGpp reporters, we sorted wild-type populations with FACS and collected the highest and lowest 10% quantiles, as has been done previously in a persistence study with P*tnaC-gfp* (Vega et al., 2012). Since both P*wrbA-gfp* and P*osmE-gfp* increase fluorescence in response to ppGpp, the highest 10% of the population contains cells with high ppGpp levels, whereas the lowest 10% contains cells with low ppGpp. As depicted in Figure 5, cells with high ppGpp levels exhibited statistically significant higher levels of persistence than cells with low ppGpp levels.

To provide additional evidence supporting the role of ppGpp and SpoT as a persister-generating metabolic TA module, we sought to demonstrate that high levels of ppGpp in excess of its antitoxin, SpoT, produced bacteriostasis and increased persistence, whereas high-level expression of SpoT could rescue growth and inhibit persister formation. To do this, we constructed two plasmids that enabled orthogonal control of RelA′ and SpoT expression with isopropyl β-D-1-thiogalactopyranoside (IPTG) and arabinose, respectively (Supplemental Experimental Procedures). Induction with IPTG in the absence of arabinose with pBAD-*spoT* or in the presence of arabinose with the pBAD-empty vector control produced bacteriostasis, whereas expression of SpoT with arabinose rescued growth (Figure 5G). Further, we demonstrate that ppGpp, in excess of its antitoxin, significantly increases persistence by over

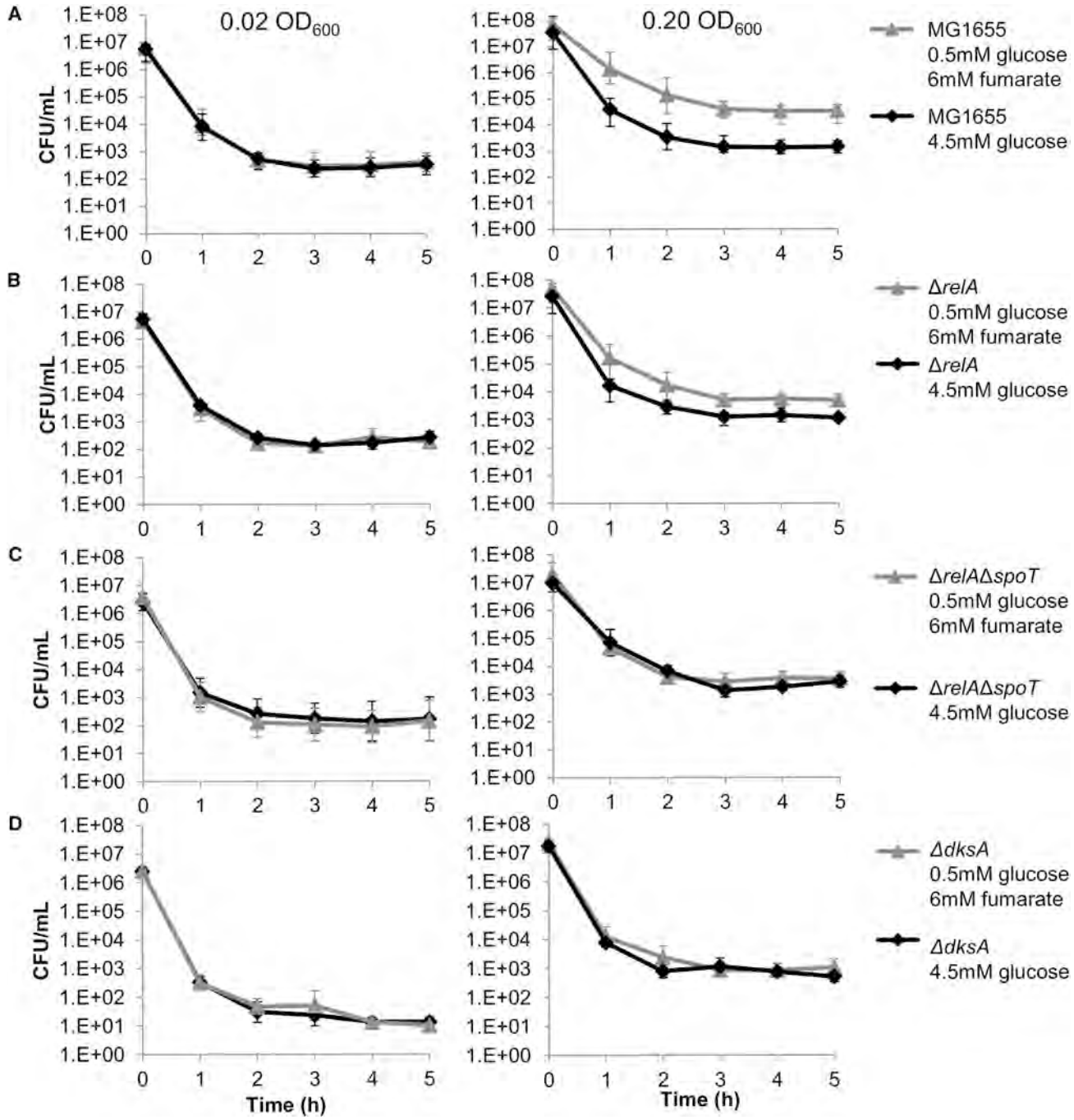

Figure 4. Carbon Source Transitions Independent of Growth Arrest Stimulate Persisters through a ppGpp-Dependent Pathway

Cells were grown in aa-supplemented minimal media and challenged with 5 μg/mL OFL at 0.02 OD_{600} and 0.20 OD_{600}, representing growth on glucose and growth after glucose exhaustion, respectively (except for 4.5 mM glucose sample). Wild-type (A) exhibited an increase in persisters after the transition from glucose to fumarate; *ΔrelA* (B) exhibited a significantly reduced increase in persister formation compared to wild-type ($p < 0.05$); Δ*relA*Δ*spoT* (C) and *ΔdksA* (D) strains exhibited nearly no increase in persister levels after glucose exhaustion compared to wild-type ($p < 0.05$). Data are averages of ≥ three independent experiments, error bars indicate data range, and significance was assessed using the null hypothesis that the mutant mean fold change in persisters was equal to the wild-type fold change in persisters. See also Figure S3 and Table S1.

100-fold (Figure 5H). These experiments, in conjunction with an inability to remove the antitoxin gene in a genetic background with the toxin, are commonly used to identify TA modules (Brown and Shaw, 2003; Christensen-Dalsgaard et al., 2010) and therefore provide strong evidence that ppGpp-SpoT functions as a TA module.

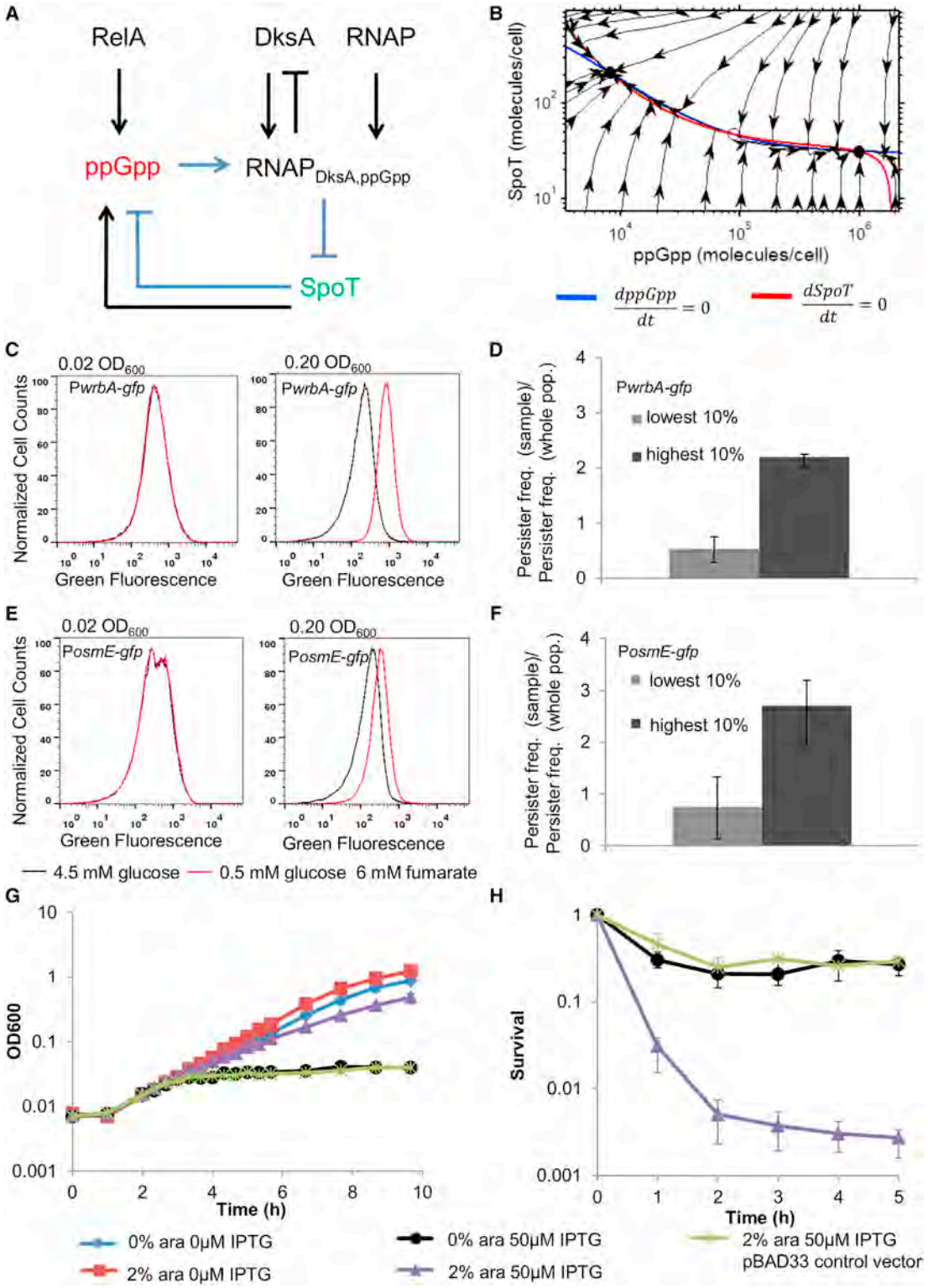

Figure 5. ppGpp-SpoT Biochemical Network as a Metabolic TA Module

(A) Within the ppGpp biochemical network is a double-negative feedback loop (blue). The toxin is ppGpp (red) and the antitoxin is SpoT (green).

(B) Blue and red curves are nullclines of equations S15 and S16 (see Supplemental Experimental Procedures). Phase space trajectories are shown in the plane (SpoT, ppGpp). Filled circles indicate stable steady states; open circle indicates an unstable steady state. The initial DksA concentration was 5,000 molecules/cell for each trajectory, and parameters used are given in Tables S3 and S4.

(legend continued on next page)

Please cite this article in press as: Amato et al., Metabolic Control of Persister Formation in *Escherichia coli*, Molecular Cell (2013), http://dx.doi.org/10.1016/j.molcel.2013.04.002

ppGpp-Dependent Persister Formation Requires Nucleoid Proteins

We sought to identify how high ppGpp levels led to tolerance toward OFL, an antibiotic that targets DNA gyrase (Maxwell, 1997). DNA gyrase is the sole enzyme responsible for negative supercoiling of DNA (Nöllmann et al., 2007), which is important for the initiation and elongation phases of transcription and DNA replication. The bactericidal activity of fluoroquinolones has been attributed to their ability to bind DNA gyrase during the negative supercoiling process and cause DNA double-strand breaks (Maxwell, 1997). We reasoned that through inhibition of transcription, DNA replication, and/or DNA gyrase negative supercoiling activity, tolerance to OFL could be achieved. Interestingly, ppGpp inhibits all three of these processes. ppGpp-DksA destabilizes RNAP-open complexes at promoters that transcribe stable RNA and numerous proteins (Potrykus and Cashel, 2008), ppGpp has been shown to inhibit DNA replication through an interaction with SeqA (Ferullo and Lovett, 2008), and high levels of ppGpp lead to overall relaxation of the chromosome, an indicator of reduced DNA gyrase activity (Ferullo and Lovett, 2008). Given these possibilities, we sought to identify those that are important for ppGpp-mediated persister formation.

We note that results presented in the preceding sections involving DksA demonstrate that the effect of ppGpp on transcription is required to form OFL persisters from carbon source transitions. To determine whether the effect of ppGpp on DNA replication contributes to persister formation, we tested mutants of CspD, SeqA, and Dam. CspD is a chromosomal inhibitor of DNA replication that previously had been implicated in bacterial persistence (Kim and Wood, 2010), and its deletion did not alter persister formation (Figure S5). SeqA is a protein that binds hemimethylated GATC sites to block initiation of DNA replication prior to full methylation by Dam (Brendler and Austin, 1999; Campbell and Kleckner, 1990). Removing SeqA and Dam abolishes stringent control of DNA replication, though the exact mechanism by which this occurs remains unknown (Ferullo and Lovett, 2008). Here we found that *ΔseqA* significantly reduced persister formation in response to glucose-fumarate transitions in aa-supplemented media, whereas *Δdam* did not alter persister formation (Figure S5). This was interesting, as ppGpp replication control was previously eliminated by both Δ*seqA* and Δ*dam* (Ferullo and Lovett, 2008). However, SeqA has an additional function as a modulator of topoisomerase activity, including that of DNA gyrase at high concentrations (Kang et al., 2003).

Topoisomerases, including DNA gyrase, work together with nucleoid-associated proteins (NAPs) to control the degree of chromosomal negative supercoiling (Travers and Muskhelishvili, 2005). DNA gyrase adds negative supercoiling, other topoisomerases relax the chromosome, and NAPs bind negatively supercoiled DNA to various degrees and affinities (Travers and Muskhelishvili, 2005). We note that chromosome relaxation occurs upon accumulation of ppGpp and that this represents DNA gyrase inhibition and/or increased activity of topoisomerases I, III, or IV (Ferullo and Lovett, 2008). Since the mechanism of ppGpp-dependent chromosome relaxation has not been delineated, we tested if DNA gyrase inhibitors, SbmC and YacG, participate in the persister formation we observe. We found that in both Δ*sbmC* and Δ*yacG*, persister formation was comparable to and not statistically different from that of wild-type (Figure S5). Given the role of NAPs in negative supercoiling, we tested mutants of the four major NAPs: FIS, HNS, HU, and IHF (Mott and Berger, 2007). We found that Δ*fis*, Δ*ihfA*, Δ*ihfB*, Δ*hupA*, and Δ*hupB* all significantly attenuated persister formation (Figure 6). These results demonstrate that FIS, HU, and IHF are all required for ppGpp to generate the majority of persisters formed in response to carbon source transitions. We note that persister levels for Δ*fis*, Δ*hupA*, and Δ*hupB* were lower than wild-type in cultures at 0.02 OD_{600} but comparable to wild-type in glucose-only cultures at 0.20 OD_{600}, where the effect of carbon source transitions was assessed. In combination with results from Δ*seqA* and previous reports that the stringent response results in chromosome relaxation (Ferullo and Lovett, 2008), these data suggest that ppGpp enables tolerance to OFL, due in part to its effect on the process of negative supercoiling.

DISCUSSION

Many studies that identify genes whose presence or absence alters persister levels have been conducted on stationary-phase or biofilm bacteria (Hansen et al., 2008; Luidalepp et al., 2011; Nguyen et al., 2011; Vega et al., 2012), presumably because that is when persisters are in the greatest abundance (Keren et al., 2004). The realization that persisters form from a multitude of stresses acting through separate TA modules suggests that persister populations in later growth stages are likely heterogeneous, containing distinct persisters from the various stresses encountered during normal growth (Allison et al., 2011; Lewis, 2010). Such complex samples would prove difficult to unravel, as removal of a single pathway may not significantly lower the total persister population by an amount that is readily observable. To identify the molecular pathways responsible for persister formation from normal growth, native stresses should be studied in isolation under defined conditions. Adopting this methodology, we identified the molecular mediators of a persister formation cascade stimulated by carbon source transitions, a stress that is commonly present in planktonic and biofilm cultures (Prüss

(C) P*wrbA-gfp* GFP distribution at 0.02 OD_{600} and 0.20 OD_{600} in glucose-fumarate and glucose media with aa supplementation.
(D) P*wrbA-gfp* persister frequency of sorted cells relative to persister frequency in the whole population was significantly increased in the highest 10% compared to the lowest 10% of the distribution ($p < 0.05$).
(E) P*osmE-gfp* GFP distribution at 0.02 OD_{600} and 0.20 OD_{600} in glucose-fumarate and glucose media with aa supplementation.
(F) P*osmE-gfp* persister frequency of sorted cells relative to persister frequency in the whole population was significantly increased in the highest 10% compared to the lowest 10% of the distribution ($p < 0.05$).
(G) Growth of Δ*relA*Δ*spoT* carrying RelA′ and SpoT overexpression plasmids under different induction conditions.
(H) Cells were grown 2 hr after RelA′ induction and challenged with 5 μg/mL OFL. Data are averages of ≥ three independent experiments, error bars indicate data range, and significance was assessed using the null hypothesis that the mean persister level relative to the whole population in the lowest 10% was equal to the mean persister level relative to the whole population in the highest 10%. See also Figure S4 and Tables S3–S5.

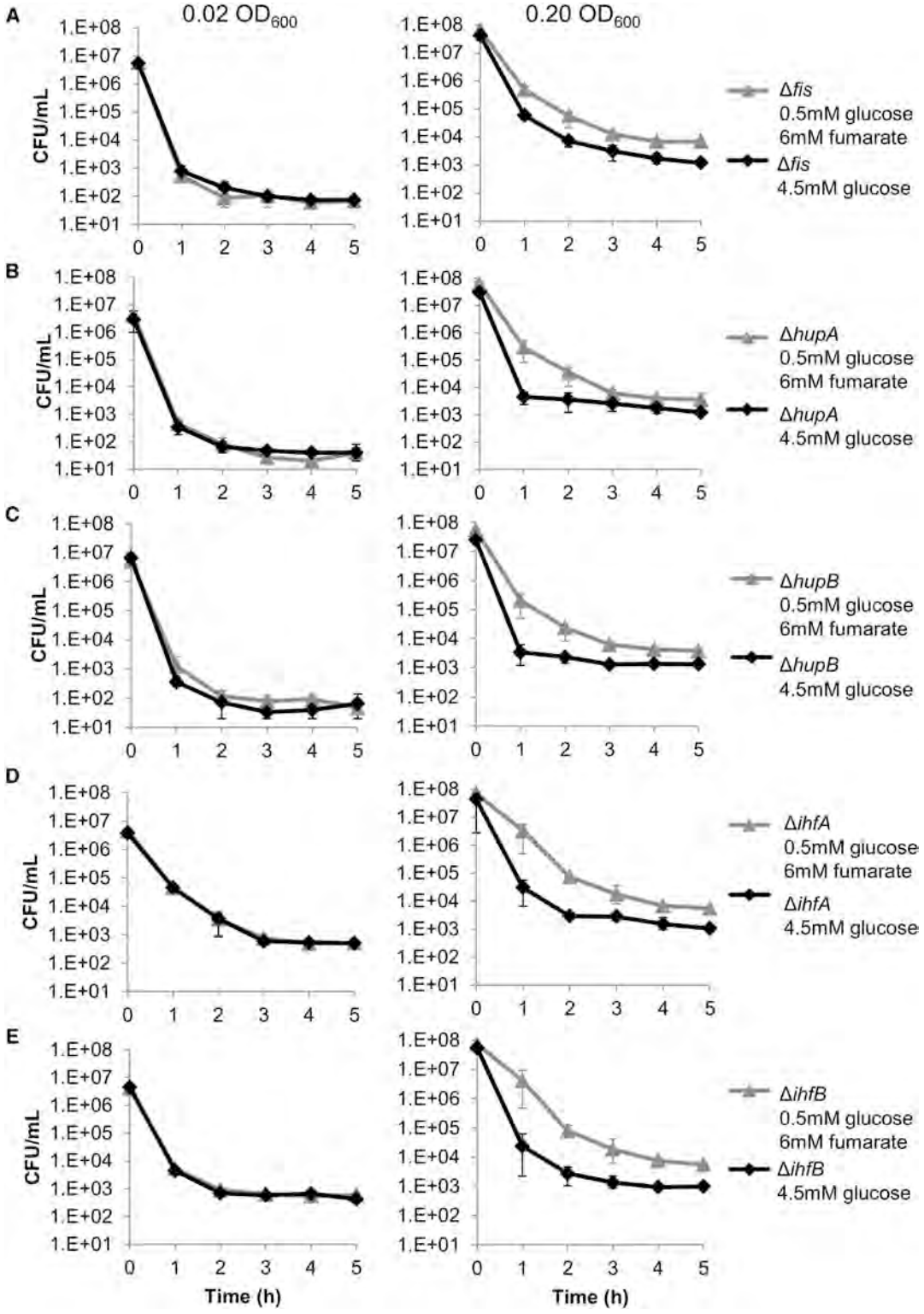

Figure 6. Nucleoid Proteins Facilitate ppGpp-Dependent Persister Formation

(A–E) Cells grown in aa-supplemented minimal media were challenged with 5 μg/mL OFL at 0.02 OD_{600} and 0.20 OD_{600}. Components of three major NAPs (Δ*fis* [A], Δ*hupA* [B], Δ*hupB* [C], Δ*ihfA* [D], Δ*ihfB* [E]) significantly reduced persister formation when compared to wild-type ($p < 0.05$). Data are averages of ≥ three independent experiments, error bars indicate data range, and significance was assessed using the null hypothesis that the mutant mean fold change in persisters was equal to the wild-type fold change in persisters. See also Figure S5 and Table S2.

Please cite this article in press as: Amato et al., Metabolic Control of Persister Formation in *Escherichia coli*, Molecular Cell (2013), http://dx.doi.org/10.1016/j.molcel.2013.04.002

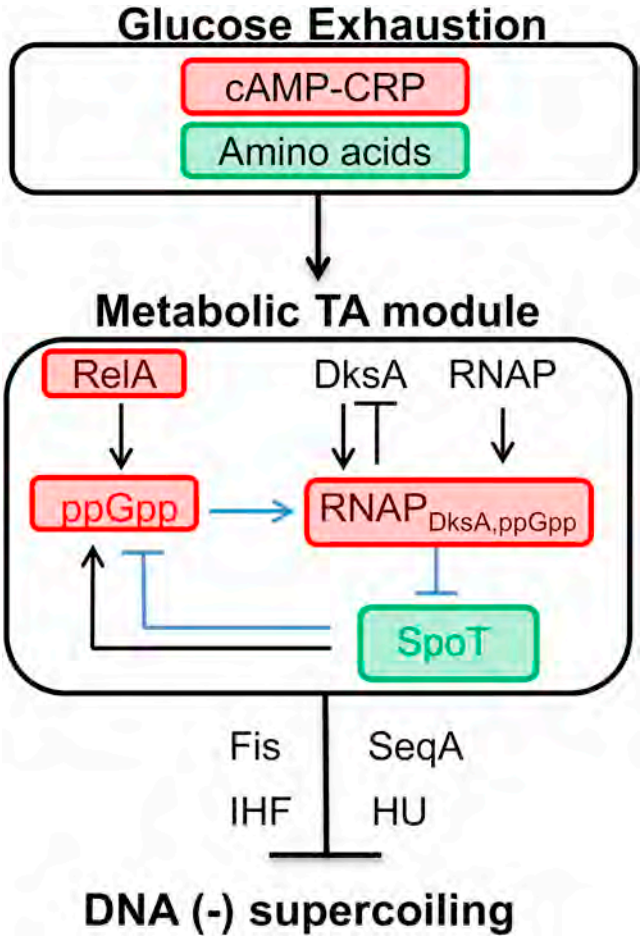

Figure 7. Model of Fluoroquinolone Persister Formation from Carbon Source Transitions

Upon glucose exhaustion, cAMP levels increase and aa limitation occurs. One or both of these events trigger the activation of the ppGpp-SpoT metabolic TA module. Increased ppGpp leads to increased DksA-dependent repression of RNAP activity. Increased ppGpp also inhibits DNA negative supercoiling, which indicated inhibition of DNA gyrase. FIS, IHF, HU, and SeqA all participate in ppGpp-dependent persister formation and modulate chromosomal negative supercoiling. All components in red increase within the model of persisters, and all components in green decrease within the model. See also Figure S6.

et al., 1994; Sezonov et al., 2007; Stewart and Franklin, 2008). This pathway explains a portion of the persister heterogeneity present in later-stage populations, but is not the only stress during normal growth with the capacity to form persisters (Vega et al., 2012). To add to persister diversity, we observed both a growth-arrest-mediated pathway generating persisters and the ppGpp-dependent pathway studied here. These data suggest not only that native stresses can generate persisters, but also that different persisters can arise from the same stress.

The persister formation cascade identified here is depicted in Figure 7. The pathway is stimulated by glucose exhaustion and results in activation of a metabolic TA module that is the source of bistability and the cause of antibiotic tolerance. The OFL tolerance of persisters was found to depend on the ability of ppGpp to inhibit transcription through DksA, as well as the presence of FIS, HU, IHF, and SeqA, all of which participate in the negative supercoiling of chromosomal DNA (Maxwell, 1997). We note that while we demonstrate that exogenous addition of cAMP can lead to persister formation through a ppGpp-dependent pathway, the involvement of cAMP and CRP under conditions of carbon source transition could not be confirmed due to the inability of Δ*crp* and Δ*cyaA* to grow past the point of glucose exhaustion. Since ppGpp accumulation following diauxie could be stimulated by reduction in amino acids (Traxler et al., 2006), we indicate that both may be involved in triggering persister formation. However, it is worth noting that we found that cAMP-CRP activity and cAMP-CRP-controlled RelA expression both increase upon glucose exhaustion in normal and persister cells (Figure S6). Interestingly, complementation of Δ*dksA* by expression of *dksA* from its native promoter on a plasmid restored wild-type persister formation both with and without the promoter's cAMP-CRP binding site (Figure S6), demonstrating that cAMP-CRP control of *dksA* expression is not required for persister formation, which agrees with previous studies citing that DksA levels remain constant over diverse conditions (Chandrangsu et al., 2011). We also note that while numerous mediators of the pathways presented in this study have been identified, the possibility exists that additional mediators, perhaps in combination, have yet to be identified.

Central to the carbon source transition pathway is the ppGpp biochemical network, which includes RelA, SpoT, and DksA. The stringent response has previously been identified as an important mediator of bacterial persistence in *E. coli*, *P. aeruginosa*, and mycobacteria (Fung et al., 2010; Hansen et al., 2008; Korch and Hill, 2006; Nguyen et al., 2011; Sureka et al., 2008). We add to this body of knowledge here by (1) elucidating a native persister formation cascade that involves ppGpp, (2) demonstrating that ppGpp-SpoT form a metabolic TA module with the capacity to generate bistability and persistence, and (3) demonstrating that ppGpp-associated persistence in this pathway requires its effect on transcription (through DksA) and the proteins FIS, HU, IHF, and SeqA, all of which participate in chromosomal negative supercoiling. Interestingly, HU and IHF have previously been implicated in the persistence phenotype for their roles as transcriptional regulators, in contrast to their roles as modulators of chromosomal negative supercoiling. We note here that ppGpp-associated persister formation may depend on both the transcriptional regulatory and negative supercoiling activity of the NAPs, but the complexity of interactions between the NAPs and ppGpp makes it difficult to discern their exact role in this mechanism (Travers and Muskhelishvili, 2005).

Here we have presented a persister formation pathway in response to a native stress experienced by bacterial cultures: carbon source transitions. Metabolism controls the initiation of this pathway (glucose exhaustion) as well as the effector of bistability and antibiotic tolerance (ppGpp-SpoT). Due to the prevalence of nutrient transitions in biofilms (Stewart and Franklin, 2008), pathways such as the one described here may represent major mechanisms of persister formation in surface-attached communities. Further, we postulate that other metabolic transitions may stimulate the formation of persisters (Grant et al., 2012) and that the total level of persisters in a population

may in fact be a sum of those formed during each transition. This potential heterogeneity represents a significant technical barrier to sterilization of any culture with antibiotics, suggesting that more knowledge is needed to quantify this heterogeneity and identify broad-spectrum methods to eliminate persisters.

EXPERIMENTAL PROCEDURES

Bacterial Strains, Plasmids, and Culture Conditions

Bacterial strains and plasmids used in this study are listed in Table S6, and details on their construction are described in Tables S7 and S8 and Supplemental Experimental Procedures. M9 minimal medium was used in all experiments. For carbon source transition experiments, 0.5 mM glucose plus 24 mM carbon of the secondary carbon source was used. Single carbon source experiments contained 27 mM carbon. The aa supplement added to specific experiments contained 400 μg/mL serine and 40 μg/mL aspartic acid, glutamic acid, histidine, isoleucine, leucine, phenylalanine, threonine, and valine. This supplement was previously determined to be the minimum aa required to allow growth of *ΔrelAΔspoT* (Potrykus et al., 2011).

Carbon Source Transition Assay

Cells from −80°C stock were grown for 4–5 hr in Luria-Bertani (LB) medium, diluted 1:100 into 1–2 mL of 10 mM M9 glucose, and grown overnight (15 hr) at 37°C and 250 rpm. Overnight cultures were diluted to 0.005 OD_{600} in 50 mL of M9 medium in a 500 mL baffled flask and cultured at 37°C and 250 rpm. Persister measurements were taken prior to glucose exhaustion (0.08 OD_{600}, Figure S1) at ~0.02 OD_{600} and after glucose exhaustion at ~0.12 OD_{600}. For experiments with aa supplementation, glucose exhausted at ~0.14 OD_{600}; therefore, persister measurements were taken at ~0.2 OD_{600} (Figure S3).

cAMP, CAM, and SHX Addition Assays

Overnight cultures were diluted to 0.005 OD_{600} in 25 mL of 4.5 mM M9 glucose medium in a 250 mL baffled flask. For each chemical treatment, two cultures were prepared: untreated and treated. Cells were cultured at 37°C and 250 rpm to 0.02 OD_{600}. Prior to addition of bacteriostatic agents CAM or SHX, an aliquot of media was removed from the culture, filter sterilized, and stored at 37°C. Cells were treated with either sterilized 8 mM cAMP, which was previously shown to eliminate the diauxic lag (Ullmann and Monod, 1968), 1 mg/mL SHX (Ferullo and Lovett, 2008), or 50 μg/mL CAM (Korch and Hill, 2006). For SHX and CAM treatment, prior to challenging with OFL, cells were washed with the sterilized media. Persisters were measured after an additional 2 hr of growth after chemical treatment.

Persistence Measurements

Persistence was measured by determining the number of colony-forming units (cfu) after exposure to 5 μg/mL OFL or 200 μg/mL AMP. At specified cell densities or time points, 500 μL aliquots of culture were removed, treated with antibiotic, and incubated at 37°C and 250 rpm. At the designated time point, samples were collected by centrifugation (3 min, 15,000 rpm), washed with PBS, serially diluted in PBS, and 10 μL was spotted onto LB agar. Plates were incubated for 16 hr at 37°C, and cfu were measured to determine persister counts. For each data point, 10–100 colonies were counted (Kohanski et al., 2007).

Statistical Analysis

Statistical significance was assessed using two-tailed t tests with unequal variances after confirming the data could be treated as near-normally distributed with a larger sample data set (Supplemental Experimental Procedures). The threshold for significance was set to the p value < 0.05 (see Supplemental Experimental Procedures for more details).

ppGpp Biochemical Network Kinetic Model and Bistability Analysis

The ppGpp biochemical network was analyzed through the construction of a kinetic model describing the production and degradation of RelA, DksA, SpoT, ppGpp, the binding events of RNAP with ppGpp and DksA, and the effects of those complexes on the expression of DksA and SpoT, which are both stringently controlled by ppGpp and DksA. A detailed description of the model and its analysis is provided in the Supplemental Experimental Procedures.

SUPPLEMENTAL INFORMATION

Supplemental Information includes six figures, eight tables, and Supplemental Experimental Procedures and can be found with this article online at http://dx.doi.org/10.1016/j.molcel.2013.04.002.

ACKNOWLEDGMENTS

We thank Professors A. James Link, Philippe Rigollet, Thomas Silhavy, and Ned Wingreen for their assistance and Christina DeCoste for her technical support with flow cytometry experiments. We thank the National BioResource Project (NIG, Japan) for their support of the distribution of the Keio collection. This research was supported by the National Science Foundation (S.M.A., Graduate Research Fellowship), the Department of the Army award number W81XWH-12-2-0138, and start-up funds from Princeton University. The authors declare that no competing interests exist.

Received: September 13, 2012
Revised: January 17, 2013
Accepted: April 1, 2013
Published: May 9, 2013

REFERENCES

Allison, K.R., Brynildsen, M.P., and Collins, J.J. (2011). Heterogeneous bacterial persisters and engineering approaches to eliminate them. Curr. Opin. Microbiol. *14*, 593–598.

An, G., Justesen, J., Watson, R.J., and Friesen, J.D. (1979). Cloning the spoT gene of Escherichia coli: identification of the spoT gene product. J. Bacteriol. *137*, 1100–1110.

Bächi, B., and Kornberg, H.L. (1975). Utilization of gluconate by Escherichia coli. A role of adenosine 3′:5′-cyclic monophosphate in the induction of gluconate catabolism. Biochem. J. *150*, 123–128.

Balaban, N.Q., Merrin, J., Chait, R., Kowalik, L., and Leibler, S. (2004). Bacterial persistence as a phenotypic switch. Science *305*, 1622–1625.

Baracchini, E., and Bremer, H. (1988). Stringent and growth control of rRNA synthesis in Escherichia coli are both mediated by ppGpp. J. Biol. Chem. *263*, 2597–2602.

Brendler, T., and Austin, S. (1999). Binding of SeqA protein to DNA requires interaction between two or more complexes bound to separate hemimethylated GATC sequences. EMBO J. *18*, 2304–2310.

Brown, J.M., and Shaw, K.J. (2003). A novel family of Escherichia coli toxin-antitoxin gene pairs. J. Bacteriol. *185*, 6600–6608.

Campbell, J.L., and Kleckner, N. (1990). E. coli oriC and the dnaA gene promoter are sequestered from dam methyltransferase following the passage of the chromosomal replication fork. Cell *62*, 967–979.

Chandrangsu, P., Lemke, J.J., and Gourse, R.L. (2011). The dksA promoter is negatively feedback regulated by DksA and ppGpp. Mol. Microbiol. *80*, 1337–1348.

Christensen-Dalsgaard, M., Jørgensen, M.G., and Gerdes, K. (2010). Three new RelE-homologous mRNA interferases of Escherichia coli differentially induced by environmental stresses. Mol. Microbiol. *75*, 333–348.

Clark, B., and Holms, W.H. (1976). Control of the sequential utilization of glucose and fructose by Escherichia coli. J. Gen. Microbiol. *96*, 191–201.

Dörr, T., Vulić, M., and Lewis, K. (2010). Ciprofloxacin causes persister formation by inducing the TisB toxin in Escherichia coli. PLoS Biol. *8*, e1000317.

Dubnau, D., and Losick, R. (2006). Bistability in bacteria. Mol. Microbiol. *61*, 564–572.

Durfee, T., Hansen, A.M., Zhi, H., Blattner, F.R., and Jin, D.J. (2008). Transcription profiling of the stringent response in Escherichia coli. J. Bacteriol. *190*, 1084–1096.

Eng, R.H., Padberg, F.T., Smith, S.M., Tan, E.N., and Cherubin, C.E. (1991). Bactericidal effects of antibiotics on slowly growing and nongrowing bacteria. Antimicrob. Agents Chemother. *35*, 1824–1828.

Ferullo, D.J., and Lovett, S.T. (2008). The stringent response and cell cycle arrest in Escherichia coli. PLoS Genet. *4*, e1000300.

Fung, D.K., Chan, E.W., Chin, M.L., and Chan, R.C. (2010). Delineation of a bacterial starvation stress response network which can mediate antibiotic tolerance development. Antimicrob. Agents Chemother. *54*, 1082–1093.

Grant, S.S., Kaufmann, B.B., Chand, N.S., Haseley, N., and Hung, D.T. (2012). Eradication of bacterial persisters with antibiotic-generated hydroxyl radicals. Proc. Natl. Acad. Sci. USA *109*, 12147–12152.

Hansen, S., Lewis, K., and Vulić, M. (2008). Role of global regulators and nucleotide metabolism in antibiotic tolerance in Escherichia coli. Antimicrob. Agents Chemother. *52*, 2718–2726.

Hong, S.H., Wang, X., O'Connor, H.F., Benedik, M.J., and Wood, T.K. (2012). Bacterial persistence increases as environmental fitness decreases. Microb. Biotechnol. *5*, 509–522.

Kang, S., Han, J.S., Park, J.H., Skarstad, K., and Hwang, D.S. (2003). SeqA protein stimulates the relaxing and decatenating activities of topoisomerase IV. J. Biol. Chem. *278*, 48779–48785.

Keren, I., Kaldalu, N., Spoering, A., Wang, Y., and Lewis, K. (2004). Persister cells and tolerance to antimicrobials. FEMS Microbiol. Lett. *230*, 13–18.

Keseler, I.M., Mackie, A., Peralta-Gil, M., Santos-Zavaleta, A., Gama-Castro, S., Bonavides-Martínez, C., Fulcher, C., Huerta, A.M., Kothari, A., Krummenacker, M., et al. (2013). EcoCyc: fusing model organism databases with systems biology. Nucleic Acids Res. *41*(Database issue), D605–D612.

Kim, Y., and Wood, T.K. (2010). Toxins Hha and CspD and small RNA regulator Hfq are involved in persister cell formation through MqsR in Escherichia coli. Biochem. Biophys. Res. Commun. *391*, 209–213.

Kohanski, M.A., Dwyer, D.J., Hayete, B., Lawrence, C.A., and Collins, J.J. (2007). A common mechanism of cellular death induced by bactericidal antibiotics. Cell *130*, 797–810.

Korch, S.B., and Hill, T.M. (2006). Ectopic overexpression of wild-type and mutant hipA genes in Escherichia coli: effects on macromolecular synthesis and persister formation. J. Bacteriol. *188*, 3826–3836.

Lemke, J.J., Sanchez-Vazquez, P., Burgos, H.L., Hedberg, G., Ross, W., and Gourse, R.L. (2011). Direct regulation of Escherichia coli ribosomal protein promoters by the transcription factors ppGpp and DksA. Proc. Natl. Acad. Sci. USA *108*, 5712–5717.

Leung, V., and Lévesque, C.M. (2012). A stress-inducible quorum-sensing peptide mediates the formation of persister cells with noninherited multidrug tolerance. J. Bacteriol. *194*, 2265–2274.

Lewis, K. (2010). Persister cells. Annu. Rev. Microbiol. *64*, 357–372.

Luidalepp, H., Jõers, A., Kaldalu, N., and Tenson, T. (2011). Age of inoculum strongly influences persister frequency and can mask effects of mutations implicated in altered persistence. J. Bacteriol. *193*, 3598–3605.

Maisonneuve, E., Shakespeare, L.J., Jørgensen, M.G., and Gerdes, K. (2011). Bacterial persistence by RNA endonucleases. Proc. Natl. Acad. Sci. USA *108*, 13206–13211.

Maxwell, A. (1997). DNA gyrase as a drug target. Trends Microbiol. *5*, 102–109.

Möker, N., Dean, C.R., and Tao, J. (2010). Pseudomonas aeruginosa increases formation of multidrug-tolerant persister cells in response to quorum-sensing signaling molecules. J. Bacteriol. *192*, 1946–1955.

Monod, J. (1942). Recherches sur la croissance des cultures bacteriennes, Second Edition (Paris, France: Hermann et Cie).

Mott, M.L., and Berger, J.M. (2007). DNA replication initiation: mechanisms and regulation in bacteria. Nat. Rev. Microbiol. *5*, 343–354.

Murray, K.D., and Bremer, H. (1996). Control of spoT-dependent ppGpp synthesis and degradation in Escherichia coli. J. Mol. Biol. *259*, 41–57.

Narang, A., and Pilyugin, S.S. (2007). Bacterial gene regulation in diauxic and non-diauxic growth. J. Theor. Biol. *244*, 326–348.

Nguyen, D., Joshi-Datar, A., Lepine, F., Bauerle, E., Olakanmi, O., Beer, K., McKay, G., Siehnel, R., Schafhauser, J., Wang, Y., et al. (2011). Active starvation responses mediate antibiotic tolerance in biofilms and nutrient-limited bacteria. Science *334*, 982–986.

Nöllmann, M., Crisona, N.J., and Arimondo, P.B. (2007). Thirty years of Escherichia coli DNA gyrase: from in vivo function to single-molecule mechanism. Biochimie *89*, 490–499.

Potrykus, K., and Cashel, M. (2008). (p)ppGpp: still magical? Annu. Rev. Microbiol. *62*, 35–51.

Potrykus, K., Murphy, H., Philippe, N., and Cashel, M. (2011). ppGpp is the major source of growth rate control in E. coli. Environ. Microbiol. *13*, 563–575.

Prüss, B.M., Nelms, J.M., Park, C., and Wolfe, A.J. (1994). Mutations in NADH:ubiquinone oxidoreductase of Escherichia coli affect growth on mixed amino acids. J. Bacteriol. *176*, 2143–2150.

Rodionov, D.G., and Ishiguro, E.E. (1995). Direct correlation between overproduction of guanosine 3′,5′-bispyrophosphate (ppGpp) and penicillin tolerance in Escherichia coli. J. Bacteriol. *177*, 4224–4229.

Roseman, S., and Meadow, N.D. (1990). Signal transduction by the bacterial phosphotransferase system. Diauxie and the crr gene (J. Monod revisited). J. Biol. Chem. *265*, 2993–2996.

Rotem, E., Loinger, A., Ronin, I., Levin-Reisman, I., Gabay, C., Shoresh, N., Biham, O., and Balaban, N.Q. (2010). Regulation of phenotypic variability by a threshold-based mechanism underlies bacterial persistence. Proc. Natl. Acad. Sci. USA *107*, 12541–12546.

Saier, M.H., Ramseier, T.M., and Reizer, J. (1996). Regulation of Carbon Utilization. In Escherichia coli and Salmonella: cellular and molecular biology, Second Edition, F.C. Neidhardt, ed. (Washington, D.C.: ASM Press).

Sezonov, G., Joseleau-Petit, D., and D'Ari, R. (2007). Escherichia coli physiology in Luria-Bertani broth. J. Bacteriol. *189*, 8746–8749.

Stewart, P.S., and Franklin, M.J. (2008). Physiological heterogeneity in biofilms. Nat. Rev. Microbiol. *6*, 199–210.

Sureka, K., Ghosh, B., Dasgupta, A., Basu, J., Kundu, M., and Bose, I. (2008). Positive feedback and noise activate the stringent response regulator rel in mycobacteria. PLoS ONE *3*, e1771.

Surette, M.G., and Bassler, B.L. (1998). Quorum sensing in Escherichia coli and Salmonella typhimurium. Proc. Natl. Acad. Sci. USA *95*, 7046–7050.

Tolosa, L., Kostov, Y., Harms, P., and Rao, G. (2002). Noninvasive measurement of dissolved oxygen in shake flasks. Biotechnol. Bioeng. *80*, 594–597.

Tosa, T., and Pizer, L.I. (1971). Biochemical bases for the antimetabolite action of L-serine hydroxamate. J. Bacteriol. *106*, 972–982.

Travers, A., and Muskhelishvili, G. (2005). DNA supercoiling - a global transcriptional regulator for enterobacterial growth? Nat. Rev. Microbiol. *3*, 157–169.

Traxler, M.F., Chang, D.E., and Conway, T. (2006). Guanosine 3′,5′-bispyrophosphate coordinates global gene expression during glucose-lactose diauxie in Escherichia coli. Proc. Natl. Acad. Sci. USA *103*, 2374–2379.

Traxler, M.F., Zacharia, V.M., Marquardt, S., Summers, S.M., Nguyen, H.T., Stark, S.E., and Conway, T. (2011). Discretely calibrated regulatory loops controlled by ppGpp partition gene induction across the 'feast to famine' gradient in Escherichia coli. Mol. Microbiol. *79*, 830–845.

Ullmann, A., and Monod, J. (1968). Cyclic AMP as an antagonist of catabolite repression in Escherichia coli. FEBS Lett. *2*, 57–60.

Vázquez-Laslop, N., Lee, H., and Neyfakh, A.A. (2006). Increased persistence in Escherichia coli caused by controlled expression of toxins or other unrelated proteins. J. Bacteriol. *188*, 3494–3497.

Vega, N.M., Allison, K.R., Khalil, A.S., and Collins, J.J. (2012). Signaling-mediated bacterial persister formation. Nat. Chem. Biol. *8*, 431–433.

Wang, X., and Wood, T.K. (2011). Toxin-antitoxin systems influence biofilm and persister cell formation and the general stress response. Appl. Environ. Microbiol. *77*, 5577–5583.

Wang, X., Lord, D.M., Cheng, H.Y., Osbourne, D.O., Hong, S.H., Sanchez-Torres, V., Quiroga, C., Zheng, K., Herrmann, T., Peti, W., et al. (2012). A new type V toxin-antitoxin system where mRNA for toxin GhoT is cleaved by antitoxin GhoS. Nat. Chem. Biol. *8*, 855–861.

Wu, Y., Vulić, M., Keren, I., and Lewis, K. (2012). Role of oxidative stress in persister tolerance. Antimicrob. Agents Chemother. *56*, 4922–4926.

Yamaguchi, Y., and Inouye, M. (2011). Regulation of growth and death in Escherichia coli by toxin-antitoxin systems. Nat. Rev. Microbiol. *9*, 779–790.

Molecular Cell, Volume *50*

Supplemental Information

Metabolic Control of Persister Formation in *Escherichia coli*

Stephanie M. Amato, Mehmet A. Orman, and Mark P. Brynildsen

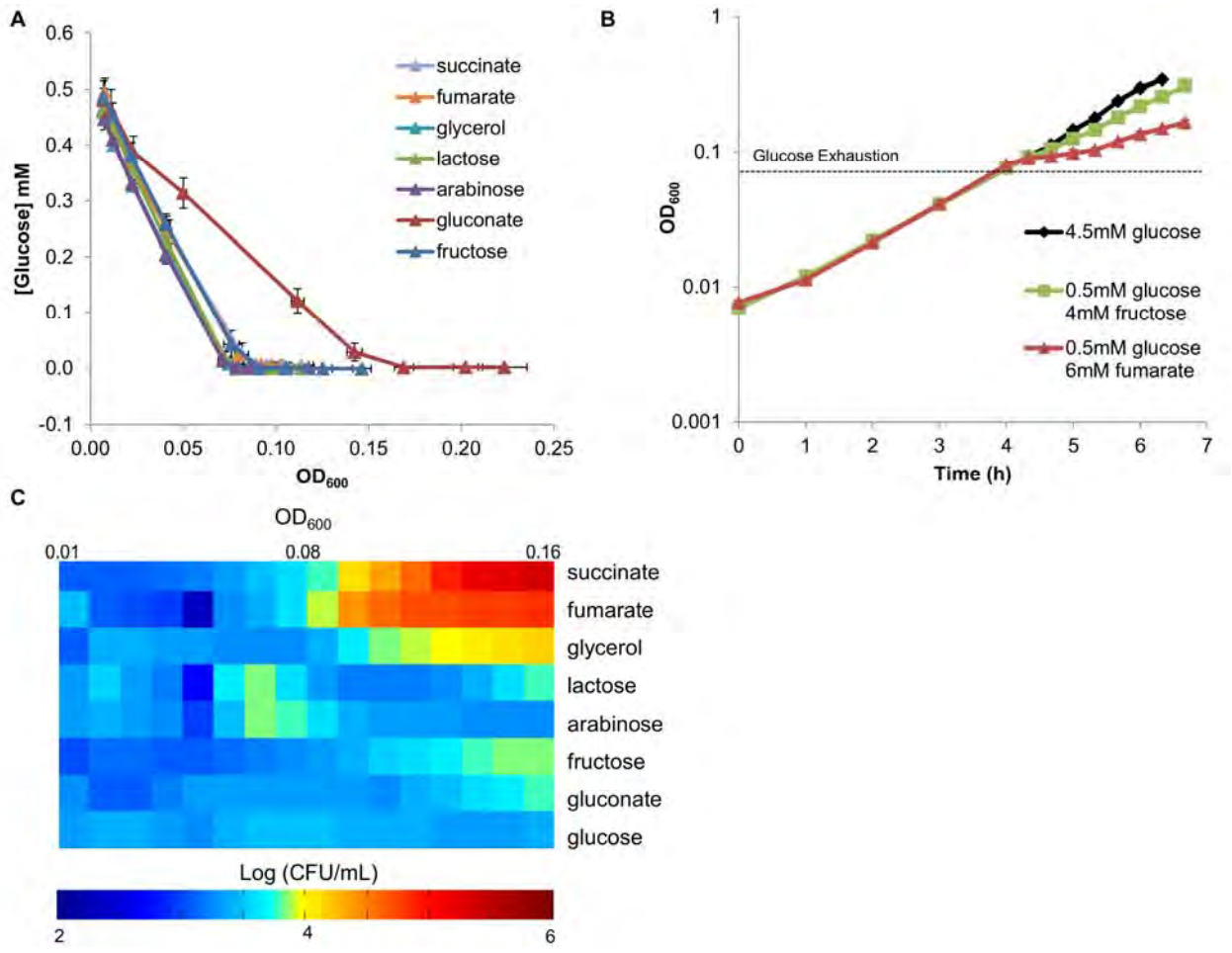

Figure S1. Glucose Consumption, Diauxic Growth, and Stimulation of Ampicillin Persisters, Related to Figure 1

(A)Glucose concentration and OD_{600} measurements were taken at specified time points to determine the OD_{600} where glucose exhausts in media composed of 0.5mM glucose and 24mM carbon from a secondary carbon source. Gluconate and glucose are co-utilized (Bachi and Kornberg, 1975) so glucose exhaustion occurs at a higher OD_{600} than other secondary carbon sources. Glucose concentrations measured using Amplex Red Glucose/Glucose Oxidase Kit (Invitrogen). (B) The OD_{600} of wild-type was measured at specified time intervals. One exponential growth phase was observed for 4.5mM glucose. Two regimes of exponential growth

were observed for 0.5mM glucose 4mM fructose media. Characteristic diauxic growth, two exponential growth phases separated by a lag phase was observed for 0.5mM glucose 6mM fumarate media. (C) *E. coli* were grown on glucose and a panel of secondary carbon sources, and at hourly time points, aliquots of culture were removed, challenged with 200μg/mL AMP for 4 h, washed, and plated to measure CFUs. To construct the color plot as a function of OD_{600}, values plotted were interpolated from two adjacent measurements. Data are averages of ≥ 3 independent experiments and error bars indicate data range.

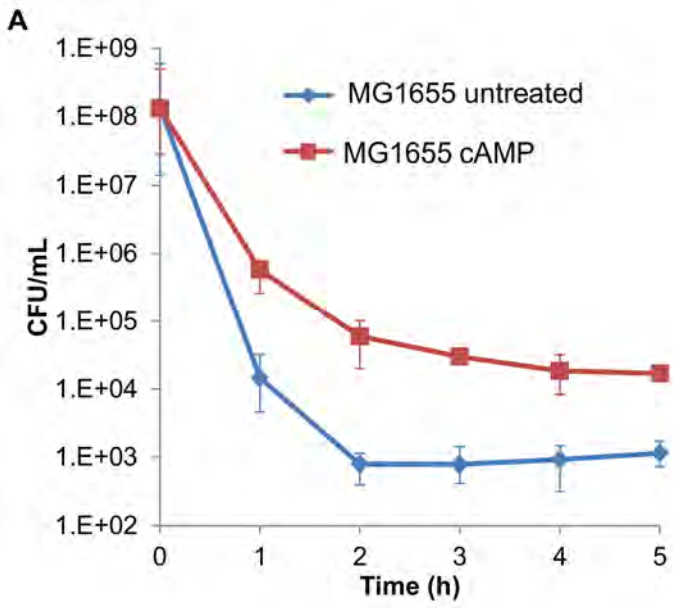

Figure S2. Effect of cAMP Addition for MG1655 in aa-Supplemented Media, Related to Figure 2

At an OD_{600} of 0.02, all strains were exposed to either 8mM cAMP or no treatment. After 2 h, the survival of the culture to 5 μg/mL OFL was measured. Data are averages of ≥ 3 independent experiments and error bars indicate data range.

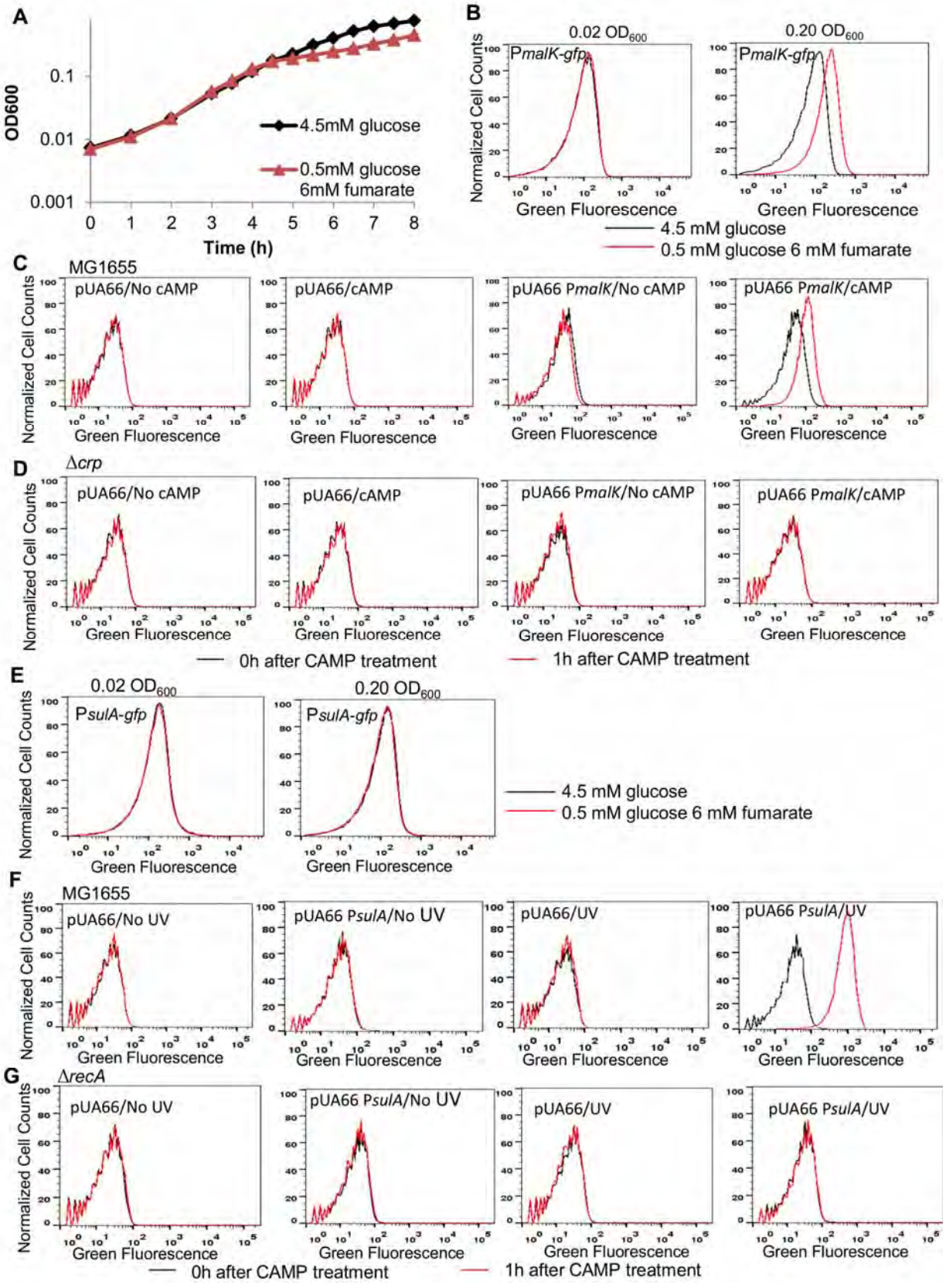
A
OD600
0.1
0.01
0.001
0 1 2 3 4 5 6 7 8
Time (h)
4.5mM glucose
0.5mM glucose
6mM fumarate
B
0.02 OD600
0.20 OD600
PmalK-gfp
Normalized Cell Counts
Green Fluorescence
4.5 mM glucose
0.5 mM glucose 6 mM fumarate
C
MG1655
pUA66/No cAMP
pUA66/cAMP
pUA66 PmalK/No cAMP
pUA66 PmalK/cAMP
D
Δcrp
0h after CAMP treatment
1h after CAMP treatment
E
0.02 OD600
0.20 OD600
PsulA-gfp
4.5 mM glucose
0.5 mM glucose 6 mM fumarate
F
MG1655
pUA66/No UV
pUA66 PsulA/No UV
pUA66/UV
pUA66 PsulA/UV
G
ΔrecA
0h after CAMP treatment
1h after CAMP treatment

Figure S3. Growth of MG1655 in aa-Supplemented Media and Tests to Discern Certain Molecular Components of the Formation Pathway, Related to Figure 4

(A) The OD_{600} of wild-type was measured at specified time intervals. (B) GFP flow cytometry data for the P*malK-gfp* cAMP reporter in glucose and glucose-fumarate before and after the carbon transition. (C) Wild-type and (D) Δ*crp* transformed with control pUA66 and P*malK-gfp* reporter plasmid were tested with flow cytometry to confirm reporter responds positively to increases in cAMP concentration. (E) GFP flow cytometry data for the P*sulA-gfp* SOS response reporter in glucose and glucose-fumarate before and after the carbon transition. (F) Wild-type and (G) Δ*recA* transformed with control pUA66 and P*sulA-gfp* reporter plasmid were tested with flow cytometry to confirm reporter responds positively to SOS response induction through DNA damage from UV light exposure. Cells for all toxin deletion strains tested were exposed to 5µg/mL OFL at 0.02 OD_{600} and 0.20 OD_{600}.

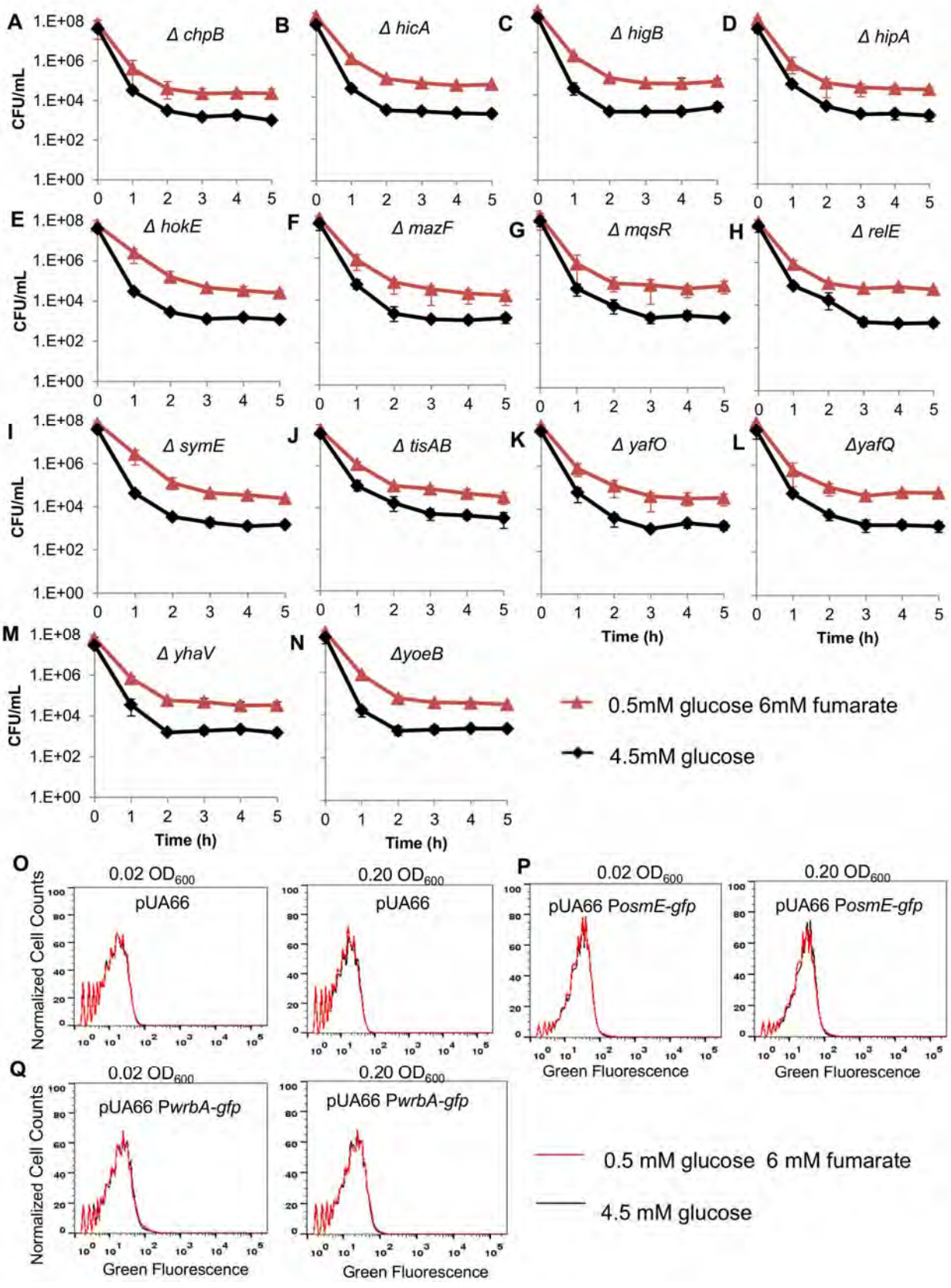
A
Δ chpB
B
Δ hicA
C
Δ higB
D
Δ hipA
E
Δ hokE
F
Δ mazF
G
Δ mqsR
H
Δ relE
I
Δ symE
J
Δ tisAB
K
Δ yafO
L
ΔyafQ
M
Δ yhaV
N
ΔyoeB
CFU/mL
1.E+08
1.E+06
1.E+04
1.E+02
1.E+00
0 1 2 3 4 5
Time (h)
0.5mM glucose 6mM fumarate
4.5mM glucose
O
P
Q
0.02 OD600
0.20 OD600
pUA66
pUA66 PosmE-gfp
pUA66 PwrbA-gfp
Normalized Cell Counts
Green Fluorescence
0.5 mM glucose 6 mM fumarate
4.5 mM glucose

Figure S4. Toxin Deletions and Controls for ppGpp Reporters, Related to Figure 5

Cells were grown in media specified with AA- supplementation. (A)Δ*chpB*, (B) Δ*hicA*, (C) Δ*higB*, (D) Δ*hipA*, (E) Δ*hokE*, (F) Δ*mazF*, (G) Δ*mqsR*, (H) Δ*relE*, (I)Δ*symE*, (J) Δ*tisAB*, (K) Δ*yafO*, (L) Δ*yafQ*, (M) Δ*yhaV*, and (N) Δ*yoeB* toxins were tested. Due to space considerations, we note all persister levels in both glucose and glucose-fumarate media at 0.02 OD_{600} were ~1000 CFU/mL. All toxin deletions at 0.20 OD_{600} produced fold-change increases in persisters (glucose-fumarate persisters/glucose-only persisters) that were quantitatively comparable to and statistically indistinguishable from that of wild-type (p-value > 0.05). Data are averages of ≥ 3 independent experiments, error bars indicate data range, and significance was assessed using the null hypothesis that the mutant mean fold-change in persisters was equal to the wild-type fold-change in persisters. To determine if the P*osmE-gfp* and P*wrbA-gfp* reporters respond properly to ppGpp in our experimental assay conditons, these reporters along with negative control pUA66 were transformed into Δ*relA*Δ*spoT*. (O) pUA66, (P) P*osmE-gfp*, and (Q) P*wrbA-gfp* were analyzed using flow cytometry at 0.02 OD_{600} and 0.20 OD_{600} in both glucose and glucose-fumarate amino acid supplemented media. Without the cellular presence of ppGpp, the GFP distribution does not increase for P*osmE-gfp* and P*wrbA-gfp* in the glucose-fumarate media after glucose exhaustion as observed in wild-type cells (Figure 5) confirming these plasmids as ppGpp reporters in our experimental conditions.

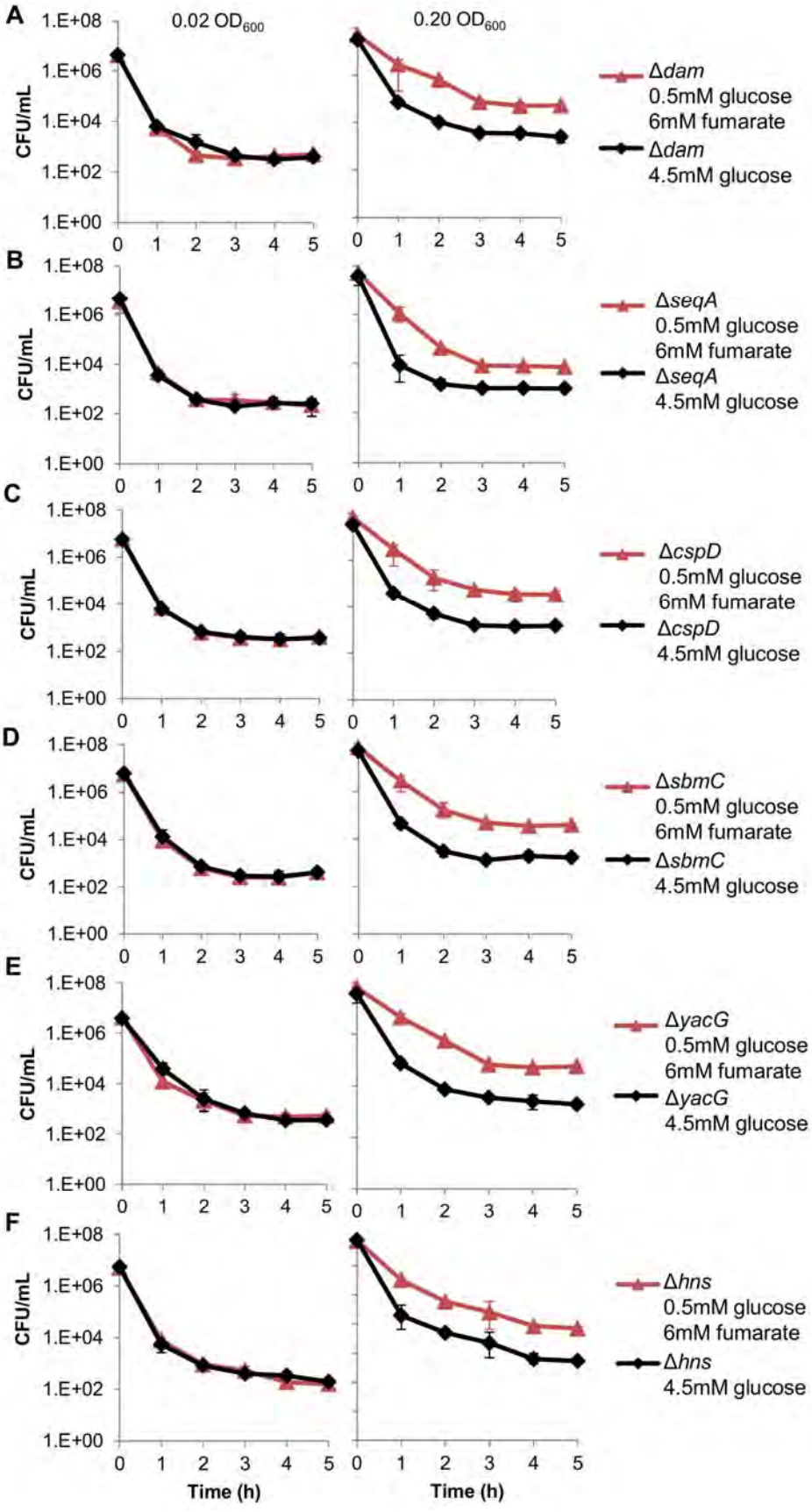
A
B
C
D
E
F
0.02 OD600
0.20 OD600
CFU/mL
1.E+08
1.E+06
1.E+04
1.E+02
1.E+00
0 1 2 3 4 5
Time (h)
Δdam
0.5mM glucose
6mM fumarate
Δdam
4.5mM glucose
ΔseqA
0.5mM glucose
6mM fumarate
ΔseqA
4.5mM glucose
ΔcspD
0.5mM glucose
6mM fumarate
ΔcspD
4.5mM glucose
ΔsbmC
0.5mM glucose
6mM fumarate
ΔsbmC
4.5mM glucose
ΔyacG
0.5mM glucose
6mM fumarate
ΔyacG
4.5mM glucose
Δhns
0.5mM glucose
6mM fumarate
Δhns
4.5mM glucose

Figure S5. Involvement of Replication and Nucleoid-Associated Proteins in ppGpp-Dependent Mechanism, Related to Figure 6

Cells were grown in minimal media supplemented with AA and challenged with 5μg/mL OFL at 0.02 OD_{600} and 0.20 OD_{600}, representing growth on glucose and growth after glucose exhaustion, respectively. (A) Δ*dam*, (C) Δ*cspD*, (D) Δ*sbmC*, (E) Δ*yacG*, and (F) Δ*hns* produced fold-change increases in persisters (glucose-fumarate persisters/glucose-only persisters) that were quantitatively comparable to and statistically indistinguishable from that of wild-type (p-value > 0.05). (B) Δ*seqA* exhibited ~ 6.8-fold increase in persisters, which was statistically different from that of wild-type (~20-fold) (p-value < 0.05). Data are averages of ≥ 3 independent experiments, error bars indicate data range, and significance was assessed using the null hypothesis that the mutant mean fold-change in persisters was equal to the wild-type fold-change in persisters.

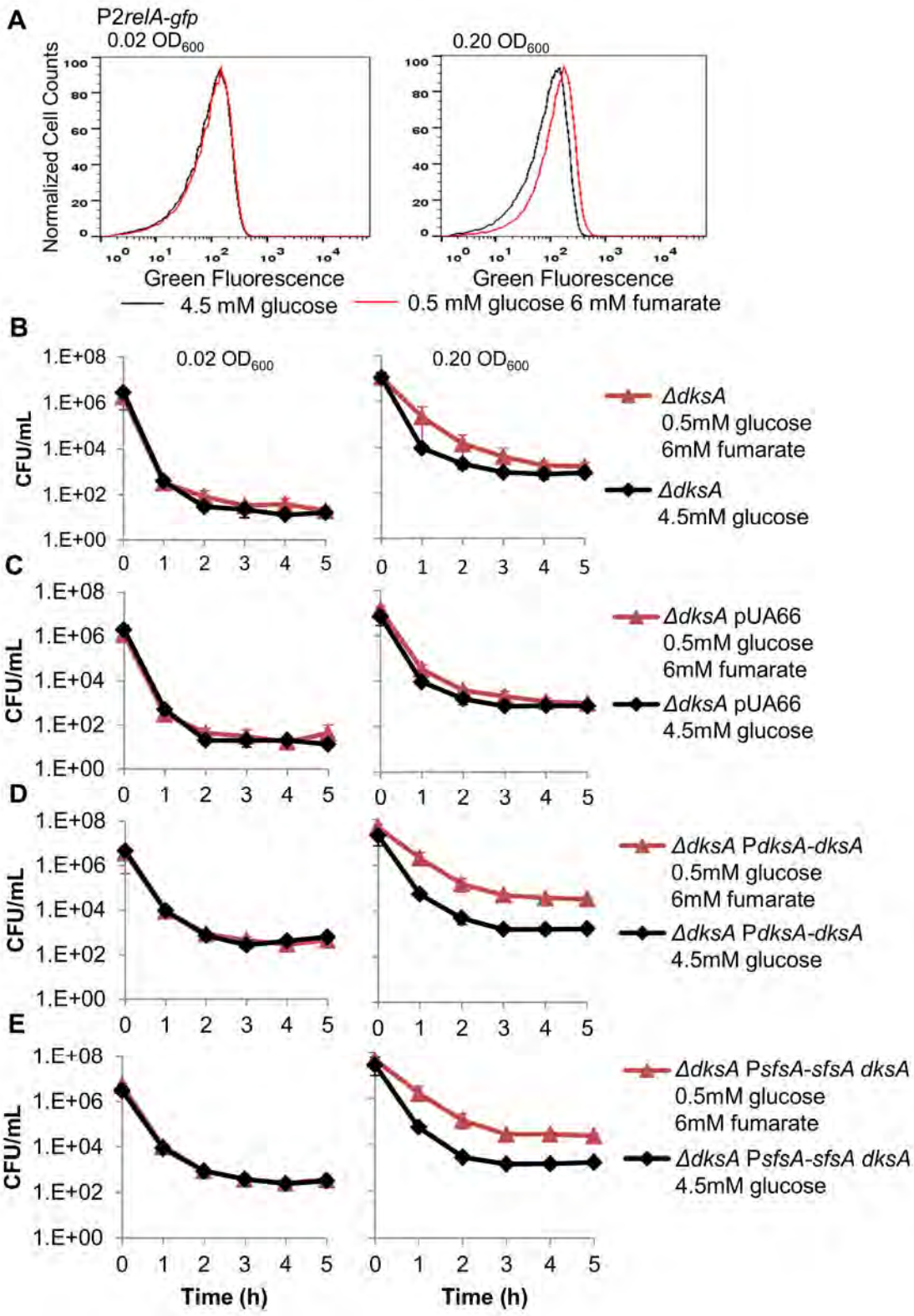
A
P2relA-gfp
0.02 OD600
0.20 OD600
Normalized Cell Counts
Green Fluorescence
Green Fluorescence
4.5 mM glucose
0.5 mM glucose 6 mM fumarate
B
C
D
E
CFU/mL
0.02 OD600
0.20 OD600
ΔdksA
0.5mM glucose
6mM fumarate
ΔdksA
4.5mM glucose
ΔdksA pUA66
0.5mM glucose
6mM fumarate
ΔdksA pUA66
4.5mM glucose
ΔdksA PdksA-dksA
0.5mM glucose
6mM fumarate
ΔdksA PdksA-dksA
4.5mM glucose
ΔdksA PsfsA-sfsA dksA
0.5mM glucose
6mM fumarate
ΔdksA PsfsA-sfsA dksA
4.5mM glucose
Time (h)
Time (h)

Figure S6. Response of RelA and DksA to cAMP Increase during aa-Supplemented Carbon Source Transition, Related to Figure 7

(A) GFP flow cytometry data for the P*2relA-gfp* reporter (an established cAMP-dependent promoter) in glucose and glucose-fumarate before and after the carbon transition. A 2-fold difference in the mean of the GFP fluorescence distribution was observed after glucose exhaustion in the glucose-fumarate media compared to the glucose media. Complementation of DksA was carried out in Δ*dksA.* The same persister levels were observed in the Δ*dksA*::kan strain as (B) Δ*dksA* without the kanamycin resistance cassette and (C) Δ*dksA* pUA66. The persister levels returned to wild-type levels when complemented with either (D) P*dksA-dksA* (no CRP binding site) or (E) P*sfsA-sfsA dksA* (CRP binding site) confirming the importance of DksA in the formation pathway and that cAMP-CRP transcriptional activation of *dksA* is not required for persistence. Data are averages of ≥ 3 independent experiments and error bars indicate data range.

Table S1. Glucose Concentrations at Persister OD_{600}s in aa-Supplemented Media, Related to Figure 4

	4.5mM glucose		0.5mM glucose 6mM fumarate	
Bacterial Strain	0.02 OD_{600}	0.20 OD_{600}	0.02 OD_{600}	0.20 OD_{600}
Wild-type	3.90 ± 0.40	3.11 ± 0.35	0.41 ± 0.02	Undetectable
ΔchpB	3.95 ± 0.28	2.76 ± 0.20	0.38 ± 0.04	Undetectable
ΔcspD	4.05 ± 0.23	3.61 ± 0.25	0.42 ± 0.03	Undetectable
Δdam	4.46 ± 0.02	3.84 ± 0.14	0.48 ± 0.002	Undetectable
ΔdksA	3.41 ± 0.03	2.96 ± 0.32	0.45 ± 0.02	Undetectable
Δfis	4.43 ± 0.15	3.49 ± 0.23	0.48 ± 0.08	Undetectable
ΔhicA	3.77 ± 0.01	3.20 ± 0.02	0.39 ± 0.03	Undetectable
ΔhigB	3.81 ± 0.001	3.11 ± 0.09	0.37 ± 0.02	Undetectable
ΔhipA	3.64 ± 0.46	2.44 ± 0.04	0.38 ± 0.02	Undetectable
Δhns	4.40 ± .006	3.96 ± 0.37	0.44 ± 0.02	Undetectable
ΔhokE	4.49 ± 0.04	3.91 ± 0.21	0.44 ± 0.01	Undetectable
ΔhupA	4.42 ± 0.02	3.73 ± 0.03	0.41 ± 0.004	Undetectable
ΔhupB	4.39 ± 0.25	3.71 ± 0.12	0.48 ± 0.03	Undetectable
ΔihfA	4.43 ± 0.11	3.80 ± 0.31	0.44 ± 0.01	Undetectable
ΔihfB	4.43 ± 0.15	3.57 ± 0.24	0.37 ± 0.02	Undetectable
ΔmazF	3.82 ± 0.02	3.03 ± 0.16	0.44 ± 0.03	Undetectable
ΔmqsR	3.88 ± 0.23	2.87 ± 0.45	0.43 ± 0.02	Undetectable
ΔrelA	3.25 ± 0.18	2.64 ± 0.03	0.43 ± 0.002	Undetectable
ΔrelAΔspoT	3.90 ± 0.40	3.21 ± 0.51	0.42 ± 0.03	Undetectable
ΔrelE	3.21 ± 0.08	2.75 ± 0.15	0.35 ± 0.02	Undetectable
ΔsbmC	4.49 ± 0.20	3.38 ± 0.14	0.41 ± 0.02	Undetectable
ΔseqA	4.35 ± 0.02	3.72 ± 0.04	0.49 ± 0.02	Undetectable
ΔsymE	4.45 ± 0.02	3.68 ± 0.15	0.49 ± 0.002	Undetectable
ΔtisAB	3.81 ± 0.33	2.93 ± 0.28	0.41 ± 0.04	Undetectable
ΔyacG	4.28 ± 0.11	3.81 ± 0.11	0.45 ± 0.01	Undetectable
ΔyafO	3.89 ± 0.32	2.87 ± 0.05	0.39 ± 0.03	Undetectable
ΔyafQ	3.74 ± 0.03	2.32 ± 0.13	0.36 ± 0.03	Undetectable
ΔyhaV	3.94 ± 0.04	3.26 ± 0.04	0.38 ± 0.04	Undetectable
ΔyoeB	3.81 ± 0.05	3.14 ± 0.01	0.39 ± 0.03	Undetectable

Glucose concentration measurements were taken at each persister sampling OD_{600} for all strains in both 4.5mM glucose and 0.5mM glucose 6mM fumarate (both cultures with AA-supplement). Measurements were made using an Amplex Red Glucose/Glucose Oxidase Kit (Invitrogen). Two replicates were conducted for each mutant and condition; error indicates maximum/minimum values.

Table S2. Significance of Genetic Deletions Analyzed

Strain	p-value	Toxin Rationale
Δ*chpB*::kan	0.625	Ribosome-independent RNA interferase implicated in persistence (Maisonneuve et al., 2011)
Δ*cspD*::kan	0.818	DNA replication inhibitor implicated in persistence (Kim et al., 2010; Kim and Wood, 2010; Langklotz and Narberhaus, 2011)
Δ*dam*::kan	0.850	N/A
Δ*dksA*::kan	0.046	N/A
Δ*fis*::kan	0.041	N/A
Δ*hicA*::kan	0.597	Ribosome-independent RNA interferase implicated in persistence (Maisonneuve et al., 2011)
Δ*higB*::kan	0.425	Ribosome-dependent RNA interferase implicated in persistence (Maisonneuve et al., 2011)
Δ*hipA*::kan	0.181	TA-module implicated in persistence(Falla and Chopra, 1998; Korch and Hill, 2006; Moyed and Bertrand, 1983)
Δ*hns*::kan	0.084	
Δ*hokE*::kan	0.883	SOS response activated toxin(Pedersen and Gerdes, 1999)
Δ*hupA*::kan	0.042	N/A
Δ*hupB*::kan	0.047	N/A
Δ*ihfA*::kan	0.038	N/A
Δ*ihfB*::kan	0.034	N/A
Δ*mazF*::kan	0.999	Ribosome-independent RNA interferase implicated in persistence (Maisonneuve et al., 2011; Vazquez-Laslop et al., 2006)
Δ*mqsR*::kan	0.749	Ribosome-independent RNA interferase implicated in persistence (Kim and Wood, 2010; Maisonneuve et al., 2011; Shah et al., 2006)
Δ*relA*::kan	0.046	N/A
Δ*relA*Δ*spoT*::kan	0.015	N/A
Δ*relE*::kan	0.240	Ribosome-dependent RNA interferase implicated in persistence (Christensen-Dalsgaard et al., 2010; Keren et al., 2004)
Δ*sbmC*::kan	0.602	DNA gyrase inhibitor activated by SOS response and cAMP-CRP(Baquero et al., 1995; Oh et al., 2001)
Δ*seqA*::kan	0.040	N/A
Δ*symE*::kan	0.583	SOS response activated toxin (Kawano et al., 2007)
Δ*tisAB*::kan	0.873	SOS response activated toxin implicated in persistence (Dorr et al., 2010)
Δ*yacG*::kan	0.604	DNA gyrase inhibitor(Sengupta and Nagaraja, 2008)
Δ*yafO*::kan	0.775	Ribosome-dependent RNA interferase activated by SOS response and implicated in persistence (Courcelle et al., 2001; Maisonneuve et al., 2011)
Δ*yafQ*::kan	0.605	Ribosome-dependent RNA interferase activated by SOS response and implicated in persistence (Courcelle et al., 2001; Maisonneuve et al., 2011)
Δ*yhaV*::kan	0.814	Ribosome-independent RNA interferase implicated in persistence (Maisonneuve et al., 2011)
Δ*yoeB*::kan	0.112	Ribosome-dependent RNA interferase implicated in persistence(Maisonneuve et al., 2011)

The table presents all genetic deletions tested in the carbon source transition assay along with the p-value associated with specific mutant's fold-change increase in persisters compared to wild-type. Significance was assessed using the null hypothesis that the mutant mean fold-change in persisters was equal to the wild-type fold-change in persisters. For the toxins listed, the link to TA-modules, cAMP, and SOS response are provided.

Table S3. Values for Parameters with Experimental Evidence, Related to Figure 5

Parameter	Description	Experimental Range	Nominal	Bistable Range	References
A	Transcription inhibition coefficient for the $RNAP_{DksA}$ complex	0.05-1 (non-dimensional)	0.633 (non-dimensional)	[0.529,1]	(Chandrangsu et al., 2011; Lemke et al., 2011)
B	Transcription inhibition coefficient for the $RNAP_{ppGpp}$ complex	0.25-1 (non-dimensional)	0.6 (non-dimensional)	[0,0.932]	(Barker et al., 2001; Chandrangsu et al., 2011; Lemke et al., 2011; Paul et al., 2004)
c	Transcription inhibition coefficient for the $RNAP_{DksA,ppGpp}$ complex	0.01-0.67 (non-dimensional)	0.01(non-dimensional)	[0.003, 0.0112]	(Barker et al., 2001; Lemke et al., 2011; Paul et al., 2004)
$K_{d,DksA}$	Concentration of DksA required to reduce open complex half-life by 50% (apparent K_d of DksA to RNAP)	30-600 molecules/cell	60 molecules/cell	(0-92]	(Lemke et al., 2011; Lennon et al., 2009; Rutherford et al., 2007)
$K_{d,ppGpp,a}$	Concentration of ppGpp required to reduce open complex half-life by 50% (apparent K_d of ppGpp to RNAP)	600-12000 molecules/cell	12,000 molecules/cell	[7675, ∞]	(Paul et al., 2004; Reddy et al., 1995)
$K_{d,ppGpp}$	Concentration of ppGpp required to reduce open complex half-life by 50% (apparent K_d of ppGpp to $RNAP_{DksA}$)	600-1200 molecules/cell	1200 molecules/cell	[1000, 1575]	(Paul et al., 2004)
$k_{deg,DksA}$	Rate constant for DksA protein degradation	0.0226 min^{-1}	0.0226 min^{-1}	(0, 0.034]	(Chandrangsu et al., 2011)
$k_{deg,SpoT,syn}$	Rate constant for SpoT synthase protein degradation	1.5 min^{-1}	1.5 min^{-1}	[1.385, 1.705]	(Murray and Bremer, 1996)
$k_{deg,SpoT,hyd}$	Rate constant for SpoT hydrolase protein degradation	0.02 min^{-1}	0.02 min^{-1}	[0, 0.22]	(Alon, 2007; Murray and Bremer, 1996)
$k_{deg,RelA}$	Rate constant for RelA protein degradation	0.02 min^{-1}	0.02 min^{-1}	[0.0177, 0.0215]	(Alon, 2007)
ATP	Concentration of ATP	$1.8 \times 10^5 – 5.8 \times 10^6$ molecules/cell	4.4×10^6 molecules/cell	[1.5×10^6, ∞]	(Bennett et al., 2009; Justesen et al., 1986; Lasko and Wang, 1996)
GTP	Concentration of GTP	$4.2 \times 10^5 – 3.0 \times 10^6$ molecules/cell	1.9×10^6 molecules/cell	[1.4×10^6, 1.2×10^7]	(Albe et al., 1990; Bennett et al., 2009; Justesen et al., 1986)
K_{ATP}	ATP Michaelis constant for RelA and SpoT	2.1×10^5 molecules/cell	2.1×10^5 molecules/cell	[0, 6.1×10^5]	(Justesen et al., 1986)
K_{GTP}	GTP Michaelis constant for RelA and SpoT	3.1×10^5 molecules/cell	3.1×10^5 molecules/cell	[7.8×10^4, 4.5×10^5]	(Enfors, 2004; Justesen et al., 1986)
K_{ppGpp}	ppGpp Michaelis constant for SpoT	2.9×10^4- 3.3×10^5 molecules/cell	2.9×10^4 molecules/cell	[2.1×10^2, 3.5×10^4]	(An et al., 1979; Heinemeyer and Richter, 1978)

This table defines each parameter in the kinetic model with experimentally established values. Experimental ranges/values for the parameter and the parameter's nominal value applied to the model are presented. Also, the parameter range for bistability in the model is provided which was determined by varying the parameter of interest while keeping all other nominal values constant.

Table S4. Uncertain Parameters Estimated to Achieve Physiological Values for RelA, DksA, and ppGpp within the Model, Related to Figure 5

Parameter	Description	Nominal	Bistable Range
β_{RelA}	RelA turnover number	1 molecule/cell min^{-1}	[0.927, 1.133]
β_{DksA}	DksA turnover number	2000 molecules/cell min^{-1}	[1300, ∞]
β_{SpoT}	SpoT turnover number	450 molecules/cell min^{-1}	[395, 490]
$k_{syn,RelA}$	Rate constant, k_{cat}, for ppGpp synthesis from RelA enzyme	1150 min^{-1}	[1070, 1300]
$k_{syn,SpoT}$	Rate constant, k_{cat}, for ppGpp synthesis from SpoT enzyme	850 min^{-1}	[0, 1480]
f	Fraction of SpoT protein concentration as synthase	0.5 (non-dimensional)	[0.481, 0.527]
$k_{deg,ppGpp}$	Rate constant, k_{cat}, for ppGpp degradation from SpoT enzyme	11,250 min^{-1}	[10,120, 12,050]
$k_{on,ppGpp}$	Rate constant for ppGpp binding to RNAP-DksA	10^{-2} $(molecules/cell)^{-1}min^{-1}$	[0, ∞]
$k_{on,DksA}$	Rate constant for DksA binding to RNAP-ppGpp	10^{-2} $(molecules/cell)^{-1}min^{-1}$	[0, ∞]

The table defines each parameter in the kinetic model where the experimental value was unknown. The values of these parameters were estimated to maintain the levels of RelA, DksA, and ppGpp at experimentally determined physiological levels. The nominal value and the bistable range for the parameters are provided. Bistable range was determined by varying the parameter of interest while keep all other parameters at their nominal value and assessing bistability.

Table S5. Steady-State Values for Significant Molecules in Model for Normal Cells and Persisters, Related to Figure 5

	Stable Steady State: Normal Cells	Stable Steady State: Persisters	Physiological Range
$DksA_{unbound}$	8.1×10^3	1.2×10^3	-
SpoT	54	8.1	-
$ppGpp_{unbound}$	8.0×10^3	9.8×10^5	-
RNAP	1.8	0.1	-
$RNAP_{DksA}$	240.5	2.2	-
$RNAP_{ppGpp}$	1.2	9.1	-
$RNAP_{DksA,ppGpp}$	1606.5	1838.6	-
$RNAP_{total}$	1850	1850	400-2000(Shepherd et al., 1980)
$DksA_{total}$	9.9×10^3	3.0×10^3	3.0×10^3-1.0×10^4(Paul et al., 2004)
$ppGpp_{total}$	9.6×10^3	9.9×10^5	5.7×10^3-1.4×10^6(Baracchini and Bremer, 1988; Murray and Bremer, 1996)

The table presents the concentrations of all major components in the model at the steady state related to normal cells and the steady state related to persistence. Physiological ranges for components provided when available.

Table S6. Bacterial Strains and Plasmids

Strain	Genotype	Source or Reference
MG1655	$F^- \lambda^-$ ilvG$^-$ rfb-50 rph-1	ATCC 700926(Kohanski et al., 2007)
SA001	MG1655 Δ*chpB*::kan	P1 Keio mutant(Baba et al., 2006) x MG1655
SA002	MG1655 Δ*crp*::kan	This work
SA003	MG1655 Δ*crp*	SA002 cured of Kan^r (Datsenko and Wanner, 2000)
SA004	MG1655 Δ*cspD*::kan	P1 Keio mutant(Baba et al., 2006) x MG1655
SA005	MG1655 Δ*dam*::kan	P1 Keio mutant(Baba et al., 2006) x MG1655
SA006	MG1655 Δ*dksA*::kan	P1 Keio mutant(Baba et al., 2006) x MG1655
SA007	MG1655 Δ*dksA*	SA006 cured of Kan^r (Datsenko and Wanner, 2000)
SA008	MG1655 Δ*fis*::kan	P1 Keio mutant(Baba et al., 2006) x MG1655
SA009	MG1655 Δ*hicA*::kan	P1 Keio mutant(Baba et al., 2006) x MG1655
SA010	MG1655 Δ*higB*::kan	P1 Keio mutant(Baba et al., 2006) x MG1655
SA011	MG1655 Δ*hipA*::kan	P1 Keio mutant(Baba et al., 2006) x MG1655
SA012	MG1655 Δ*hns*::kan	P1 Keio mutant(Baba et al., 2006) x MG1655
SA013	MG1655 Δ*hokE*::kan	P1 Keio mutant(Baba et al., 2006) x MG1655
SA014	MG1655 Δ*hupA*::kan	P1 Keio mutant(Baba et al., 2006) x MG1655
SA015	MG1655 Δ*hupB*::kan	P1 Keio mutant(Baba et al., 2006) x MG1655
SA016	MG1655 Δ*ihfA*::kan	P1 Keio mutant(Baba et al., 2006) x MG1655
SA017	MG1655 Δ*ihfB*::kan	This work
SA018	MG1655 Δ*mazF*::kan	P1 Keio mutant(Baba et al., 2006) x MG1655
SA019	MG1655 Δ*mqsR*::kan	P1 Keio mutant(Baba et al., 2006) x MG1655
SA020	MG1655 Δ*recA*	This work
SA021	MG1655 Δ*relA*::kan	P1 Keio mutant(Baba et al., 2006) x MG1655
SA022	MG1655 Δ*relA*Δ*spoT*::kan	This work
SA023	MG1655 Δ*relA*Δ*spoT*	SA022 cured of Kan^r (Datsenko and Wanner, 2000)
SA024	MG1655 Δ*relE*::kan	This work
SA025	MG1655 Δ*sbmC*::kan	P1 Keio mutant(Baba et al., 2006) x MG1655
SA026	MG1655 Δ*seqA*::kan	P1 Keio mutant(Baba et al., 2006) x MG1655
SA027	MG1655 Δ*symE*::kan	P1 Keio mutant(Baba et al., 2006) x MG1655
SA028	MG1655 Δ*tisAB*::kan	This work
SA029	MG1655 Δ*yacG*::kan	P1 Keio mutant(Baba et al., 2006) x MG1655
SA030	MG1655 Δ*yafO*::kan	P1 Keio mutant(Baba et al., 2006) x MG1655
SA031	MG1655 Δ*yafQ*::kan	P1 Keio mutant(Baba et al., 2006) x MG1655
SA032	MG1655 Δ*yhaV*::kan	P1 Keio mutant(Baba et al., 2006) x MG1655
SA033	MG1655 Δ*yoeB*::kan	P1 Keio mutant(Baba et al., 2006) x MG1655
Plasmid	Genotype	Source or Reference
pBAD33	Vector, pACYC ori, P_{BAD} arabinose-inducible Cm^r	(Guzman et al., 1995)
pQE80	Vector, ColE1 ori, P_{T5} IPTG-inducible Amp^r	QIAGEN
pSA01	pBAD33 P_{BAD} *spoT* Cm^r	This work
pSA02	pQE80 P_{T5} *relA'* Amp^r	This work
pUA66	Vector, SC101ori, Kan^r, *gfp*mut2 reporter	(Zaslaver et al., 2006)
pSA03	pUA66 P*malK-gfp*mut2 Kan^r	This work
pSA04	pUA66 P*osmE-gfp*mut2 Kan^r	(Zaslaver et al., 2006)
pSA05	pUA66 P2*relA-gfp*mut2 Kan^r	This work
pSA06	pUA66 P*sulA-gfp*mut2 Kan^r	(Zaslaver et al., 2006)
pSA07	pUA66 P*wrbA-gfp*mut2 Kan^r	(Zaslaver et al., 2006)
pSA08	pUA66 P*dksA- dksA* Kan^r	This work
pSA09	pUA66 P*sfsA -sfsA dksA* Kan^r	This work

Table S7. DNA Primers for Datsenko and Wanner Single Gene Deletions and Plasmid Construction

Datsenko Wanner oligonucleotides		
Strain	Forward	Reverse
Δ*crp*::kan	5’-AGCGGCGTTATCTGGCTCTGGAGAAAGCTTATAACAGAGGATTAACCGCGCATGGTGTAGGCTGGAGCTGCTTCG-3’	5’-TACCAGGTAACGCGCCACTCCGACGGGATTAACGAGTGCCGTAAACGACTGACCATATGAATATCCTCCTTAGTTCCTATTC-3’
Δ*ihfB*::kan	5'-CAGCCGCTTAATTTGCCTTTAAGGAACCGGAGGAATCATGGTGTAGGCTGGAGCTGCTTC-3'	5'-TCAAGTTTGAGTAAAAAACTTAACCGTAAATATTGGCGCGACGGCTGACATGGGAATTAG-3'
Δ*recA*::kan	5’-CAACAGAACATATTGACTATCCGGTATTACCCGGCATGACAGGAGTAAAAATGGTGTAGGCTGGAGCTGCTTCG-3’	5’-ATGCGACCCTTGTGTATCAAACAAGACGATTAAAAATCTTCGTTAGTTTCCATATGAATATCCTCCTTAGTTCCTATTC-3’
Δ*relE*::kan	5’-GAACGGCTTCGTAATCCTAAGCCAGTACGTGTGACGCTGGATGAACTCTGATGGTGTAGGCTGGAGCTGCTTCG-3’	5’-GGTGCGAAACAGAGATGTCATGCTTTGGTTCAGAGAATGCGTTTGACCGCCATATGAATATCCTCCTTAGTTCCTATTC-3’
Δ*spoT*::kan	5’-CCGTTACCGCTATTGCTGAAGGTCGTCGTTAATCACAAAGCGGGTCGCCCTTGGTGTAGGCTGGAGCTGCTTCG-3’	5’-CGTGCATAACGTGTTGGGTTCATAAAACATTAATTTCGGTTTCGGGTGACCATATGAATATCCTCCTTAGTTCCTATTC-3’
Δ*tisAB*::kan	5’-GAAACGGGTGGTGGCCGTCAGCGCCTTAACCCCGCGTGAGCACACTGTGTTATGGTGTAGGCTGGAGCTGCTTCG-3’	5’-GCTCCCCTTTGGTGCGACTTGAATCTGAATTACTTCAGGTATTTCAGAACCTATTGCATATCCTCCTTAGTTCCTATTC-3’
Plasmid construction oligonucleotides		
P*malK*	5'-GCGCGGCTCGAGTAGCTGCGTGCACCTGTTTTTATT-3'	5'-GCGCGGGGATCCCCAGGCTTTCGTTACATTTTG-3'
P*2relA*	5'-GCGCGGCTCGAGTAGCAAACAATGCCCCATTTTAGC-3'	5'-GCGCGGGGATCCCTTCTACACCGACCACACTGG-3'
pBAD33-*spoT*	5’-GCGCGGTCTAGATAGCAGGAGAGGTCGCCCTTGTATCTGTTTGAA-3’	5’-GCGCGGAAGCTTTTAATTTCGGTTTCGGGTGA-3’
pQE80-*relA’*	5'-GCGCATGAATTCATTAAAGAGGAGAAGAGGACGATGGTTGCGGTA-3'	5'-GCGCGGAAGCTTTCACAGCTGGTAGGTGAACG-3'
P*dksA- dksA*	5'-GCGCGGCTCGAGTAGCACTATTGTCAGAAGCTCAACAGAG-3'	5'-GCGCGGCCTGCAGGTTAGCCAGCCATGTGTTTTTC-3'
P*sfsA -sfsA dksA*	5'-GCGCGGCTCGAGTAGCCAATCGTCCGTTTCATCCA-3'	5'-GCGCGGCCTGCAGGTTAGCCAGCCATGTGTTTTTC-3'

Table S8. DNA Primers to Confirm Gene Deletion and Kanamycin Resistance Cassette Insertion

Strain	Upstream Forward Primer	Internal Forward Primer	Internal Reverse Primer
Δ*chpB*::kan	5'-ACTTACAGCCGGGGCAGAG-3'	5'-GTGAATTTGAACGGGGAGAC-3'	5'-CGCGATAAATAAACACACCTTATTC-3'
Δ*crp*::kan	5'-GGAAGCATATTTCGGCAATCC-3'	5'-ACTCTCGAATGGTTCTTGTCTC-3'	5'-ACGATGGTTTTACCGTGTGC-3'
Δ*cspD*::kan	5'-TGTCCCCTGTCAAATGCTTG-3'	5'-GAAGCATGGAAAAGGGTACTGT-3'	5'-GCGACTGCCGCTTCTACTT-3'
Δ*dam*::kan	5'-CAGATGTCCAGGCCAAAAAC-3'	5'-ATGTCTGGTTGAGCCTTTTGTA-3'	5'-CGCCGTTGCTGCTTATACTG-3'
Δ*dksA*::kan	5'-CGCAAATACGCTTTTCCTCAC-3'	5'-GGCAAAACCGTAAAACATCG-3'	5'-CTGTAATTAGCCAGCCATCTGT-3'
Δ*fis*::kan	5'-GACTTTTATGGTCCGGCAAA-3'	5'-GAACAACGCGTAAATTCTGAC-3'	5'-GCGCATCACCGTGAATAATG-3'
Δ*hicA*::kan	5'-CGTAAACATCCTGCCACCTT-3'	5'-CGTAAACATCCTGCCACCTT-3'	5'-TTAGAGGCGACGCTCAAAGG-3'
Δ*higB*::kan	5'-CTTATCCGGCCTACGTTCAG-3'	5'-GATAACTCAAAAAGCATTGAAAGAT-3'	5'-GTACGATGAACAGCGGTAAAGA-3'
Δ*hipA*::kan	5'-ATTAAGCAGGCGACGATTTC-3'	5'-TAGCAAGCCCTTATGCCAGA-3'	5'-TCTCAGCACCTTTGCTGTCG-3'
Δ*hns*::kan	5'-CTGCGAAATCATCGGTGTAA-3'	5'-CGAAGCACTTAAAATTCTGAACA-3'	5'-TTGCTTGATCAGGAAATCGTC-3'
Δ*hokE*::kan	5'-GGAGTGAGAAGTCCGAAACAGG-3'	5'-GGAGTGAGAAGTCCGAAACAGG-3'	5'-TATTACGTTCCTTCACCGTAAAC-3'
Δ*hupA*::kan	5'-TTTAACGCCTGATTTGTCGTA-3'	5'-TGCAGAGAAAGCAGAACTGTCC-3'	5'-TGGTCTTCAGCAAATCCACT-3'
Δ*hupB*::kan	5'-ACTCTGGCGCTGCAAAATG-3'	5'-ATTGCTTCCGTAACTGAATCTCTG-3'	5'-TGTAACAACACTCCGCTGTAGA-3'
Δ*ihfA*::kan	5'-GGTATAAGAGCCTCGCCATAAG-3'	5'-CTGGTTTTGGTAACTTCGATCTG-3'	5'-GAATTTGCCAGACGAACAGT-3'
Δ*ihfB*::kan	5'-TGCAGGTTTCGTCCTGTAA-3'	5'-GCCAAGACGGTTGAAGATG-3'	5'-TCCGCTAATTATGCATACACC-3'
Δ*mazF*::kan	5'-TAATGCAGGCGCTCAATCTG-3'	5'-GTACCCGATATGGGCGATCT-3'	5'-GTCAGGTGGAAACCTGTGAC-3'
Δ*mqsR*::kan	5'-CGGATGTTTATGTGCCGTTG-3'	5'-CACATACACGTTTGAGTCAGGTTA-3'	5'-GGCAAACCGGACATTTCATA-3'
Δ*recA*	5'-CTGGTTTGCTTTTGCCACTG-	5'-TGGAAACCATCTCTACCGGTT	5'-GACGAACAGAGGCGTAGAA

	3’	C-3'	T-3'
Δ*relA*::kan	5’-TGGCGATGCTGGATATGTTC-3’	5’-GGTGTTGAGATGGTGGAGAT-3’	5’-ATCTCTTCCTGCCACGCAAT-3’
Δ*relE*::kan	5’-GCATTAACCTGCGTATTGACGA-3’	5'-CACTAAAGGAATGGCGAAAG-3'	5'-CTTCCGAGCGTTCTCTTTTCC-3'
Δ*sbmC*::kan	5’-TTCTCGCCTGAGTGATTATTTCC-3’	5'-GGAGGCGTCATGAACTACGA-3'	5'-GCCCTGAGATGAATTAGTGATG-3'
Δ*seqA*::kan	5'-CCACAGGGCTGCAACAAATA-3'	5'-TGCCAGCCACACTAAGCATATC-3'	5'-GATAGTTCCGCAAACCTTCTCA-3'
Δ*symE*::kan	5’-CACGCCAATCATAACCCACA-3’	5'-ACTGACACGCATTCTATTGCAC-3'	5'-GCTGTTACGCGACTTTCTGTT-3'
Δ*spoT*::kan	5’-CGCGAAATCGAAGAAGGTCT-3’	5’-TTTGAAAGCCTGAATCAACTG-3’	5’-TACGGATCTGGACCTCAACC-3’
Δ*tisAB*::kan	5’-TCACAGTTTGCGTTTTGTCC-3’	5'-AAGCACAACGTTTCTCCTTGAG-3'	5'-GCGGGAGAGGAATCTATCAC-3'
Δ*yacG*::kan	5'-CCGTAAACAAACCAGCCTGA-3'	5'-TATTACGGTGAATTGCCCAAC-3'	5'-TGTAGGTCGGATAAGGCGTTC-3'
Δ*yafO*::kan	5’-CCGGTTGCGGTTCTTTCTAA-3’	5'-TAAGGATGCGGGTATTCAAA-3'	5'-CGCCAGGCTGATAGTTTCTTA-3'
Δ*yafQ*::kan	5’-TGGTTCGCATAACCCTCACA-3’	5'-TGAATACTCGGGACAATATTCAAA-3'	5'-GGAAGGCTCACATTATCACCAA-3'
Δ*yhaV*::kan	5'-CTGGGAGATGAACAGGAGGA-3'	5'-AATAATGGATTTTCCACAAAGG-3'	5'-TGGGTTTCTTCTGTTTCTCG-3'
Δ*yoeB*::kan	5’-GAAAGCCGTTGAAGATCATGC-3’	5'-AAACTAATCTGGTCTGAGGAATCA-3'	5'-CGTATCAAAACTGACAATTCATTC-3'

Supplemental Experimental Procedures

Genetic Perturbations

Genetic deletions were either generated using the method of Datsenko and Wanner (Datsenko and Wanner, 2000) or transduced from the Keio collection (Baba et al., 2006) using the standard P1 phage method. The kanamycin resistance marker was removed from specified strains by FLP recombinase. The primers used for those genes deleted using the Datsenko and Wanner method are presented in Table S7. To generate the Δ*relA*Δ*spoT*::kan strain, the kanamycin resistance cassette was removed by FLP recombinase from the Δ*relA*::kan MG1655 strain (SA021), and then *spoT* was deleted using the method of Datsenko and Wanner (Datsenko and Wanner, 2000). All gene deletions were confirmed using PCR and two sets of primers (Table S8). One set confirmed the presence of the kanamycin resistance cassette in the proper chromosomal location using a forward primer upstream of the intended insertion site and a kanamycin resistance cassette reverse primer, 5'- ATGATGGATACTTTCTCGGCAGGAG-3'. The second set confirmed the absence of a duplicate gene, and contained primers within the gene of interest. Separate colonies were used for each of three replicate experiments.

Plasmid Constructions

Plasmids pSA03 containing the *malK* promoter and pSA05 containing the cAMP dependent *relA* P2 promoter (Nakagawa et al., 2006) were constructed by cloning the proper promoters from the MG1655 chromosome into the XhoI/BamHI sites of vector pUA66 using primers defined in Table S7. The plasmids pSA04, *osmE* promoter, pSA06, *sulA* promoter, and pAS07, *wrbA* promoter were taken from a commercial library (Zaslaver et al., 2006).

The pSA01 pBAD33-*spoT* plasmid was constructed by cloning the *spoT* gene from the MG1655 chromosome into the XbaI/HindIII site of vector pBAD33 using primers defined in Table S7. The pSA02 pQE80-*relA*' plasmid was constructed by cloning the 55-kD truncated *relA* gene described previously (Schreiber et al., 1991) from the MG1655 chromosome into the EcoRI/HindIII site of vector pQE80 using primers defined in Table S7. The *relA'* open reading frame was chosen to overexpress functional RelA protein without association to the ribosome (Schreiber et al., 1991). Plasmids pSA01 and pSA02 used to overexpress SpoT and RelA' respectively were transformed into MG1655 Δ*relA*Δ*spoT* (SA023) so the strain possessed both plasmids. The control strain was MG1655 Δ*relA*Δ*spoT* with the empty pBAD33 vector and pSA02.

For complementation, the *dksA* locus was cloned into the pUA66 vector. To assess the importance of the cAMP-CRP transcriptional regulation for DksA's involvement in persistence, two complementation plasmids were constructed, one containing the cAMP-CRP binding site upstream of the *sfsA* promoter and one lacking the cAMP-CRP binding using the *dksA* specific promoter. Plasmids pSA08 (PsfsA) and pSA09 (PdksA) were constructed by cloning the *dksA* locus with the designated promoter and transcriptional regulation into the XhoI/SbfI sites of the pUA66 vector using primers specified in Table S7.

Statistical Analysis for Genetic Mutants

To determine which two-carbon media, chemical treatments, and genetic deletions were significant to persister formation, the 5h persister measurements were used. This data point was selected since the cultures were in the second regime of biphasic killing, where only persisters are capable of generating a CFU (Lewis, 2010). To determine if a genetic deletion was

significant to the persister formation pathway the fold-change, defined as the ratio of persisters in glucose-fumarate media to persisters in glucose media, was calculated for the 5h time point for both the genetic mutant and the wild-type culture ran during that assay as a control.

The CFU method was first tested to confirm that the data can be treated as normally distributed. Since wild-type samples were run in parallel every time deletion mutants were tested, 31 CFU measurements were available for wild-type in AA-supplemented media. The normality of these data along with their fold-change values, glucose-fumarate persisters/glucose-only persisters, was assessed using the Anderson-Darling and Shapiro-Wilk tests. Both the CFU/mL values and fold-change values after 5 h OFL treatment were considered normally distributed by both tests. The normality plots of the two datasets are shown below.

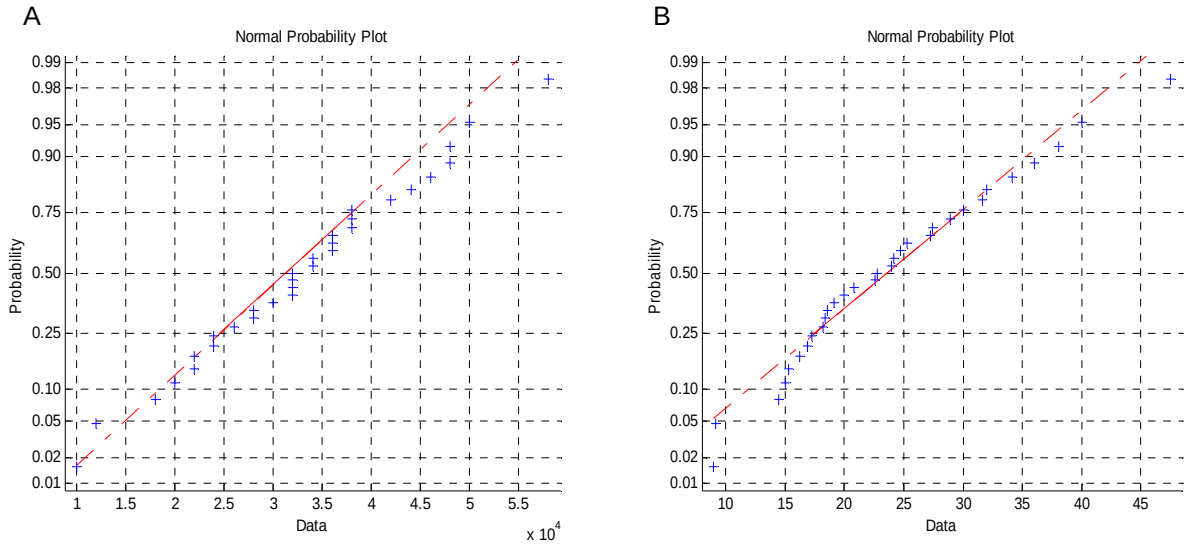

Normality plot for large dataset. (A) Dataset for wild-type persisters at 5h OFL treatment in glucose-fumarate AA supplemented media and (B) the fold-change for wild-type persisters at 5hr OFL treatment after the carbon source transition demonstrate near-normality

After confirming the data can be considered near-normally distributed, 2-tailed t-tests with unequal variances were used to assess statistical significance due to a small sample size

(n=3). Statistical significance was assessed in three ways, 1) a t-test was performed on CFU/mL measurements obtained after 5 h of OFL treatment using the null hypothesis that the means of both samples were equal, 2) a t-test was performed on fold-change measurements, (CFU/mL glucose-fumarate/CFU/mL glucose-only), between deletion mutants and wild-type samples using the null hypothesis that the mean of the mutant fold-change was equal to the wild-type fold-change, and 3) a t-test was performed on persister frequency relative to the whole population for the highest and lowest 10% for FACS using the null hypothesis that the mean persister level relative to the whole population in the lowest 10% was equal to the mean persister level relative to the whole population in the highest 10%. For each test, if the p-value < 0.05, the null hypothesis was rejected. Table S2 displays the p-values for all gene deletions tested.

Transcriptional Reporter Experiments

Flow Cytometry

All strains including controls were analyzed by LSRII (BD Biosciences, San Jose, CA) flow cytometer before sorting. Microorganisms were determined using forward and side scatter parameters (FSC and SSC). The bacteria were assayed with a laser emitting at 488nm for green proteins, and green fluorescence was collected by 525/50 bandpass filter. Data were acquired and analyzed using FACSDiVa software (BD Biosciences, San Jose, CA). The control experiments and their results are explained below.

ppGpp Reporter Control

The *osmE* and *wrbA* promoters were selected as transcriptional reporters for ppGpp. In addition to previous experimental evidence that these promoters respond positively to increases

in ppGpp levels (Durfee et al., 2008; Traxler et al., 2011), the responses of these promoters to increases in ppGpp levels in our experimental conditions were tested to assure the reporters responded to the proper stimuli. Plasmids pUA66 (promoterless) as a negative control, pSA04 (*osmE),* and pSA07 (*wrbA*) were individually transformed into MG1655 Δ*relA*Δ*spoT* (SA019). Kanamycin (50µg/mL) was present during growth to retain the plasmid in the cell. Cells were prepared as described in the Experimental Procedures (main text) under carbon source transition assay. At 0.02 OD_{600} (before glucose exhaustion) and at 0.20 OD_{600} (after glucose exhaustion), cells were collected, washed in 1X PBS, and diluted to approximately 10^6 cells/mL. Samples were then analyzed by LSRII flow cytometry as described above.

cAMP Reporter Control

The *malK* promoter was selected as a cAMP transcriptional reporter since this promoter contains multiple cAMP-CRP binding sites that activate transcription (Raibaud, 1989; Raibaud et al., 1989; Vidal-Ingigliardi and Raibaud, 1991). The reporter was tested for its ability to respond to cAMP levels. Plasmid pUA66 (promoterless) as a negative control and pSA03 (*malK*) were individually transformed into MG1655 and MG1655 *Δcrp* (SA003). Kanamycin (50µg/mL) was present during growth for plasmid retention. Cells were prepared as described in the Experimental Procedures (main text). At 0.02 OD_{600}, cultures were treated with filter sterilized cAMP to a final concentration of 8mM. Cells were collected prior to cAMP addition as a reference state and at 1 h after cAMP addition. Cells were washed in 1X PBS and analyzed by LSRII flow cytometry as described above. Once the reporter was confirmed to respond to the proper cAMP stimuli, MG1655 pSA03 was grown in the carbon source transition assay conditions and FACS was conducted as described below. The GFP distributions are presented in

Figure S3 (B). The persister levels were evenly distributed throughout the population, and not statistically different between the lowest and highest 10% quantile.

SOS Response Reporter Control

The *sulA* promoter was selected as an SOS response transcriptional reporter as chosen previously (Dorr et al., 2010). The reporter was tested for its ability to respond to SOS response induction through DNA damage. Plasmids pUA66 (promoterless) as a negative control and pSA06 (*sulA*) were individually transformed into MG1655 and MG1655 Δ*recA* (SA020). Kanamycin (50µg/mL) was present during growth to retain the plasmid in the cell. Overnight cultures were prepared as described in Experimental Procedures (main text). Cells from the overnight culture were diluted to an OD_{600} of 0.005 in 25mL of 4.5mM M9 glucose medium in a 250mL baffled flask and cultured in a shaker at 37°C and 250rpm to an OD_{600} of 0.02. Cells were then exposed to 254 nm ultraviolet (UV) light for 30s in a biological safety cabinet (Labconco Class II, Type A2 Biosafety Cabinets, Kansas City, MO). Cells were collected prior to UV exposure as a reference state and at 1 h after UV exposure. All samples were washed in 1X PBS and analyzed by LSRII flow cytometry as described above. Once the reporter was confirmed to respond to the proper DNA damage stimuli, MG1655 pSA06 was grown in the carbon source transition assay conditions and FACS was conducted as described below. The GFP distributions are presented in Figure S3 (E). The persister levels were evenly distributed throughout the population, and not statistically different between the lowest and highest 10% quantile.

Cell Sorting and Persister Assay

Cells were sorted using Reflection (Sony-iCyt Mission Technology, Champaign, IL) cell sorter at 30psi with a 70micron nozzle. Microorganisms were determined by forward and side scatter parameters (FSC and SSC), and physiologically distinct subpopulations were identified using a 488nm excitation laser and 525/50 bandpass filter. The gates of subpopulations were determined by analyzing wild type cells with/without promoterless pUA66 plasmids (negative control) and strains including plasmids with GFP. The sheath fluid used in the sorter was 1X PBS.

Cells were collected prior to glucose exhaustion (0.02 OD_{600}) and after glucose exhaustion (0.20 OD_{600}) in AA-supplemented media and were diluted in filter-sterilized culture media taken at sampling time to obtain approximately 10^6cells/mL. Cells taken from glucose-fumarate media at 0.20 OD_{600} were segregated into the lowest and highest 10% quantiles based on the GFP signal. Approximately $5x10^5$ cells for each quantile collected were sorted in 0.5 mL PBS, mixed 1:1 with filter-sterilized culture medium to decrease the effect of medium-composition on persistence, treated with 5 μg/mL OFL, and incubated at 37 ºC and 250 rpm. After 5h OFL treatment, cells were collected by centrifugation (3 minutes, 15000 rpm), washed with PBS, resuspended in 100μL PBS, and 10μL of samples were serially diluted in PBS and plated on LB agar to incubate for 16 hours at 37 ºC for CFU counts. The remaining 90 μL were also plated on LB agar in case CFU counts from 10 μL samples might be under the limit of detection.

DksA Complementation Assay

Plasmids pUA66 (promoterless), pSA08, and pSA09 were individually transformed into MG1655 Δ*dksA* (SA007). The carbon source transition assay was performed using MG1655, MG1655 Δ*dksA::kan*, MG1655 Δ*dksA (*control for curing out kanamycin), MG1655 Δ*dksA* pUA66 (empty vector control), MG1655 Δ*dksA* pSA08, and MG1655 Δ*dksA* pSA09 for complementation as described in the Experimental Procedures (main text).

RelA-SpoT Overexpression

Overnight cultures of MG1655 Δ*relA*Δ*spoT* pSA01 pSA02 grown with 100µg/mL AMP and 50µg/mL CAM for selection were diluted to 0.005 OD_{600} in 25mL of 4.5mM M9 glucose medium supplemented with AA in a 250mL baffled flask. When indicated, induction of P_{BAD} was performed with 2% arabinose at the time of inoculation. Cells were cultured in a shaker at 37°C and 250rpm to 0.02 OD_{600}, at which time 50µM IPTG was added to cultures if indicated to activate the P_{T5} promoter. Growth was monitored by measuring OD_{600}. Persister measurements were taken 2 h post IPTG induction. Cells were plated on LB agar with 2% arabinose to facilitate growth of cells inhibited by RelA'.

ppGpp Biochemical Network Kinetic Model

Model Construction

The ppGpp biochemical network is presented mathematically as a system of ordinary differential equations describing changes in the concentration of RelA, DksA, SpoT, ppGpp, and all four RNAP forms over time (Eqns. S1-S8).

$$\frac{d[RelA]}{dt} = \beta_{RelA} RNAP_{activity} - k_{\deg,RelA}[RelA] \quad \text{(S1)}$$

$$\frac{d[DksA]}{dt} = \beta_{DksA} RNAP_{activity} - k_{\deg,DksA}[DksA] - k_{on,RNAPDksA}[DksA][RNAP]$$
$$+ k_{off,RNAPDksA}[RNAP_{DksA}] - k_{on,RNAPDksA}[DksA][RNAP_{ppGpp}] + k_{off,RNAPDksA}[RNAP_{DksA,ppGpp}] \quad \text{(S2)}$$

$$\frac{d[SpoT]}{dt} = \beta_{SpoT} RNAP_{activity} - k_{\deg,SpoT,hyd}(1-f)[SpoT] - k_{\deg,SpoT,syn} f[SpoT] \quad \text{(S3)}$$

$$\frac{d[ppGpp]}{dt} = \frac{k_{syn,\mathrm{Re}lA}[RelA][GTP][ATP]}{[ATP][GTP] + K_{ATP}[GTP] + K_{GTP}[ATP]} + \frac{k_{syn,SpoT} f[SpoT][GTP][ATP]}{[ATP][GTP] + K_{ATP}[GTP] + K_{GTP}[ATP]}$$
$$- \frac{k_{\deg,ppGpp}(1-f)[SpoT][ppGpp]}{[ppGpp] + K_{ppGpp}} - k_{on,RNAPppGpp,a}[ppGpp][RNAP]$$
$$+ k_{off,RNAPppGpp,a}[RNAP_{ppGpp}] - k_{on,RNAPppGpp}[ppGpp][RNAP_{DksA}] + k_{off,RNAPppGpp}[RNAP_{DksA,ppGpp}] \quad \text{(S4)}$$

$$\frac{d[RNAP]}{dt} = -k_{on,RNAPDksA}[DksA][RNAP] + k_{off,RNAPDksA}[RNAP_{DksA}] \quad \text{(S5)}$$
$$- k_{on,RNAPppGpp,a}[ppGpp][RNAP] + k_{off,RNAPppGpp,a}[RNAP_{ppGpp}]$$

$$\frac{d[RNAP_{ppGpp}]}{dt} = k_{on,RNAPppGpp,a}[ppGpp][RNAP] - k_{off,RNAPppGpp,a}[RNAP_{ppGpp}] \quad \text{(S6)}$$
$$- k_{on,RNAPDksA}[RNAP_{ppGpp}][DksA] + k_{off,RNAPDksA}[RNAP_{DksA,ppGpp}]$$

$$\frac{d[RNAP_{DksA}]}{dt} = k_{on,RNAPDksA}[DksA][RNAP] - k_{off,RNAPDksA}[RNAP_{DksA}] \quad \text{(S7)}$$
$$- k_{on,RNAPppGpp}[RNAP_{DksA}][ppGpp] + k_{off,RNAPppGpp}[RNAP_{DksA,ppGpp}]$$

$$\frac{d[RNAP_{DksA,ppGpp}]}{dt} = k_{on,RNAPDksA}[DksA][RNAP_{ppGpp}] - k_{off,RNAPDksA}[RNAP_{DksA,ppGpp}] \quad \text{(S8)}$$
$$+ k_{on,RNAPppGpp}[RNAP_{DksA}][ppGpp] - k_{off,RNAPppGpp}[RNAP_{DksA,ppGpp}]$$

The concentration of RelA is denoted by [RelA], the concentration of DksA is denoted by [DksA], the concentration of SpoT is denoted by [SpoT], the concentration of ppGpp is denoted by [ppGpp], the concentration of free RNAP is denoted by [RNAP], the concentration of RNAP bound by ppGpp is denoted by [$RNAP_{ppGpp}$], the concentration of RNAP bound by DksA is denoted by [$RNAP_{DksA}$], and the concentration of RNAP bound with both DksA and ppGpp is denoted by [$RNAP_{DksA,ppGpp}$]. Definitions of all other parameters are presented in Table S3 and Table S4.

The turnover numbers, β, for each protein described in the model are combined parameters encompassing transcription and translation rates assuming mRNA production is at steady state.

$$\frac{d[mRNA]}{dt} = k_{transcription} - k_{\deg,mRNA}[mRNA] = 0 \quad \text{(S9.a)}$$

$$[mRNA] = \frac{k_{transcription}}{k_{\deg,mRNA}} \quad \text{(S9.b)}$$

Where [mRNA] is the concentration of mRNA, $k_{transcription}$ is the rate constant for transcription of the gene of interest, and $k_{deg,mRNA}$ is the rate constant for mRNA degradation. Therefore, the steady state value of mRNA (Eqn. S9.b) can be applied to the equation describing protein production (Eqn. S9.c).

$$\frac{d[protein]}{dt} = k_{translation}[mRNA] - k_{\deg,protein}[protein] = \frac{k_{translation}k_{transcription}}{k_{\deg,mRNA}} - k_{\deg,protein}[protein] \quad \text{(S9.c)}$$
$$= \beta_{protein} - k_{\deg,protein}[protein]$$

$$\beta_{protein} = \frac{k_{translation}k_{transcription}}{k_{\deg,mRNA}} \quad \text{(S9.d)}$$

Where [protein] is the concentration of the protein of interest, $k_{translation}$ is the rate constant for translation, $k_{deg,protein}$ is the rate constant for protein degradation, and $\beta_{protein}$ is defined as the turnover number for the protein of interest.

The repression of DksA and SpoT expression by DksA and ppGpp is achieved by modulating the turnover number for the protein by a factor $RNAP_{activity}$, since different RNAP complexes have different affinities to the promoter and, therefore, alter $k_{transcription}$. The $RNAP_{activity}$ is defined as the ratio of RNAP complexes transcriptionally active versus total RNAP.

$$RNAP_{activity} = \frac{RNAP_{active}}{RNAP_{total}} = \frac{[RNAP] + a[RNAP_{DksA}] + b[RNAP_{ppGpp}] + c[RNAP_{DksA,ppGpp}]}{[RNAP] + [RNAP_{DksA}] + [RNAP_{ppGpp}] + [RNAP_{DksA,ppGpp}]} \quad \text{(S10)}$$

The four different forms of RNAP, free RNAP, $RNAP_{ppGpp}$, $RNAP_{DksA}$, and $RNAP_{DksA,ppGpp}$ each have their own transcription activity, which corresponds to its binding affinity to promoters. We assume free RNAP is fully active, while other complexes' transcriptional activity is modulated by the coefficients a, b, or c. Calculation of the inhibition coefficients is described below. We assume the *relA* promoter is not stringently controlled so that for Eqn. S1, $RNAP_{activity}$=1 (*i.e.* a=b=c=1).

The SpoT protein can act as either a synthase or a hydrolase but cannot have both functionalities simultaneously. It is unknown what causes the protein to possess one functionality versus the other (Murray and Bremer, 1996) so the parameter *f* was used to quantify the fraction of SpoT protein acting as a ppGpp synthase. It is assumed that the SpoT synthase and hydrolase enzyme have different degradation rates since the synthase is considered unstable while the hydrolase is considered stable (Murray and Bremer, 1996; Richter et al., 1979).

The product of RelA and SpoT synthases using ATP and GTP as substrates is guanosine pentaphosphate (pppGpp). This nucleotide is hydrolyzed to ppGpp by the Gpp enzyme (Somerville and Ahmed, 1979). We assume (p)ppGpp to be collectively termed ppGpp for all analyses. Two substrate Michaelis Menten enzyme kinetics was assumed for ppGpp synthesis by RelA and SpoT. Since no mechanism for this enzymatic reaction is known, we applied the two most common bi-substrate enzymatic mechanisms, ping-pong and sequential. The mechanism used in Eqn. S4 and for all model simulations was ping-pong (Splittgerber, 1983). The kinetic expression for a sequential mechanism was tested and did not alter results. The ATP and GTP Michealis constants for SpoT synthase are unknown and therefore assumed to be the same as those for RelA synthase since the two proteins have a very high sequence homology (Murray and Bremer, 1996). ppGpp degradation was described by single substrate Michaelis Menten kinetics.

To simplify the kinetic model for bistability analysis, we assumed all binding events involving ppGpp, DksA, and RNAP rapidly approached equilibrium. With this assumption, the rate of ppGpp/DksA binding to RNAP is equal to the rate of ppGpp/DksA unbinding to RNAP.

$$RNAP + DksA \xleftrightarrow{K_{d,DksA}} RNAP_{DksA} \quad \text{(S11.a)}$$

$$k_{on,RNAPDksA}[RNAP][DksA] = k_{off,RNAPDksA}[RNAP_{DksA}] \quad \text{(S11.b)}$$

$$[RNAP_{DksA}] = \frac{k_{on,RNAPDksA}[RNAP][DksA]}{k_{off,RNAPDksA}} = \frac{[RNAP][DksA]}{K_{d,DksA}} \quad \text{(S11.c)}$$

$$RNAP + ppGpp \xleftrightarrow{K_{d,ppGpp,a}} RNAP_{ppGpp} \quad \text{(S12.a)}$$

$$k_{on,RNAPppGpp,a}[RNAP][ppGpp] = k_{off,RNAPppGpp,a}[RNAP_{ppGpp}] \quad \text{(S12.b)}$$

$$[RNAP_{ppGpp}] = \frac{k_{on,RNAPppGpp,a}[RNAP][ppGpp]}{k_{off,RNAPppGpp,a}} = \frac{[RNAP][ppGpp]}{K_{d,ppGpp,a}} \quad \text{(S12.c)}$$

$$RNAP_{ppGpp} + DksA \xleftrightarrow{K_{d,DksA}} RNAP_{DksA,ppGpp}$$
$$RNAP_{DksA} + ppGpp \xleftrightarrow{K_{d,ppGpp}} RNAP_{DksA,ppGpp} \quad \text{(S13.a)}$$

$$k_{on,RNAPppGpp}[RNAP_{DksA}][ppGpp] + k_{on,RNAPDksA}[RNAP_{ppGpp}][DksA] = (k_{off,RNAPppGpp} + k_{off,RNAPDksA})[RNAP_{DksA,ppGpp}] \quad \text{(S13.b)}$$

$$[RNAP_{DksA,ppGpp}] = \frac{k_{on,RNAPppGpp}[RNAP_{DksA}][ppGpp] + k_{on,RNAPDksA}[RNAP_{ppGpp}][DksA]}{k_{off,RNAPppGpp} + k_{off,RNAPDksA}}$$
$$= \frac{\frac{k_{on,RNAPppGpp}[RNAP][DksA][ppGpp]}{K_{d,DksA}} + \frac{k_{on,RNAPDksA}[RNAP][DksA][ppGpp]}{K_{d,ppGpp,a}}}{k_{on,RNAPppGpp}K_{d,ppGpp} + k_{on,RNAPDksA}K_{d,DksA}} \quad \text{(S13.c)}$$

Where $k_{on,DksA}$ and $k_{off,DksA}$ are the binding and dissociating rate constants for DksA to RNAP or $RNAP_{ppGpp}$, $k_{on,ppGpp,a}$ and $k_{off,ppGpp,a}$ are the binding and dissociating rate constants for ppGpp to RNAP, $k_{on,ppGpp}$ and $k_{off,ppGpp}$ are the binding and dissociating rate constants for ppGpp to $RNAP_{DksA}$, and the dissociation constant for each binding event is defined as $K_d = \frac{k_{off}}{k_{on}}$. These terms for the various RNAP complexes were applied to Eqn. S10.

The three simplified equations shown below were ultimately applied to the model for bistability analysis.

$$\frac{d[DksA]}{dt} = \beta_{DksA} RNAP_{activity} - k_{\deg,DksA}[DksA] \quad \text{(S14)}$$

$$\frac{d[SpoT]}{dt} = \beta_{SpoT} RNAP_{activity} - k_{\deg,SpoT,hyd}(1-f)[SpoT] - k_{\deg,SpoT,syn} f[SpoT] \quad \text{(S15)}$$

$$\frac{d[ppGpp]}{dt} = \frac{k_{syn,\mathrm{Re}lA}[RelA][GTP][ATP]}{[ATP][GTP] + K_{ATP}[GTP] + K_{GTP}[ATP]} + \frac{k_{syn,SpoT} f[SpoT][GTP][ATP]}{[ATP][GTP] + K_{ATP}[GTP] + K_{GTP}[ATP]} - \frac{k_{\deg,ppGpp}(1-f)[SpoT][ppGpp]}{[ppGpp] + K_{ppGpp}} \quad \text{(S16)}$$

$$RNAP_{activity} = \frac{1 + a\left(\frac{[DksA]}{K_{d,DksA}}\right) + b\left(\frac{[ppGpp]}{K_{d,ppGpp,a}}\right) + c\left(\frac{[ppGpp][DksA]\left(\frac{k_{on,ppGpp}}{K_{d,DksA}} + \frac{k_{on,DksA}}{K_{d,ppGpp,a}}\right)}{k_{on,DksA}K_{d,DksA} + k_{on,ppGpp}K_{d,ppGpp}}\right)}{1 + \frac{[DksA]}{K_{d,DksA}} + \frac{[ppGpp]}{K_{d,ppGpp,a}} + \frac{[ppGpp][DksA]\left(\frac{k_{on,ppGpp}}{K_{d,DksA}} + \frac{k_{on,DksA}}{K_{d,ppGpp,a}}\right)}{k_{on,DksA}K_{d,DksA} + k_{on,ppGpp}K_{d,ppGpp}}} \quad \text{(S17)}$$

Bistability analysis was performed by initially solving for the steady-state concentration of DksA in terms of ppGpp by setting Eqn. S14 equal to zero. This expression for DksA was applied to Eqn. S15, which reduced the system to two ordinary differential equations. Both the modified Eqn. S15 and Eqn. S16 were set to zero and equations for the nullclines of each were determined. Points of intersection between nullclines designate a steady state. Therefore, bistability was present if the two nullclines intersected more than once. System dynamics were analyzed using the integrator ode15s in MATLAB to determine the stability of each steady state and the initial conditions required to drive the system to a particular steady state for the given parameter set.

Parameterization

We sought to inform our kinetic model as accurately and completely as possible with experimentally determined parameter values so as to produce physiologically relevant results. Different categories of parameters emerged: those with only a single experimental value, those

with known experimental ranges, and those with no experimentally determined values. Unknown values were chosen to align steady state results with known physiological ranges. All parameter values applied to the model and known experimental ranges are presented in Table S3 and Table S4.

In the instance where only one experimental value for the given parameter was known, that value was applied to the model. These parameters included protein degradation rate constants where the protein was estimated to have a half-life of a stable protein (Alon, 2007) and the ATP and GTP Michaelis constants for RelA and SpoT for ppGpp synthesis. Parameters with known experimental ranges included inhibition coefficients, the dissociation coefficients, K_d, for the various binding events, concentrations of proteins and metabolites, and the ppGpp Michaelis constant for SpoT.

Inhibition coefficients were calculated from transcriptional fold-inhibition by specific RNAP complexes. Experimental evidence has shown that ppGpp and DksA individually can inhibit translation at stringent promoters, but greater inhibition of transcription occurs when both molecules are present and work synergistically (Chandrangsu et al., 2011; Lemke et al., 2011; Paul et al., 2004). We assumed that unbound RNAP is fully active. To determine the degree of repression each bound complex should contribute, we analyzed data from *in vitro* transcription assays. The coefficients of inhibition for the $RNAP_{DksA}$ and $RNAP_{ppGpp}$ were determined using 1.5-fold inhibition of transcription (Chandrangsu et al., 2011). Coefficient for the $RNAP_{DksA,ppGpp}$ complex was calculated using 20-fold inhibition of transcription (Paul et al., 2004) (See table below).

Concentrations and parameters for calculation of inhibition coefficient

	A	B	c
fold-change inhibition	1.5	1.5	20
$RNAP_{total}$	6 molecules/cell	6 molecules/cell	6 molecules/cell
$DksA_{initial}$	600 molecules/cell	600 molecules/cell	120 molecules/cell
$ppGpp_{initial}$	60000 molecules/cell	60,000 molecules/cell	120,000 molecules/cell
RNAP	0.55 molecules/cell	1 molecules/cell	0.03 molecules/cell
DksA	594 molecules/cell	-	114.3 molecules/cell
ppGpp	-	59,995 molecules/cell	119,994 molecules/cell
$RNAP_{DksA}$	5.45 molecules/cell	-	0.05 molecules/cell
$RNAP_{ppGpp}$	-	5 molecules/cell	0.3 molecules/cell
$RNAP_{DksA,ppGpp}$	-	-	5.62 molecules/cell
Coefficient	0.633	0.600	.01
Reference	(Chandrangsu et al., 2011)	(Chandrangsu et al., 2011)	(Paul et al., 2004)

Concentrations and parameters for calculation of inhibition coefficient. The fold-inhibition by each RNAP complex was determined using *in vitro* transcription assay data. This table provides concentrations of RNAP, DksA, ppGpp and RNAP complexes used to calculate inhibition coefficients for each RNAP complex.

$$\frac{RNAP + aRNAP_{DksA}}{RNAP_{total}} = \frac{1}{fold, inhibition} \quad \text{(S18.a)}$$

$$\frac{RNAP + bRNAP_{ppGpp}}{RNAP_{total}} = \frac{1}{fold, inhibition} \quad \text{(S18.b)}$$

$$\frac{RNAP + aRNAP_{DksA} + bRNAP_{ppGpp} + cRNAP_{DksA, ppGpp}}{RNAP_{total}} = \frac{1}{fold, inhibition} \quad \text{(S18.c)}$$

Eqns. S18.a, S18.b, and S18.c were applied to solve for the coefficients a, b, and c.

The ppGpp Michaelis constant for SpoT hydrolase has been stated in literature (An et al., 1979; Heinemeyer and Richter, 1978). However, values were reported without the supporting

calculations from experimental data. Therefore, the experimental data of ppGpp decay versus time during the initial velocity of the reaction was fit to the two kinetic parameters, V_{max} and K_{ppGpp} (Heinemeyer and Richter, 1978). The data was fit using a MATLAB nonlinear least squares minimization function, lsqcurvefit, to determine the kinetic parameters (see figure below). The V_{max}= 15.4μM/min= 9274 molecules/cell/min and K_{ppGpp}=49.3μM= 2.9 x 10^4 molecules/cell. Another source reported that K_{ppGpp}=3.3 x 10^5 molecules/cell (An et al., 1979), which is significantly higher than that determined from the data reported by Heinemeyer and Richter. This K_m value is higher than that of most enzymes with their substrates, and it is representative of a very poor binding affinity of ppGpp with SpoT (Berg et al., 2012). Since the assay of Heinemeyer and Richter was performed on whole cell lysates and that of An and colleagues was performed on partially purified protein, it is possible that an allosteric activator of SpoT might have been absent in the reaction contents of the purified enzyme leading to the large K_m for isolated SpoT.

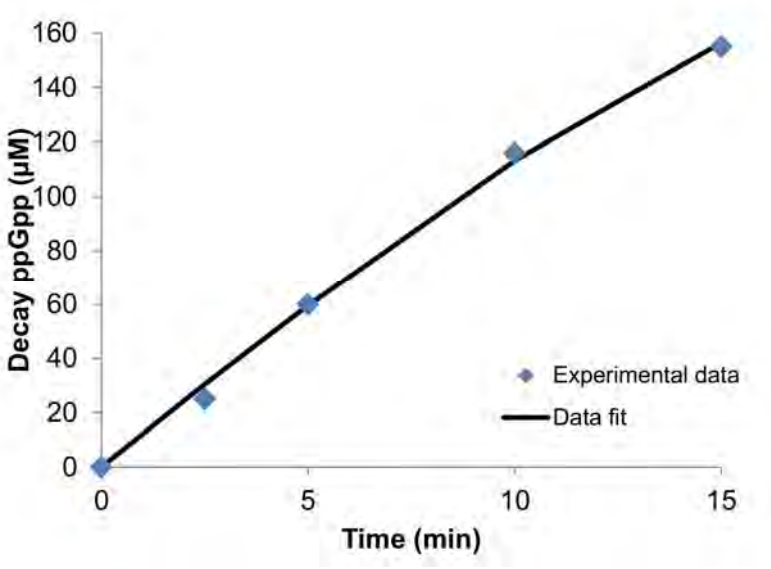

Data fit for ppGpp Km for SpoT hydrolase. Simulation of ppGpp decay was fit to reported experimental data to determine the optimal value for V_{max} and K_m as described. The data fit resulted in V_{max}=9274 molecules/cell/min and

Uncertain parameter values (Table S4) were estimated using experimental evidence available to achieve physiological values for RelA, DksA, and ppGpp. These parameter values

included turnover numbers, catalytic rate constants for ppGpp synthesis and degradation, the fraction of SpoT molecules in the synthase state, and the rate constant for either ppGpp or DksA binding to RNAP.

Modulating turnover numbers allowed the model to achieve steady-state levels for ppGpp, RelA, and DksA to be within physiological ranges. The average concentration of RelA is 50 molecules/cell since there is approximately 1 RelA molecule for every 200 ribosomes (Srivatsan and Wang, 2008) and a typical *E. coli* cell contains 10^4 ribosomes (Alon, 2007). Since RelA is considered a stable protein and its degradation rate constant is 0.02 min^{-1} and the steady state concentration of RelA, 50 molecules/cell, is defined by setting Eqn. S1 equal to zero as:

$$[RelA]_{steadystate} = \frac{\beta_{RelA}}{k_{\deg,RelA}} \quad \text{(S19)}$$

Therefore, the turnover number for RelA was set to 1 molecule/cell. DksA is reported to be present at approximately 3,000-10,000 molecules/cell (Paul et al., 2004). The turnover number for DksA was modulated to achieve a total DksA concentration within this range. The turnover number selected at 2000 molecules/cells keeps the concentration of DksA within this range for both the normal and persister cells as presented in Table S4. The physiological range of SpoT protein in the cell has not been determined. Therefore, we assumed the protein concentration of SpoT in normal cells to be analogous to RelA protein concentration since the two proteins are highly homologous. The turnover number of SpoT set to 450 molecules/cell provides a SpoT concentration of approximate 50 molecules/cell in normal cells (see Table S5) similar to RelA.

The ppGpp synthesis and degradation rate constants were selected to keep the steady state characterized by lower ppGpp levels within the physiologically observed range during

exponential growth (5,700-34,000 molecules/cell) (Murray and Bremer, 1996). An estimate of $k_{syn,RelA}$ was determined using *in vitro* RelA synthase data (Pedersen and Kjeldgaard, 1977). From the % ppGpp converted from GTP vs [RelA] data, using specified protein and nucleotide concentrations, and Michealis constants determined in Table S3, the $k_{syn,RelA}$ was estimated by applying a two-substrate ping-pong Michealis Menten kinetic rate equation to the presented data. The $k_{syn,RelA}$ was determined to be on the order of $1000min^{-1}$. Since *in vitro* data for SpoT synthase activity is not available, we assumed the $k_{syn,SpoT}$ to be similar to $k_{syn,RelA}$ due to the strong sequence homology between the two enzymes. An estimate for the catalytic rate constant for SpoT hydrolase was determined using the data presented above to determine the K_m and V_{max} for the hydrolase (Heinemeyer and Richter, 1978). The SpoT present in the crude cell extract protein was assumed to be similar to that of RelA protein content. Then, the equation for Vmax was applied shown in Eqn. S20.

$$V_{\max} = k_{\deg, ppGpp}[SpoT] \quad \text{(S20)}$$

The degradation rate constant was determined to be on the order of $10{,}000min^{-1}$. Since the proportion of SpoT synthase to SpoT hydrolase present in the cell is not known, we assumed half of the SpoT protein was a synthase and half was a hydrolase setting f=0.5.

The forward rate constants for ppGpp binding to $RNAP_{DksA}$ and DksA binding to $RNAP_{ppGpp}$ are unknown, but the equilibrium rate constant of the binding is experimentally determined (Table S4). Since the model is analyzing steady states, these parameter values are not significant. Altering the value of these parameters did not alter the nullclines.

Bistability Analysis

We used the parameter values and ranges in Table S3 and Table S4 to analyze bistability in our system. The experimental range of each parameter is provided as a basis for the physiological relevance of the nominal values. Nominal values are those used to generate the nullclines and phase space trajectories in Figure 5B.

For each parameter, we establish the range of values for which bistability is maintained in the system. Each parameter value was altered while keeping all other parameters constant at their nominal values and bistability was assessed. The bistable range presented in Table S3 and Table S4 represent the values of these parameters where bistability is maintained. Since many of these parameters are interrelated within the model, altering the nominal value of one parameter may affect the bistable ranges of other parameters. Therefore, the values presented in the bistable range may not be the only values of that particular parameter where bistability may occur if nominal values of other parameters are altered.

Bistability was most sensitive to the coefficient c and therefore, the extent of repression from the $RNAP_{DksA,ppGpp}$ complex. When repression was strong, bistability was present with all other parameters at their nominal values. As repression from this complex was weakened, the concentration of SpoT was no longer reduced enough to observe the high ppGpp state. The bistability was not as sensitive to the regulation by $RNAP_{DksA}$ or $RNAP_{ppGpp}$, most likely due to the small concentrations of these complexes at high ppGpp concentrations. We note that in Table S3, we report a narrow range, in comparison to the experimental range, for the parameter c where bistability is achieved. This reflects a requirement of very strong repression from this

complex to enable bistability. The bistable range reported in Tables S3 and S4 is that which applies when c is varied and all other parameters are kept at their nominal values. The parameters within this model are interrelated, and the range of values for c which enable bistability will only increase beyond that which we report here if a more extensive analysis is performed. For instance, a combinatorial analysis, where all values are adjusted simultaneously, would expand the range of c values that enable bistability. Therefore, the bistable range of c-values reported here should not be considered the maximal range, but simply one that applies for the nominal values used in this study.

The effect of ppGpp and DksA on transcription has been shown to be promoter specific exhibiting varying degrees of repression (Chandrangsu et al., 2011; Lemke et al., 2011). This can be incorporated into our model by designating different a, b, and c values for DksA and SpoT. Weakening the repression of DksA expression by these complexes did not alter the model results significantly, when SpoT repression was kept strong. However, weakening the repression of SpoT regardless of repression on DksA eventually eliminated the presence of two steady states. Therefore, bistability present in the ppGpp biochemical network was highly dependent on the repression of SpoT production by ppGpp and DksA.

The ppGpp Michaelis constant, K_{ppGpp}, for SpoT hydrolase was also an important parameter for bistability. The Michaelis constant represents the substrate concentration at which the reaction rate is half maximal (Splittgerber, 1983), therefore, lower K_{ppGpp} values suggest the SpoT enzyme degrades ppGpp more efficiently than at higher K_{ppGpp} values. Increasing K_{ppGpp} from its nominal value toward the upper physiological range eliminated the bistability and only the high ppGpp state remained (Table S3). This suggests that as the affinity of the enzyme for its

substrate drops, it can no longer degrade ppGpp efficiently enough to keep the ppGpp levels low. These results highlight the importance of not only strong repression of SpoT expression by $RNAP_{DksA,ppGpp}$, but also proficient degradation of ppGpp by SpoT hydrolase for the biochemical network to exhibit bistability.

We assumed that SpoT synthase is functionally and/or physically unstable because of the inability to detect SpoT synthase in cell extracts (Richter et al., 1979) and the requirement of continued protein synthesis for functionality (Murray and Bremer, 1996). Since both the nominal value of *f* and $k_{deg,SpoT,syn}$ are assumptions and are interrelated within our model, we explored varying both of these parameters simultaneously to determine if making the SpoT synthase more stable while altering the synthase fraction can yield a bistable system. The parameter $k_{deg,SpoT,syn}$ was varied from a discretized range of [0.015,1.5] and the parameter *f* was varied from a discretized range of [0,1] while keeping all other parameters at their nominal values. The model simulation was run for 10,000 iterations while randomly selecting values for the two parameters within their specified ranges. For each pair of $k_{deg,SpoT,syn}$ and *f*, bistability was assessed. The figure below presents the data sets that exhibited bistability. It was observed that when the stability of the SpoT synthase was increased, the system required a higher fraction of SpoT synthase to maintain bistability. Bistability was observed with a ~5-fold increase in synthase activity. These results suggest a range of values for $k_{deg,SpoT,syn}$ and *f* exist for the system to be bistable.

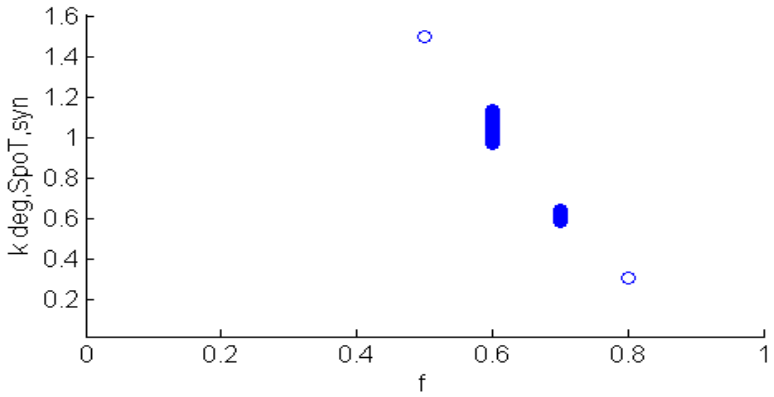

Simultaneous $k_{deg,SpoT,syn}$ and f parameter variation to assess bistable range. The parameter values that exhibit bistability when varying the stability of the SpoT synthase and the fraction of SpoT synthase present in the system.

As mentioned in the main text, *ΔrelAΔspoT* and *ΔdksA* experimentally remove the persister population formed from the ppGpp-dependent pathway. These results support our model since removing RelA/SpoT and DksA individually from the network simulations by setting their initial concentrations and turnover numbers to 0 to mimic genetic deletions also removed bistability. Elimination of RelA and SpoT removed all steady states from the model since ppGpp is neither produced nor degraded. Elimination of DksA yielded only one steady state, characterized by low ppGpp concentration and high SpoT concentration, when keeping all other parameters at their nominal value.

Supplemental References

Albe, K.R., Butler, M.H., and Wright, B.E. (1990). Cellular concentrations of enzymes and their substrates. Journal of theoretical biology *143*, 163-195.

Alon, U. (2007). An introduction to systems biology : design principles of biological circuits (Boca Raton, FL: Chapman & Hall/CRC).

An, G., Justesen, J., Watson, R.J., and Friesen, J.D. (1979). Cloning the spoT gene of Escherichia coli: identification of the spoT gene product. Journal of bacteriology *137*, 1100-1110.

Baba, T., Ara, T., Hasegawa, M., Takai, Y., Okumura, Y., Baba, M., Datsenko, K.A., Tomita, M., Wanner, B.L., and Mori, H. (2006). Construction of Escherichia coli K-12 in-frame, single-gene knockout mutants: the Keio collection. Molecular systems biology *2*, 2006 0008.

Bachi, B., and Kornberg, H.L. (1975). Utilization of gluconate by Escherichia coli. A role of adenosine 3':5'-cyclic monophosphate in the induction of gluconate catabolism. The Biochemical journal *150*, 123-128.

Baquero, M.R., Bouzon, M., Varea, J., and Moreno, F. (1995). sbmC, a stationary-phase induced SOS Escherichia coli gene, whose product protects cells from the DNA replication inhibitor microcin B17. Molecular microbiology *18*, 301-311.

Baracchini, E., and Bremer, H. (1988). Stringent and growth control of rRNA synthesis in Escherichia coli are both mediated by ppGpp. The Journal of biological chemistry *263*, 2597-2602.

Barker, M.M., Gaal, T., Josaitis, C.A., and Gourse, R.L. (2001). Mechanism of regulation of transcription initiation by ppGpp. I. Effects of ppGpp on transcription initiation in vivo and in vitro. Journal of molecular biology *305*, 673-688.

Bennett, B.D., Kimball, E.H., Gao, M., Osterhout, R., Van Dien, S.J., and Rabinowitz, J.D. (2009). Absolute metabolite concentrations and implied enzyme active site occupancy in Escherichia coli. Nature chemical biology *5*, 593-599.

Berg, J.M., Tymoczko, J.L., and Stryer, L. (2012). Biochemistry, 7th edn (New York: W.H. Freeman).

Chandrangsu, P., Lemke, J.J., and Gourse, R.L. (2011). The dksA promoter is negatively feedback regulated by DksA and ppGpp. Molecular microbiology *80*, 1337-1348.

Christensen-Dalsgaard, M., Jorgensen, M.G., and Gerdes, K. (2010). Three new RelE-homologous mRNA interferases of Escherichia coli differentially induced by environmental stresses. Molecular microbiology *75*, 333-348.

Courcelle, J., Khodursky, A., Peter, B., Brown, P.O., and Hanawalt, P.C. (2001). Comparative gene expression profiles following UV exposure in wild-type and SOS-deficient Escherichia coli. Genetics *158*, 41-64.

Datsenko, K.A., and Wanner, B.L. (2000). One-step inactivation of chromosomal genes in Escherichia coli K-12 using PCR products. Proceedings of the National Academy of Sciences of the United States of America *97*, 6640-6645.

Dorr, T., Vulic, M., and Lewis, K. (2010). Ciprofloxacin causes persister formation by inducing the TisB toxin in Escherichia coli. PLoS biology *8*, e1000317.

Durfee, T., Hansen, A.M., Zhi, H., Blattner, F.R., and Jin, D.J. (2008). Transcription profiling of the stringent response in Escherichia coli. Journal of bacteriology *190*, 1084-1096.

Enfors, S.O. (2004). Physiological stress responses in bioprocesses. In Advances in biochemical engineering/biotechnology, (Berlin ; New York, Springer,), pp. x, 244 p. ill. 224 cm.

Falla, T.J., and Chopra, I. (1998). Joint tolerance to beta-lactam and fluoroquinolone antibiotics in Escherichia coli results from overexpression of hipA. Antimicrobial agents and chemotherapy *42*, 3282-3284.

Guzman, L.M., Belin, D., Carson, M.J., and Beckwith, J. (1995). Tight regulation, modulation, and high-level expression by vectors containing the arabinose PBAD promoter. Journal of bacteriology *177*, 4121-4130.

Heinemeyer, E.A., and Richter, D. (1978). Characterization of the guanosine 5'-triphosphate 3'-diphosphate and guanosine 5'-diphosphate 3'-diphosphate degradation reaction catalyzed by a specific pyrophosphorylase from Escherichia coli. Biochemistry *17*, 5368-5372.

Justesen, J., Lund, T., Skou Pedersen, F., and Kjeldgaard, N.O. (1986). The physiology of stringent factor (ATP:GTP 3'-diphosphotransferase) in Escherichia coli. Biochimie *68*, 715-722.

Kawano, M., Aravind, L., and Storz, G. (2007). An antisense RNA controls synthesis of an SOS-induced toxin evolved from an antitoxin. Molecular microbiology *64*, 738-754.

Keren, I., Shah, D., Spoering, A., Kaldalu, N., and Lewis, K. (2004). Specialized persister cells and the mechanism of multidrug tolerance in Escherichia coli. Journal of bacteriology *186*, 8172-8180.

Kim, Y., Wang, X., Zhang, X.S., Grigoriu, S., Page, R., Peti, W., and Wood, T.K. (2010). Escherichia coli toxin/antitoxin pair MqsR/MqsA regulate toxin CspD. Environmental microbiology *12*, 1105-1121.

Kim, Y., and Wood, T.K. (2010). Toxins Hha and CspD and small RNA regulator Hfq are involved in persister cell formation through MqsR in Escherichia coli. Biochemical and biophysical research communications *391*, 209-213.

Kohanski, M.A., Dwyer, D.J., Hayete, B., Lawrence, C.A., and Collins, J.J. (2007). A common mechanism of cellular death induced by bactericidal antibiotics. Cell *130*, 797-810.

Korch, S.B., and Hill, T.M. (2006). Ectopic overexpression of wild-type and mutant hipA genes in Escherichia coli: effects on macromolecular synthesis and persister formation. Journal of bacteriology *188*, 3826-3836.

Langklotz, S., and Narberhaus, F. (2011). The Escherichia coli replication inhibitor CspD is subject to growth-regulated degradation by the Lon protease. Molecular microbiology *80*, 1313-1325.

Lasko, D.R., and Wang, D.I. (1996). On-line monitoring of intracellular ATP concentration in Escherichia coli fermentations. Biotechnology and bioengineering *52*, 364-372.

Lemke, J.J., Sanchez-Vazquez, P., Burgos, H.L., Hedberg, G., Ross, W., and Gourse, R.L. (2011). Direct regulation of Escherichia coli ribosomal protein promoters by the transcription factors ppGpp and DksA. Proceedings of the National Academy of Sciences of the United States of America *108*, 5712-5717.

Lennon, C.W., Gaal, T., Ross, W., and Gourse, R.L. (2009). Escherichia coli DksA binds to Free RNA polymerase with higher affinity than to RNA polymerase in an open complex. Journal of bacteriology *191*, 5854-5858.

Lewis, K. (2010). Persister cells. Annual review of microbiology *64*, 357-372.

Maisonneuve, E., Shakespeare, L.J., Jorgensen, M.G., and Gerdes, K. (2011). Bacterial persistence by RNA endonucleases. Proceedings of the National Academy of Sciences of the United States of America *108*, 13206-13211.

Moyed, H.S., and Bertrand, K.P. (1983). hipA, a newly recognized gene of Escherichia coli K-12 that affects frequency of persistence after inhibition of murein synthesis. Journal of bacteriology *155*, 768-775.

Murray, K.D., and Bremer, H. (1996). Control of spoT-dependent ppGpp synthesis and degradation in Escherichia coli. Journal of molecular biology *259*, 41-57.

Nakagawa, A., Oshima, T., and Mori, H. (2006). Identification and characterization of a second, inducible promoter of relA in Escherichia coli. Genes & genetic systems *81*, 299-310.

Oh, T.J., Jung, I.L., and Kim, I.G. (2001). The Escherichia coli SOS gene sbmC is regulated by H-NS and RpoS during the SOS induction and stationary growth phase. Biochemical and biophysical research communications *288*, 1052-1058.

Paul, B.J., Barker, M.M., Ross, W., Schneider, D.A., Webb, C., Foster, J.W., and Gourse, R.L. (2004). DksA: a critical component of the transcription initiation machinery that potentiates the regulation of rRNA promoters by ppGpp and the initiating NTP. Cell *118*, 311-322.

Pedersen, F.S., and Kjeldgaard, N.O. (1977). Analysis of the relA gene product of Escherichia coli. European journal of biochemistry / FEBS *76*, 91-97.

Pedersen, K., and Gerdes, K. (1999). Multiple hok genes on the chromosome of Escherichia coli. Molecular microbiology *32*, 1090-1102.

Raibaud, O. (1989). Nucleoprotein structures at positively regulated bacterial promoters: homology with replication origins and some hypotheses on the quaternary structure of the activator proteins in these complexes. Molecular microbiology *3*, 455-458.

Raibaud, O., Vidal-Ingigliardi, D., and Richet, E. (1989). A complex nucleoprotein structure involved in activation of transcription of two divergent Escherichia coli promoters. Journal of molecular biology *205*, 471-485.

Reddy, P.S., Raghavan, A., and Chatterji, D. (1995). Evidence for a ppGpp-binding site on Escherichia coli RNA polymerase: proximity relationship with the rifampicin-binding domain. Molecular microbiology *15*, 255-265.

Richter, D., Fehr, S., and Harder, R. (1979). The guanosine 3',5'-bis(diphosphate) (ppGpp) cycle. Comparison of synthesis and degradation of guanosine 3',5'-bis(diphosphate) in various bacterial systems. European journal of biochemistry / FEBS *99*, 57-64.

Rutherford, S.T., Lemke, J.J., Vrentas, C.E., Gaal, T., Ross, W., and Gourse, R.L. (2007). Effects of DksA, GreA, and GreB on transcription initiation: insights into the mechanisms of factors that bind in the secondary channel of RNA polymerase. Journal of molecular biology *366*, 1243-1257.

Schreiber, G., Metzger, S., Aizenman, E., Roza, S., Cashel, M., and Glaser, G. (1991). Overexpression of the relA gene in Escherichia coli. The Journal of biological chemistry *266*, 3760-3767.

Sengupta, S., and Nagaraja, V. (2008). YacG from Escherichia coli is a specific endogenous inhibitor of DNA gyrase. Nucleic acids research *36*, 4310-4316.

Shah, D., Zhang, Z., Khodursky, A., Kaldalu, N., Kurg, K., and Lewis, K. (2006). Persisters: a distinct physiological state of E. coli. BMC microbiology *6*, 53.

Shepherd, N.S., Churchward, G., and Bremer, H. (1980). Synthesis and activity of ribonucleic acid polymerase in Escherichia coli. Journal of bacteriology *141*, 1098-1108.

Somerville, C.R., and Ahmed, A. (1979). Mutants of Escherichia coli defective in the degradation of guanosine 5'-triphosphate, 3'-diphosphate (pppGpp). Molecular & general genetics : MGG *169*, 315-323.

Splittgerber, A.G. (1983). Simplified treatment of two-substrate enzyme kinetics. Journal of Chemical Education *60*, 651.

Srivatsan, A., and Wang, J.D. (2008). Control of bacterial transcription, translation and replication by (p)ppGpp. Current opinion in microbiology *11*, 100-105.

Traxler, M.F., Zacharia, V.M., Marquardt, S., Summers, S.M., Nguyen, H.T., Stark, S.E., and Conway, T. (2011). Discretely calibrated regulatory loops controlled by ppGpp partition gene induction across the 'feast to famine' gradient in Escherichia coli. Molecular microbiology *79*, 830-845.

Vazquez-Laslop, N., Lee, H., and Neyfakh, A.A. (2006). Increased persistence in Escherichia coli caused by controlled expression of toxins or other unrelated proteins. Journal of bacteriology *188*, 3494-3497.

Vidal-Ingigliardi, D., and Raibaud, O. (1991). Three adjacent binding sites for cAMP receptor protein are involved in the activation of the divergent malEp-malKp promoters. Proceedings of the National Academy of Sciences of the United States of America *88*, 229-233.

Zaslaver, A., Bren, A., Ronen, M., Itzkovitz, S., Kikoin, I., Shavit, S., Liebermeister, W., Surette, M.G., and Alon, U. (2006). A comprehensive library of fluorescent transcriptional reporters for Escherichia coli. Nature methods *3*, 623-628.

Establishment of a Method To Rapidly Assay Bacterial Persister Metabolism

Mehmet A. Orman and Mark P. Brynildsen
Antimicrob. Agents Chemother. **2013, 57(9):4398. DOI: 10.1128/AAC.00372-13.**
Published Ahead of Print 1 July 2013.

AAC Journals.ASM.org

Establishment of a Method To Rapidly Assay Bacterial Persister Metabolism

Mehmet A. Orman, Mark P. Brynildsen

Department of Chemical and Biological Engineering, Princeton University, Princeton, New Jersey, USA

Bacterial persisters exhibit an extraordinary tolerance to antibiotics that is dependent on their metabolic state. Although persister metabolism promises to be a rich source of antipersister strategies, there is relatively little known about the metabolism of these rare and transient phenotypic variants. To address this knowledge gap, we explored the use of several techniques, and we found that only one measured persister metabolism. This assay was based on the phenomenon of metabolite-enabled aminoglycoside killing of persisters, and we used it to characterize the metabolic heterogeneity of different persister populations. From these investigations, we determined that glycerol and glucose are the most ubiquitously used carbon sources by various types of *Escherichia coli* persisters, suggesting that these metabolites might prove beneficial to deliver in conjunction with aminoglycosides for the treatment of chronic and recurrent infections. In addition, we demonstrated that the persister metabolic assay developed here is amenable to high-throughput screening with the use of phenotype arrays.

Persisters are phenotypic variants that are tolerant to extraordinary concentrations of antibiotics. Persisters in biofilms have been hypothesized to underlie the proclivity of biofilm infections to relapse (1), and until recently there was no effective way to eliminate persisters. Two promising studies have demonstrated metabolism-dependent killing of persisters: one that potentiates aminoglycoside (AG) activity by stimulating proton motive force generation in persisters (2), and another that stimulates persister awakening (3). These methods suggest that knowledge of persister metabolic capabilities would expedite the discovery and development of antipersister therapies. Consequently, perturbations to numerous metabolic genes and regulators have been shown to alter persister levels (4–9, 30, 31), further supporting a central role for metabolism in maintenance of this phenotypic state. In addition, persisters have recently been shown to largely adopt a metabolically quiescent state that must be achieved and sustained by coordinated metabolic actions (10). Unfortunately, persister metabolism has not been sufficiently studied, and knowledge of the metabolic activities of these phenotypic variants remains limited. In part, this is due to difficulties associated with isolation of persisters from normally growing cultures, where current techniques provide only modest persister enrichment (11, 12).

In this study, we sought to measure the metabolic activities of natively generated *Escherichia coli* persisters, not those obtained synthetically by overexpression of a toxin (13) or treatment with persister-stimulating agents (14). First, we attempted to use the only isolation technique previously described to produce pure persister samples (15). In this method, normally growing bacteria are lysed with ampicillin (AMP), and the remaining cells, considered persisters, are sedimented by centrifugation. However, by using LIVE/DEAD staining, a fluorescent indicator of cell lysis, a metabolic assay, and persister measurements, we found that exponential-phase cultures of wild-type *E. coli* treated with AMP contained almost 100-fold more viable but nonculturable cells (VBNCs) than persisters and that VBNC metabolic activity obscured measurement of persister metabolism. In the absence of a high-fidelity isolation technique, it was necessary to base the measurements of persister metabolism on the fundamental definition of persistence, antibiotic tolerance exhibited by a reduced killing rate in a biphasic kill curve, followed by growth resumption on standard media. This definition distinguishes persisters from normal and dead cells as well as VBNCs and, therefore, must be used to measure persister physiology in the absence of improved isolation techniques. Since persisters can only be killed by AGs if they metabolize carbon sources to generate proton motive force (PMF) (2), we adapted the AG potentiation assay to rapidly measure persister metabolism in a high-throughput manner with the use of phenotype microarrays. We used this method to measure the metabolism of various persisters (e.g., AMP and ofloxacin [OFX], during the exponential and stationary phases), and we found that glycerol and glucose were the most commonly metabolized substrates by *E. coli* persisters, establishing these carbon sources as prime candidates for combination therapy with AGs. The method described here can be used to explore persister metabolism and build back their active metabolic networks, while simultaneously probing for the best adjuvants for AG therapy of relapsing infections.

MATERIALS AND METHODS

Bacterial strains. All strains were derived from *E. coli* MG1655. The MG1655 *hipA7* mutant was a generous gift from the James J. Collins Lab (Boston University, Boston, MA). Generation of MO001, which contained a chromosomally integrated *lacI*^{q} promoter in place of the *lacI* promoter and a chromosomally integrated *T5p-mCherry* in place of *lacZYA*, was described in a previous study (10). Genetic deletions (Δ*gldA*, Δ*glpK*, Δ*gldA*Δ*glpK*, and Δ*ptsI*) were transduced from the Keio Collection by using the standard P1 phage method (16). When necessary, the kanamycin resistance gene was removed using FLP recombinase (17). All mu-

Received 20 February 2013 Returned for modification 18 March 2013
Accepted 25 June 2013
Published ahead of print 1 July 2013
Address correspondence to Mark. P. Brynildsen, mbrynild@princeton.edu.
Supplemental material for this article may be found at http://dx.doi.org/10.1128/AAC.00372-13.

doi:10.1128/AAC.00372-13

tations were confirmed using PCR and/or DNA sequencing (Genewiz, South Plainfield, NJ).

Chemicals, media, and growth conditions. All chemicals, unless noted below, were purchased from Fisher Scientific or Sigma-Aldrich. A LIVE/DEAD bacterial viability kit was purchased from Life Technologies, Invitrogen (Grand Island, NY). Fluorescent particles for cell counting were purchased from Spherotech, Inc. (Lake Forest, IL). WST-1 was purchased from Dojindo Molecular Technologies (Rockville, MD), and isopropyl-β-D-thiogalactopyranoside (IPTG) was purchased from Gold Biotechnology (St. Louis, MO). Phenotype microarrays were purchased from Biolog, Inc. (Hayward, CA). LB medium (10 g/liter tryptone, 5 g/liter yeast extract, and 10 g/liter NaCl) and LB agar plates (LB with 15 g/liter agar) were used for planktonic growth and enumeration of CFU, respectively. When necessary, 0.22-μm filter-sterilized pyruvate, α-ketoglutarate, or catalase solutions were aseptically spread on the surface of LB agar plates at concentrations of 0.1% pyruvate, 0.1% α-ketoglutarate, and 2,000 U catalase per plate (18). For persister assays, 200 μg/ml AMP and 5 μg/ml OFX were used. For the AG potentiation assay, 25 μg/ml kanamycin (KAN) was used. For mutant selection, 50 μg/ml KAN was utilized. To inhibit cytochrome activity, 1 mM KCN was used (2). To prepare the overnight cultures, cells from a 25% glycerol, −80°C stock were incubated in 2 ml LB medium at 37°C with shaking (250 rpm) for 24 h. The overnight cultures were diluted 1,000-fold in 50 ml of fresh LB medium in a 500-ml baffled flask and incubated for 90 min at 37°C and 250 rpm before antibiotic treatment. To enumerate CFU, cells were washed and diluted in phosphate-buffered saline (PBS), plated on LB agar, and incubated at 37°C for 16 h.

LIVE/DEAD staining assay. SYTO 9 and propidium iodide (PI) staining were performed according to the manufacturer's instructions. Exponential-phase and AMP-treated cell cultures were washed and diluted in sterile 0.85% NaCl buffer to reach a final density of 1×10^6 cells/ml. Then, cells were stained with SYTO 9 and PI simultaneously, at concentrations of 5 μM and 30 μM, respectively, and incubated at room temperature for approximately 15 min before flow cytometry analysis. As controls, approximately 1×10^6 exponential-phase cells were either incubated in 1 ml of 70% ethanol solution for 1 h or sonicated at 10% amplitude with a sonic dismembrator (Fisher Scientific, Pittsburgh, PA) in 1 ml of 0.85% NaCl buffer on ice for 30 min prior to staining.

Fluorescent indicator (mCherry) of cell lysis assay. MO001 cells were cultured as described above, except that 1 mM IPTG was included in the overnight and exponential growth cultures. After AMP treatment, 1-ml samples were collected at the indicated time points, washed, diluted in PBS, and analyzed by flow cytometry to count the unlysed cells. For the control, exponential-phase cells were sonicated in PBS as described above prior to the flow cytometry assay.

Flow cytometry analysis. All samples were analyzed with an LSRII flow cytometer (BD Biosciences, San Jose, CA). Microorganisms were identified using forward and side scatter parameters (FSC and SSC). SYTO 9/PI-stained cells and mCherry-expressing cells were assayed with lasers emitting at 488 nm and 560 nm, respectively, and fluorescence intensities were collected by using a green fluorescence (525/50 nm) bandpass filter for SYTO 9 and a red fluorescence (610/20 nm) bandpass filter for both PI and mCherry. Data were acquired and analyzed using FACSDiVa software (BD Biosciences, San Jose, CA).

Cell sorting. All cell sorting experiments were performed using a FACSVantage SE cell sorter with DiVa (BD Biosciences, San Jose, CA) at 16 lb/in^2 with a 70-μm nozzle. Microorganisms were determined using forward and side scatter parameters. mCherry-positive cells were identified by measuring red fluorescence (561-nm excitation with a 615/30-bandpass filter). Cells were sorted using sterile 1× PBS as sheath fluid in the sorter. mCherry-positive cells after AMP treatment (approximately 10,000 cells) were sorted in microcentrifuge tubes, plated on LB agar, and incubated at 37°C for 16 h to count CFU. These data were used to calculate the persister/VBNC ratio. To determine the VBNC levels prior to antibiotic treatment, single cells from exponential-phase MG1655 cultures were delivered to individual wells of 96-well plates filled with 200 μl LB agar. The plates were incubated for 16 h at 37°C. Wells that failed to grow were inoculated with a dead cell or VBNC, whereas wells with measureable growth were inoculated with a normal cell or a persister.

Persister and VBNC enumeration. MIC ranges for MG1655 cells were found to be 1.5 to 3 μg AMP/ml, 0.075 to 0.15 μg OFX/ml, and 3 to 6 μg KAN/ml by using the method based on serial 2-fold dilutions of antibiotics in LB medium (10). Exponential-phase cultures (50 ml) were treated with either AMP (200 μg/ml) or OFX (5 μg/ml), while stationary-phase cultures (2 ml) were only treated with OFX (5 μg/ml), and all cultures were incubated at 37°C and 250 rpm. To enumerate the persister levels, samples were collected at the indicated time points, washed, and serially diluted in PBS, and then 10-μl samples were plated on LB agar. VBNC levels at the indicated time points during the AMP treatment were enumerated by flow cytometry with fluorescent counting particles with either SYTO 9/PI-stained wild-type cells or mCherry-expressing cells as described above. To determine whether VBNCs from these experiments could be resuscitated (18), antibiotic-treated samples were plated on LB, LB plus pyruvate (0.1%), LB plus α-ketoglutarate (0.1%), or LB plus catalase (2,000 U/plate).

Tetrazolium assay. For the tetrazolium assay, the detection reagent was prepared according to the methods described by Tsukatani and coworkers (19). WST-1 and 2-methyl-1,4-naphthoquinone were dissolved in distilled water and ethanol at concentrations of 11.1 mM and 8 mM, respectively, and then they were mixed at a ratio of 9:1, yielding 10 mM tetrazolium salt and 0.8 mM electron mediator. The reagent was filter sterilized with a membrane filter (0.2 μm).

Cells from 50-ml exponential-phase cultures treated with AMP (5 or 20 h) were pelleted at 4,000 rpm for 15 min using a centrifuge (5810R; Eppendorf AG, Hamburg, Germany) and resuspended in 1 ml of sterile 1.25× M9 salt solution, including AMP (125 μg/ml). Then, 80 μl of microbial resuspension, 10 μl of detection reagent, and 10 μl of carbon source solution (600 mM carbon) were added to each well of 96-well microtiter plates. This yielded approximately 10^7 live cells (VBNCs plus persisters), 1 mM WST-1, 0.08 mM electron mediator, and 60 mM carbon per well. As a control, 10 μl sterile water was added to this mixture instead of a carbon source. We note that all carbon sources were dissolved in distilled water and then filter sterilized. Ninety-six-well plates were covered with sterile, gas-permeable sealing membranes (Breath-Easy; Sigma-Aldrich). Cell cultures were incubated at 37°C and 250 rpm, and the A_{438} was measured at the indicated time points by using a Synergy H1 hybrid multimode microplate reader (BioTek, Winooski, VT). The same procedures were applied to stationary- and exponential-phase cultures before AMP treatment to measure their metabolic activities. The cell density in all samples was ~10^7 live cells/well.

To understand if the debris from lysed cells affected formazan production, 2 ml of exponential-phase cells before the AMP treatment was washed with 1.25× M9 salt solution as described above and sonicated at 10% amplitude for 30 min on ice. This method did not result in protein denaturation, which was confirmed by measuring the fluorescence intensities of samples before and after sonication using a microplate reader (560-nm excitation, 610-nm emission). Lysis of all cells was confirmed by flow cytometry. A colorimetric microbial assay was performed for both sonicated and unsonicated exponential-phase cells that had been chilled on ice as described above.

Aminoglycoside potentiation assay. For the AG potenitation assay, cells from 50-ml exponential-phase cultures treated with AMP (200 μg/ml) or OFX (5 μg/ml) were pelleted and suspended in 1 ml of sterile 1.25× M9 salt solution as described above without antibiotic. Then, 80 μl of cell suspension, 10 μl of KAN solution, and 10 μl of carbon source solution were mixed in each well of the plates, resulting in ~10^5 AMP or ~10^6 OFX persisters, 25 μg/ml KAN, and 60 mM carbon per well. The plates were covered with sterile, gas-permeable sealing membranes and incubated at 37°C and 250 rpm, and 5-μl samples were removed from each well at the indicated time points and diluted 60-fold in PBS into another 96-well

plate, to reduce the antibiotic concentrations to sub-MIC levels. Then, 10-μl aliquots of these samples were further diluted and plated onto LB agar. Where indicated, KCN, AMP, or OFX was added to a 1.25× M9 suspension buffer (controls). The final concentrations of these chemicals in the cultures were, respectively, 1 mM, 100 μg/ml, and 5 μg/ml. The same procedures were applied to stationary-phase OFX persisters. Overnight cultures in 2 ml LB were treated with OFX (5 μg/ml) to obtain stationary-phase persisters.

Competition assay. To understand if VBNCs interfere with the AG potentiation assay (e.g., consume a carbon source and generate a product that potentiates AG activity in persisters), a competition assay was performed. Antibiotic-treated samples of wild-type and mutant (Δ*gldA* Δ*glpK* or Δ*ptsI*) cells from either exponential- or stationary-phase cultures were pelleted and suspended in 1 ml of sterile 1.25× M9 salt solution as described above. Wild-type and mutant cells (Δ*gldA* Δ*glpK* or Δ*ptsI*) were mixed so as to obtain an approximate 50/50 proportion of persisters. Then, 80 μl of cell suspension, 10 μl of KAN solution, and 10 μl of carbon source solution were mixed in each well of the plates, resulting in ~10^5 persisters, 25 μg/ml KAN, and 60 mM carbon per well. For controls, wild-type-only and mutant-only cell suspensions were treated with KAN. All mixed cultures had the same amount of wild-type or mutant persisters as wild-type-only or mutant-only cultures. Where indicated, KCN and AMP were added to 1.25× M9 suspension buffer. Where indicated, cell densities were decreased (10-fold) to minimize the effects of surrounding cells on persisters, and KAN and carbon source concentrations were kept constant. The plates were then covered with sterile, gas-permeable sealing membranes and were incubated at 37°C and 250 rpm. After 2 h of incubation, cell cultures (100 μl) were transferred to sterile microcentrifuge tubes and washed with PBS to remove the antibiotics, and 10-μl aliquots of these samples were further diluted and plated onto LB agar. The remaining 90 μl of the cultures was also plated in case the CFU were not measured from the 10-μl spot. To confirm that mixed-cell cultures were enriched with mutants after 2 h of incubation with KAN and the nonutilized carbon source (glycerol for Δ*gldA* Δ*glpK* and glucose for Δ*ptsI*), at least 24 colonies from mixed cultures were grown in 200 μl M9-glycerol or M9-glucose medium (60 mM carbon), in 96-well plates, for 24 h at 37°C and 250 rpm. This allowed quantification of the proportion of surviving cells that were mutants, since Δ*gldA* Δ*glpK* and Δ*ptsI* cannot grow in M9-glycerol or M9-glucose medium, respectively, whereas wild-type cells can grow in both media.

Phenotype microarray assay. Phenotype microarrays (PM) were used to measure AG potentiation and cell growth in a high-throughput manner. Stationary-phase cells in 2 ml LB treated with OFX for 5 h were washed and diluted 10-fold in 1× M9 salt solution, including 25 μg/ml KAN, and 100-μl aliquots of samples from this cell suspension were added to the wells of a PM. Plates were covered with sterile, gas-permeable sealing membranes and incubated at 250 rpm and 37°C. At the indicated time points, 5-μl samples were removed for CFU enumeration as described above. When indicated, KCN or AMP was added to the 1× M9 suspension buffer (controls). To determine the cell growth rates, stationary-phase cells without antibiotic treatment were washed and diluted 10-fold in 1× M9 salt solution, and 100-μl aliquots of the cell suspension were added to wells of a PM. Cells were incubated at 250 rpm and 37°C for 6 h, and at the indicated time points, 10-μl aliquots of cultures were mixed with 290 μl of 1× M9 salt solution to measure the optical density at 600 nm.

Statistical analysis. All experiments were independently repeated at least 3 times. Pairwise comparison was performed using a two-tailed *t* test, and a *P* value threshold of 0.05 was used to identify statistically significant differences. Each data point is represented by the mean value ± the standard error.

RESULTS

Ampicillin-lysed cultures include more VBNCs than persisters. Persisters cannot be isolated from untreated cultures, due to isolation difficulties that originate from their transient nature, low abundance, and a lack of high-fidelity biomarkers. Fluorescence-activated cell sorting (FACS) methods used for persister isolation based on an rRNA reporter (an indicator of protein synthesis) (11) and a fluorescent indicator of cell division (10, 12) provide samples that are enriched in persisters but remain highly contaminated with other cell types, such as normal cells and VBNCs. Another technique that has been described for persister isolation involves treatment of cultures with β-lactams and sedimentation of nonlysed cells (15, 20). As evidence that the sedimented cells are persisters, Keren and colleagues performed LIVE/DEAD (SYTO/PI) staining to show that all remaining cells stained as live cells (15). However, the claim that these sedimented cells are all persisters has come under scrutiny due to additional studies that have demonstrated that cell lysis by β-lactams leaves many more cells with intact membranes than there are persisters in the population (7, 12, 21). Here, we sought to determine if β-lactam lysis would be useful for isolation of wild-type *E. coli* persisters for metabolic measurements. After 24 h of incubation in LB, the overnight cells were inoculated in fresh medium and cultured for 90 min (doubling time, ~25 min). Exponential-phase cells were then treated with AMP, live cells were counted by flow cytometry, and CFU were measured by plating on LB agar. The LIVE/DEAD probes, SYTO 9 and PI, which are, respectively, green and red fluorescent nucleic acid stains that differ in their ability to penetrate bacterial cells (22), were used to enumerate live cells, as Keren and colleagues had done (15). While SYTO 9 can stain all cells, PI only stains cells with damaged membranes (qualified as dead). To determine the gates of live and dead cell subpopulations, exponential-phase cells were treated with ethanol (standard control) or sonicated until all cells were killed and then stained with SYTO 9 and PI dyes (Fig. 1A). We reasoned that sonication was an important control due to the fact that AMP lyses cells. As depicted in Fig. 1A, dead cells were differentially stained by these two dyes. When we compared these data with a stained AMP-treated culture (Fig. 1B and C), sonicated samples more closely resembled AMP-treated cells than ethanol-treated cells. When we monitored the live cell and persister levels for 5 h during AMP treatment, we found that the level of live cells was almost 2 orders of magnitude higher than the level of persisters (Fig. 1G), consistent with previous studies (7, 12, 21). Cells that cannot form a colony on standard media but stain as live are known as VBNCs (23). Under specific circumstances, VBNCs have been observed to return to culturability by plating on media with antioxidants, such as pyruvate, α-ketoglutarate, or catalase (18). To determine if such resuscitation was possible under our experimental conditions, antibiotic-treated samples were plated on LB alone, LB with pyruvate, LB with α-ketoglutarate, and LB with catalase, and CFU were measured. As depicted in Fig. S1 in the supplemental material, the addition of these components could not resuscitate VBNCs, suggesting that the distinction between VBNC and persister was robust to the medium variation in this study.

To corroborate the LIVE/DEAD staining, we measured the level of intact cells by using a fluorescent protein (12). In this method, the fluorescent protein is expressed and then cells are treated with AMP. Normal cells lyse and their fluorescent signals are lost, whereas unlysed cells retain their high fluorescence. Here, we used an *mCherry* gene under the control of a strong, synthetic, IPTG-inducible promoter (T5) that was knocked into the chromosome of an *E. coli* strain carrying a chromosomally integrated

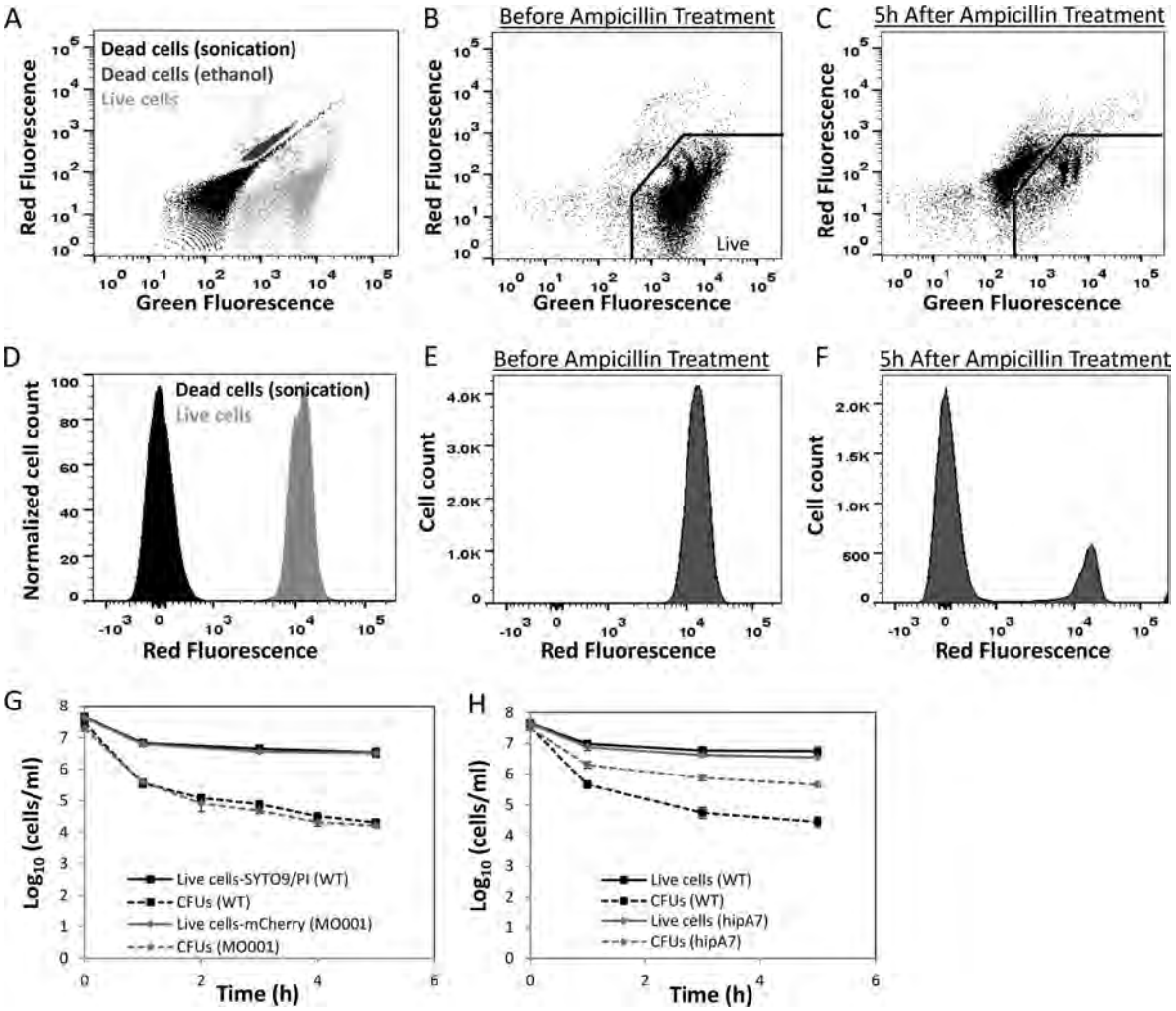

FIG 1 Enumeration of persister and VBNC levels in exponential-phase cultures. (A) Wild-type live and dead cells (sonicated or ethanol treated) stained with SYTO9/PI were analyzed by flow cytometry to determine the live and dead cell regions. (B and C) Exponential-phase cells were treated with AMP for 5 h, and samples were taken before and after the treatment for staining with SYTO9/PI. (D) Similarly, mCherry-expressing live and dead (sonicated) cells (MO001) were analyzed by flow cytometry to determine the live and dead cell cell counts. (E and F) Samples taken before and after the AMP treatment were assayed with flow cytometry. K indicates the cell count values (*y* axis) should be multiplied by 1,000. (G) VBNC and persister levels were monitored in both wild-type and MO001 cell types for 5 h during the AMP treatment. Significant differences were not observed when persister levels ($P > 0.30$) or VBNC levels ($P > 0.90$) of wild-type and MO001 strains were compared after 5 h of AMP treatment. (H) VBNC and persister levels of *hipA7* mutant were monitored for 5 h during the AMP treatment. A significant difference between wild-type and *hipA7* strains was not observed when VBNC levels ($P > 0.10$) were compared after 5 h of AMP treatment; however, persister levels were significantly higher in the *hipA7* strain than wild-type ($P < 0.001$). CFU were enumerated from antibiotic-treated samples by plating on LB agar, whereas live cells were enumerated by counting the unlysed cells using flow cytometry as a function of time. Error bars indicate the standard errors of the means.

LacI^q promoter mutation (MO001) (10). IPTG was applied to induce *mCherry* expression during both the overnight and exponential growth period to maintain the high fluorescent signals of unlysed cells. As a control, exponential-phase MO001 cells expressing mCherry were sonicated to lyse the population and determine the region of lysed cells on the flow diagram (Fig. 1D), which was consistent with that of AMP-treated cells (Fig. 1E and F). Using this technique, the level of live cells in exponential MO001 cultures was monitored for 5 h during AMP treatment and found to be statistically indistinguishable from the level of live cells in wild-type cultures, as enumerated with SYTO/PI (Fig. 1G). Further, persister levels of wild-type and MO001 cells were statistically indistinguishable (Fig. 1G), and when cells from the live subpopulation of an antibiotic-treated MO001 cell culture were sorted, only 0.59% ± 0.21% of those cells regrew, a result that was consistent with the 2 orders of magnitude difference observed between the levels of live cells and persisters when using LIVE/DEAD staining (see Fig. S2 in the supplemental material). These results demonstrated that AMP-treated wild-type cultures contain significantly more VBNCs than persisters. We also performed analogous experiments with a *hipA7* mutant and found that the level of VBNCs was comparable to that of the wild type, whereas the level of persisters was over an order of magnitude higher (Fig. 1H). This result agrees with a previous study that demonstrated that the AMP lysis technique was insufficient to isolate persisters from *hipA7* cultures (7).

To determine whether VBNCs may be problematic for persister isolation from untreated cultures, we measured the proportions of normal cells, dead cells, VBNCs, and persisters in wild-type cultures prior to antibiotic treatment. Using single-cell-mode FACS, single cells were delivered to individual wells of 96-well plates filled with LB agar. Wells that produced a colony arise from a normal cell or persister, whereas wells without a colony received either a dead cell or VBNC. The frequency of dead cells was quantified using LIVE/DEAD staining, and the frequency of persisters was quantified in antibiotic tolerance assays. With this combination of assays, each subpopulation could be quantified, and the results are presented in Table S1 of the supplemental material. Notably, we observed that VBNCs were far more abundant than persisters in untreated wild-type samples. When analogous experiments were performed on the *hipA7* mutant, the proportions of normal cells, dead cells, and VBNCs were comparable to that of the wild type, whereas the proportion of persisters was over an order of magnitude higher (Fig. 1H; see also Table S1 in the supplemental material). These data demonstrated that VBNCs are more abundant than persisters in untreated cultures and confirmed that, similar to the β-lactam technique (15, 20), methods for persister isolation from untreated samples are also complicated by the presence of VBNCs (11).

VBNCs exhibit significantly reduced metabolic activity. Although VBNCs preserve their membrane integrity, it remained unclear whether VBNCs exhibited significant metabolic activity. If VBNCs were metabolically inactive, AMP-treated samples might still be useful for measurement of persister metabolic activities. To determine whether AMP-treated samples exhibited metabolic activity, we adapted an assay that uses a water-soluble tetrazolium salt (WST-1) in conjunction with an electron mediator (2-methyl-1,4-naphthoquinone) to facilitate dye reduction (see Materials and Methods). WST-1 is reduced extracellularly to its soluble formazan by electron transport across the membrane of metabolically active cells (19, 24). The color change during formazan production can be detected by absorbance measurements, which correlate with the cellular dehydrogenase and reductase activities (24). This method enabled us to test numerous carbon sources simultaneously.

To measure metabolic activity from AMP-treated samples, cells were washed in M9 minimal medium without a carbon source to remove LB, and approximately 1×10^7 nonlysed cells (VBNCs plus persisters) were incubated in 100 μl/well M9 medium containing various carbon sources (60 mM carbon) in a 96-well plate. AMP at 100 μg/ml was also added to prevent growth resumption. A carbon source-free control was used to measure the background reduction of the water-soluble tetrazolium salt by the different cell suspensions. When absorbance measurements were taken at the indicated time points (Fig. 2A), the nonlysed cells could metabolize several of the carbon sources tested, including glycerol, glucose, mannitol, fructose, and succinate (see Fig. S3 in the supplemental material for all carbon sources tested). To verify that debris from lysed cells was not responsible for the measured WST-1 reduction, we measured the metabolic activities of samples that were lysed by a sonication procedure that did not denature proteins (see Fig. S4 in the supplemental material), and we found that cell debris was an insignificant source of formazan production (see Fig. S4). However, it was unclear whether VBNCs or persisters were responsible for the observed metabolic activity. Although the VBNC levels were ~2 orders of magnitude higher than persister levels, the VBNCs could have been far less metabolically active. Therefore, we sought to measure metabolic activity from samples where the abundance of one cell type was approximately constant and the abundance of the other cell type was altered by orders of magnitude. Interestingly, when exponential-phase cells were treated with 200 μg/ml AMP for 20 h, VBNC levels did not change, whereas persister levels decreased by ~100-fold (Fig. 2C and D). This phenomenon allowed determination of whether the metabolic signal obtained from AMP-treated samples was from VBNCs or persisters. As depicted in Fig. 2A, B, and E, 20-h AMP-treated samples displayed a metabolic activity that was strikingly similar to that obtained from 5-h AMP-treated samples (see Fig. S3 in the supplemental material for all carbon sources tested). This experiment suggested that the metabolic activity of AMP-lysed cultures is dominated by VBNCs that mask the contribution by persisters. To ensure that the WST-1 absorbance measurements showed metabolic activity, VBNCs from mutants that cannot utilize glycerol and glucose, Δ*glpK* Δ*gldA* and Δ*ptsI*, respectively (see Fig. S5 in the supplemental material), were assayed for their ability to reduce WST-1. As depicted in Fig. 2F and G, VBNCs from the Δ*glpK* Δ*gldA* mutants were unable to reduce WST-1 in the presence of glycerol, whereas VBNCs from Δ*ptsI* mutants were unable to reduce WST-1 in the presence of glucose.

Since the WST-1 assay as applied to AMP-treated samples indicates VBNC metabolism, we compared the metabolism of VBNCs with that of stationary- and exponential-phase cells from the same cultures. Overnight cells, exponential-phase cells (before AMP treatment), and VBNCs (after AMP treatment) were similarly incubated in M9 minimal medium as described above. We defined the metabolic activity rates as the slopes of the A_{438} during the first 2 h of incubation with WST-1. As shown in Fig. 3, VBNC metabolism was significantly reduced (approximately 5-fold and 2-fold compared to exponential- and stationary-phase cells, respectively) but surprisingly similar to that of exponential- and stationary-phase cells. Glucose, glycerol, mannitol, and fructose were highly utilized by all three cell types.

Aminoglycoside potentiation can identify persister metabolic activities. Since VBNCs are orders of magnitude more abundant than persisters and these nonlysed cells have metabolic activity, the metabolic activity of persisters could not be assayed by the WST-1 method. The inability to isolate persisters to homogeneity, either from normally growing or antibiotic-treated cultures, precludes direct measurement of persister metabolism. The distinguishing characteristic of persisters that is not shared with other cell types (e.g., normal, dead, or VBNCs) is an enhanced ability to tolerate antibiotic treatment (second regimen of a biphasic kill curve) followed by resumption of growth on standard media. Recently, we discovered that persisters can metabolize specific carbon sources and become susceptible to AG (2). AG susceptibility was conferred by increased AG uptake, facilitated by catabolism of carbon sources to generate a proton motive force. Notably, persister killing could be eliminated through perturbations to the respiratory chain, including treatment with KCN, which blocks cytochrome oxidoreductase activity. Since AG potentiation is measured by a reduction in CFU, it provided an opportunity to measure persister metabolism in antibiotic-treated samples, where persisters are the only cell type capable of colony formation on standard media.

To adapt the AG potentiation phenomenon for the purpose of rapidly measuring persister metabolism, we sought to (i) identify

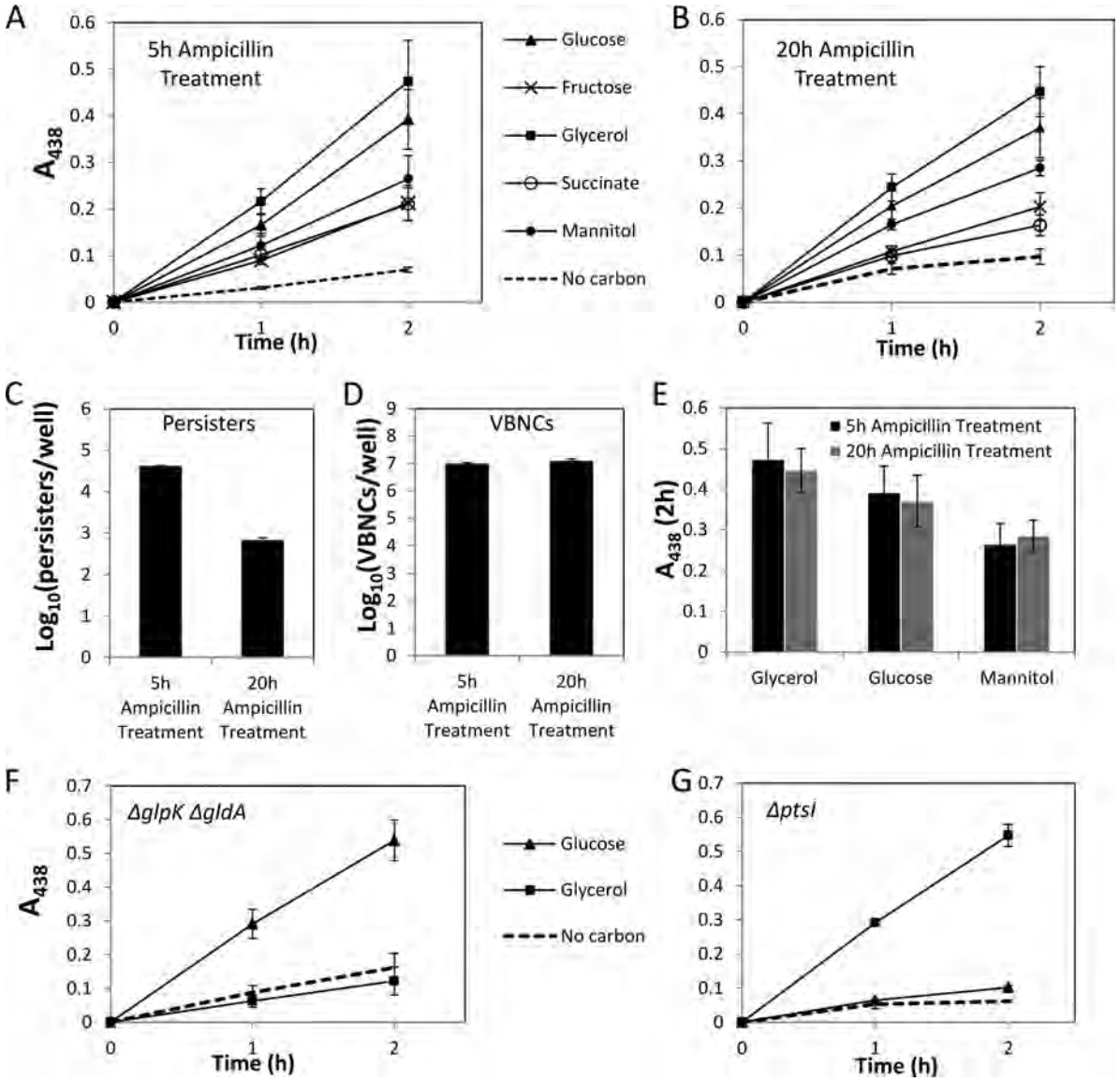

FIG 2 Metabolic activity measurements of ampicillin-treated cultures. (A) Live cells (VBNCs and persisters) after 5 h of AMP treatment were incubated in M9 minimal medium with various carbon sources, WST-1, and an electron mediator in 96-well plates, and absorbance (A_{438}) was measured at the indicated time points. (B) Similarly, absorbance was measured from 20-h AMP-treated cultures. (C to E) Persister and VBNC levels, as well as absorbance measurements from 5- and 20-h AMP-treated samples, were compared. Persister levels were significantly different ($P < 0.001$), whereas VBNC levels and absorbance measurements for both cultures were similar ($P > 0.5$). VBNCs were enumerated by counting mCherry-positive cells in the antibiotic-treated samples using flow cytometry. (F and G) Δ*gldA* Δ*glpK* and Δ*ptsI* cells after 5 h of AMP treatment were incubated in M9 minimal medium with glycerol, glucose, or no carbon (control), and absorbance was measured at the indicated time points. Error bars indicate the standard errors of the means.

conditions where many metabolites could be assayed in a single experiment without the need for wash steps and (ii) confirm that the assay results were attributable to persister metabolism. To accomplish the first task, the AG assay was scaled to a 96-well plate filled with 100-μl culture volumes and 25 μg/ml of KAN (see Materials and Methods). After exponential-phase cells in LB were treated with AMP for 5 h, cells were washed and incubated with KAN in M9 minimal medium with different carbon sources (60 mM carbon). To confirm that persisters remained nonreplicative and retained their antibiotic tolerance, AMP was used as a control (Fig. 4A). To confirm that the same AG potentiation phenomenon was being measured, KCN was used to block respiration and proton motive force generation. In addition, a control that provided no carbon source was used to measure inherent AG activity, from which enhancements from metabolite exposure could be quantified (Fig. 4A). Results from this assay (Fig. 4B) demonstrated that glycerol and glucose efficiently potentiated AG activity in AMP persisters from exponential-phase cultures (see Fig. S6A in the supplemental material for the potentiation of other carbon sources). To demonstrate that this assay measured metabolic activity, we confirmed that AG potentiation by glycerol was eliminated in the Δ*gldA* Δ*glpK* strain and AG potentiation by glucose was eliminated in the Δ*ptsI* strain (Fig. 4C).

To accomplish the second task, we sought to confirm that the

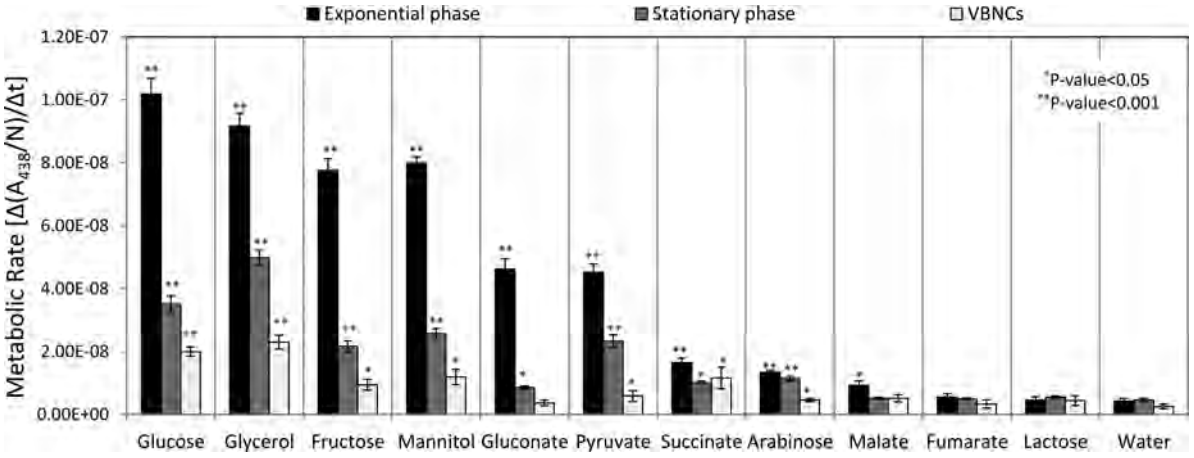

FIG 3 Comparison of metabolic activities of exponential- and stationary-phase cells and VBNCs. Stationary- and exponential-phase cells as well as VBNCs from 5-h AMP-treated exponential-phase cultures were incubated in M9 minimal medium with various carbon sources, and absorbance was measured during the first 2 h of incubation with WST-1 and an electron mediator. Metabolic activity rates were defined as the slopes of absorbance curves during the first 2 h (*n* is the number of total live cells determined by flow cytometry). In each group, metabolic activity rates with different carbon sources were compared to baseline values (no-carbon control) by using the *t* test. Error bars indicate the standard errors of the means.

dead cells and VBNCs in antibiotic-treated samples were not influencing assay results. We reasoned that since VBNCs are the dominant metabolically active subpopulation in antibiotic-treated samples, it was possible that they might consume a carbon source and generate a product that would potentiate AG activity in persisters, thus interfering with interpretation of assay results. To determine if such a phenomenon was present, we performed competition assays where antibiotic-treated samples of the wild type and mutants (Δ*gldA* Δ*glpK* or Δ*ptsI*) were mixed so as to obtain an approximate 50/50 proportion of persisters (see Materials and Methods). The mixed samples were then assayed for AG potentiation with the differentiating carbon source. If persisters were not influenced by surrounding cells, treatment of wild-type and Δ*gldA* Δ*glpK* samples with glycerol and KAN or wild-type and Δ*ptsI* samples with glucose and KAN would yield a 2-fold reduction in the persister level, and all remaining persisters would be Δ*gldA* Δ*glpK* or Δ*ptsI*. In wild-type plus Δ*gldA* Δ*glpK* samples, upon glycerol and KAN treatment all remaining CFU were Δ*gldA* Δ*glpK*, but a significant portion of Δ*gldA* Δ*glpK* persisters were eliminated (10-fold reduction) (Fig. 5A). With the controls, we found that AMP failed to eliminate persisters, and KCN prevented AG-dependent killing. These data demonstrated that wild-type persisters were far more susceptible to AG potentiation with glycerol than Δ*gldA* Δ*glpK* cells in mixed samples, and we identified an interesting phenomenon that was not apparent in the sole Δ*gldA* Δ*glpK* cultures. Elimination of Δ*gldA* Δ*glpK* persisters by glycerol and KAN in mixed samples may be attributable to any subpopulation within the wild-type sample (dead, VBNC, or persister cells), since assays performed without those cells failed to reduce CFU (Fig. 4C). We reasoned that reducing the total cell density of the assay would minimize the effects of surrounding cells and enhance the direct effect of the carbon source on persisters. As demonstrated in Fig. 5B, a 10-fold reduction in cell density yielded conditions under which all wild-type persisters in a mixed sample were eliminated by glycerol and KAN, whereas all Δ*gldA* Δ*glpK* persisters survived. These data demonstrated assay conditions that exclusively reported persister metabolic activity, since persisters must consume the carbon source and drive respiration in order to be eliminated, and all surviving persisters were those unable to metabolize the carbon source. When these experiments were performed with wild-type plus Δ*ptsI* samples (Fig. 5C and D), a significant elimination of Δ*ptsI* persisters by glucose and KAN was not observed under the assay conditions with a high or low cell density, verifying that persisters consume glucose to potentiate AG activity.

Since the low-density assay was not amenable to high-throughput screening, due to the need for wash steps to remove KAN, we used the high-density assay as a prescreen, to identify carbon sources with the potential to be metabolized by persisters, followed by the low-density assay for a conclusive demonstration of persister metabolism. We noted that carbon sources that did not reduce CFU in the high-density assay also failed to reduce CFU in the low-density assay, as confirmed with malate and gluconate (Fig. 5E).

Glycerol and glucose are the most desirable carbon sources in different persisters. Due to recent literature suggesting heterogeneity in persister populations (6, 8, 25), we sought to measure the metabolic activity of OFX persisters obtained from exponential-phase cultures. Exponential-phase cells were treated with OFX for 5 h (Fig. 6A), and then the high-density AG potentiation assay was performed as described above. We confirmed that OFX persisters remained nonreplicative, AG potentiation was eliminated by blocking respiration with KCN (Fig. 6B), and that the AG potentiation reflected metabolic activity (Fig. 6C and D). We observed that glycerol and glucose most strongly potentiated AG activity in both AMP and OFX persisters obtained from exponential-phase cultures (Fig. 4B and 6C). Furthermore, AG potentiation largely eliminated OFX persisters when mannitol, pyruvate, succinate, or fructose was present (Fig. 6C; see also Fig. S6B in the supplemental material). For glucose and glycerol, we confirmed with the low-density assay that persisters metabolized these substrates (see Fig. S7 in the supplemental material).

To understand how persister metabolism varies as a function of growth stage, we applied the AG potentiation assay to stationary-phase persisters obtained after 5 h of OFX treatment of overnight cells. Among the tested carbon sources, malate, fumarate, succinate, lactose, arabinose and gluconate did not potentiate the

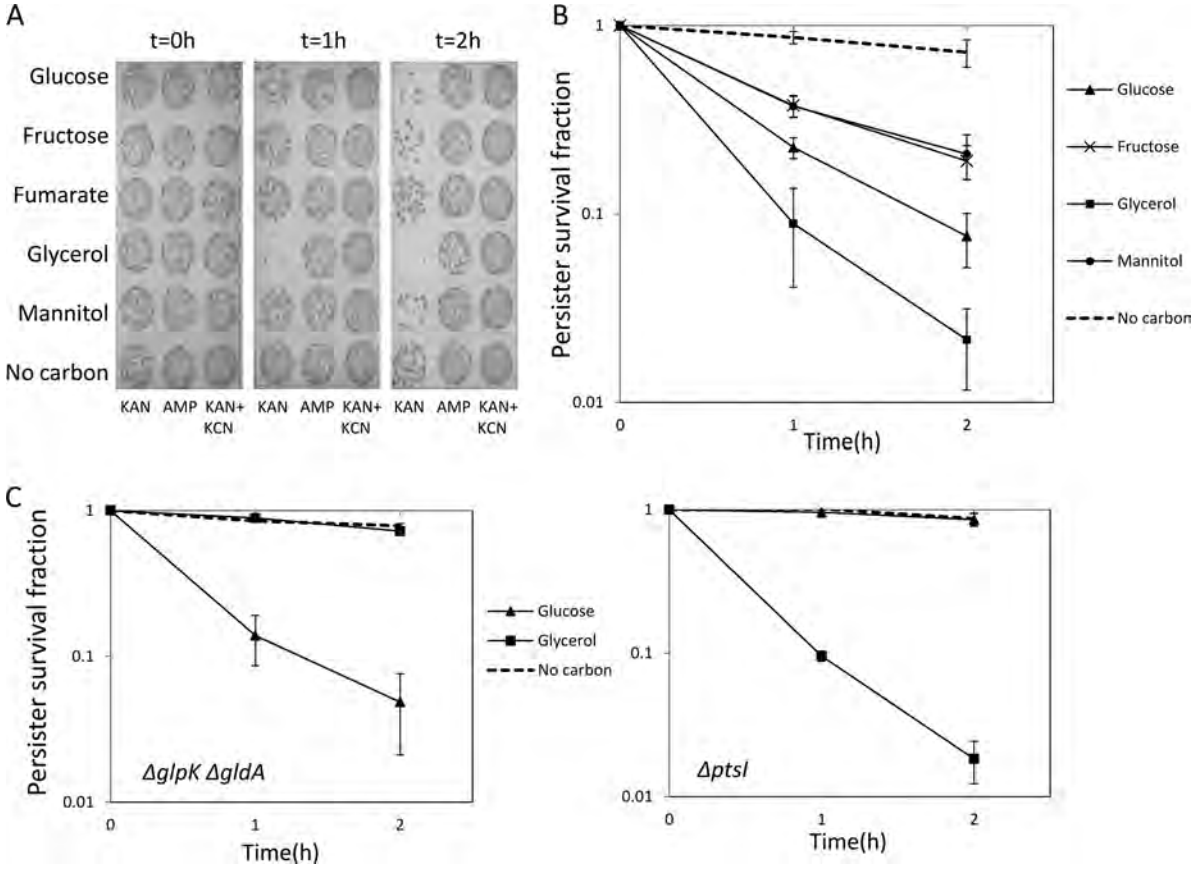

FIG 4 AG potentiation assay for ampicillin persisters. (A) After exponential-phase cells were treated with AMP for 5 h, cells were incubated with KAN (25 μg/ml) in M9 minimal medium with different carbon sources using 96-well plates. For controls, AMP (100 μg/ml) and KCN (1 mM) were used. AMP is required to confirm that persisters are nonreplicative in M9-minimal medium, whereas KCN blocks respiration and eliminates AG potentiation. (B) The survival fraction was monitored based on CFU. (C) Similarly, Δ*gldA* Δ*glpK* (deficient in glycerol utilization) and Δ*ptsI* (deficient in glucose utilization) persisters were incubated with KAN in M9 minimal medium, and the survival fraction was monitored. Error bars indicate the standard errors of the means.

AG activity (see Fig. S8 in the supplemental material). However, glycerol, pyruvate, mannitol, or glucose, or to a lesser extent fructose, efficiently potentiated AG activity (Fig. 7). This was in contrast to the results from exponential-phase persisters, where only glycerol and glucose were the major carbon sources to potentiate AG activity in persisters. For glucose and glycerol, we confirmed with the low-density assay that stationary-phase OFX persisters metabolized these substrates (see Fig. S9 in the supplemental material). These potentiation substrates differed slightly from those identified previously (2), and this difference was likely caused by the assay conditions, which included 100-μl samples treated in a 96-well plate. For example, increased AG activity in glycerol samples identified here might have been due to more efficient oxygenation, since the glycerol degradation pathway requires glycerol-3-phosphate dehydrogenase, an aerobic respiratory enzyme that catalyzes the oxidation of glycerol-3-phosphate to dihydroxyacetone phosphate.

The AG metabolic assay can be successfully applied to phenotype microarrays. We demonstrated that the AG potentiation method provides information regarding the metabolic capabilities of persisters, and we wanted to translate the high-density portion of the assay to a high-throughput screening format. Using a PM with stationary-phase persisters to OFX (5-h treatment), we tested 95 different carbon sources in a high-throughput manner to identify substrates that persisters catabolized for respiratory activity (Fig. 8). The controls included a cell suspension without any metabolite but including KAN (Fig. 8, box with bold outline) and analogous plates treated with KAN plus KCN or AMP only. All controls produced negligible killing of persisters (data not shown). We identified that glycerol, glucose, glycerol phosphate, glucose-6-phosphate, and glucose-1-phosphate all effectively potentiated AG activity in persisters. The carbon sources mannose, fructose, sorbitol, pyruvate, methyl pyruvate, lactate, and acetate potentiated AG activity in comparison to the no-carbon control, but did so less effectively than glucose and glycerol. Further, this assay showed that thymidine, uridine, and inosine could potentiate AG activity in persisters, suggesting that persisters may have an active nucleotide salvage pathway (Fig. 8).

After demonstrating that phenotype arrays could be used to perform the high-density assay, we sought to determine whether growth of normal cells on a substrate was predictive of AG potentiation in persisters. Therefore, we measured the ability of normal cells to grow in the PM plate and compared those results to AG potentiation results from persisters. As depicted in Table S2 of the supplemental material, there does appear to be a slight dependency between the ability of a metabolite to support normal cell growth and to potentiate AG against persisters. However, although normal cells can utilize maltriose as efficiently as glucose,

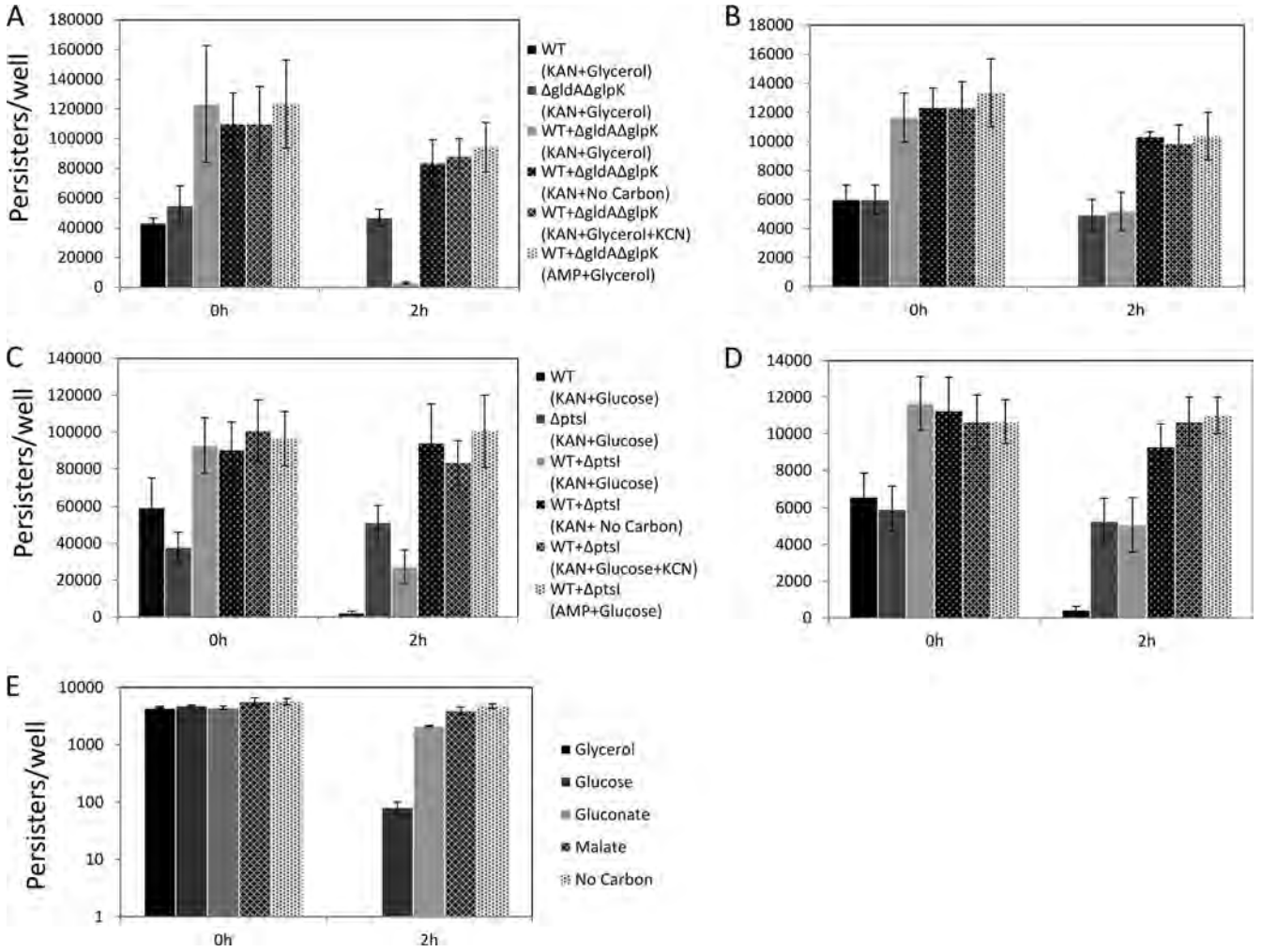

FIG 5 Competition assay. (A) After 5 h of treatment of exponential-phase cells with AMP, wild-type only, Δ*gldA* Δ*glpK* only, and mixed cell cultures (approximate 50/50 proportion of persisters) were treated for 2 h as indicated. (B) The same experiments were repeated following a 10-fold reduction in cell densities. (C and D) Similar experiments were performed for wild-type and Δ*ptsI* at both high (C) and low (D) cell densities. When KCN was used with KAN or a carbon source was absent, AG potentiation was eliminated. AMP confirmed that persisters are nonreplicative in M9-minimal medium. (E) AG potentiation of various carbon sources was tested in low-cell-density assays. Note that, in low-cell-density assays, no detectable CFU were counted after 2 h of treatment with KAN and glycerol (B and E). Mixed cultures had the same number of wild-type persisters as wild-type-only cultures and the same number of mutant persisters as mutant-only cultures. Error bars indicate the standard errors of the means.

glycerol, and glucose-6-phosphate for growth, this substrate cannot effectively potentiate AG activity in persisters. Further, specific substrates, such as methyl pyruvate and acetic acid, were poor growth substrates but led to significant potentiation of AG in persisters. This interesting phenomenon, which has not been observed previously, might be clinically desirable, since until now the AG adjuvants identified have all been able to support rapid bacterial growth.

DISCUSSION

Recent studies have found that persisters can be eliminated by targeting their metabolism (2, 3). Persisters are arguably the most clinically important cell type in an antibiotic-treated culture, since they are the only cell type capable of resuming growth once antibiotics have killed all normal cells and been removed from the system. Increased knowledge and understanding of persister metabolism will facilitate the development of antipersister therapies that increase antibiotic activity in persisters, disrupt persister homeostasis, and/or promote exit from the phenotype. However, measurement of persister metabolism is difficult and must be performed under experimental conditions where alternative cell types (e.g., normal cells and VBNCs) do not interfere with measurements. Unfortunately, current isolation techniques do not provide the purity necessary to perform metabolic measurements directly. The method of Shah and colleagues produced persister samples where ~70% of the population was not antibiotic tolerant (11). Further, the abundance of persisters in their normal cell sample (~2%) was approximately 100-fold higher than the level that is commonly observed from exponentially growing wild-type *E. coli* in rich media (10, 26). This suggests that the antibiotic tolerance measured by Shah and colleagues did not reflect the persistence phenotype. The β-lactam isolation method of Keren and colleagues (15), which we have shown here, produces orders of magnitude more VBNCs than persisters, and the VBNCs retain

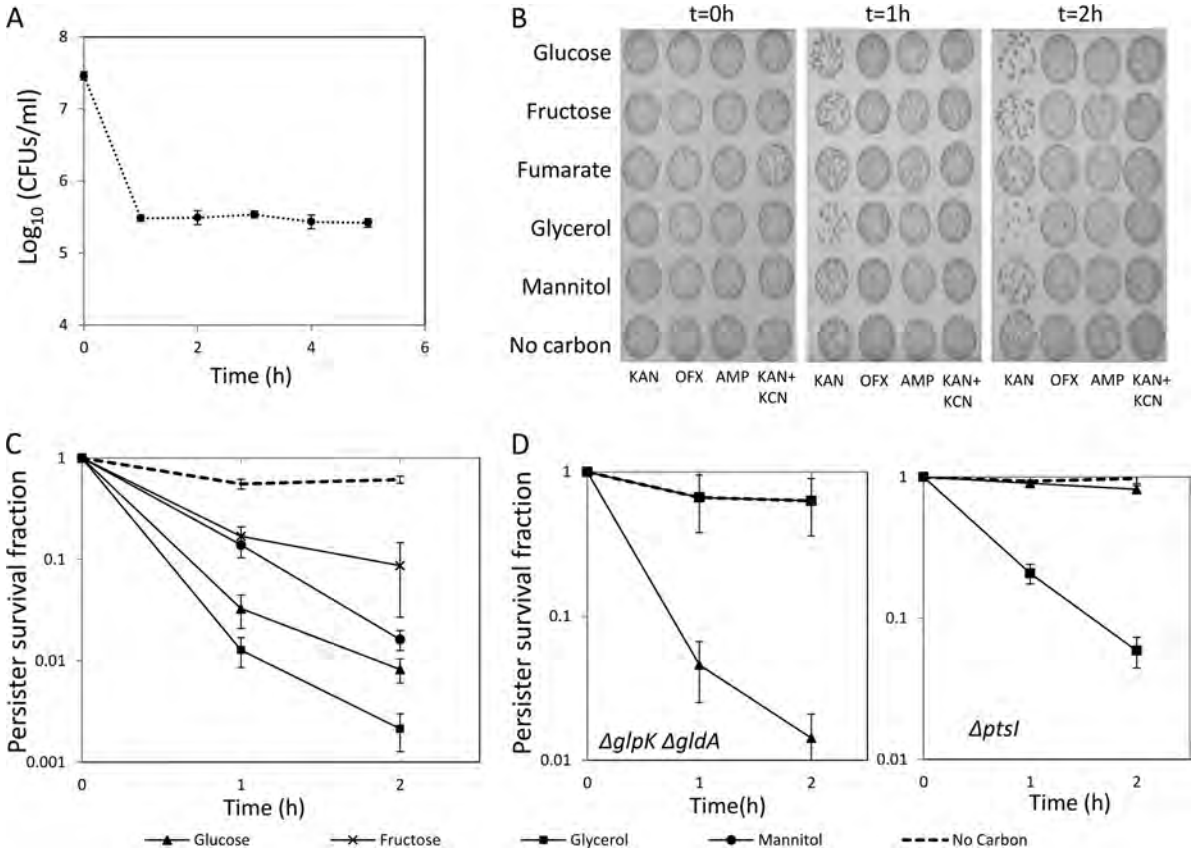

FIG 6 AG potentiation assay for ofloxacin persisters. (A to C) OFX persisters (5-h treatment) (A) were similarly incubated with KAN in M9 minimal medium with different carbon sources, and the survival fraction was monitored by CFU (B and C). For controls, AMP only, OFX only, or both KCN and KAN were used (B). (D) Survival fractions for Δ*gldA* Δ*glpK* and Δ*ptsI* persisters were monitored during the AG potentiation assay. Error bars indicate the standard errors of the means.

sufficient metabolic activity to preclude direct measurement of persister metabolism from the samples. Microscopy-based techniques applied to characterize the persister physiology (27, 28) are also difficult to use for isolation due to the similarities between persisters and VBNCs. Both cell types stain as live cells, retain metabolic activity, and often appear as nongrowing. The main distinction between persisters and VBNCs is the ability of persisters to resume normal growth after antibiotic treatment. However, upon growth resumption, the cell is no longer a persister, and thus experimental conditions where VBNCs are significantly less abundant than persisters are a prerequisite for isolation by microscopy. Unfortunately, we also demonstrated here that under normal culturing conditions, VBNCs are in much greater abundance than persisters in untreated samples.

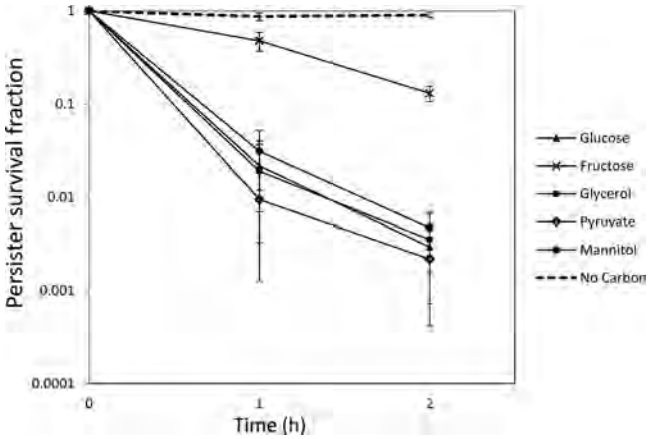

FIG 7 Metabolic properties of stationary-phase persisters. After stationary-phase cells were treated with OFX for 5 h, cells were incubated with KAN in M9 minimal medium with different carbon sources, and the survival fraction was monitored based on CFU. Error bars indicate the standard errors of the means.

In the absence of high-fidelity persister isolation techniques, any phenotypic measurement of persister physiology must be based on their ability to tolerate antibiotics and resume growth on standard media. Inspired by the phenomenon of metabolite-enabled AG potentiation, we developed a high-throughput method to measure persister metabolism that is not influenced by the presence of other cell types, including VBNCs. An important aspect to note is that the standard method by which phenotype microarrays measure metabolic activity involves reduction of a water-soluble tetrazolium salt (29), and we demonstrated here that such an assay measures VBNC metabolism and not the metabolism of persisters in antibiotic-treated samples. In contrast, AG potentiation measures the metabolism of persisters, because it is based on a loss of culturability. This loss in culturability of persisters may arise from cell death or a transition to the VBNC state, which are both possible outcomes. Unfortunately, distinguishing between these out-

Negative control 0.870±0.049 0.777±0.074	L-Arabinose 0.761±0.062 0.159±0.081	N-Acetyl-D-Glucosamine 0.142±0.072 0.014±0.011	D-Saccharic Acid 0.680±0.193 0.446±0.122	Succinic Acid 0.408±0.136 0.157±0.051	D-Galactose 0.538±0.151 0.375±0.098	L-Aspartic Acid 0.749±0.102 0.393±0.164	L-Proline 0.740±0.119 0.506±0.199	D-Alanine 0.568±0.101 0.450±0.225	D-Trehalose 0.556±0.122 0.326±0.109	D-Mannose 0.161±0.067 0.015±0.008	Dulcitol 0.662±0.134 0.525±0.098
D-Serine 0.394±0.124 0.106±0.051	D-Sorbitol 0.125±0.059 0.021±0.005	Glycerol 0.004±0.002 0.000±0.000	L-Fucose 0.569±0.186 0.308±0.094	D-Glucoronic Acid 0.377±0.124 0.147±0.042	D-Gluconic Acid 0.326±0.088 0.097±0.030	D,L-α-Glycerol P 0.016±0.008 0.000±0.000	D-Xylose 0.679±0.196 0.488±0.209	L-Lactic Acid 0.378±0.122 0.072±0.012	Formic Acid 0.504±0.071 0.430±0.063	D-Mannitol 0.081±0.032 0.006±0.002	L-Glutamic Acid 0.416±0.043 0.552±0.176
D-Glucose-6-Phosphate 0.045±0.018 0.003±0.001	D-Galactonic Acid-γ-Lactone 0.428±0.099 0.393±0.164	D,L-Malic Acid 0.463±0.132 0.378±0.173	D-Ribose 0.480±0.024 0.428±0.150	Tween 20 0.312±0.119 0.231±0.088	L-Rhamnose 0.597±0.131 0.604±0.106	Fructose 0.201±0.091 0.029±0.015	Acetic Acid 0.293±0.210 0.023±0.009	α-D-Glucose 0.073±0.050 0.008±0.003	Maltose 0.437±0.020 0.251±0.039	D-Melibiose 0.668±0.101 0.475±0.089	Thymidine 0.226±0.054 0.072±0.010
L-Asparagine 0.572±0.117 0.349±0.186	D-Aspartic acid 0.580±0.103 0.507±0.107	D-Glucosaminic Acid 0.694±0.170 0.445±0.077	1,2-Propanediol 0.411±0.128 0.481±0.202	Tween 40 0.452±0.171 0.328±0.119	α-Keto-Glutaric Acid 0.366±0.111 0.455±0.126	α-Keto-Butyric Acid 0.716±0.050 0.527±0.166	α-Methyl-D-Galactoside 0.491±0.124 0.518±0.103	α- D-Lactose 0.456±0.089 0.329±0.112	Lactulose 0.374±0.077 0.476±0.151	Sucrose 0.588±0.136 0.542±0.181	Uridine 0.235±0.145 0.056±0.021
L-Glutamine 0.510±0.220 0.310±0.184	m-Tartaric Acid 0.909±0.077 0.566±0.088	D-Glucose-1-Phosphate 0.090±0.062 0.008±0.003	D-Fructose-6-Phosphate 0.311±0.178 0.041±0.016	Tween 80 0.377±0.145 0.294±0.102	α-Hydroxy Glutaric A.-γ-Lactone 0.616±0.186 0.695±0.159	α-Hydroxy Butyric Acid 0.461±0.174 0.430±0.193	β-Methyl-D-Glucoside 0.271±0.150 0.152±0.038	Adonitol 0.444±0.209 0.381±0.080	Maltotriose 0.282±0.192 0.105±0.025	2-Deoxy Adenosine 0.507±0.223 0.112±0.024	Adenosine 0.395±0.173 0.117±0.037
Glycyl-L-Aspartic Acid 0.542±0.208 0.126±0.034	Citric Acid 0.690±0.142 0.505±0.134	m-Inositol 0.520±0.144 0.416±0.083	D-Threonine 0.485±0.238 0.376±0.112	Fumaric Acid 0.615±0.173 0.461±0.220	Bromo Succinic Acid 0.310±0.075 0.440±0.083	Propionic Acid 0.423±0.122 0.447±0.152	Mucic Acid 0.622±0.031 0.534±0.117	Glycolic Acid 0.541±0.111 0.491±0.026	Glyoxylic Acid 0.649±0.195 0.705±0.133	D-Cellobiose 0.511±0.217 0.319±0.065	Inosine 0.228±0.147 0.028±0.013
Glycyl-L-Glutamic Acid 0.564±0.172 0.242±0.107	Tricarballylic Acid 0.577±0.125 0.500±0.112	L-Serine 0.476±0.153 0.284±0.132	L-Threonine 0.692±0.212 0.436±0.194	L-Alanine 0.551±0.189 0.244±0.058	L-Alanyl-Glycine 0.486±0.164 0.320±0.061	Acetoacetic acid 0.533±0.162 0.339±0.127	N-Acetyl-β-D-Mannosamine 0.171±0.082 0.068±0.026	Mono Methyl Succinate 0.459±0.138 0.236±0.079	Methyl Pyruvate 0.326±0.131 0.023±0.005	D-Malic Acid 0.895±0.029 0.657±0.137	L-Malic Acid 0.722±0.162 0.317±0.104
Glycyl-L-Proline 0.447±0.157 0.480±0.173	p-Hydroxy Phenyl Acetic Acid 0.541±0.159 0.464±0.113	m-Hydroxy Phenyl Acetic Acid 0.572±0.124 0.479±0.166	Tyramine 0.719±0.092 0.579±0.162	D-Psicose 0.498±0.179 0.255±0.015	L-Lyxose 0.636±0.149 0.426±0.059	Glucuronamide 0.460±0.186 0.226±0.115	Pyruvic acid 0.385±0.148 0.022±0.008	L-Galactonic Acid-γ-Lactone 0.689±0.139 0.544±0.180	D-Galacturonic Acid 0.543±0.253 0.115±0.034	Phenylethyl amine 0.749±0.102 0.548±0.067	2-Aminoethanol 0.611±0.105 0.451±0.038

FIG 8 Persister survival fractions determined in the phenotype microarray. Stationary-phase cells treated with OFX for 5 h were incubated with KAN in M9 minimal medium with different carbon sources in a PM, and the survival fraction was monitored based on CFU. Note that in each cell, the first number indicates the first-hour survival fraction, and the second number indicates the second-hour survival fraction. Black, second-hour survival fraction < 0.01; dark grey, $0.01 <$ second-hour survival fraction < 0.05; light grey, $0.05 <$ second-hour survival fraction < 0.1. The no-carbon control is highlighted with bold outline. Error bars indicate the standard errors of the means.

comes is not technically possible, given the extremely low abundance of persisters compared to VBNCs and dead cells in antibiotic-treated samples (see Fig. S10 in the supplemental material). However, regardless of whether a persister dies or becomes a VBNC by AG potentiation, the method described here still measures persister metabolism, since either transition is facilitated by metabolic events within persisters; this was demonstrated both genetically with knockouts and chemically with KCN.

With the high-cell-density AG potentiation assay, we rapidly tested various carbon sources, as a prescreen, to identify those with the potential to be metabolized by persisters. We then performed a low-cell-density AG potentiation assay to unambiguously measure persister metabolism, and we found that glycerol and glucose were the most commonly catabolized carbon sources. We note that the need for both the high-density and low-density AG potentiation assays originated from the scalability of the high-density assay to high-throughput screening, and the results of the competition assay (wild-type and mutant mixed samples), where low-cell-density conditions demonstrated that all surviving persisters were those that could not metabolize the carbon source and that all persisters that could not metabolize the carbon source survived in the assay. Though we did not identify the underlying cause as to why Δ*gldA* Δ*glpK* persisters were killed in the presence of glycerol, KAN, and antibiotic-treated wild-type cells under high cell density conditions, we postulate that wild-type VBNCs, which are the dominant metabolically active subpopulation within antibiotic-treated samples (Fig. 2), were most likely metabolizing glycerol and excreting a substrate that Δ*gldA* Δ*glpK* could consume to drive respiration and AG uptake. The absence of this phenomenon for Δ*ptsI* cells in mixed culture may originate from VBNCs not processing glucose to a product that potentiates AG activity in Δ*ptsI* persisters.

The results demonstrating that diverse persister populations (exponential- and stationary-phase persisters; AMP and OFX persisters) consume glycerol and glucose suggest that there might be an active core metabolic network in persisters that is independent of the antibiotic tolerance mechanism and growth stage, suggesting the feasibility of a universal persister elimination strategy. In addition, we identified novel carbon sources that potentiate AG activity in persisters, including mannose, sorbitol, acetic acid, lactic acid, methyl pyruvate, inosine, thymidine, and uridine. To confirm that persisters metabolize these carbon sources, low-density assays will need to be performed. Of these carbon sources, methyl pyruvate and acetate are particularly interesting, since they do not support robust growth of *E. coli* but are efficient at potentiating the activity of AGs in persisters. Such metabolic adjuvants are potentially attractive, as they would not facilitate outgrowth of

potential survivors after the majority of persisters had been eliminated.

The technique presented here is the first method to rapidly assay persister metabolism, and we demonstrated that it is amenable to high-throughput screening through the use of phenotype microarrays. This assay, which includes both a high- and low-cell-density portion, provides a platform to more effectively explore the metabolic potential of persisters and provides data in the form of metabolic input (consumed substrate) and output (cytochrome activity). However, the network between input and output in persisters is not delineated with this assay. To explore such connections in persisters, genetic knockouts can be used (2), and we performed such an analysis here to determine that GlpK and not GldA was responsible for glycerol catabolism in persisters (see Fig. S11 in the supplemental material). To comprehensively identify the active metabolic network of persisters, the metabolic data can be analyzed with computational approaches to identify candidate networks capable of generating the metabolic output from the input. These candidate networks can then be analyzed to identify genetic perturbations for validation. In this manner, an iterative experimental and computational approach can be employed to reconstruct the metabolic networks of persisters and uncover novel strategies to eliminate persisters as a source of chronic and recurrent infection.

ACKNOWLEDGMENTS

We thank Christina J. DeCoste for technical support with flow cytometry and James J. Collins and Kyle R. Allison for providing the MG1655 *hipA7* strain. We also acknowledge Brittany Williams and Nicolas Ugaz for their help with the WST-1 assay. We thank the National BioResource Project (NIG, Japan) for their support of the distribution of the Keio collection.

Research reported in this publication was supported by the National Institute of Allergy and Infectious Diseases of the National Institutes of Health under award number R21AI105342, the Department of the Army under award number W81XWH-12-2-0138, and with starup funds from Princeton University.

The content is solely the responsibility of the authors and does not necessarily represent the official views of the funding agencies.

REFERENCES

1. **Lewis K.** 2007. Persister cells, dormancy and infectious disease. Nat. Rev. Microbiol. **5:**48–56.
2. **Allison KR, Brynildsen MP, Collins JJ.** 2011. Metabolite-enabled eradication of bacterial persisters by aminoglycosides. Nature **473:**216–220.
3. **Kim JS, Heo P, Yang TJ, Lee KS, Cho DH, Kim BT, Suh JH, Lim HJ, Shin D, Kim SK, Kweon DH.** 2011. Selective killing of bacterial persisters by a single chemical compound without affecting normal antibiotic-sensitive cells. Antimicrob. Agents Chemother. **55:**5380–5383.
4. **Hansen S, Lewis K, Vulic M.** 2008. Role of global regulators and nucleotide metabolism in antibiotic tolerance in Escherichia coli. Antimicrob. Agents Chemother. **52:**2718–2726.
5. **Korch SB, Henderson TA, Hill TM.** 2003. Characterization of the hipA7 allele of Escherichia coli and evidence that high persistence is governed by (p)ppGpp synthesis. Mol. Microbiol. **50:**1199–1213.
6. **Li YF, Zhang Y.** 2007. PhoU is a persistence switch involved in persister formation and tolerance to multiple antibiotics and stresses in Escherichia coli. Antimicrob. Agents Chemother. **51:**2092–2099.
7. **Luidalepp H, Jõers Kaldalu AN, Tenson T.** 2011. Age of inoculum strongly influences persister frequency and can mask the effects of mutations implicated in altered persistence. J. Bacteriol. **193:**3598–3605.
8. **Ma C, Sim SZ, Shi WL, Du LJ, Xing DM, Zhang Y.** 2010. Energy production genes sucB and ubiF are involved in persister survival and tolerance to multiple antibiotics and stresses in Escherichia coli. FEMS Microbiol. Lett. **303:**33–40.
9. **Spoering AL, Vulic M, Lewis K.** 2006. GlpD and PlsB participate in persister cell formation in Escherichia coli. J. Bacteriol. **188:**5136–5144.
10. **Orman MA, Brynildsen MP.** 2013. Dormancy is not necessary or sufficient for bacterial persistence. Antimicrob. Agents Chemother. **57:**3230–3239.
11. **Shah D, Zhang ZG, Khodursky A, Kaldalu N, Kurg K, Lewis K.** 2006. Persisters: a distinct physiological state of E-coli. BMC Microbiol. **6:**53. doi:10.1186/1471-2180-6-53.
12. **Roostalu J, Joers A, Luidalepp H, Kaldalu N, Tenson T.** 2008. Cell division in Escherichia coli cultures monitored at single cell resolution. BMC Microbiol. **8:**68. doi:10.1186/1471-2180-8-68.
13. **Vázquez-Laslop N, Lee H, Neyfakh AA.** 2006. Increased Persistence in Escherichia coli caused by controlled expression of toxins or other unrelated proteins. J. Bacteriol. **188:**3494–3497.
14. **Kwan BW, Valenta JA, Benedik MJ, Wood TK.** 2013. Arrested protein synthesis increases persister-like cell formation. Antimicrob. Agents Chemother. **57:**1468–1473.
15. **Keren I, Shah D, Spoering A, Kaldalu N, Lewis K.** 2004. Specialized persister cells and the mechanism of multidrug tolerance in Escherichia coli. J. Bacteriol. **186:**8172–8180.
16. **Baba T, Ara T, Hasegawa M, Takai Y, Okumura Y, Baba M, Datsenko KA, Tomita M, Wanner BL, Mori H.** 2006. Construction of Escherichia coli K-12 in-frame, single-gene knockout mutants: the Keio collection. Mol. Syst. Biol. **2:**2006.0008. doi:10.1038/msb4100050.
17. **Datsenko KA, Wanner BL.** 2000. One-step inactivation of chromosomal genes in Escherichia coli K-12 using PCR products. Proc. Natl. Acad. Sci. U. S. A. **97:**6640–6645.
18. **Mizunoe Y, Wai SN, Takade A, Yoshida S-I.** 1999. Restoration of culturability of starvation-stressed and low-temperature-stressed Escherichia coli O157 cells by using H_2O_2-degrading compounds. Arch. Microbiol. **172:**63–67.
19. **Tsukatani T, Suenaga H, Higuchi T, Akao T, Ishiyama M, Ezoe K, Matsumoto K.** 2008. Colorimetric cell proliferation assay for microorganisms in microtiter plate using water-soluble tetrazolium salts. J. Microbiol. Methods **75:**109–116.
20. **Keren I, Minami S, Rubin E, Lewis K.** 2011. Characterization and transcriptome analysis of Mycobacterium tuberculosis persisters. mBio **2**(3):e00100–11. doi:10.1128/mBio.00100-11.
21. **Jõers A, Kaldalu Tenson N, T.** 2010. The frequency of persisters in Escherichia coli reflects the kinetics of awakening from dormancy. J. Bacteriol. **192:**3379–3384.
22. **Berney M, Weilenmann H-U, Egli T.** 2006. Flow-cytometric study of vital cellular functions in Escherichia coli during solar disinfection (SODIS). Microbiology **152:**1719–1729.
23. **Oliver JD.** 2005. The viable but nonculturable state in bacteria. J. Microbiol. **43:**93–100.
24. **Berridge MV, Herst PM, Tan AS.** 2005. Tetrazolium dyes as tools in cell biology: new insights into their cellular reduction, vol 11. Elsevier Science, Amsterdam, Netherlands.
25. **Allison KR, Brynildsen MP, Collins JJ.** 2011. Heterogeneous bacterial persisters and engineering approaches to eliminate them. Curr. Opin. Microbiol. **14:**593–598.
26. **Keren I, Kaldalu N, Spoering A, Wang YP, Lewis K.** 2004. Persister cells and tolerance to antimicrobials. FEMS Microbiol. Lett. **230:**13–18.
27. **Balaban NQ, Merrin J, Chait R, Kowalik L, Leibler S.** 2004. Bacterial persistence as a phenotypic switch. Science **305:**1622–1625.
28. **Gefen O, Gabay C, Mumcuoglu M, Engel G, Balaban NQ.** 2008. Single-cell protein induction dynamics reveals a period of vulnerability to antibiotics in persister bacteria. Proc. Natl. Acad. Sci. U. S. A. **105:**6145–6149.
29. **Bochner BR, Gadzinski P, Panomitros E.** 2001. Phenotype microarrays for high-throughput phenotypic testing and assay of gene function. Genome Res. **11:**1246–1255.
30. **Amato SM, Orman MA, Brynildsen MP.** 2013. Metabolic control of persister formation in *Escherichia coli*. Mol. Cell **50:**475–487.
31. **Vega NM, Allison KR, Khalil AS, Collins JJ.** 2012. Signaling-mediated bacterial persister formation. Nat. Chem. Biol. **8:**431–433.

SUPPLEMENTAL MATERIALS

Establishment of a method to rapidly assay bacterial persister metabolism

Mehmet A Orman and Mark P Brynildsen*

Department of Chemical and Biological Engineering, Princeton University, Princeton, New Jersey, United States of America.

*E-mail: mbrynild@princeton.edu.

Running title: Persister metabolism

Table S1. Dead, VBNC and persister levels in bacterial cultures before and after the antibiotic treatment.

WT	Before antibiotic treatment	After antibiotic treatment
Normal cells (%)	88.42 ± 3.40	-
Dead cells (%)	6.84 ± 0.93	85.26 ± 5.89
VBNCs (%)	4.68 ± 2.55	14.68 ± 5.89
Persisters (%)	0.06 ± 0.00	0.06 ± 0.00
hipA7		
Normal cells (%)	87.66 ± 0.90	-
Dead cells (%)	5.56 ± 1.15	91.74 ± 3.02
VBNCs (%)	5.83 ± 0.89	7.31± 2.88
Persisters (%)	0.95 ± 0.21	0.95 ± 0.21

Table S2. Cell growth in phenotype microarray (ΔOD_{600} after 6 hours of incubation).

Negative control 0.00±0.00	L-Arabinose 0.74±0.05	N-Acetyl-D-Glucosamine 1.13±0.07	D-Saccharic Acid 0.02±0.02	Succinic Acid 0.47±0.11	D-Galactose 0.17±0.02	L-Aspartic Acid 0.31±0.06	L-Proline 0.00±0.00	D-Alanine 0.09±0.04	D-Trehalose 0.22±0.03	D-Mannose 0.28±0.04	Dulcitol 0.13±0.13
D-Serine 0.24±0.03	D-Sorbitol 0.35±0.03	Glycerol 0.53±0.04	L-Fucose 0.38±0.03	D-Glucoronic Acid 0.60±0.04	D-Gluconic Acid 0.55±0.06	D,L-α-Glycerol P. 0.26±0.06	D-Xylose 0.45±0.04	L-Lactic Acid 0.30±0.05	Formic Acid 0.00±0.00	D-Mannitol 0.72±0.07	L-Glutamic Acid 0.00±0.00
D-Glucose-6-Phosphate 0.60±0.03	D-Galactonic Acid-γ-Lactone 0.33±0.03	D,L-Malic Acid 0.35±0.05	D-Ribose 0.07±0.01	Tween 20 0.26±0.05	L-Rhamnose 0.13±0.03	Fructose 0.75±0.07	Acetic Acid 0.08±0.03	α-D-Glucose 1.47±0.12	Maltose 0.49±0.02	D-Melibiose 0.29±0.06	Thymidine 0.32±0.05
L-Asparagine 0.24±0.03	D-Aspartic acid 0.00±0.00	D-Glucosaminic Acid 0.00±0.00	1,2-Propanediol 0.00±0.00	Tween 40 0.25±0.04	α-Keto-Glutaric Acid 0.26±0.07	α-Keto-Butyric Acid 0.18±0.03	α-Methyl-D-Galactoside 0.39±0.05	α- D-Lactose 0.77±0.04	Lactulose 0.01±0.01	Sucrose 0.00±0.00	Uridine 0.24±0.02
L-Glutamine 0.01±0.01	m-Tartaric Acid 0.05±0.03	D-Glucose-1-Phosphate 0.66±0.05	D-Fructose-6-Phosphate 0.62±0.07	Tween 80 0.23±0.03	α-Hydroxy Glutaric A.-γ-Lactone 0.02±0.01	α-Hydroxy Butyric Acid 0.20±0.05	β-Methyl-D-Glucoside 0.13±0.03	Adonitol 0.01±0.01	Maltotriose 1.00±0.07	2-Deoxy Adenosine 0.37±0.03	Adenosine 0.27±0.02
Glycyl-L-Aspartic Acid 0.28±0.03	Citric Acid 0.00±0.00	m-Inositol 0.00±0.00	D-Threonine 0.00±0.00	Fumaric Acid 0.34±0.07	Bromo Succinic Acid 0.21±0.04	Propionic Acid 0.11±0.04	Mucic Acid 0.36±0.03	Glycolic Acid 0.04±0.04	Glyoxylic Acid 0.31±0.27	D-Cellobiose 0.01±0.01	Inosine 0.31±0.06
Glycyl-L-Glutamic Acid 0.19±0.05	Tricarballylic Acid 0.01±0.01	L-Serine 0.39±0.05	L-Threonine 0.06±0.03	L-Alanine 0.30±0.05	L-Alanyl-Glycine 0.35±0.07	Acetoacetic acid 0.03±0.02	N-Acetyl-β-D-Mannosamine 0.11±0.04	Mono Methyl Succinate 0.03±0.03	Methyl Pyruvate 0.02±0.02	D-Malic Acid 0.30±0.09	L-Malic Acid 0.33±0.09
Glycyl-L-Proline 0.25±0.01	p-Hydroxy Phenyl Acetic Acid 0.02±0.02	m-Hydroxy Phenyl Acetic Acid 0.01±0.01	Tyramine 0.00±0.00	D-Psicose 0.00±0.00	L-Lyxose 0.00±0.00	Glucuronamide 0.02±0.02	Pyruvic acid 0.29±0.03	L-Galactonic Acid-γ-Lactone 0.31±0.06	D-Galacturonic Acid 0.73±0.08	Phenylethyl amine 0.00±0.00	2-Aminoethanol 0.00±0.00

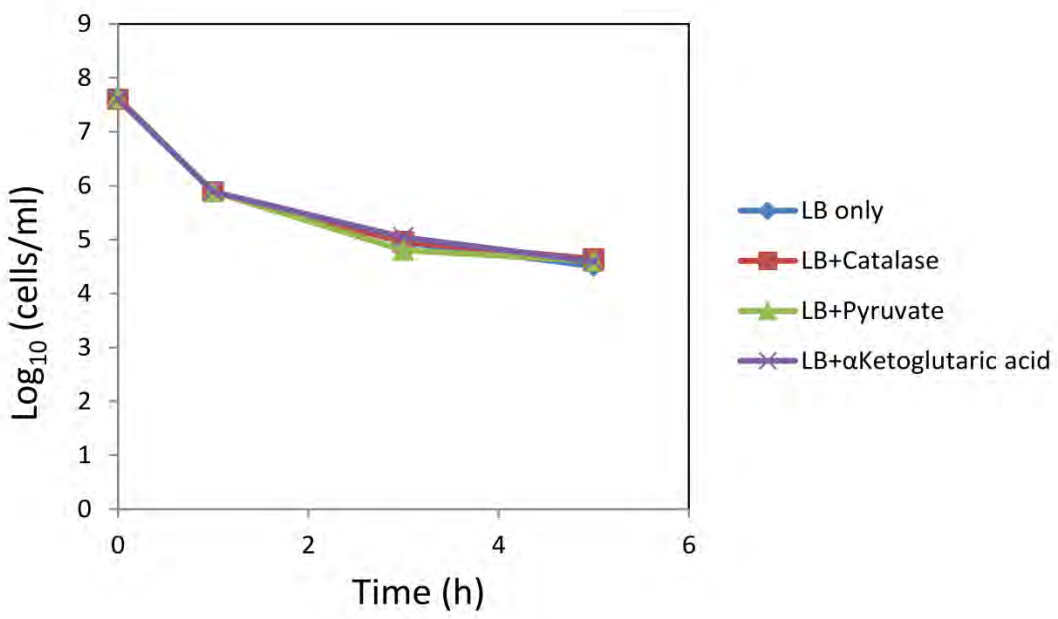

Figure S1. Resuscitation of VBNCs. Exponential phase cells treated with ampicillin for 5 hours were plated on LB, LB + pyruvate (0.1%), LB + α-ketoglutarate (0.1%) and LB + catalase (2000U/ plate) agar plates (replicated 3 times). Error bars indicate the standard error of the mean.

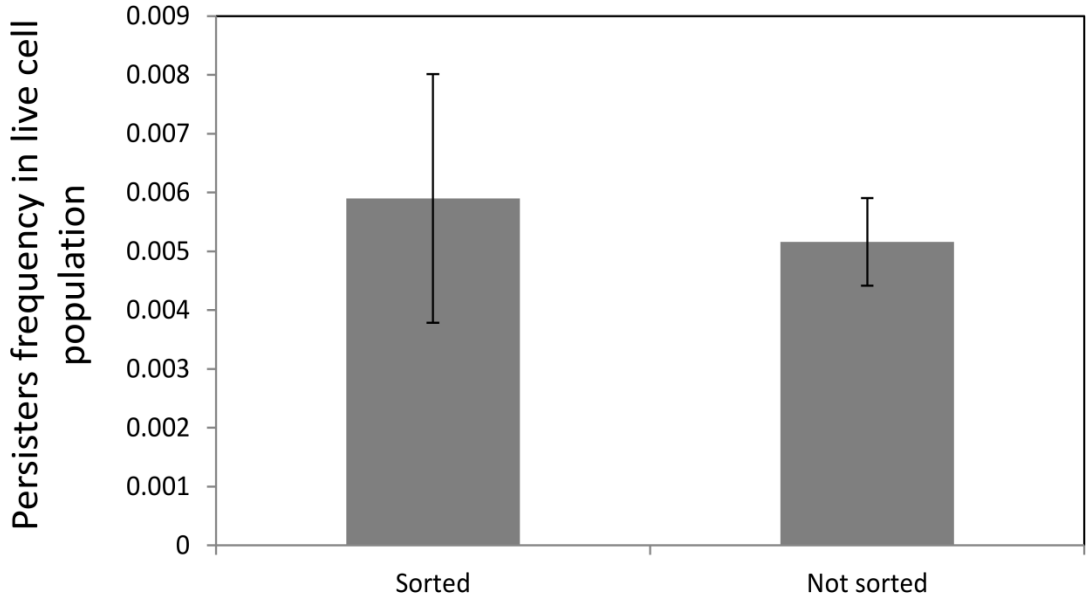

Figure S2. Persister frequency in live cell population after ampicillin treatment. Approximately 10,000 mCherry positive cells (live) after 5 hour ampicillin treatment were sorted and plated on LB agar to count CFUs (persisters). Ampicillin-treated cultures were also plated without sorting, and the number of live cells (mCherry positive cells) was enumerated by flow cytometry with fluorescent counting particles. Error bars indicate the standard error of the mean.

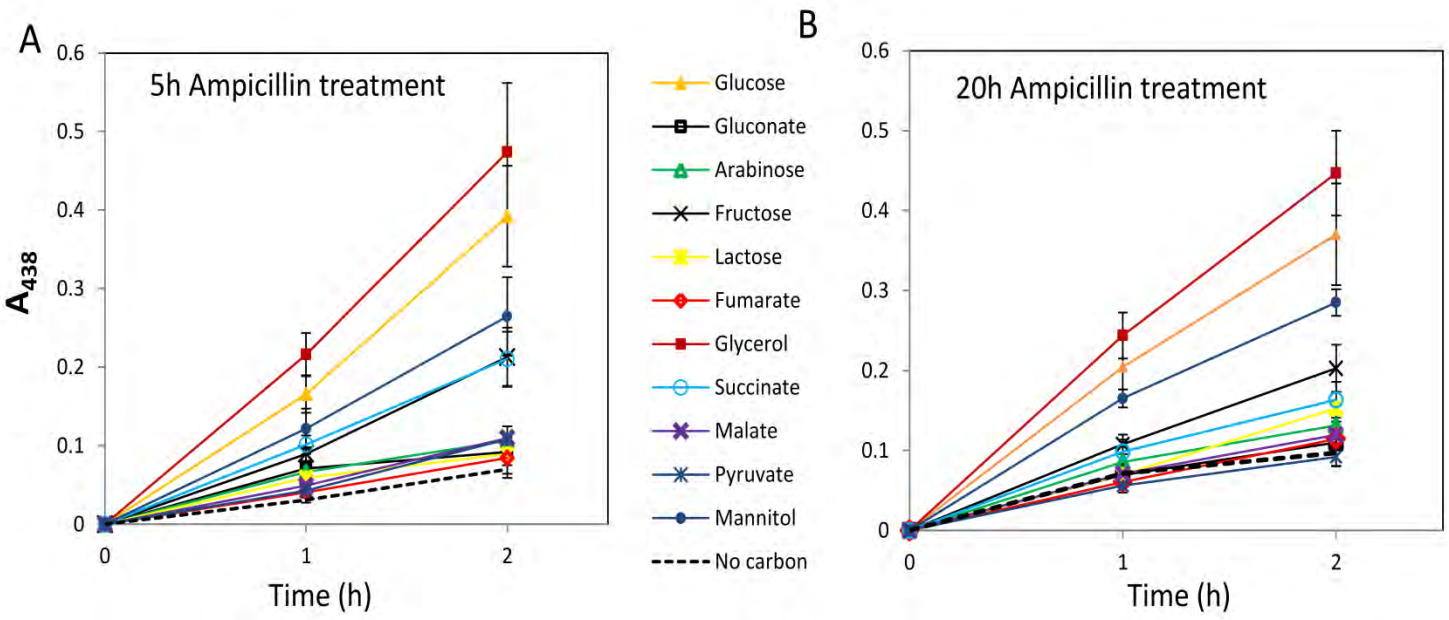

Figure S3. Metabolic activity measurement of ampicillin-treated cultures. Live cells (VBNCs and persisters) after 5 hour (A) or 20 hour (B) ampicillin treatment were incubated in M9 minimal media with various carbon sources, WST-1 and electron mediator by using microplates, and absorbance (A_{438}) was measured at indicated time points. Error bars indicate the standard error of the mean.

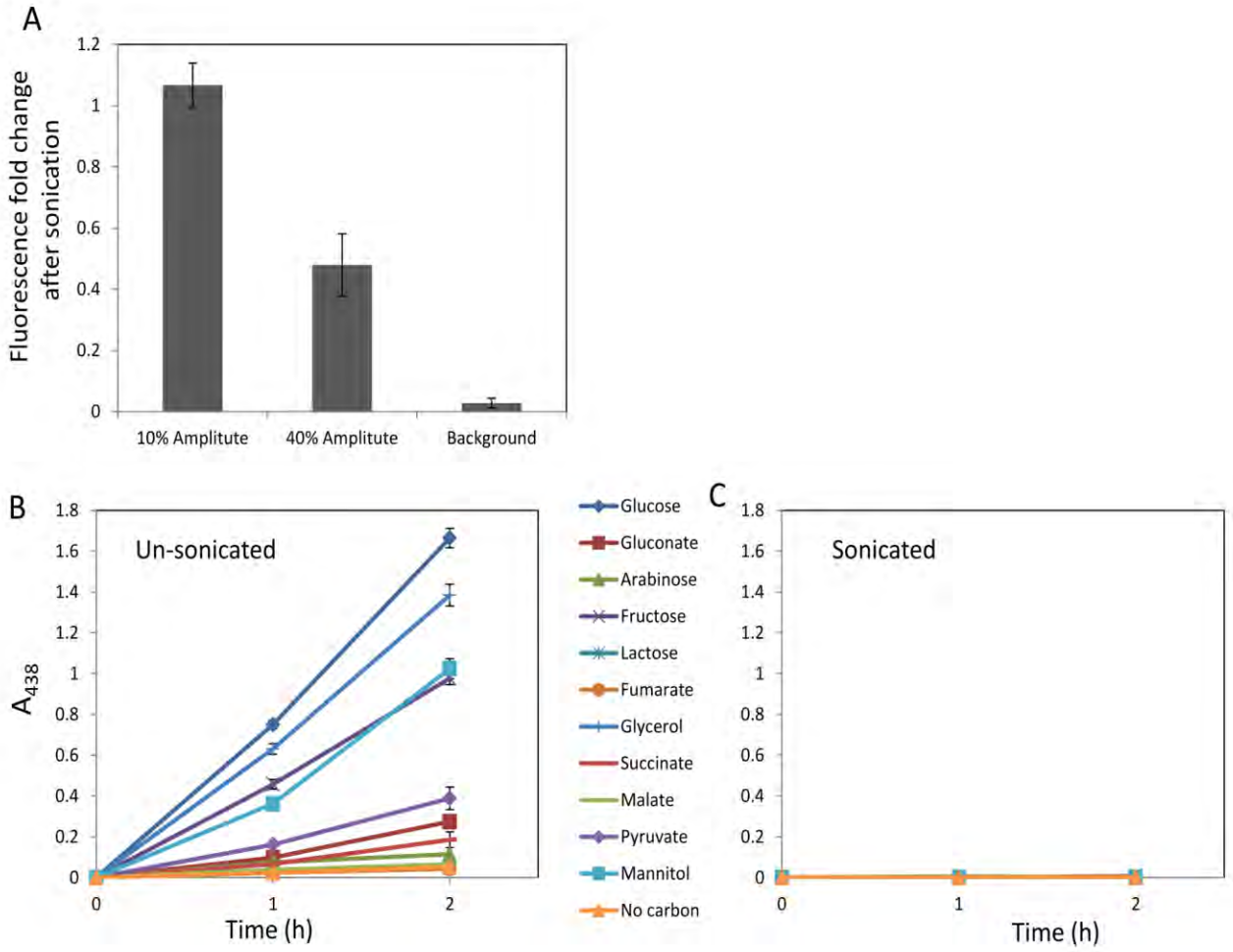

Figure S4. Comparison of metabolic activities of lysed (sonicated) and exponential phase cells. Exponential phase MO001 cultures (2mL) were washed and diluted in M9 salt solution and sonicated at the specified amplitude for 30 minutes on ice, fluorescence was measured before and after sonication using a plate reader (560 nm excitation, 610nm emission) (A). Data indicated that 10% amplitude failed to denature mCherry, but mCherry could serve as an indicator of denaturation, since 40% amplitude significantly reduced fluorescence. Background was fluorescence of sonicated wild-type cells (non-mCherry expressing) during exponential phase. Fluorescence intensities measured after sonication were normalized to fluorescence intensities of unsonicated MO001 cultures. Both sonicated (10% amplitude) and un-sonicated cells chilled on ice were incubated in M9 media with various carbon sources and absorbance measurements were taken at indicated time points (B and C). Error bars indicate the standard error of the mean.

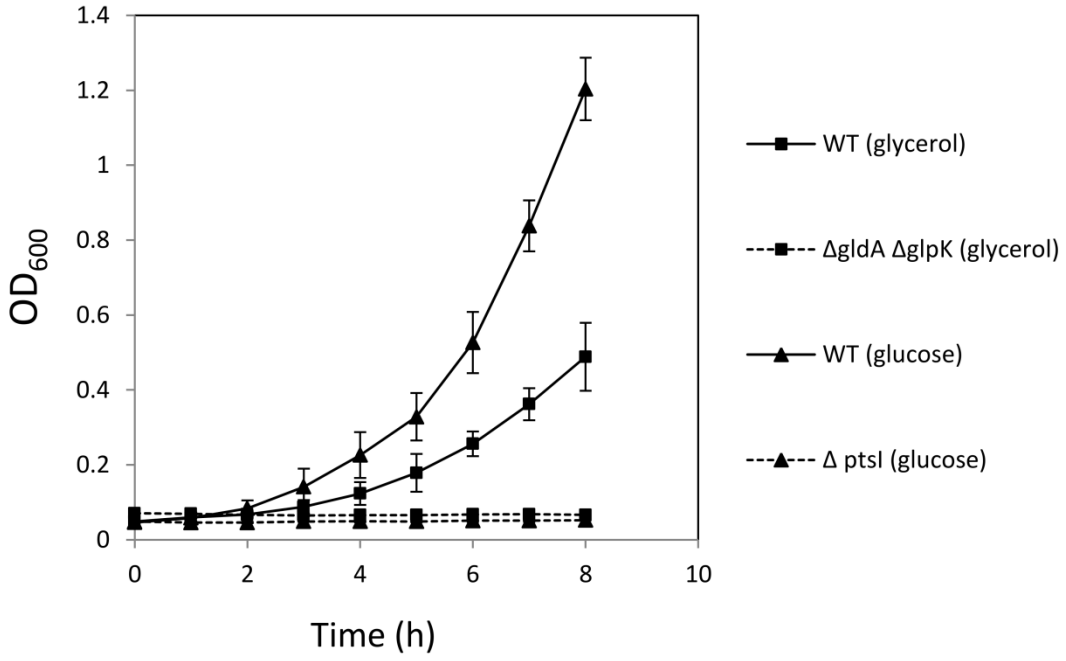

Figure S5. Growth curves of *ΔgldA ΔglpK* and *ΔptsI* in minimal media. Overnight cells in LB were diluted 100-fold in M9 minimal media with indicated carbon sources (60mM carbon) in 250mL flask, and incubated at 37°C and 250rpm. OD_{600} measurements were taken at indicated time points. Error bars indicate the standard error of the mean.

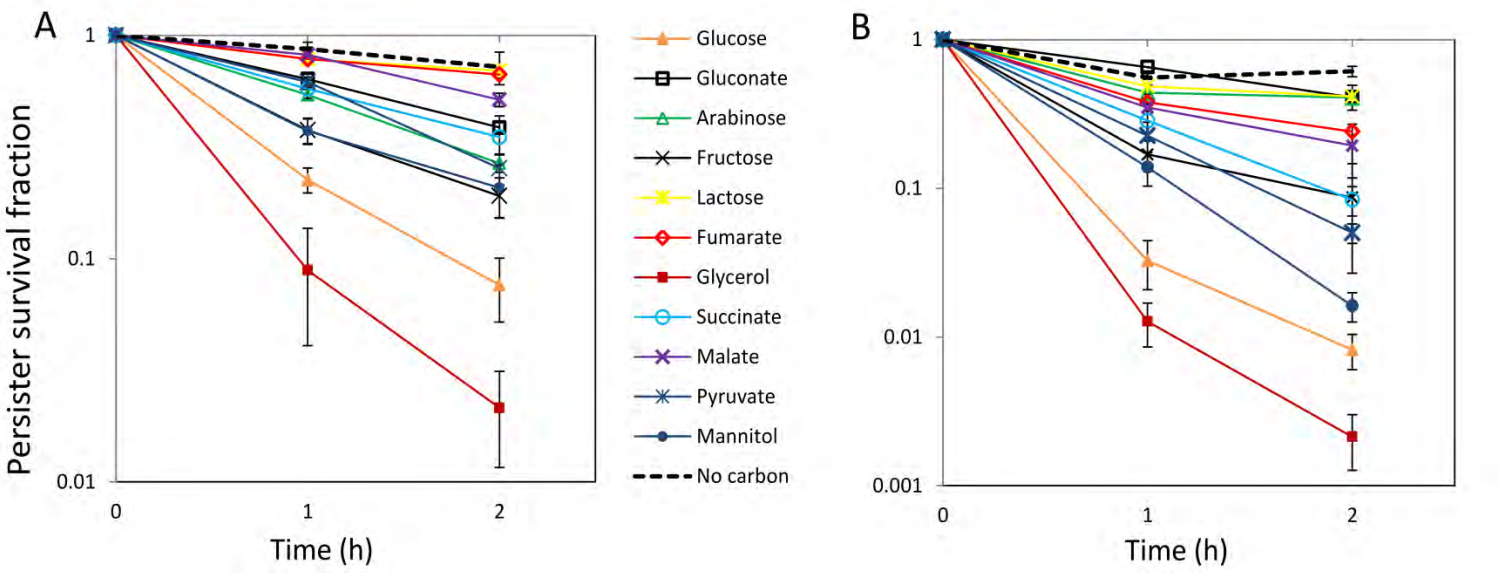

Figure S6. AG potentiation assay for exponential-phase persisters. After exponential-phase cells were treated with ampicillin (A) or ofloxacin (B) for 5 hours, cells were incubated with kanamaycin (KAN) (25μg/mL) in M9 minimal media with different carbon sources using 96-well plates. Changes in CFUs were monitored during the 2 hour assay. Error bars indicate the standard error of the mean.

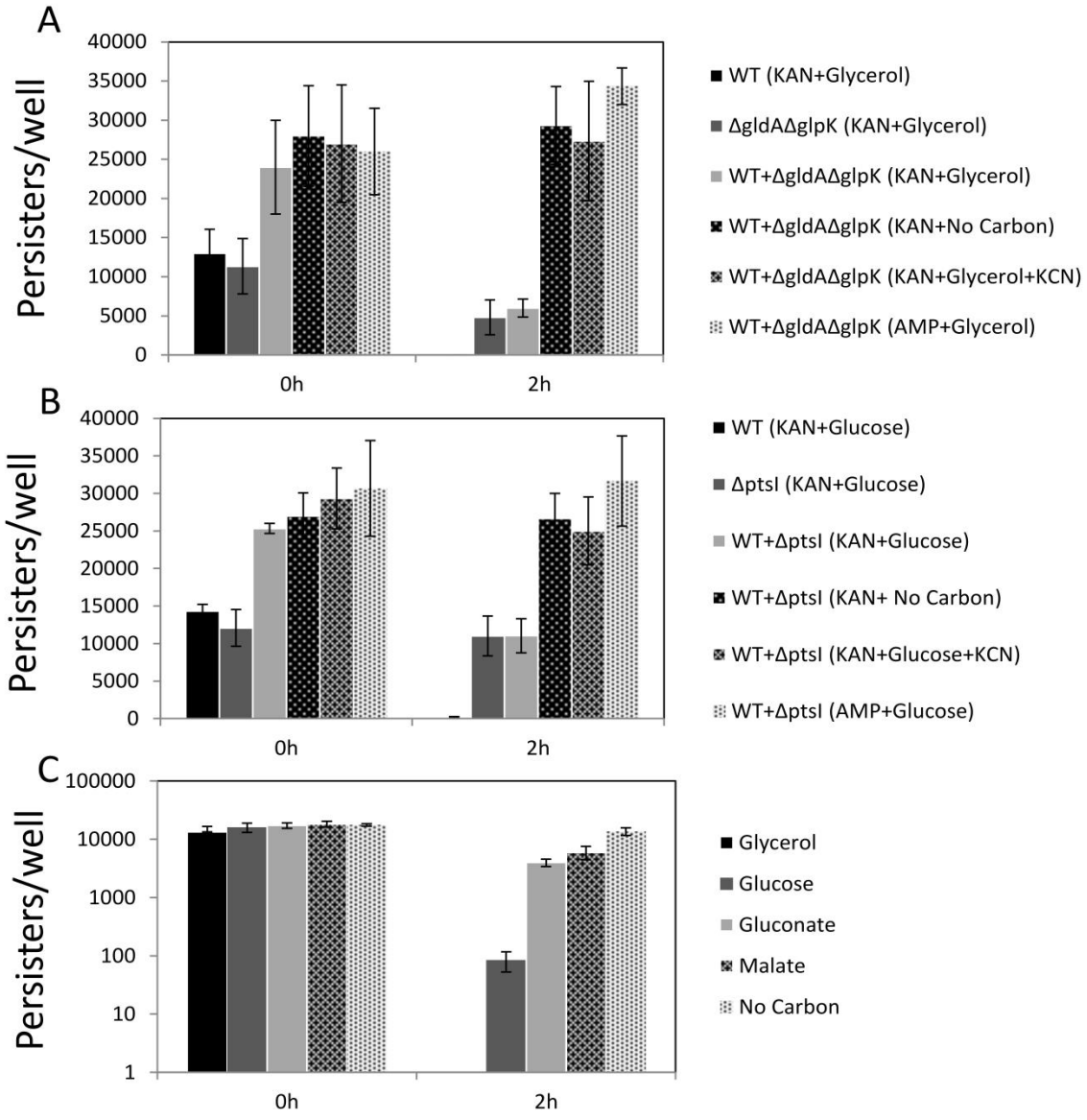

Figure S7. Competition assay for exponential-phase cells treated with ofloxacin. After 5 hour treatment of exponential phase cells with OFX, wild-type only, *ΔgldAΔglpK* only and mixed cell cultures (approximately 50/50 proportion of persisters) at low cell densities were treated for 2 hours with KAN and glycerol (A). The same experiments were repeated for wild-type and *Δpts1* cultures (B). When KCN was used with KAN, AG potentiation was eliminated. Without a carbon source, all cells survived in the presence of KAN. AG potentiation of various carbon sources was tested in low cell density assay (C). Note that, in low cell density assays, no detectable CFUs were counted after 2 hour of treatment with KAN and glycerol (A and C). Error bars indicate the standard error of the mean.

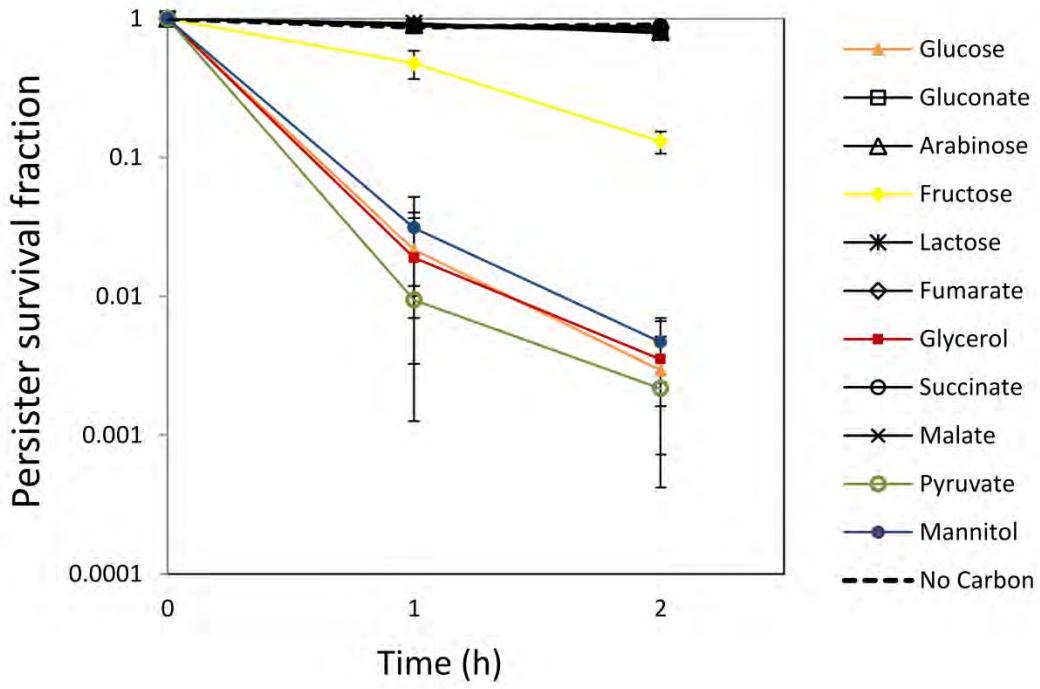

Figure S8. AG potentiation assay for stationary-phase persisters. After stationary-phase cells were treated with OFX for 5 hours, cells were incubated with kanamycin (KAN) (25μg/mL) in M9 minimal media with different carbon sources using 96-well microplates. Survival fraction was monitored by CFU. Error bars indicate the standard error of the mean.

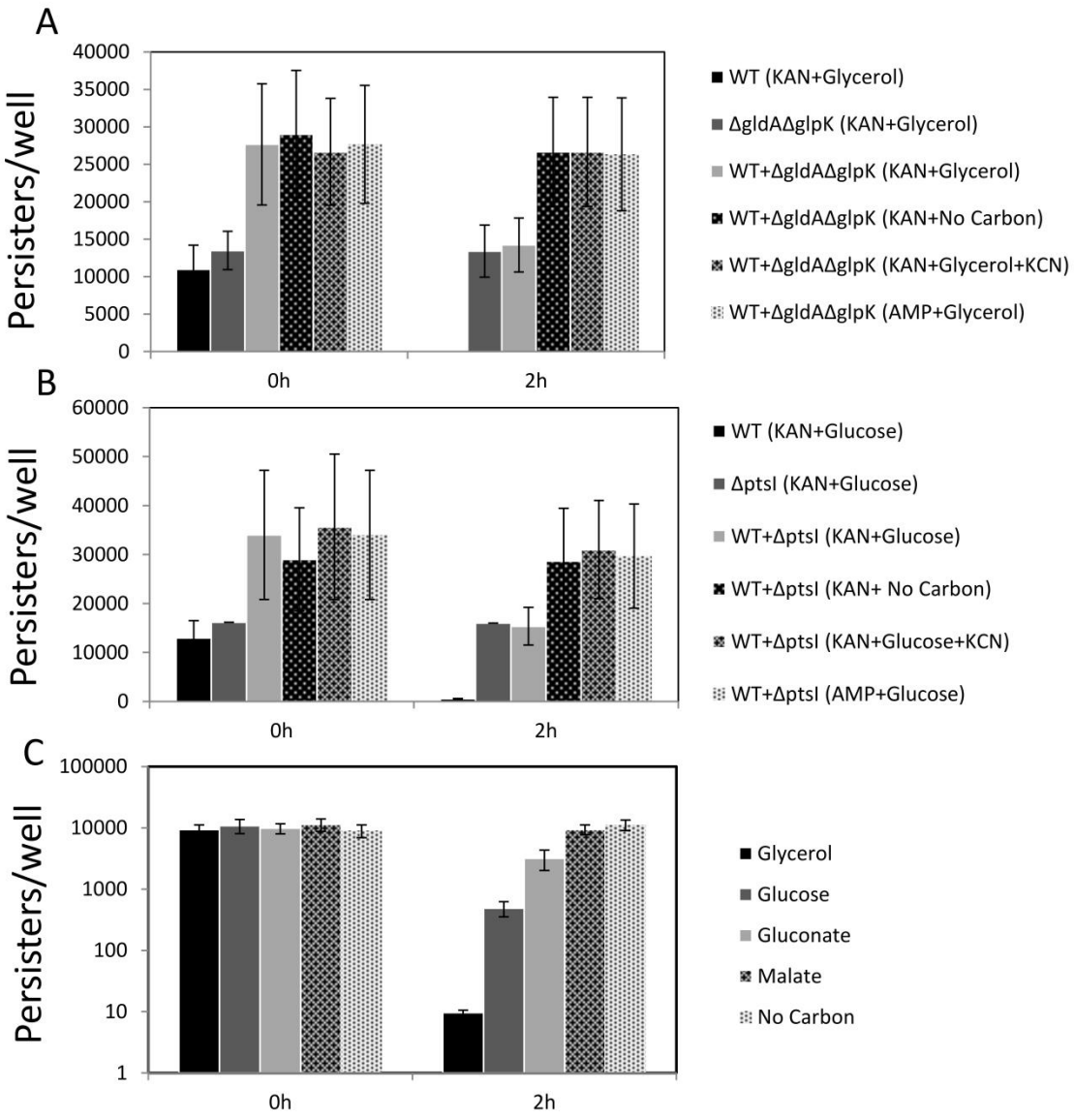

Figure S9. Competition assay for stationary-phase cells treated with ofloxacin. After 5 hour treatment of stationary-phase cells with OFX, wild-type only, *ΔgldAΔglpK* only and mixed cell cultures (50/50 proportion of persisters) at low cell densities were treated with KAN and glycerol for 2 hours (A). The same experiments were repeated for wild-type and *ΔptsI* cultures (B). AG potentiation of various carbon sources was tested in low cell density assay (C). Error bars indicate the standard error of the mean.

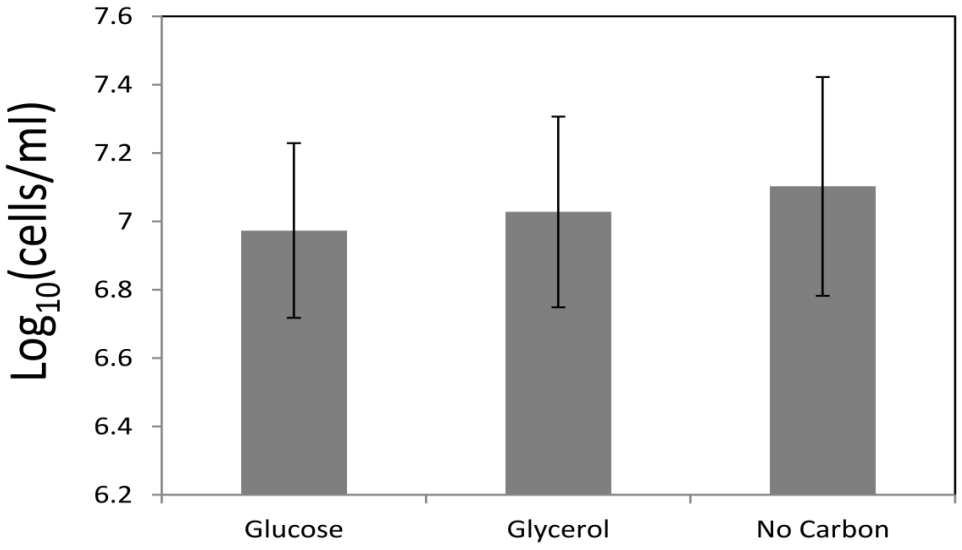

Figure S10. Enumeration of live cells during AG assay. Ampicillin-treated exponential phase cells were treated with KAN and glucose or glycerol. The cells were stained with SYTO9 and PI after 2 hour of AG treatment, and analyzed by flow cytometry to enumerate live cells. As a control, ampicillin-treated cells were not exposed to a carbon source during the AG treatment. Error bars indicate the standard error of the mean.

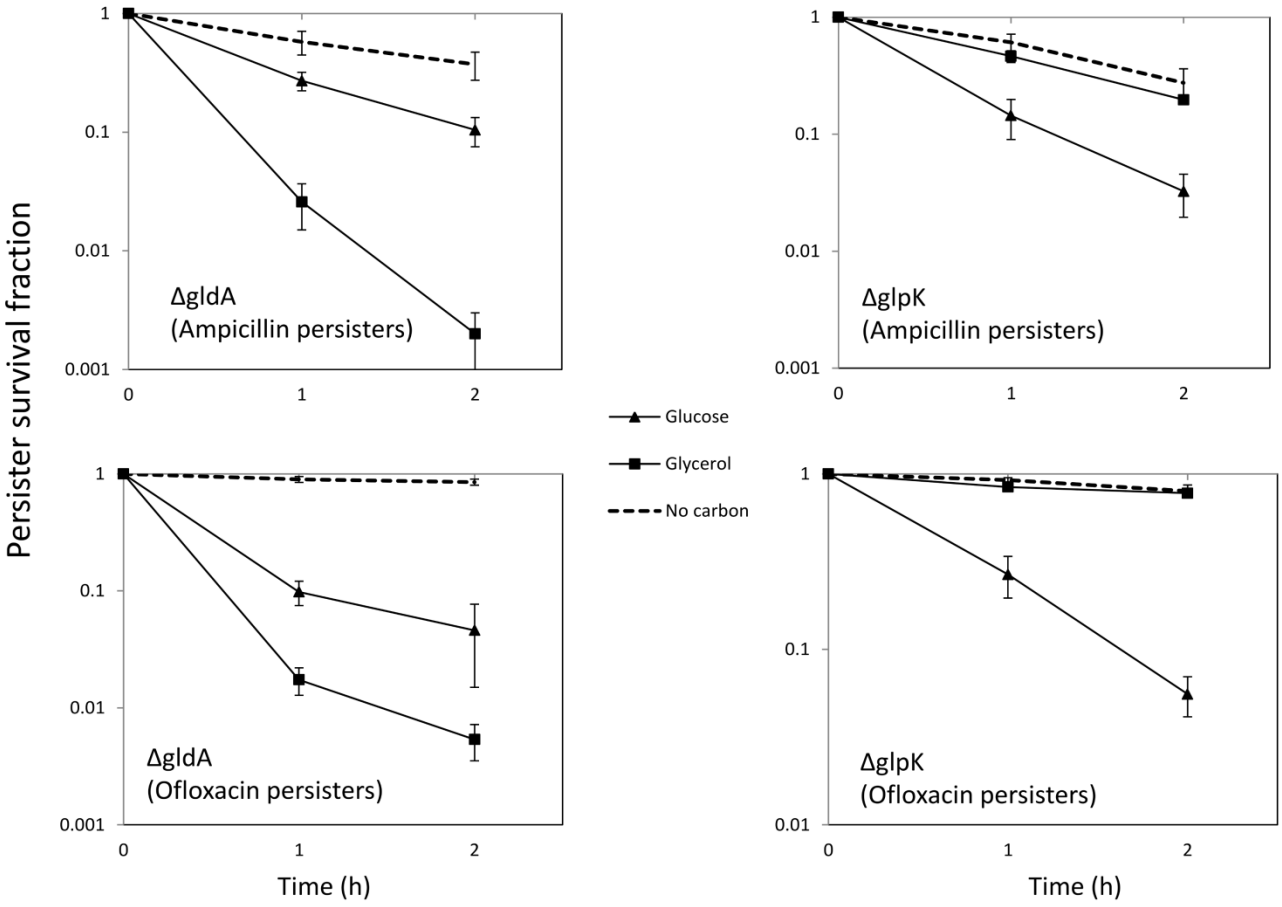

Figure S11. Identification of active glycerol degradation pathway in persisters. Ampicillin and ofloxacin persisters from *ΔgldA* and *ΔglpK* cell types at exponential phase stage were treated with kanamycin in M9 minimal media with indicated carbon sources, and the persister survival fractions were monitored for 2 hours. Error bars indicate the standard error of the mean.

Dormancy Is Not Necessary or Sufficient for Bacterial Persistence

Mehmet A. Orman and Mark P. Brynildsen
Antimicrob. Agents Chemother. **2013, 57(7):3230. DOI: 10.1128/AAC.00243-13.**
Published Ahead of Print 29 April 2013.

AAC Journals.ASM.org

Dormancy Is Not Necessary or Sufficient for Bacterial Persistence

Mehmet A. Orman, Mark P. Brynildsen

Department of Chemical and Biological Engineering, Princeton University, Princeton, New Jersey, USA

The antibiotic tolerances of bacterial persisters have been attributed to transient dormancy. While persisters have been observed to be growth inhibited prior to antibiotic exposure, we sought to determine whether such a trait was essential to the phenotype. Furthermore, we sought to provide direct experimental evidence of the persister metabolic state so as to determine whether the common assumption of metabolic inactivity was valid. Using fluorescence-activated cell sorting (FACS), a fluorescent indicator of cell division, a fluorescent measure of metabolic activity, and persistence assays, we found that bacteria that are rapidly growing prior to antibiotic exposure can give rise to persisters and that a lack of replication or low metabolic activity prior to antibiotic treatment simply increases the likelihood that a cell is a persister. Interestingly, a lack of significant growth or metabolic activity does not guarantee persistence, as the majority of even "dormant" subpopulations (>99%) were not persisters. These data suggest that persistence is far more complex than dormancy and point to additional characteristics needed to define the persister phenotype.

Bacterial persisters are rare phenotypic variants with the ability to tolerate extraordinary levels of antibiotics (1). This tolerance has commonly been attributed to transient growth inhibition and the resulting inactivity of essential cell functions (2). Convincing evidence in support of this model was obtained by time-lapse fluorescence microscopy, as growth-inhibited cells from high-persister mutants survived prolonged antibiotic treatment and resumed normal replication upon removal of the antibiotic (3). That study, by Balaban and colleagues, undoubtedly demonstrated that persisters can originate from growth-inhibited cells (3), and dormancy has since been deemed a trait of persisters, permeating to aspects of their physiology, such as metabolism, for which only indirect evidence of reduced activity exists (4–6). However, it remains unclear to what extent dormancy is a characteristic of persisters or if persister antibiotic tolerances require growth inhibition. Two notable studies used single-cell growth reporters to study persistence, but neither presented data that answer the question of whether persistence requires dormancy (5, 7). Shah and colleagues segregated an exponential-phase population by using an rRNA reporter and found antibiotic-tolerant cells in the subpopulation that was growth inhibited as well as the subpopulation that was growing normally (5). Unfortunately, the antibiotic treatment used to enumerate tolerant cells was performed in a nonnutritive buffer and yielded persister levels (~1:50) that were over 2 orders of magnitude higher than those routinely measured in exponential-phase *Escherichia coli* cultures (<1:5,000) (8). Such a discrepancy suggests that the tolerant cells identified were not representative of normal persister physiology. Roostalu and colleagues segregated growing and nongrowing cells by using a cell division reporter and found that 0.2 to 10% of the nongrowing cells were tolerant to ampicillin treatment (7). Though this result suggested that only a fraction of the nongrowing cells were tolerant to ampicillin, the necessity of growth inhibition for persistence was not queried, since the persistence of the growing subpopulation was not measured.

Recently, persister formation in response to a variety stresses was observed, demonstrating that nonpersister cells can be transformed into the persistent state through the action of signal transduction cascades (9–13, 37). While supportive of the hypothesis that persister populations are heterogeneous (14), these studies do not provide evidence regarding the growth state of the persisters formed and whether growth inhibition prior to antibiotic challenge is a requirement of persistence. Dorr and colleagues demonstrated that ciprofloxacin can induce persistence in a subpopulation of exponential-phase cells through the action of the SOS response, but they did not determine whether those cells that became persisters were growth inhibited prior to antibiotic exposure (9, 10). Moker and colleagues found that a quorum sensing molecule increased persistence in *Pseudomonas aeruginosa*, but they also did not establish the growth state of persisters prior to antibiotic exposure (13). Vega and colleagues found that indole induces persister formation, and they elegantly demonstrated with a microfluidic device that the strength of indole sensing is predictive of tolerance to 1 h of ampicillin treatment (11). However, the tolerant subpopulation in the microfluidic device was much higher than that obtained when exponential-phase cells were exposed to indole (20% compared to 1%), suggesting that tolerance measured in the device might not be translatable to normal culture conditions. Wu and colleagues found that paraquat at a concentration close to that which completely inhibits growth induces persister formation, but the growth characteristics of the culture and persister subfractions were not reported (12). Interestingly, despite the growing body of literature on persister formation and physiology (14–16), we cannot definitively say whether growth inhibition is necessary or sufficient for persistence. Analogously, and to a greater extent, we do not know whether persister antibiotic tolerances require metabolic dormancy. All insights into persister metabolism have been obtained indirectly from gene expres-

Received 4 February 2013 Returned for modification 24 February 2013
Accepted 23 April 2013
Published ahead of print 29 April 2013
Address correspondence to Mark P. Brynildsen, mbrynild@princeton.edu.
Supplemental material for this article may be found at http://dx.doi.org/10.1128/AAC.00243-13.

doi:10.1128/AAC.00243-13

sion of persister-enriched samples (4–6) or potentiation of aminoglycoside activity (17).

Here we answer two fundamental questions about bacterial persistence. (i) Can bacteria that are normally replicating prior to antibiotic treatment be persisters? (ii) Are persisters metabolically dormant prior to antibiotic treatment, as most research assumes (3, 5, 7, 18), or can they exhibit a range of metabolic activities? To answer these questions, we employed fluorescence-activated cell sorting (FACS), a fluorescent indicator of cell division (7), a fluorescent measure of metabolic activity (19, 20), and persistence assays to rigorously quantify the metabolic and cell division distributions of persisters within an exponentially growing *E. coli* culture. Using the cell division reporter, we found that the nongrowing subpopulation was far more enriched with persisters (~1%) than the growing subpopulation (~0.01%), but due to the relative abundances of the growing and nongrowing subpopulations, ~20% of all persisters originated from growing cells. Surprisingly, even the most rapidly growing subpopulation gave rise to persisters, demonstrating that growth inhibition prior to antibiotic exposure is not required for persistence. Using a fluorescent measure of metabolic activity, redox sensor green (RSG), we found that within an exponential-phase *E. coli* population, cells with low reductase activity were ~40 times more likely to be persisters than cells with high reductase activity. These are the first direct measurements of metabolic activity in persisters, and interestingly, persisters appear to display a range of metabolic activities. We subsequently performed a two-dimensional (2D) FACS experiment (red channel, cell division; and green channel, metabolism) and found that persisters were enriched in the subpopulation with low reductase activity due to the prevalence of persisters in the nongrowing subpopulation, whose metabolic activity was significantly less than that of the growing subpopulation. Overall, the experimental evidence presented in this study supports the emerging hypothesis that persister subpopulations are highly diverse (14–16) and provides a more holistic view of the persistence phenomenon, one in which inhibition of replication or metabolism enhances the likelihood of a cell to be a persister but in itself cannot adequately explain the phenotype.

MATERIALS AND METHODS

Bacterial strains. All strains were derived from *E. coli* MG1655. Strain MO001 contained a chromosomally integrated *lacI*^{q} promoter in place of the *lacI* promoter and a chromosomally integrated *T5p-mCherry* cassette in place of *lacZYA*. This was done in order to eliminate plasmid copy number as a variable. The T5 promoter (T5p) is a strong, IPTG (isopropyl-β-D-thiogalactopyranoside)-inducible promoter under the control of two *lac* operator sites (21). Using the forward and reverse primers indicated in Table S1 in the supplemental material, the T5p was amplified from the pQE-80L plasmid (Qiagen, Valencia, CA). Both *lacI*^{q}*p* and *T5p-mCherry* were integrated into the chromosome by using the method of Datsenko and Wanner (22). All primers used, as well as a description of the cloning steps, are presented in Table S1. All mutations were confirmed using PCR and/or DNA sequencing (Genewiz, South Plainfield, NJ).

Chemicals, media, and growth conditions. All chemicals, unless noted below, were purchased from Fisher Scientific or Sigma-Aldrich. RSG and a Live/Dead (Syto9/PI) staining kit were purchased from Life Technologies, Invitrogen (Grand Island, NY), and IPTG was purchased from Gold Biotechnology (St. Louis, MO). LB medium (10 g/liter tryptone, 5 g/liter yeast extract, and 10 g/liter NaCl) and LB-agar plates (LB plus 15 g/liter agar) were used for planktonic growth and enumeration of CFU, respectively. Antibiotics were used at the following concentrations for selection or translational inhibition: 50 μg/ml kanamycin, 50 μg/ml chloramphenicol, and 100 μg/ml ampicillin. For persister assays, 200 μg/ml ampicillin (23) and 5 μg/ml ofloxacin (8) were used. Unless otherwise noted, overnight cultures were prepared by culturing cells from a 25% glycerol, −80°C stock in 2 ml LB medium at 37°C with shaking (250 rpm) for 24 h. Overnight cultures were then diluted 1,000-fold in 50 ml of fresh LB medium in 500-ml baffled flasks and incubated for 2.5 h at 37°C and 250 rpm, at which time an optical density at 600 nm (OD_{600}) of ~0.1 was achieved. CFU were enumerated by washing and diluting samples in phosphate-buffered saline (PBS), plating them on LB-agar plates, and incubating them at 37°C for 16 h. MICs of antibiotics for both wild-type MG1655 and MO001 at exponential phase were determined by serial 2-fold dilution of antibiotics in LB broth (24). MIC ranges for both strains were found to be 1.5 to 3 μg ampicillin/ml and 0.075 to 0.15 μg ofloxacin/ml.

Staining with redox sensor green. Cell staining was performed according to the manufacturer's instructions, with some modifications. Briefly, cells were cultured as described above, and after 2.5 h at 37°C and 250 rpm, 1 ml of exponential-phase culture was stained with 1 μM RSG and incubated in the dark at room temperature for approximately 30 min before sorting. As controls, 1-ml samples were first incubated with carbonyl cyanide *m*-chlorophenylhydrazone (CCCP) or potassium cyanide (KCN) at 10 μM or 1 mM, respectively, for 5 min prior to addition of RSG. To analyze the effect of RSG on cell viability, CFU in samples were measured before staining and 30 min after staining.

Single-cell division assay. MO001 cells were cultured as described above, except that 1 mM IPTG was included overnight to express *mCherry*, and following the overnight incubation, IPTG was removed by centrifugation (3 min at 15,000 rpm), removal of the supernatant, and resuspension of the culture in fresh LB. Washed cells were then diluted 1,000-fold in 50 ml fresh LB and cultured as described above. One milliliter of the culture was analyzed by flow cytometry to sort the growing and nongrowing cells. To compare MO001 background fluorescence to that of the parent strain (without *mCherry*), MO001 was incubated without IPTG during overnight growth and then inoculated into fresh medium with or without IPTG, and fluorescence intensities of exponential-phase cultures were measured by flow cytometry (see Fig. S1 in the supplemental material). To verify that mCherry was not degraded during the time frame of the experiment, the washed overnight culture was diluted in LB with 50 μg/ml chloramphenicol, and 1-ml samples were analyzed by flow cytometry (see Fig. S2).

Microscopy imaging. Phase-contrast and fluorescence images of induced MO001 were taken by a Nikon Eclipse 90i microscope equipped with a 100×/1.40-numerical-aperture (NA) phase objective, a Q Imaging Rolera-XR camera, and NIS Elements software. Cells were stabilized on 1% agarose pads during the imaging process. To do this, 200 μl of fully dissolved warm agarose was transferred to the middle of a clean microscope slide, and then another slide was placed on top of the agarose to attain a flat surface (air bubbles were avoided). After the agarose solidified, the upper glass slide was carefully removed, and 2.5 μl of cell culture was loaded on the solid medium and covered with a coverslip to be analyzed with the microscope.

Flow cytometry analysis. All samples, including controls, were analyzed by an LSRII flow cytometer (BD Biosciences, San Jose, CA). Microorganisms were identified using forward and side scatter parameters (FSC and SSC, respectively). Stained bacteria were assayed with a laser emitting at 488 nm for RSG and 561 nm for mCherry; fluorescence was collected using green and red fluorescence filters (525/50- and 610/20-nm-band-pass filters, respectively). Data were acquired and analyzed using FACSDiVa software (BD Biosciences, San Jose, CA).

Cell sorting. Cells were sorted using either a FACSVantage SE w/DiVa (BD Biosciences, San Jose, CA) cell sorter at 16 lb/in^2 with a 70-μm nozzle or a Reflection (Sony-iCyt Mission Technology, Champaign, IL) cell sorter at 30 psi with a 70-μm nozzle. Microorganisms were determined using forward and side scatter parameters (FSC and SSC), and physiologically distinct subpopulations were identified by measuring green and red fluorescence (488-nm excitation with 530/30-nm-band-pass filter and

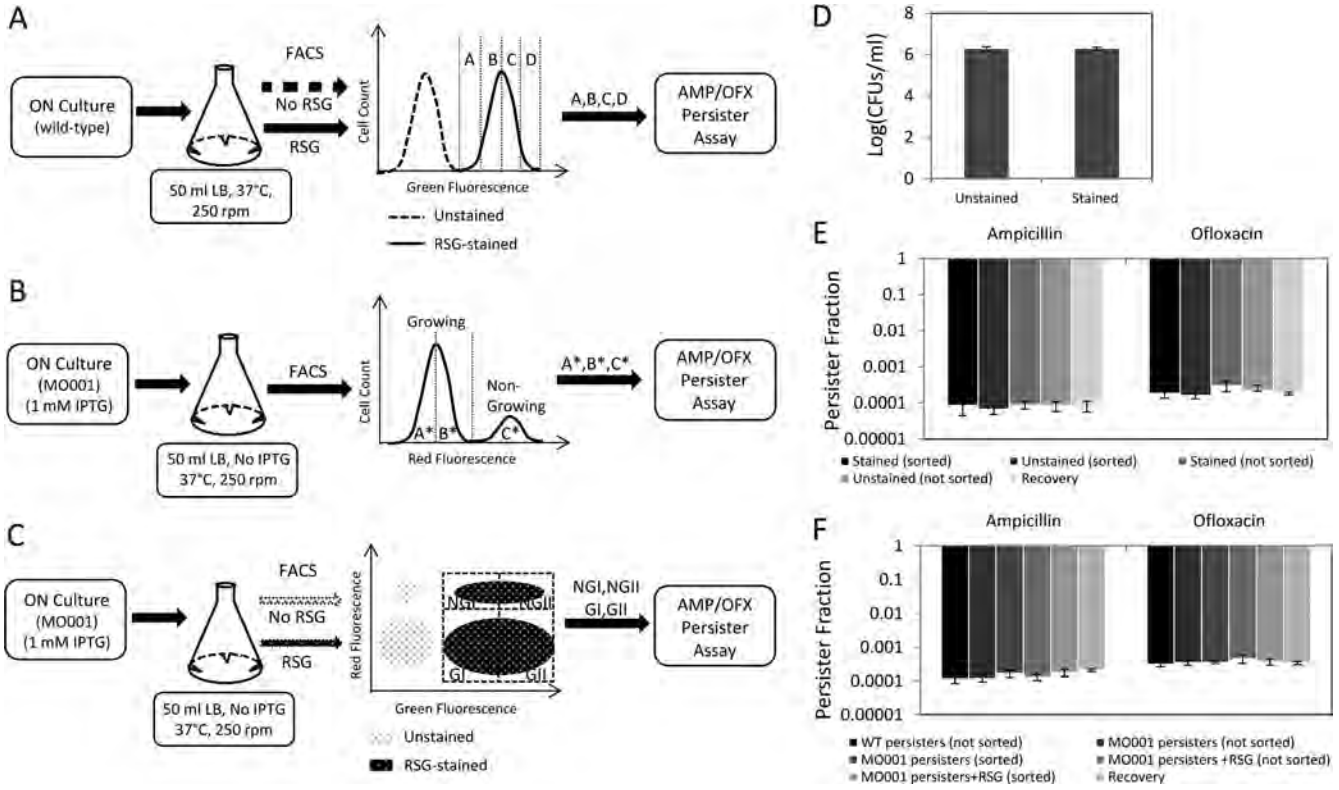

FIG 1 FACS methods and control experiments. (A to C) Exponential-phase cells were sorted from the indicated regions (gates) in order to quantify the metabolic and cell division distributions of persisters. Gates were determined by using a fluorescent measure of metabolic activity (RSG) (A), a cell division reporter (*mCherry* with an IPTG-inducible promoter) (B), or both (C). ON, overnight. (D) RSG staining did not affect cell viability ($P = 0.94$ by the *t* test). (E) RSG staining, cell sorting, and segregation did not change the persister levels of exponential-phase *E. coli* cultures sorted as illustrated in panel A ($P = 0.97$ for the ampicillin group and $P = 0.52$ for the ofloxacin group, using ANOVA). (F) RSG staining, cell sorting, and segregation did not alter persister levels of mCherry-expressing cells sorted as in panel C ($P = 0.31$ for the ampicillin group and $P = 0.75$ for the ofloxacin group, using ANOVA). Recovery is the calculated frequency of persisters in the total population, based on the persister frequencies measured from the segregated quantiles (see Materials and Methods).

561-nm excitation with 615/30-nm-band-pass filter, respectively) and by running unstained samples, RSG-only-stained cells, mCherry-expressing cells, and mCherry-expressing cells stained with RSG. Cells were sorted using sterile 1× PBS as sheath fluid in the sorter.

As a test to quantify the number of nongrowing cells (C* region in Fig. 1B) that were improperly sorted into the fastest-growing quantile (A* region in Fig. 1B), approximately 5×10^5 cells were sorted from the A* or C* region. The sorter sample line was then immediately washed first with 10% bleach for 5 min and then with PBS for 5 min to remove any cell remnants from the previous sample. The sorted cells from A* and C* were reanalyzed separately by the same sorter to assess the proportion of persisters in the fastest-growing subpopulation that may have arisen from nongrowing cells (see Fig. S3 in the supplemental material). The sorter was washed as described above between analyzing A* and C*.

Persister assays. After determining the fluorescence quantiles to be sorted (Fig. 1A to C), approximately 1×10^6 cells from each subpopulation were collected in 1 ml of PBS. Cells were sorted at room temperature, and each sorting procedure lasted 15 min or less, depending on the percentage of the population corresponding to the region to be sorted. The collected cells were then mixed 1:1 with a rich medium (2× tryptone, 2× yeast extract, and 1× NaCl) to produce a medium similar to LB. One milliliter of this culture, containing 5×10^5 cells, was immediately treated with either ampicillin (200 μg/ml) or ofloxacin (5 μg/ml). Cells were then incubated in a shaker at 37°C and 250 rpm for 5 h. Samples at designated time points were collected by centrifugation for 3 min at 15,000 rpm, washed with PBS twice, and resuspended in 100 μl of PBS. Next, 10 μl of the sample was serially diluted in PBS and spotted on LB agar to measure the CFU. The remaining 90-μl sample was also plated on LB agar in case the CFU from the 10-μl sample might be under the limit of detection. To analyze the effect of RSG on persister levels, unstained cells (negative control) were sorted and treated with antibiotics as described above to enumerate the level of persisters, which was compared to the persister levels obtained from RSG-stained samples. To determine the effect of flow through the sorter on persister levels, cells that were not sorted were diluted in 1 ml fresh LB to obtain approximately 5×10^5 cells and then were treated with antibiotics, and CFU were measured at the indicated time points.

To quantitatively estimate the percentage of nongrowing cells that started to grow during the antibiotic treatment period, the sorted cells from the C* region (Fig. 1B) were treated with or without antibiotics for 5 h in LB as described above, and the number of cells retaining high mCherry levels was quantified by LSRII flow cytometry with the use of fluorescent counting particles (Spherotech Inc., Lake Forest, IL). To determine the number of dead cells in the nongrowing subpopulation, stationary-phase cultures diluted 1,000-fold in 1 ml 0.85% NaCl buffer were stained with Syto9 and propidium iodide (PI) simultaneously at concentrations of 5 μM and 30 μM, respectively, and then incubated at room temperature for approximately 15 min before flow cytometry analysis. This method enumerates dead cells in the nongrowing subpopulation, under the assumption that dead cells within this subpopulation arose from 24-h stationary-phase inoculums. As a control, stationary-phase cells were incubated in 1 ml of 70% ethanol solution for 1 h.

The dilution/growth experiment described by Keren et al. (8) was applied in order to demonstrate that the persister levels measured with the

FACS procedure were identical to those measured on the bench. Cells with mCherry protein from overnight cultures were diluted 1:1,000 in 50 ml fresh medium in a 500-ml baffled flask without inducer and cultured at 37°C and 250 rpm. When the cell culture reached an OD_{600} of 0.1, the cells were diluted 1:50 in fresh medium and cultured in the same way until the OD_{600} reached 0.1 again. This dilution/growth cycle was repeated twice, thus resulting in three rounds in total (R_0, R_1, and R_2). At the end of each round, cells were analyzed by FACS and sorted to determine the persister levels as described above.

The frequency of persisters (f) was calculated as the ratio of the number of persisters in a sample to the initial number of sorted cells before antibiotic treatment. Persister frequencies of all sorted regions are provided in Table S2 in the supplemental material. We defined recovery (R) as follows: $R = p_A f_A + p_B f_B + p_C f_C + p_D f_D$, where p_A is the proportion of the total population in the A quantile and f_A is the frequency of persisters in the A quantile (Fig. 1A). Recovery is the frequency of persisters in the total population, as calculated from the segregated quantiles, and thus was used as an internal consistency check, since it should equal the frequency of persisters obtained from a nonsegregated sample. The persister fraction from a region (such as region A) is the ratio of persisters in that region to the total number of persisters in the whole population, which was calculated as $p_A f_A/R$. We note that the sum of persister fractions from all quantiles equals 1. To illustrate, persister frequencies of the A*, B*, and C* regions (Fig. 1B; see Fig. 3A) were found to be 4.47×10^{-5}, 5.8×10^{-5}, and 4.27×10^{-3} (see Fig. 3C), respectively. Since $p_{A^*} = 0.48$, $p_{B^*} = 0.48$, and $p_{C^*} = 0.04$ (see Fig. 3A), the recovery is calculated as follows: $R = 4.47 \times 10^{-5} \times 0.48 + 5.8 \times 10^{-5} \times 0.48 + 4.27 \times 10^{-3} \times 0.04 = 2.2 \times 10^{-4}$, which also corresponds to the frequency of persisters in the total population. The persister fraction of A* was calculated as $4.47 \times 10^{-5} \times 0.48/2.2 \times 10^{-4} = 0.1$; similarly, the B* and C* fractions were found to be 0.12 and 0.78, respectively (see Fig. 3D). All experiments were repeated 3 times in this study. One-way analysis of variance (ANOVA) was used to test the null hypothesis that the population means for all conditions, including the treatment and control groups, were the same. Pairwise comparisons were performed using the two-tailed t test. A significance P value threshold of 0.05 was selected. Data points in figures are average values for experimental repeats. Error bars represent standard errors.

RESULTS

FACS methods to quantify persister metabolic and cell division distributions. To determine whether persisters needed to be growth inhibited or metabolically inactive prior to antibiotic treatment, we required a method to quantify persister phenotype distributions. Previous studies have monitored persister growth rates in cultures of high-persistence (*hipA7* and *hipQ*) mutants by using fluorescence microscopy (3); however, the low abundance of persisters in wild-type *E. coli* populations necessitated the use of a more rapid screening technique. FACS is a rapid, single-cell, quantitative screening method that has been used to study different aspects of the persistence phenotype (5, 7, 11, 25). Here we used FACS to quantify growth rate and metabolic activity distributions for persisters from exponential-phase *E. coli* cultures. In brief, FACS was used to segregate cultures into quantiles based on fluorescence signals (Fig. 1A to C), and each quantile was then treated with an antibiotic (ampicillin or ofloxacin) to enumerate the number of persisters present. To demonstrate that the FACS procedure did not alter persistence within the culture, we verified that fluorescence labeling (e.g., metabolic staining and fluorescent protein expression), flow cytometry, and segregation all did not change the level of persisters in the population (Fig. 1D to F).

To monitor growth rate, we adapted the methodology of Roostalu and colleagues (7), which tracks cell division by dilution of a fluorescent protein. To generate a strain whose cell division could be monitored by red fluorescence, we knocked the *mCherry* gene, under the control of a strong, synthetic, IPTG-inducible promoter (*T5p*) (21), into the chromosome of an *E. coli* strain carrying a chromosomally integrated *lacI*^{q} promoter mutation (MO001) (26). Background fluorescence from MO001 (without IPTG) was comparable to that of the parent strain without *mCherry*, whereas full induction produced fluorescence that was orders of magnitude above the background, providing us with a large dynamic range (see Fig. S1 in the supplemental material). To verify that this method monitored cell division, *mCherry* expression was induced during the overnight culture, and cells were washed to remove the inducer and inoculated into fresh medium without inducer. The dilution of mCherry protein within the cells due to cell proliferation was monitored using flow cytometry and fluorescence microscopy. As depicted in Fig. 2A to C, all cells started with high red fluorescence, and as cells divided, the red fluorescence of the population declined, except for a small subpopulation whose fluorescence remained constant due to a lack of division. To verify that mCherry was not degraded during the time frame of the experiments, cells were incubated in medium with chloramphenicol, an inhibitor of protein synthesis, and were demonstrated to retain their red fluorescence throughout the time course (see Fig. S2). These results demonstrate that this FACS method monitors cell division at the single-cell level.

To study single-cell metabolic activity, we employed RSG, a fluorogenic redox indicator that yields green fluorescence when reduced by bacterial reductases (19, 27, 28). To ensure that the measured fluorescence reported on metabolic activity, we used the chemical inhibitor KCN to block respiration and CCCP to deplete the proton motive force. As depicted in Fig. 2D and E, both CCCP and KCN significantly reduced staining with RSG, demonstrating that RSG is a robust indicator of bacterial metabolism ($P = 0.024$ and 0.030 for mean fluorescence values of CCCP- and KCN-treated samples, respectively, compared with that of RSG-only-stained samples, using the t test).

Persisters can originate from the fastest-growing subpopulation of cells. To separate the nongrowing cells from the growing subpopulation in exponential-phase cultures, *mCherry* expression was induced from MO001 during overnight culture, and cells were washed to remove the inducer and inoculated into fresh medium without inducer. At 2.5 h postinoculation ($OD_{600} = 0.1$), the nongrowing population constituted approximately 4% of all cells (Fig. 3A). To enumerate persisters, FACS-sorted samples were treated with ampicillin or ofloxacin and CFU were monitored as a function of time. As depicted in Fig. 3B and C, a rapid killing regimen, representing the death of normal cells, was followed by a slower killing regimen, indicating the presence of persisters. This biphasic kill curve verified that 5 h of antibiotic treatment under the conditions described here was sufficient to quantify persister levels (15). Figure 3B and C also demonstrate that MO001 had persister levels indistinguishable from those of the wild type. To determine whether the nongrowing subpopulation was enriched with persisters, we sorted the population into three regions based on red fluorescence and treated the samples with ampicillin or ofloxacin for 5 h. While the majority of persisters were found to be within the nongrowing subpopulation (77.26% ± 6.11% of ampicillin persisters and 78.55% ± 3.61% of ofloxacin persisters), we also measured persisters within the growing subpopulation (Fig. 3D and E). Surprisingly, 22.73% ± 6.42% of ampicillin persisters and 21.44% ± 3.79% of ofloxacin persist-

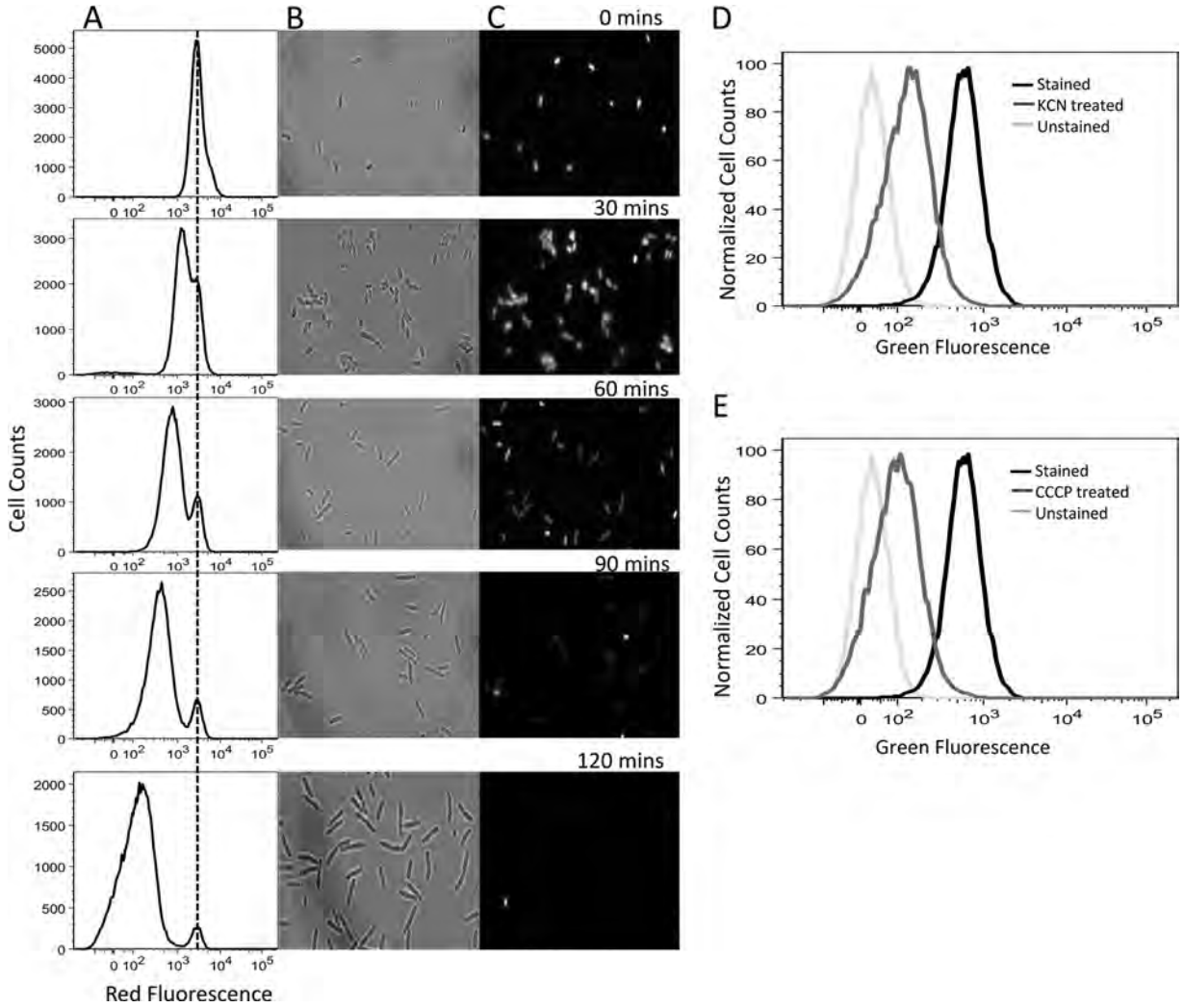

FIG 2 Cell division and metabolic activity reporters. Division at the single-cell level was monitored by flow cytometry and microscopy. After accumulation of mCherry protein during overnight culture, cells were washed to remove the inducer and inoculated into fresh medium without inducer. When the cells started to divide, the red fluorescence of the population decreased, except for a small subpopulation whose fluorescence remained constant (nongrowing cells). Panel A shows the flow cytometry data, whereas panels B and C show phase-contrast and fluorescence images taken by microscopy, respectively, at the indicated time points during exponential-phase growth. (D and E) Cellular metabolic activity was characterized by RSG staining. RSG produces a stable green fluorescence signal when reduced by bacterial reductases. The fluorescence signals were reduced when the cells were treated with KCN and CCCP, which block respiration and deplete the proton motive force, respectively.

ers were within the growing subpopulation. We note that a previous study has shown that persisters can replicate at rates that are 10-fold lower than those of normal cells (3) but that this is the first report of persisters being found in the fastest-dividing subpopulation (A*) of an exponentially growing culture (doubling time of 25.41 ± 0.38 min) (see Fig. S4 in the supplemental material).

To confirm that persisters can arise from the growing subpopulation, we sought to provide further evidence in support of our FACS results. Specifically, we sought to (i) quantify the precision of our FACS experiments by measuring the number of nongrowing cells that were improperly sorted into the fastest-growing quantile and (ii) demonstrate further that our FACS technique does not generate persisters (in addition to the controls depicted in Fig. 1D to F). Measuring the precision of our FACS procedure allowed calculation of the proportion of persisters in the fastest-growing subpopulation that may have arisen from nongrowing cells and was an important control given the ~100-fold difference in persister frequencies between the nongrowing and growing subpopulations (Fig. 3D). To generate these data, we performed a tandem FACS experiment where cells were sorted and then immediately reanalyzed on the same cell sorter (see Materials and Methods). We determined that <0.2% of cells in the fastest-growing subpopulation (A*) were subsequently sorted as nongrowing cells (C*) (see Fig. S3 in the supplemental material). Given the frequencies of persisters in A* and C*, we calculated that >80% of persisters measured in A* were normally replicating cells. Although the cells were replicating normally prior to sorting, the possibility remained that the FACS procedure stimulated some cells to become persisters. As depicted in Fig. 1D to F, we performed a control to test this for the entire population and showed that the persister levels were indistinguishable with and without sorting (as analyzed by ANOVA). However, to lend further experimental

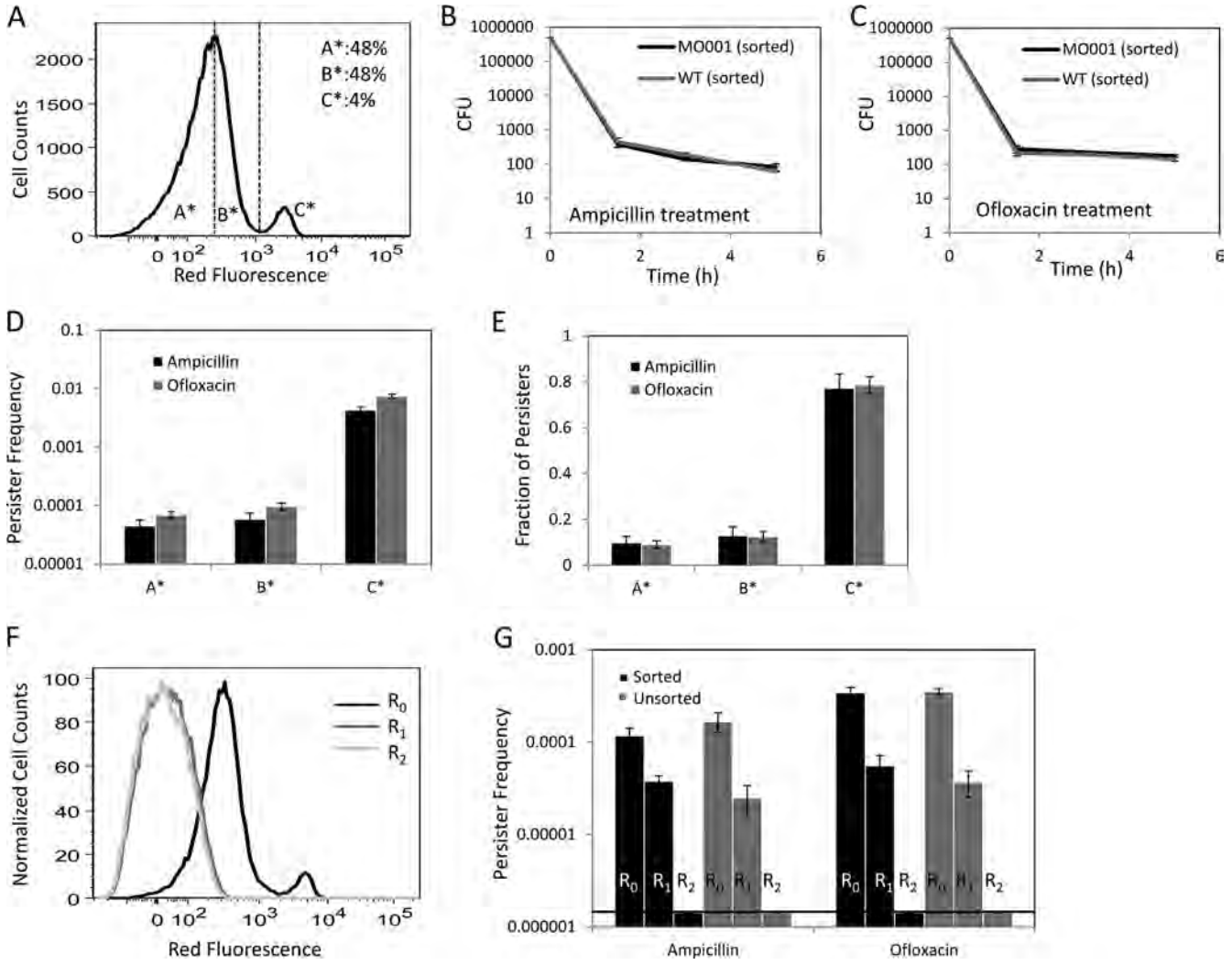

FIG 3 Cell division properties of persisters. (A) The regions to be sorted (A*, B*, and C*) were determined based on the proliferation rates of exponential-phase cells. A* and B* comprised approximately 96% of the population (48% each), whereas C* contained approximately 4% of all cells. (B and C) CFU were counted at the indicated time points during the ampicillin or ofloxacin treatment of FACS-sorted or nonsorted cells. MO001 had statistically indistinguishable persister levels compared to the wild type ($P = 0.38$ for ampicillin persisters at the 5-h time point and 0.30 for ofloxacin persisters at the 5-h time point, by the *t* test). (D and E) Persister frequencies and fractions of A*, B*, and C* were determined 5 h after antibiotic treatment. The frequency is the ratio of persisters to the initial number of FACS-sorted cells. The fraction of persisters of a region such as A* is the ratio of persisters in A* to the total number of persisters in the culture. (F) Repeated inoculation into fresh medium eliminated the nongrowing subpopulation. Overnight cultures of cells with mCherry protein were inoculated (1:1,000) into fresh medium without inducer and cultured until the OD_{600} reached 0.1. The cells were then diluted 1:50 in fresh medium and cultured identically until the OD_{600} again reached 0.1, and this cycle was repeated twice, resulting in three rounds in total (R_0, R_1, and R_2). (G) At the end of each round, cells were sorted by FACS to determine the persister levels. No significant differences were observed between bench-top- and FACS-sorted samples ($P = 0.37$ for R_0-ampicillin samples, 0.88 for R_0-ofloxacin samples, 0.30 for R_1-ampicillin samples, and 0.42 for R_1-ofloxacin samples, using the *t* test). Note that *P* values for R_2 samples could not be determined because the number of persisters was found to be under the limit of detection for these samples.

support for our FACS procedure, we sought to execute the same protocol on a population of exponential-phase cells devoid of persisters and to show that persisters were unequivocally not generated by our method. To do this, we sought to demonstrate that our results were in agreement with those of Keren and colleagues (8), who found that continued culturing by dilution in fresh medium eliminates persisters from a culture. We repeated this experiment under normal assay conditions (bench top) as well as with our FACS method (see Materials and Methods) and found the results between the two to be indistinguishable (Fig. 3G). Repeated inoculation into fresh medium eliminated the nongrowing subpopulation (Fig. 3F), as well as all persisters from the growing subpopulation (Fig. 3G). These results are consistent with those of Keren and colleagues and provide further evidence that our FACS method does not alter persister levels. Interestingly, normally dividing cells lose the ability to become persisters after continued culturing, suggesting that aspects of their physiology that confer persistence are lost by continued rounds of replication. We note that in order for cells to be within the A* region of Fig. 3A, they had to divide, on average, >3 times after inoculation from stationary phase, whereas cells present in the R_2 culture, which did not contain persisters, divided, on average, >14 times. Altogether, these data demonstrate that while nongrowing cells are more likely to be persisters than growing cells, persisters can be found in the nor-

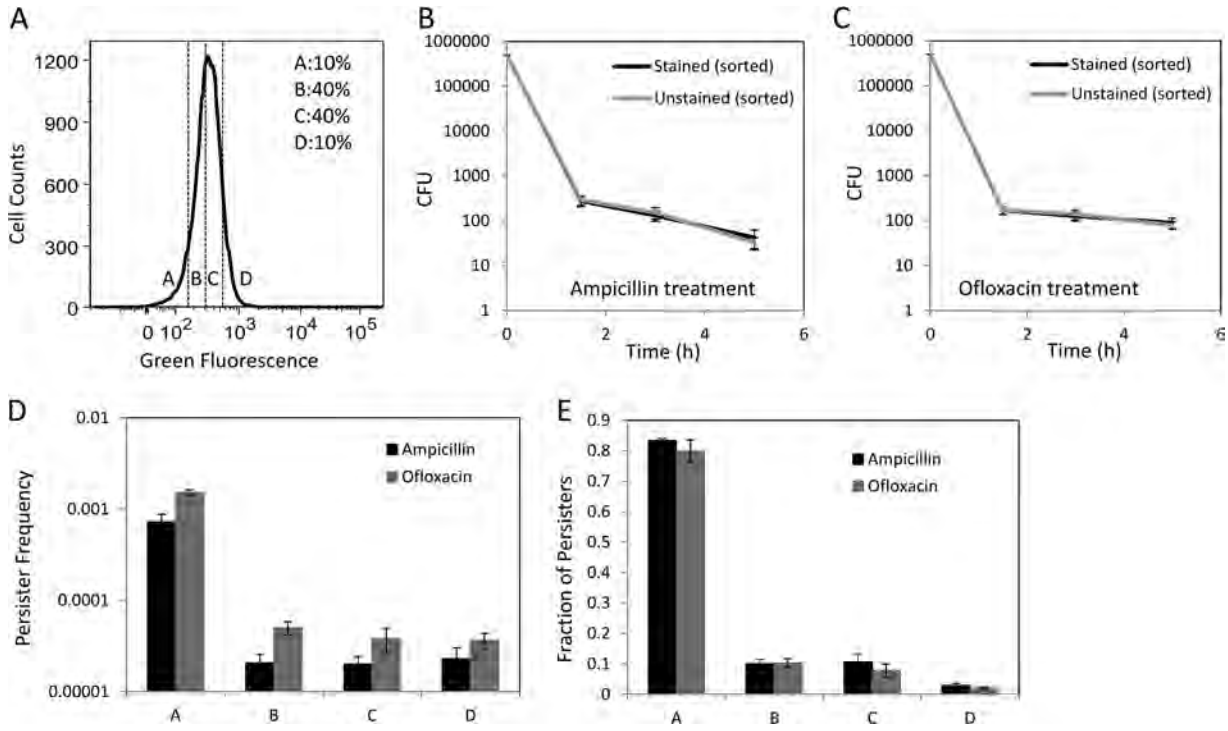

FIG 4 Metabolic activity of persisters. (B and C) CFU were determined at the indicated time points during the antibiotic treatment. RSG staining did not affect the persister levels ($P = 0.58$ for ampicillin persisters at the 5-h time point and 0.52 for ofloxacin persisters at the 5-h time point, using the *t* test). Persister frequencies (D) as well as fractions (E) were quantified after 5 h of antibiotic treatment of FACS-sorted cells from regions A, B, C, and D, based on RSG staining (A).

mally dividing subpopulation, and that a lack of growth does not confer persistence, since 99.57% ± 0.048% of nongrowing cells are not ampicillin persisters, and similarly, 99.26% ± 0.064% of nongrowing cells are not ofloxacin persisters.

Persisters exhibit heterogeneous metabolic activity. Cells from early exponential phase ($OD_{600} = 0.1$) were incubated with RSG for 30 min and analyzed by flow cytometry (see Materials and Methods). As expected, staining of cells with RSG exhibited increased green fluorescence compared to that of the unstained, CCCP-treated, and KCN-treated controls (Fig. 2D and E). To determine where persisters existed within the phenotypic distribution of reductase activity, we sorted cells from four different regions of the distribution, as indicated in Fig. 4A. The A region contained cells with metabolic activity in the lowest ~10% of the population, the B region contained cells with low-intermediate metabolic activity (~40% of the population), the C region contained cells with intermediate-high metabolic activity (~40% of the population), and the D region contained cells with metabolic activity in the highest ~10% of the population. To enumerate persisters, FACS-sorted samples were treated with ampicillin or ofloxacin and CFU were monitored. The biphasic kill curves verified that 5 h of antibiotic treatment under the conditions described here was sufficient to quantify persister levels (Fig. 4B and C). Furthermore, Fig. 4B and C demonstrate that RSG staining had no effect on the persistence of the population. The frequencies of persisters within these populations are presented in Fig. 4D, whereas the fraction of persisters from the total population in each quantile is provided in Fig. 4E. We found that 83.33% ± 0.67% and 79.92% ± 3.62% of all ampicillin and ofloxacin persisters, respectively, were present in region A of the reductase distribution, demonstrating that 4 of 5 persisters contained low reductase activity (Fig. 4E). This is the first direct measurement of metabolic activity in persisters, and while the data are supportive of the notion that persisters are largely metabolically dormant, the regions with higher reductase activity (B, C, and D) did contain a nonnegligible portion of persisters: ~20%. These data demonstrate that persisters can be metabolically active and retain their antibiotic tolerances, suggesting that metabolic dormancy prior to antibiotic treatment is not a requirement of persistence. In addition, the frequency of persisters in the region of low reductase activity (A) was only 0.07% ± 0.01% for ampicillin and 0.15% ± 0.01% for ofloxacin, suggesting that metabolic dormancy is not sufficient to confer persistence.

Most persisters exhibit low metabolic activity due to their nonreplicating state. Since low metabolic activity and lack of replication are predictive of persister enrichment, we sought to determine whether these results were coupled or could be used in conjunction to further increase the persister frequency in a sample. To do this, we performed a 2D FACS experiment in which growing and nongrowing cells could be discerned using mCherry (Fig. 5A), and metabolic activity was measured using RSG. We observed that the nongrowing subpopulation fluoresced far less on the green channel (RSG) than the growing subpopulation ($P = 0.022$ by the *t* test), suggesting that nongrowing cells generally harbored lower reductase activity than growing cells (Fig. 5B). After verifying that RSG-stained, mCherry-expressing cells did not have a changed persistence phenotype (Fig. 5C and D), we found that the persister enrichment associated with low metabolic activity was dependent

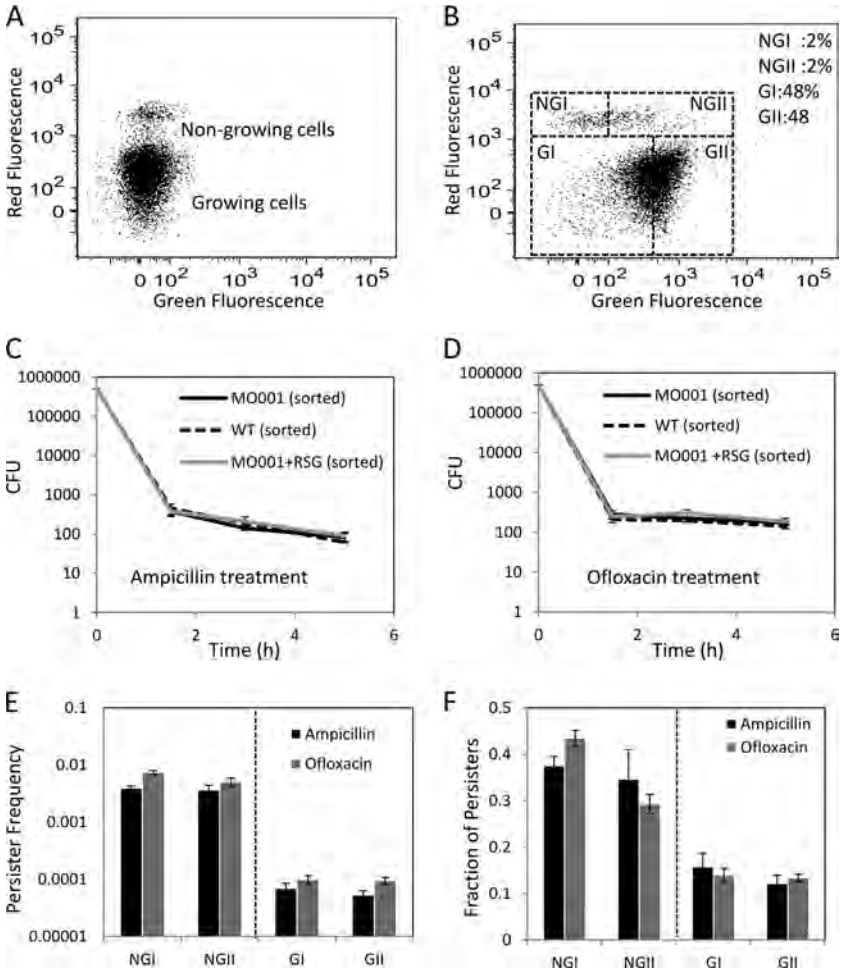

FIG 5 2D FACS sorting. (A) Unstained exponential-phase MO001 cells. (B) RSG-stained MO001 cells. (C and D) CFU were determined at the indicated time points during the antibiotic treatment. Persister frequencies (E) as well as fractions (F) were quantified after 5 h of antibiotic treatment of FACS-sorted cells from the NGI, NGII, GI, and GII regions (B). There was no significant difference in persister frequencies between NGI and NGII ($P = 0.77$ for ampicillin samples and $P = 0.09$ for ofloxacin samples, using the *t* test) or between GI and GII ($P = 0.45$ for ampicillin samples and $P = 0.86$ for ofloxacin samples, using the *t* test).

on replication (Fig. 5E and F). When the growing and nongrowing subpopulations were split in half based on metabolic activity (GI and GII populations and NGI and NGII populations), indistinguishable persister frequencies were obtained (Fig. 5E). These data demonstrate that persistence depends more on replication status than on metabolic activity, and thus 2D sorting based on metabolic status and growth rate is unlikely to yield persister enrichment beyond that which is attained based simply on growth rate.

DISCUSSION

The dominant model of persistence posits that persisters are growth-inhibited cells with depressed cellular functions whose corruption by bactericidal antibiotics fails to produce cellular death (3). This model has stimulated a significant amount of research into different mechanisms of growth inhibition and their association with persistence (5, 9, 10, 14–16, 18, 29–31) and has facilitated the extrapolation of dormancy to additional cellular processes, such as metabolism, for which supporting evidence remains indirect (4–6). However, it has remained unclear to what extent growth inhibition prior to antibiotic treatment characterizes persistence. Several studies have shown that specific antibiotics can kill bacteria in nongrowing cultures (8, 17, 32, 33), and data from Roostalu and colleagues suggest that a lack of growth under growth-promoting conditions is insufficient to confer persistence in response to ampicillin (7). The results presented here agree with and expand upon these findings, as ampicillin and ofloxacin persisters were found to be rare (<1%) within the nongrowing subpopulation of an exponential-phase culture. These data suggest that factors beyond lack of growth define which nongrowing cells become persisters and which do not. Possible reasons for why nongrowing cells might not be persisters include the following: the cells may have been dead prior to antibiotic treatment or may have resumed replication during antibiotic treatment (3, 15, 23). We note that under the experimental conditions investigated here, 2.93% ± 0.68% of the nongrowing subpopulation could have been dead prior to antibiotic treatment, 29.17% ± 14.94% of the nongrowing subpopulation began replicating after 5 h of incubation in the absence of antibiotic, and 24.08% ± 11.92% and 19.83% ± 9.28% of the nongrowing subpopulation experienced a reduction in mCherry content after 5 h of incubation in the presence of ampicillin and ofloxacin, respectively. The remaining nongrowing subpopulation can be classified as viable but noncul-

turable (VBNC), since its members stained as live cells, did not resume replication during antibiotic treatment, and failed to form a colony afterward. These data, in conjunction with the previous investigations discussed above, demonstrate that growth inhibition is insufficient to confer persistence.

Though insufficient, growth inhibition prior to antibiotic exposure has commonly been considered a necessary condition of persistence (34). Several recent studies have investigated stress-induced persistence, a phenomenon in which a nonpersister cell is transformed into a persister cell through the action of signal transduction pathways (9, 10). However, it is important that none of these studies determined the growth state of the persisters formed prior to antibiotic treatment. Indeed, even the study of Dorr and colleagues, in which ciprofloxacin itself stimulated persister formation through the SOS response, did not determine whether the persisters formed were growing normally prior to antibiotic exposure (9, 10). Most recently, a study by Wakamoto and colleagues established that persisters observed in response to a prodrug antibiotic can be replicating normally prior to and during exposure (35). Cell death was found to be associated with the presence of catalase, the prodrug-activating enzyme, and independent of growth. While Wakamoto and colleagues established that persistence in response to prodrugs does not require growth inhibition, the same phenomenon for antibiotics that do not require activation (e.g., β-lactams and fluoroquinolones) had not been established. Here we discovered that growth inhibition prior to antibiotic challenge is not necessary for a cell to be a persister in response to ampicillin and ofloxacin, both of which are antibiotics that do not require activation by an enzyme to kill bacteria. We demonstrated that persisters can arise from normally replicating bacteria, though at significantly lower frequencies than those observed for nongrowing bacteria, and that the proportion of persisters from normally replicating bacteria is significant compared to that originating from nongrowing bacteria, amounting to approximately 20% of all persisters present. This observation challenges what most investigations had assumed was a requirement of the persistence phenotype (2, 34) and highlights the diversity of persisters present in bacterial populations (14).

Interestingly, we observed that the ability of a normally replicating cell to form a persister is lost after continuous exponential-phase propagation, a result that is consistent with observations from a previous study (8). Though we did not identify the cause of this phenotypic change, we postulate that this phenomenon is associated with dilution of a specific component, perhaps a protein, that is present in stationary phase and requires a >512-fold dilution to drop to levels that no longer confer persistence. From Fig. 3, it is obvious that the R_0 population retained stationary-phase characteristics, as the mCherry concentration remained largely above background. The fluorescence of the R_1 population resembles the background fluorescence and that of R_2, but cells in R_1 had undergone 5 or 6 fewer divisions than those in R_2. Since the number of persisters in R_1 exceeded that which could have originated from the nongrowing subpopulation of R_0 (at most, 1 to 3 in 500,000 cells could have been persisters from the R_0 nongrowing subpopulation), the ability to form persisters was still retained by the growing subpopulation. This ability was lost after 5 or 6 subsequent divisions, which characterizes R_2. Specifically, in the absence of degradation or export, stationary-phase components would be diluted 512-fold, on average, in R_1 and 16,384-fold in R_2. Since specific protein concentrations can exceed 200,000 molecules per cell in stationary-phase cells (36), there are stationary-phase characteristics that are more likely to be lost in cells of R_2 than in cells of R_1. To determine whether this is the case is an interesting topic for a future investigation.

In association with growth inhibition, metabolic dormancy has been a commonly cited characteristic of persisters, despite the existence of only indirect evidence (17, 34). Therefore, in addition to cell division, we monitored the metabolic state of cells and found that a lower reductase activity prior to antibiotic treatment increased the likelihood that a cell would be a persister. Interestingly, lower reductase activity was also insufficient to define persistence, and we further found that sorting based on cell division and reductase activity did not provide improved persister enrichment beyond that attained with cell division alone. Though persister metabolism could not be leveraged in conjunction with cell division to improve persister enrichment, the metabolic measurements presented here suggest that persisters can contain a wide range of metabolic activities and thereby support the idea of persister diversity (14). Inherently, persister diversity will complicate efforts to eradicate these cells as sources of chronic and recurrent infections; however, charting persister diversity, as was done in this study, will place the field in the best position possible to develop broad-spectrum antipersister therapies.

ACKNOWLEDGMENTS

We thank Christina J. DeCoste and Christi A. O'Donnell for their technical support with flow cytometry and Zemer Gitai and his lab for providing pAS08.3 *mCherry* and for technical support with fluorescence microscopy. We also thank A. James Link and Ned Wingreen for their thoughtful suggestions.

Research reported in this publication was supported by the National Institute of Allergy and Infectious Diseases of the National Institutes of Health under award number R21AI105342, by the Department of the Army under award number W81XWH-12-2-0138, and with start-up funds from Princeton University.

The content is solely the responsibility of the authors and does not necessarily represent the official views of the funding agencies.

REFERENCES

1. **Spoering AL, Lewis K.** 2001. Biofilms and planktonic cells of Pseudomonas aeruginosa have similar resistance to killing by antimicrobials. J. Bacteriol. **183**:6746–6751.
2. **Lewis K.** 2010. Persister cells. Annu. Rev. Microbiol. **64**:357–372.
3. **Balaban NQ, Merrin J, Chait R, Kowalik L, Leibler S.** 2004. Bacterial persistence as a phenotypic switch. Science **305**:1622–1625.
4. **Keren I, Shah D, Spoering A, Kaldalu N, Lewis K.** 2004. Specialized persister cells and the mechanism of multidrug tolerance in Escherichia coli. J. Bacteriol. **186**:8172–8180.
5. **Shah D, Zhang ZG, Khodursky A, Kaldalu N, Kurg K, Lewis K.** 2006. Persisters: a distinct physiological state of E. coli. BMC Microbiol. **6**:53. doi:10.1186/1471-2180-6-53.
6. **Kaldalu N, Mei R, Lewis K.** 2004. Killing by ampicillin and ofloxacin induces overlapping changes in Escherichia coli transcription profile. Antimicrob. Agents Chemother. **48**:890–896.
7. **Roostalu J, Joers A, Luidalepp H, Kaldalu N, Tenson T.** 2008. Cell division in Escherichia coli cultures monitored at single cell resolution. BMC Microbiol. **8**:68. doi:10.1186/1471-2180-8-68.
8. **Keren I, Kaldalu N, Spoering A, Wang YP, Lewis K.** 2004. Persister cells and tolerance to antimicrobials. FEMS Microbiol. Lett. **230**:13–18.
9. **Dorr T, Lewis K, Vulic M.** 2009. SOS response induces persistence to fluoroquinolones in Escherichia coli. PLoS Genet. **5**:e1000760. doi:10.1371/journal.pgen.1000760.
10. **Dorr T, Vulic M, Lewis K.** 2010. Ciprofloxacin causes persister formation by inducing the TisB toxin in Escherichia coli. PLoS Biol. **8**:e1000317. doi:10.1371/journal.pbio.1000317.

11. **Vega NM, Allison KR, Khalil AS, Collins JJ.** 2012. Signaling-mediated bacterial persister formation. Nat. Chem. Biol. **8**:431–433.
12. **Wu YX, Vulic M, Keren I, Lewis K.** 2012. Role of oxidative stress in persister tolerance. Antimicrob. Agents Chemother. **56**:4922–4926.
13. **Moker N, Dean CR, Tao JS.** 2010. Pseudomonas aeruginosa increases formation of multidrug-tolerant persister cells in response to quorum-sensing signaling molecules. J. Bacteriol. **192**:1946–1955.
14. **Allison KR, Brynildsen MP, Collins JJ.** 2011. Heterogeneous bacterial persisters and engineering approaches to eliminate them. Curr. Opin. Microbiol. **14**:593–598.
15. **Gefen O, Balaban NQ.** 2009. The importance of being persistent: heterogeneity of bacterial populations under antibiotic stress. FEMS Microbiol. Rev. **33**:704–717.
16. **Kint CI, Verstraeten N, Fauvart M, Michiels J.** 2012. New-found fundamentals of bacterial persistence. Trends Microbiol. **20**:577–585.
17. **Allison KR, Brynildsen MP, Collins JJ.** 2011. Metabolite-enabled eradication of bacterial persisters by aminoglycosides. Nature **473**:216–220.
18. **Kwan BW, Valenta JA, Benedik MJ, Wood TK.** 2013. Arrested protein synthesis increases persister-like cell formation. Antimicrob. Agents Chemother. **57**:1468–1473.
19. **Kalyuzhnaya MG, Lidstrom ME, Chistoserdova L.** 2008. Real-time detection of actively metabolizing microbes by redox sensing as applied to methylotroph populations in Lake Washington. ISME J. **2**:696–706.
20. **Gray DR, Yue S, Chueng CY, Godfrey W.** 2005. Bacterial vitality detected by a novel fluorogenic redox dye using flow cytometry, p 331. Abstr. 105th Gen. Meet. Am. Soc. Microbiol.
21. **Bujard H, Gentz R, Lanzer M, Stueber D, Mueller M, Ibrahimi I, Haeuptle MT, Dobberstein B.** 1987. A T5 promoter-based transcription translation system for the analysis of proteins in-vitro and in-vivo. Methods Enzymol. **155**:416–433.
22. **Datsenko KA, Wanner BL.** 2000. One-step inactivation of chromosomal genes in Escherichia coli K-12 using PCR products. Proc. Natl. Acad. Sci. U. S. A. **97**:6640–6645.
23. **Jõers A, Kaldalu N, Tenson T.** 2010. The frequency of persisters in Escherichia coli reflects the kinetics of awakening from dormancy. J. Bacteriol. **192**:3379–3384.
24. **Ma C, Sim SZ, Shi WL, Du LJ, Xing DM, Zhang Y.** 2010. Energy production genes sucB and ubiF are involved in persister survival and tolerance to multiple antibiotics and stresses in Escherichia coli. FEMS Microbiol. Lett. **303**:33–40.
25. **Kim J-S, Heo P, Yang T-J, Lee K-S, Jin Y-S, Kim S-K, Shin D, Kweon D-H.** 2011. Bacterial persisters tolerate antibiotics by not producing hydroxyl radicals. Biochem. Biophys. Res. Commun. **413**:105–110.
26. **Calos MP.** 1978. DNA sequence for a low-level promoter of the lac repressor gene and an 'up' promoter mutation. Nature **274**:762–765.
27. **Hyser JM, Utama B, Crawford SE, Estes MK.** 2012. Genetic divergence of rotavirus nonstructural protein 4 results in distinct serogroup-specific viroporin activity and intracellular punctate structure morphologies. J. Virol. **86**:4921–4934.
28. **Lidstrom ME, Konopka MC.** 2010. The role of physiological heterogeneity in microbial population behavior. Nat. Chem. Biol. **6**:705–712.
29. **Vázquez-Laslop N, Lee H, Neyfakh AA.** 2006. Increased persistence in Escherichia coli caused by controlled expression of toxins or other unrelated proteins. J. Bacteriol. **188**:3494–3497.
30. **Kim Y, Wang X, Zhang X-S, Grigoriu S, Page R, Peti W, Wood TK.** 2010. Escherichia coli toxin/antitoxin pair MqsR/MqsA regulate toxin CspD. Environ. Microbiol. **12**:1105–1121.
31. **Falla TJ, Chopra I.** 1998. Joint tolerance to beta-lactam and fluoroquinolone antibiotics in Escherichia coli results from overexpression of hipA. Antimicrob. Agents Chemother. **42**:3282–3284.
32. **Fung DKC, Chan EWC, Chin ML, Chan RCY.** 2010. Delineation of a bacterial starvation stress response network which can mediate antibiotic tolerance development. Antimicrob. Agents Chemother. **54**:1082–1093.
33. **Nguyen D, Joshi-Datar A, Lepine F, Bauerle E, Olakanmi O, Beer K, McKay G, Siehnel R, Schafhauser J, Wang Y, Britigan BE, Singh PK.** 2011. Active starvation responses mediate antibiotic tolerance in biofilms and nutrient-limited bacteria. Science **334**:982–986.
34. **Lewis K.** 2007. Persister cells, dormancy and infectious disease. Nat. Rev. Microbiol. **5**:48–56.
35. **Wakamoto Y, Dhar N, Chait R, Schneider K, Signorino-Gelo F, Leibler S, McKinney JD.** 2013. Dynamic persistence of antibiotic-stressed mycobacteria. Science **339**:91–95.
36. **Nair S, Finkel SE.** 2004. Dps protects cells against multiple stresses during stationary phase. J. Bacteriol. **186**:4192–4198.
37. **Amato SM, Orman MA, Brynildsen MP.** 9 May 2013, posting date. Metabolic control of persister formation in *Escherichia coli*. Mol. Cell doi: 10.1016/j.molcel.2013.04.002.

Supplemental Material

Dormancy is not necessary or sufficient for bacterial persistence

Mehmet A Orman and Mark P Brynildsen*

Department of Chemical and Biological Engineering, Princeton University, Princeton, New Jersey, United States of America.

*E-mail: mbrynild@princeton.edu.

Running title: Persister dormancy

Table S1. Primer list.

Forward primer (5`---3`)	Reverse primer(5`---3`)	Explanation
TCTGGTGGCCGGAAGGCGAAG CGGCATGCATTTACGTTGATGC AGCATTACACGTCTTGA	**TGCCTAATGAGTGAGCTAACTCAC ATTAATTGCGTTGCGC**CAAGATCC GCAGTTCAACCT	Primers for using Datsenko and Wanner method to knock-out chromosomal *LacI* including promoter. Primers amplified *Kan*^{R} cassette from pKD4 plasmid, and have 40-nt homology regions (bold).
TCTGGTGGCCGGAAGGCGAAG CGGCATGCATTTACGTTGACAC CATCGAATGGTGCAAAA	**TCCAGCCTACACAATCGCTC**TCAC TGCCCGCTTTCCAGTC	Primers for amplifying *LacI*^{q} gene from pQE80L plasmid (Qiagen). The forward primer has a 40-nt homology extension (bold) for up-stream sequence of chromosomal *LacI* gene, and the reverse primer has a 20-nt homology extension (bold) to append *Kan*^{R} cassette to the 3` end of *LacI*^{q} coding strand.
GAGCGATTGTGTAGGCTGGA	**TGCCTAATGAGTGAGCTAACTCAC ATTAATTGCGTTGCGC**TTAACGGC TGACATGGGAAT	Primers for amplifying *Kan*^{R} cassette from pKD4 plasmid. Forward primer is homologous to reverse primer of *LacI*^{q} for overlap extension, and reverse primer has a 40-nt homology extension (bold) for down-stream sequence of chromosomal *LacI* gene. *LacI*^{q}*+Kan*^{R} DNA fragment was chromosomally integrated in place of *LacI* using Datsenko & Wanner method.
ATTAATGTGAGTTAGCTCACTC ATTAGGCACCCCAGGCTTCTCG AGAAATCATAAAAAAT	**TCCTCGCCCTTGCTCACCAT**AGTT AATTTCTCCTCTTTAA	Primers for amplifying *T5* promoter from pQE-80L plasmid. The forward primer has a 40-nt homology extension (bold) for up-stream sequence of *Lac* operon, and the reverse primer has a 20-nt homology extension (bold) to append *mCherry* gene to the 3` end of *T5p* coding strand.
ATGGTGAGCAAGGGCGAGGA	**CGATCCTCATCCTGTCTCTTGAT**C TTCTACTTGTACAGCTCGTCCATG	Primers for amplifying *mCherry* gene from pAS08.3 plasmid. Forward primer is homologous to reverse primer of *T5p* (overlap extension), and reverse primer has a 23-nt homology extension (bold) to append *Kan*^{R} gene to the 3` end of *mCherry* coding strand.
ATCAAGAGACAGGATGAGGAT CG	**TGTAGATCGCTGAACTTGTAGGC CTGATAAGCGCAGCGTATCAGGC AATT**TCAGAAGAACTCGTCAAGAA GG	Primers for amplifying *Kan*^{R} gene. Forward primer is homologous to reverse primer of *mCherry* for overlap extension, and reverse primer has a homology region (bold) for down-stream sequence of chromosomal *Lac* operon. *T5p+mCherry+Kan*^{R} DNA fragment was chromosomally integrated in place of *Lac* operon using Datsenko & Wanner method.
ATCGAATGGCGCAAAACCT	TTCCAGTCGGGAAACCTGT	Internal primers for *LacI* to confirm the absence of duplicate gene after knocking out chromosomal *LacI*.
GGGATCAGGAGGAGAAGATCG		Forward primer for upstream sequence of the *LacI* gene. This primer and a Kan^R reverse primer (see below) were used to confirm the presence of the kanamycin resistance cassette in the proper chromosomal location.
AGGACAGTCGTTTGCCGTCT	ATCGACAGATTTGATCCAGCG	Internal primers for *LacZ* to confirm the absence of duplicate gene after knocking out chromosomal *Lac* operon.
CCGATTTGGCTACATGACATC	AAACAGACCAGATAAATCGTCGC	Internal primers for *LacY* to confirm the absence of duplicate gene after knocking out chromosomal *Lac* operon.
GCCAATGACCGAAAGAATAAGA	GAAATAATAGTGCTTATCCCGGTC	Internal primers for *LacA* to confirm the absence of duplicate gene after knocking out chromosomal *Lac* operon.
CGGTAGTGGGATACGACGATAC		Forward primer for upstream sequence of the *Lac* operon. This primer and *Kan*^{R} or *mCherry* reverse primer were used to confirm the presence of the kanamycin resistance cassette or *mCherry* gene in the proper chromosomal location.
	ATGATGGATACTTTCTCGGCAGGAG	*Kan*^{R} reverse primer

Table S2. Persister Frequencies.

Persister frequencies of mCherry expressing cells		
	Ampicillin	**Ofloxacin**
A*	4.47E-05 ± 1.17E-05	6.93E-05 ± 9.33E-06
B*	5.80E-05 ± 1.59E-05	9.60E-05 ± 1.33E-05
C*	4.27E-03 ± 4.81E-04	7.40E-03 ± 6.43E-04
Persister frequencies of RSG stained cells		
A	7.19E-04 ± 1.55E-04	1.52E-03 ± 1.03E-04
B	2.05E-05 ± 4.99E-06	5.00E-05 ± 8.29E-06
C	2.00E-05 ± 4.24E-06	3.80E-05 ± 1.17E-05
D	2.30E-05 ± 7.14E-06	3.65E-05 ± 6.95E-06
Persister frequencies of RSG stained-mCherry expressing cells		
NGI	3.93E-03 ± 3.33E-04	7.40E-03 ± 5.77E-04
NGII	3.67E-03 ± 7.51E-04	5.07E-03 ± 8.11E-04
GI	6.93E-05 ± 1.57E-05	9.93E-05 ± 1.64E-05
GII	5.33E-05 ± 9.96E-06	9.53E-05 ± 1.34E-05

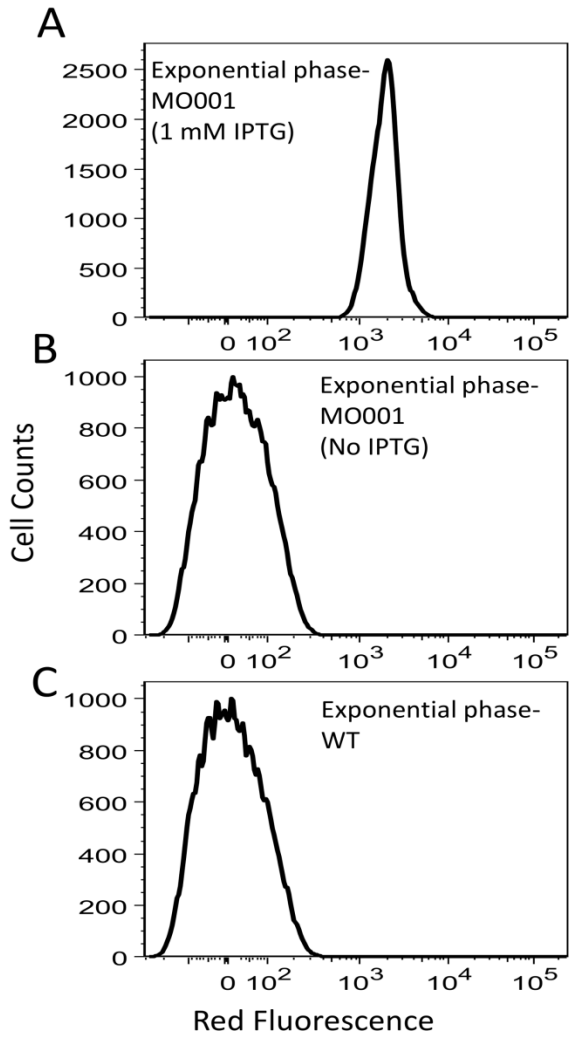

Figure S1. MO001 background fluorescence is as low as that of the parent strain (without *mCherry*). MO001 was incubated without IPTG during the overnight and both with and without IPTG during the exponential growth (A, B), and fluorescence intensities were measured by flow cytometry. Exponential wild-type cells were used to determine the background fluorescence (C).

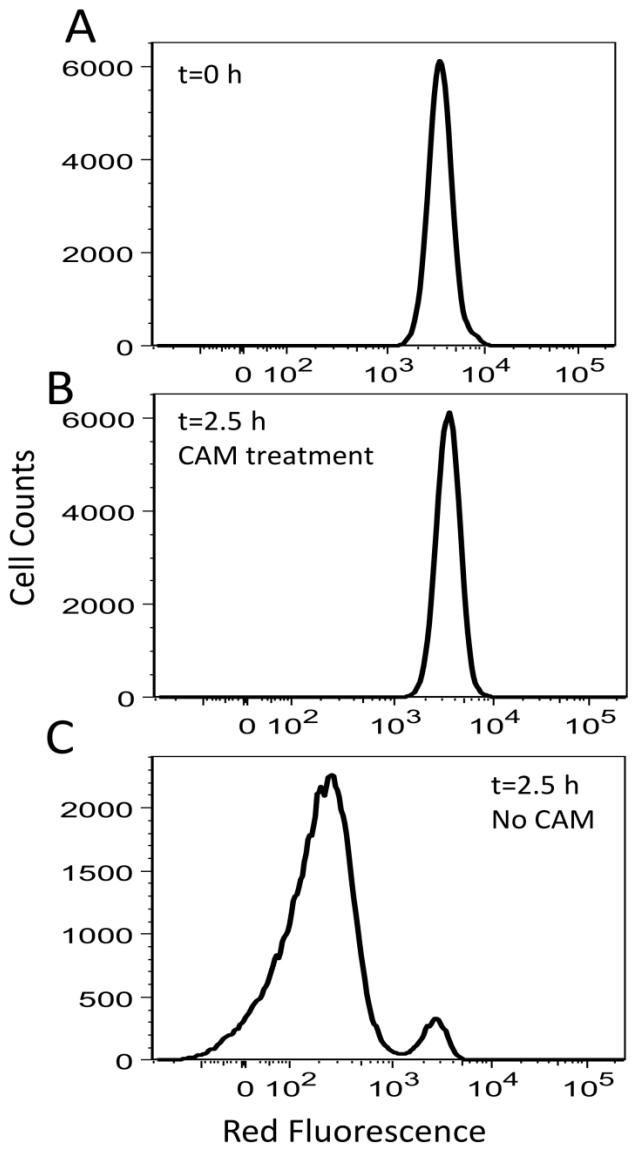

Figure S2. mCherry was not degraded during the time-frame of the experiment. After accumulation of mCherry protein during the overnight culture (t=0 h) (A), cells were inoculated in fresh media (without IPTG) with 50μg/mL chloramphenicol (B) or without chloramphenicol (C). Exponential-phase samples (2.5 h after the inoculation) were analyzed by flow cytometry.

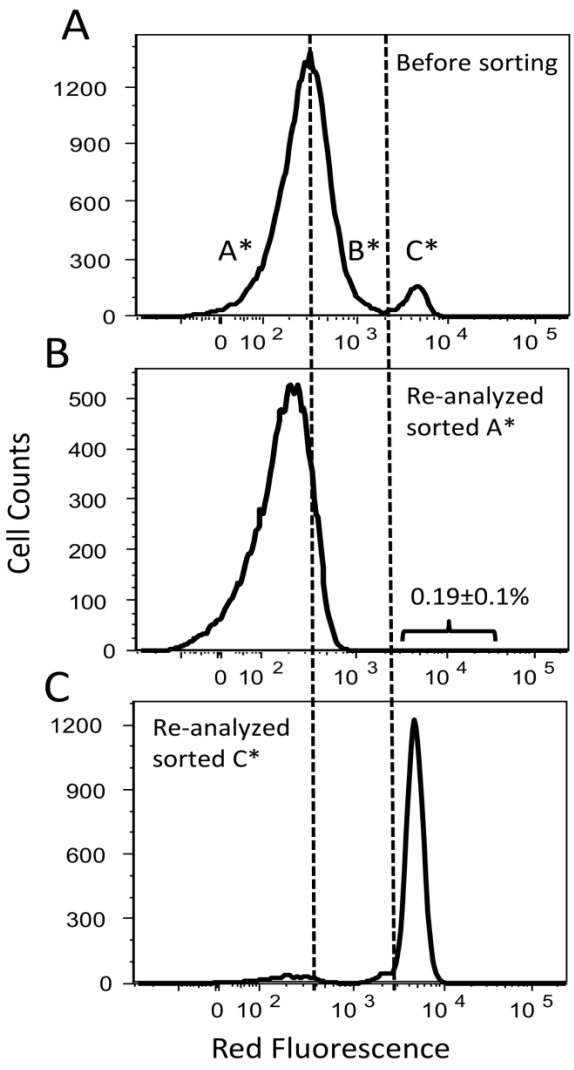

Figure S3. The number of non-growing cells that were improperly sorted into the fastest-growing quantile was measured. After sorting approximately $5x10^5$ cells from the A* or C* regions (A), the cells from A* and C* were separately reanalyzed by the same sorter (B and C, respectively). It was found that 0.19±0.1% of cells in A* were non-growing cells.

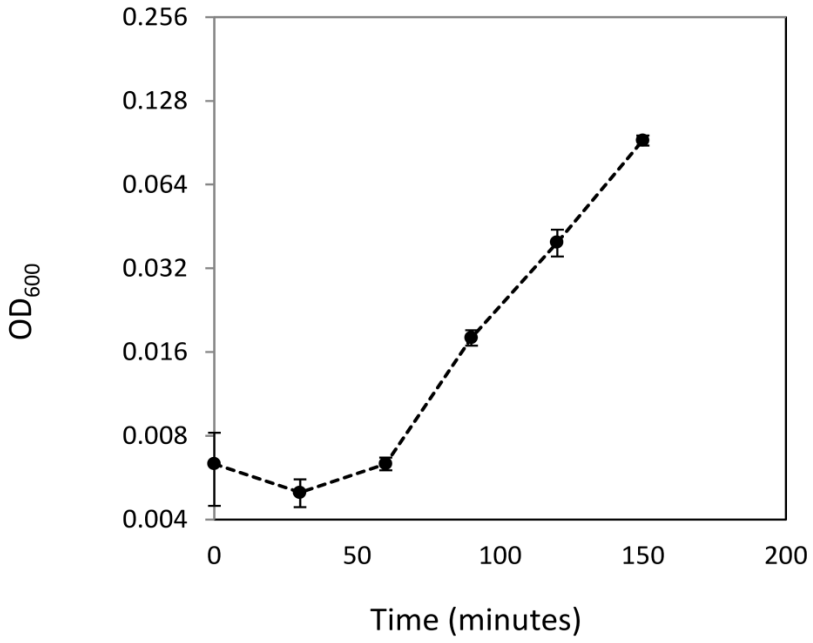

Figure S4. Growth of MO001 cells. After inoculation of overnight culture in fresh media (1:1000), OD_{600} was monitored every 30 minutes, and the growth rate was calculated using exponential fit between 60 to 150 minutes time points.